

**Molecular aspects of plant disease susceptibility:
Arabidopsis genes affecting downy mildew infection**

Moleculaire aspecten van vatbaarheid voor plantenziekten:
Arabidopsis-genen betrokken bij infectie door valse meeldauw
(met een samenvatting in het Nederlands)

Proefschrift

ter verkrijging van de graad van doctor aan de Universiteit Utrecht op
gezag van de rector magnificus, prof.dr. G.J. van der Zwaan, inge-
volge het besluit van het college voor promoties in het openbaar te
verdedigen op maandag 2 december 2013 des middags te 12.45 uur

door

Dmitry Lapin

geboren op 6 februari 1987
te Shchukovo, Rusland

Promotor: prof. dr. ir. C.M.J. Pieterse
Co-promotor: dr. A.F.J.M. Van den Ackerveken

This thesis was accomplished with financial support from The Lever-
hulme trust and Utrecht University

Table of contents

<i>Chapter 1: General Introduction</i>	5
Plant disease susceptibility: more than a failure of host immunity	
<i>Outline</i>	15
<i>Chapter 2</i>	17
Broad spectrum resistance of Arabidopsis C24 to downy mildew is mediated by different combinations of isolate-specific loci	
<i>Chapter 3</i>	37
Two interacting downy mildew resistance loci in the Arabidopsis accession C24 revealed by whole genome sequencing of backcross lines	
<i>Chapter 4</i>	57
Association mapping reveals a potential role for <i>CYTOKININ RESPONSE FACTOR 1</i> in Arabidopsis susceptibility to downy mildew	
<i>Chapter 5</i>	87
Disease-related N-glycoproteins of Arabidopsis infected by downy mildew	
<i>Chapter 6: General discussion</i>	111
<i>References</i>	117
<i>Summary</i>	139
<i>Samenvatting</i>	140
<i>Acknowledgements/Благодарности</i>	141
<i>Curriculum vitae</i>	143
<i>List of publications</i>	145

Chapter 1: General Introduction

Plant disease susceptibility: more than a failure of host immunity

Dmitry Lapin and Guido Van den Ackerveken

Plant–Microbe Interactions, Utrecht University, Padualaan 8, 3584 CH, Utrecht, The Netherlands

Trends in Plant Science, doi 10.1016/j.tplants.2013.05.005

Abstract

Susceptibility to infectious diseases caused by pathogens affects most plants in their natural habitat and leads to yield losses in agriculture. However, plants are not helpless because their immune system can deal with the vast majority of attackers. Nevertheless, adapted pathogens are able to circumvent or avert host immunity making plants susceptible to these uninvited guests. In addition to the failure of the plant immune system, there are other host processes that contribute to plant disease susceptibility. In this review we discuss recent studies that show the active role played by the host in supporting disease, focusing mainly on biotrophic stages of infection. Plants attract pathogens, enable their entry and accommodation, and facilitate nutrient provision.

Forced hospitality enables infection

Plants possess a dedicated immune system to fend off infection by pathogens such as viruses, bacteria, fungi, oomycetes, and nematodes. The activation of plant defense responses is triggered by the recognition of invading organisms by immune receptors. These can be plasma membrane-bound receptors that monitor the extracellular environment or intracellular receptors that detect the presence or activity of pathogen-derived effectors. An important class of receptors recognizes molecules known as pathogen or microbe-associated molecular patterns (PAMPs/MAMPs), which are exposed or released by a broad range of invading organisms. Well-known examples are the pattern recognition receptors FLS2 (FLAGELLIN-SENSITIVE 2) for bacterial flagellin and the CERK1 (CHITIN ELICITOR RECEPTOR KINASE 1) for fungal chitin. Recognition of PAMPs/MAMPs results in the activation of the plant immune system [1]. Plants have the intrinsic capacity to detect and respond to invading pathogens and, therefore, are resistant to the majority of potential pathogens [2-4].

However, the plant immune system is rendered ineffective by adapted pathogens that have evolved ways to interfere with host defense (see Box 1). The ensuing failure of the plant immune system allows further ingress of invading pathogens, however, not without the ‘collaboration’ of the host. The focus of this review is on non-immunity-related plant processes that contribute to the susceptibility of plants to pathogens at the level of (i) pathogen attraction and attachment to the host, (ii) accommodation of infection structures in plant cells, and (iii) nutrient production and transport from the host (Figure 1). We will mainly focus on the susceptibility of plants to pathogens that have a biotrophic lifestyle either during initial stages of infection (e.g. *Phytophthora* spp., *Colletotrichum* spp.) or throughout their life cycle (e.g. the powdery and downy mildews) (see Glossary for terminology).

Plant signals as cues for pathogen development

The effect of signals from the host plant on early pathogen development was convincingly

illustrated in a recent analysis of gene expression in germinating spores of the hemibiotrophic fungus *Colletotrichum higginsianum*, which showed that the transcription of >1700 genes is induced when the spores are on a host plant surface rather than on an artificial polystyrene surface [14]. Plant-derived molecules such as flavonoids, fatty acids, alcohols, and aldehydes are known to serve as signals to attract pathogens, stimulate attachment to the plant surface, and induce germination and formation of penetration structures named appressoria.

Flavonoids are released into the soil from the roots of many plant species where they can attract soil-borne pathogens. It has been shown that isoflavonoids released by the roots of soybean (*Glycine max*) and other plants attract zoospores of *Phytophthora* spp., which are oomycete pathogens [15]. Flavonoids can also stimulate spore germination, as shown for the fungal legume pathogen *Fusarium solani* [16]. However, these compounds have not been reported to stimulate the development of infection structures *in vivo*.

Other compounds, for example plant hormones, are known to trigger pathogen development. Ethylene released by ripening fruits stimulates both spore germination and appressorium formation of the fungus *Colletotrichum gloeosporioides* [17]. There are indications that strigolactones also influence *in vitro* growth of phytopathogenic fungi [18], although it is not clear how they influence plant infection.

Components of plant surface waxes (see Glossary), such as long-chain alcohols and aldehydes, play an important role in pathogen spore germination. Leaves of the maize (*Zea mays*) *glossy11* mutant, in which very-long-chain aldehydes are depleted from surface waxes, are poor substrates for the germination of spores of the barley powdery mildew *Blumeria graminis* f.sp. *hordei*. Exogenous application of the C26 aldehyde n-hexacosanal on *glossy11* leaves restored efficient spore germination demonstrating that it serves as a cue for pathogen

Glossary

Biotroph – pathogen that lives and multiplies only on living host tissues [22, 23]. The examples of plant biotrophic pathogens are viruses, viroids, downy and powdery mildews, rusts.

Cutin - a polymer of long-chain fatty acids and their derivatives on the plant surface, the main component of surface cuticle [24].

Effector – microbial and pest secreted molecules that alter host cell processes or structures generally promoting the interaction with the host [12].

Endoreduplication – modification of the cell cycle in which nuclear DNA undergoes replication without subsequent cell division that leads to formation of nuclei with increased ploidy level [25]. The resulting ploidy level is expressed as the amount of DNA compared to that of a haploid nucleus. For example, normal diploid cell (2n) has 2C amount of DNA.

G-proteins - GTP hydrolyzing proteins (GTPases) that work as molecular switches in regulating a broad range of cell processes. Plant G-proteins are broadly classified into small G-proteins (including ROPs), heterotrimeric G-proteins and unconventional G-proteins [26, 27]

Hemibiotroph – pathogen for which only a part of the life cycle is dependent on living host tissues. For example, the oomycete pathogen *Phytophthora capsici* starts infection process in *Arabidopsis thaliana* as a biotrophic pathogen but later switches to the necrotrophic stage [28, 29].

Necrotroph - pathogen feeding on dead host tissues. The plant necrotrophic pathogens are exemplified by the grey mold fungus *Botrytis cinerea* and the oomycete parasites *Pythium* [30].

Strigolactones - carotenoid-derived plant hormones originally identified as molecules from root exudates stimulating germination of seeds of parasitic plants in the periphery of the host plant. Strigolactones are not only signals in the rhizosphere but also play an important role as hormones in plant development [31].

Waxes – a complex mixture of highly hydrophobic long-chain alkanes, alcohols and fatty acids frequently found on the surface cuticles [24].

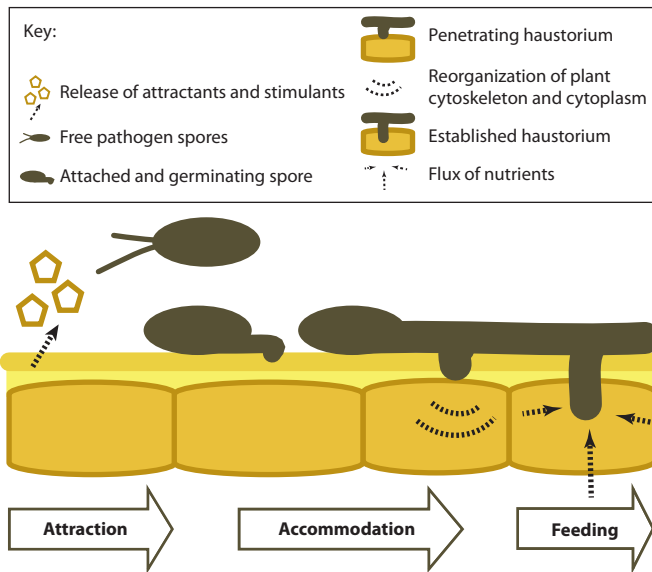


Figure 1. The host plant promotes susceptibility to pathogen infection at several key steps: (i) attracting pathogens by plant-derived molecules and stimulating their attachment and development on the host surface, (ii) accommodating pathogen infection structures, for example, haustoria, and (iii) feeding the uninvited guests.

development [19]. Similarly, on leaves of the *Medicago truncatula irg1* (*inhibitor of rust germ tube differentiation 1*) mutant, spores of the fungi *Colletotrichum trifolii* (a pathogen of *Medicago*) and *Phakopsora pachyrhizi* (for which *Medicago* is a non-host) showed reduced differentiation rates. The *irg1* mutant has an altered composition of surface waxes because it is severely depleted in C30 primary alcohols. Transcriptome analysis of the *irg1* mutant revealed downregulation of *ECERIFERUM4*, implicated in primary alcohol biosynthesis, and *MYB96*, a transcriptional regulatory gene of wax biosynthesis [20]. In addition, barley (*Hordeum vulgare*) and wheat (*Triticum aestivum*) wax components, such as C26 and C28

Box 1. Suppression of plant immunity

Adapted pathogens have evolved effector proteins and small molecules to suppress PAMP/MAMP-triggered immunity [5-7] and can thereby establish effector-triggered susceptibility (ETS). A second class of plant immune receptors, encoded by resistance genes, has evolved to recognize these effectors or their activity. Effector recognition activates a defense response referred to as effector-triggered immunity (ETI). However, this second layer of immunity can also be rendered ineffective by other effectors that can suppress ETI, for example, by acting on downstream signaling components [5]. The striking feature that many of these effectors have in common is that they act within the host cell and require specialized transport mechanisms to get there. Gram-negative bacteria use a type III secretion system to 'inject' proteins into the host cell [8, 9]. Nematodes can also insert proteins directly into plant cells by means of their stylet. By contrast, biotrophic fungi and oomycetes secrete proteins from their hyphae or haustoria followed by uptake or translocation over the plant cell membrane into the host cell [10]. Research on the mode of action of effectors has revealed intriguing ways of host manipulation, for example, by manipulating host target proteins, mostly aimed at disabling the plant immune system [11-13]. The resulting suppression is important in the early stages of infection and remains throughout the infection process so that biotrophic pathogens can complete their life cycle without being killed or arrested by plant defense responses. Interestingly, some effectors stimulate susceptibility by other means: for example, by interfering with nutrient metabolism or transport (see text for further discussion).

n-alcohols and even-numbered C22–C30 n-aldehydes, are known to induce germination of powdery mildew spores *in vitro* [21].

Cutin (see Glossary) also plays a signaling role in pathogen development. *M. truncatula ram2* mutant plants, which are missing a glycerol-3-phosphate acyltransferase enzyme involved in cutin biosynthesis, showed increased resistance to the oomycete *Phytophthora palmivora* as a result of reduced appressoria formation by the pathogen. Application of the C16:0 monomer of cutin 1,16-hexadecanediol not only stimulated appressoria formation of *P. palmivora* on a polypropylene surface but also increased the susceptibility of the *Medicago* roots to oomycete infection [32]. Cutin monomers (hydroxy-fatty acids) also stimulate appressorium formation and regulate the hyphal development of the obligate biotroph *Ustilago maydis* [33]. We can conclude that plant compounds can act as important attractants for pathogens, as well as triggers for the formation of penetration structures, thereby contributing to disease susceptibility.

Pathogen accommodation

The accommodation of pathogens during biotrophic stages of infection often involves specialized structures, such as haustoria, which could be important for nutrition uptake, as shown for soybean rust (*Uromyces fabae*) [34], and for effector translocation into host cells (see below). The cytoplasm of host cells remains separated from the invading fungal or oomycete haustoria by a host-derived extrahaustorial membrane that is continuous with the plant cell membrane but has a distinct set of membrane-associated proteins [35, 36]. Accommodation of the invading pathogen inside the plant cell involves large changes in host membrane and cytoskeleton organization to which the host actively contributes.

Rho-like GTPases of plants (ROPs, also called RACs) (see Glossary) are well-known for their involvement in development and interaction with the environment [37]. In addition, there is evidence that these proteins play a role in disease susceptibility. Silencing of the rice (*Oryza sativa*) *OsRAC4* and *OsRAC5* genes led to reduced susceptibility to the blast fungus *Magnaporthe grisea* [38]. Similarly, expression of a dominant negative form of ROP6 enhanced resistance of *Arabidopsis* (*Arabidopsis thaliana*) to powdery mildew independently of salicylic acid-mediated immunity [39]. By contrast, constitutively active forms of barley RAC3 and HvRACB, homologs of the *Arabidopsis* ROP6, increased susceptibility of transgenic tobacco (*Nicotiana tabacum*) plants to the powdery mildew fungus *Golovinomyces cichoracearum* and the bacterium *Pseudomonas syringae* pv. *tabaci* [40]. Silencing of the barley HvRACB in single epidermal cells showed that this ROP is indeed required for successful powdery mildew haustorium accommodation [41–43]. Furthermore, a regulator of ROP activity, the *Arabidopsis* receptor-like kinase FERONIA (FER) was found to be important for successful powdery mildew infection and for pollen tube growth [44]. Given that FER [45] as well as the barley HvRACB and *Arabidopsis* ROP6 [41, 46] are also linked to root hair formation, this suggests that the accommodation of fungal haustoria, pollen tube growth and root hair development share a similar signaling pathway. Furthermore, the *ROP6* and *ROP1* genes influence the interaction of *Arabidopsis* with the root endophyte *Piriformospora indica* because their mutation affects plant cytoskeleton reorganization during fungal penetration and the growth-promoting effect by the fungus [47]. Interestingly, ROPs also play a role in the accommodation of symbiotic *Rhizobium* bacteria as shown for the *Lotus japonicus* *ROP6*, which is important for infection thread formation that precedes the accommodation of rhizobacteria [48]. Also, in the interaction with arbuscular mycorrhizal fungi, a pre-penetration apparatus is assembled in epidermal root cells of *M. truncatula* and of *Daucus carota* (carrot), a process that requires reorganization of cytoskeleton and endoplasmic reticulum components [49, 50]. Reorganization of host plasma membrane and aggregation of organelles was also observed at penetration sites in *Arabidopsis* inoculated with the powdery mildew *G. cichoracearum* [36], suggesting that prepenetration complexes, involving ROPs and other proteins, are needed for accommodation of symbiont and pathogen infection structures.

Not only do plants enable and support the accommodation of pathogens but they also

contribute to the transport of effector proteins (see Glossary and Box 1) into the host cell. Over the past decade many secreted oomycete and fungal proteins have been identified that show activity inside the host cell, the so-called host-translocated or cytoplasmic effectors [10]. Pioneering electron microscopy has revealed that the immuno gold-labeled rust transferred proteins *Uf-RTP1p* and *Us-RTP1p* from the rust fungi *Uromyces fabae* and *Uromyces striatus*, respectively, are transported from haustoria into plant cells [51]. Two recent studies have shown that fungal effectors localize to specific compartments at the host–pathogen interface, from where they are secreted. In *Magnaporthe oryzae*-infected rice cells, this structure was named the biotrophic interfacial complex [52], and similar structures were found in infections with the hemibiotroph *C. higginsianum*, showing stage-specific foci of effector accumulation at discrete sites on its invasive hyphae [53]. The question remains how effectors end up in the host cell cytoplasm after being secreted to the extracellular interface between the host and the pathogen. Data collected so far points to pathogen-independent uptake by plant cells, possibly via an endocytic route, as was observed for several oomycete and fungal effectors [54-56]. Inhibition of lipid raft-mediated endocytosis with filipin and nystatin was shown to block uptake of the oomycete effector Avr1b into the plant cells. Given that multiple effectors

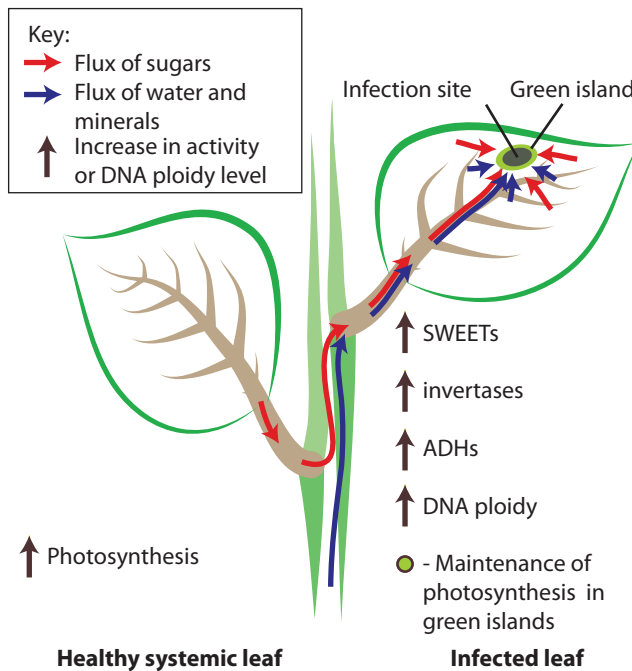


Figure 2. Changes in plant physiology during infection by biotrophic and hemibiotrophic pathogens. Leaves infected with oomycete, fungal, bacterial and protist pathogens show elevated expression of SWEET sugar transporters and cell-wall-bound and vacuolar invertases that facilitate phloem unloading and the flux of sugars to the infection site. ‘Green islands’ are known to surround rusts and powdery mildew infection sites and maintain photosynthesis in the otherwise senescing host tissues. Powdery mildew infection activates host alcohol dehydrogenases (ADHs) that might play a role in the synthesis of specific metabolites beneficial for the fungus and induces increased DNA ploidy levels in mesophyll cells underneath the infected epidermal cells that could contribute to increased metabolite production. Successful infection can also lead to systemic changes in plant physiology, for example, by stimulating photoassimilation in uninfected leaves.

from plant pathogenic oomycetes and fungi were described to bind the phosphoinositide phosphatidylinositol-3-phosphate present in the host plasma membrane, it was suggested that binding initiates effector translocation [54, 57, 58]. However this could not be reproduced by four independent laboratories [59, 60], suggesting that alternative mechanisms of translocation exist. Host cells also enable cell-to-cell movement of effector proteins, for example, the chorismate mutase Cmu1 and PWL2 (for Prevents pathogenicity toward Weeping Lovegrass) secreted by *U. maydis* and *M. oryzae*, respectively, that can move to plant cells next to the infected cells. The movement is likely to be through the plasmodesmata because Cmu1 was not observed in guard cells that lack symplastic connections [52, 61]. It is tempting to speculate that mobile effectors could make distant tissues more accessible to infection thereby possibly contributing to the phenomenon of “induced accessibility”.

Provision of food for pathogenic guests

In addition to accommodation, host plants also ‘offer’ nutrients to their pathogenic guests. In particular, in biotrophic interactions, the plant provides carbon and other nutrients to infecting pathogens. The photosynthetically active tissues of the plant produce organic carbon in the form of sugars. Surprisingly, a reduction of plant photosynthesis rates has been observed in tissues infected with biotrophic and hemibiotrophic leaf pathogens, both in susceptible and resistant plants [62]. The demand for carbon in the infected tissue requires that there is compensation by carbon allocation from non-infected tissues, in particular in non-photosynthetically active tissues, such as in leaf epidermal cells infected by powdery mildews, or root cells parasitized by nematodes. The infected tissues become an important sink so that nutrients, including sugars, are transported there. Transport of sucrose from source to sink tissues requires efficient unloading of the phloem into the apoplast and further transport of sugars to the surrounding cells. The strength of the sink is largely determined by the level of phloem unloading which, in turn, is strongly influenced by the activity of sugar transporters and cell-wall-bound invertases, which are highly expressed in sink tissues [63] (Figure 2).

The discovery of the SWEET family of plant transmembrane proteins was a major breakthrough because several SWEET proteins were shown to transport glucose and sucrose across cell membranes, thus contributing to phloem unloading [64, 65]. A subset of *SWEET* genes in *Arabidopsis* and rice are transcriptionally induced during bacterial and fungal infection [64, 65]. In grapevine (*Vitis vinifera*), the *SWEET* orthologs *VvHT1* and *VvHT5* (hexose transporters) are also transcriptionally activated after powdery and downy mildew infection. Notably, analysis of *VvHT5* spatial expression showed that the gene is actively transcribed in veins of diseased leaves, with the highest abundance close to the infection site [66]. Thus, by unloading phloem, sugar transporters are likely to mediate carbon transport to bacterial, fungal and oomycete infection sites.

The importance of these sugar transporters for disease susceptibility has been revealed in rice. Transcription of the *OsSWEET11/Xa13* gene is activated by the *Xanthomonas oryzae* pv. *oryzae* (*Xoo*) transcription-activator like (TAL) effector PthXo1 through its specific binding to the *OsSWEET11* promoter. Interestingly, recessive resistance to *Xoo* mediated by *xa13* alleles is based on promoter mutations that make the *OsSWEET11* gene non-responsive to the PthXo1 effector [65, 67]. Apparently, the mutated promoter leads to lower transporter levels and consequently a diminished flow of sugars to *Xoo* resulting in a large decrease in susceptibility. Additional support for the importance of sugar transport during infection came from studies showing that other *Xoo* strains have evolved ways to activate the expression of a different rice sucrose and glucose transporter gene, *OsSWEET14*, by another TAL effector, AvrXa7 [64, 65, 68]. In this way, *Xoo* is thought to stimulate the release of sugars needed for bacterial growth. This strategy is likely to be used by other pathogens given that the transcriptional activation of SWEET genes was also observed during infection by fungi and oomycetes [65, 66] (Figure 3).

Alternatively, SWEET transporters could increase susceptibility of rice to *Xoo* by regulating host copper redistribution. Rice *OsSWEET11* interacts both *in vivo* and *in vitro* with the

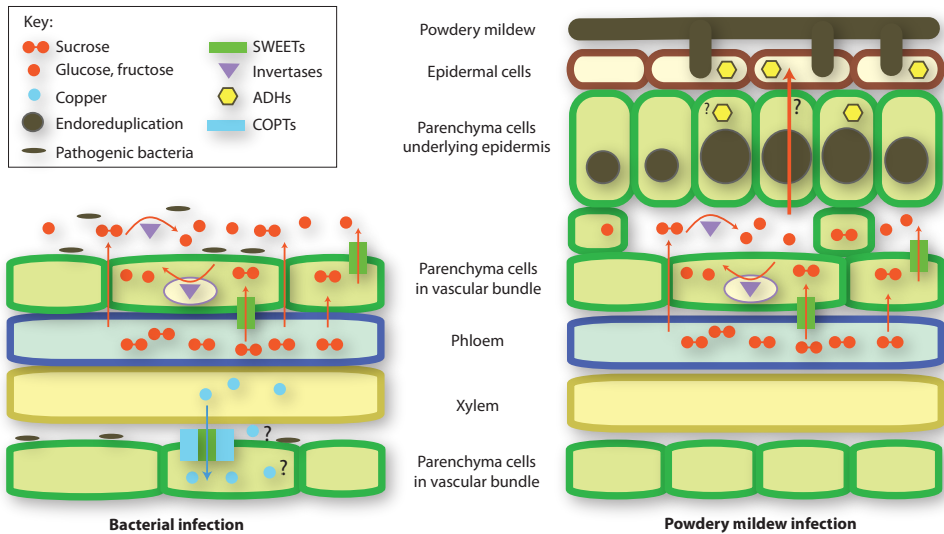


Figure 3. Model of plant susceptibility factors enabling bacterial (left panel) and fungal (right panel) pathogens to be fed by the plant, depicted in a schematic partial cross section of a leaf. On the schematic leaf cross section, genes encoding SWEET sugar transporters are transcriptionally induced after infection with fungal, oomycete and bacterial pathogens. In powdery and downy mildew-infected leaves, the induction of SWEET genes is associated with vascular tissues. SWEETs are suggested to unload sucrose from the phloem into the apoplast, besides symplastic unloading via plasmodesmata. Subsequently, cell-wall-bound or vacuolar invertases, activated during infection, hydrolyze sucrose into fructose and glucose. Invertase activity, typically linked to sink tissues, promotes phloem unloading and sugar delivery to pathogens. Nuclei of mesophyll cells underlying powdery mildew-infected epidermal cells undergo endoreduplication cycles that are suggested to enhance metabolic rates contributing to successful pathogen development. Host alcohol dehydrogenase activity induced during powdery mildew infection might help to reroute plant cell metabolism to produce compounds beneficial for the pathogen. Finally, the sugar transporter OsSWEET11 together with copper transporters OsCOPT1 and OsCOPT5 might also play a role in removing copper, which is toxic to the pathogenic bacteria *Xanthomonas oryzae* pv. *oryzae*, from rice xylem sap.

copper transporters OsCOPT1 and OsCOPT5 at the plasma membrane. Remarkably, all three genes, *OsSWEET11*, *OsCOPT1* and *OsCOPT5*, show increased transcript abundance during *Xoo* infection in rice, and are needed for copper uptake. Their constitutive expression led to increased copper content in rice leaf tissues, except in the xylem where the copper content was reduced. Infection with *Xoo* strain PXO99 also led to the accumulation of copper in leaves, to which bacteria show high sensitivity. *OsSWEET11*, together with the *OsCOPTs*, is suggested to limit toxic effects on the vascular pathogen *Xoo* by transporting copper out of the xylem during infection [69] (Figure 3).

The increased activity of the cell wall-bound invertases is often associated with pathogen infection and could enhance the sink strength to provide carbon to the pathogen. In grapevine leaves, the cell wall-bound invertase gene *Vvvcw-INV* is indeed transcriptionally induced during infection with downy and powdery mildews [66]. Accordingly, in transgenic tomato (*Solanum lycopersicum*) plants in which the major cell wall-bound invertase isoforms had been silenced, starch accumulation in leaves was reduced, suggesting that cell wall-bound invertases restrict sucrose export [70]. So, cell wall-bound invertases could facilitate efficient sugar allocation to

the infected tissues. In *Arabidopsis* roots, the cell wall-bound invertase gene *AtcwINV1* and the vacuolar invertase gene *Atβfruct4* show enhanced expression upon infection with the clubroot pathogen *Plasmodiophora brassicae*. Inhibition of the invertases at the infection sites of the *Arabidopsis* root via the root-specific expression of the invertase inhibitor genes *AtC/VIF1* and *AtC/VIF2* led to reduced gall formation by the pathogen [71], suggesting that both vacuolar and cell wall invertases could increase disease susceptibility by enhancing the sink strength (Figure 3). However, the role of extracellular invertases in disease susceptibility is likely to be more complex. For example, inhibition of cell wall-bound invertases in *Arabidopsis* by acarbose led to enhanced susceptibility to *Pseudomonas syringae* pv. *tomato* DC3000 [72], indicating that cell wall-bound invertases positively affect immunity. In addition, effectors of *Xanthomonas campestris* pv. *vesicatoria* were shown to suppress cell wall-bound invertase activity, thereby reducing sugar-mediated immunity [73]. Therefore, it is possible that pathogens adjust plant invertase activity so that host immune responses and efficient sugar transport are balanced.

Host plants are likely to provide additional forms of organic carbon to their microbial guests. In the nitrogen-fixing nodules on legume roots, carbon is transported to the infected cells not only in the form of sugars, but also in other organic forms, presumably tricarboxylates, from the surrounding uninfected cells [74, 75]. In barley, alcohol dehydrogenase (ADH) activity is induced during infection with *B. graminis* f. sp. *hordei*. Treatment with pyrazole, an inhibitor of ADH-catalyzed alcohol oxidation, reduced the disease symptoms and hyphal growth of the powdery mildew fungus and, accordingly, transient overexpression of the barley *HvADH1* increased the number of successfully established fungal infection sites [76]. Elevated ADH activity could lead to the production of alternative sources of organic carbon for pathogens. This was observed in grapevine, in which overexpression of *VvADH2* led to the accumulation of diverse secondary metabolites, such as shikimates, norisoprenoids, and terpenes [77]. Furthermore, ADH activity is induced under hypoxic conditions in maize [78] and *Arabidopsis* [79], and *ADH1* overexpression enables *Arabidopsis* plants to maintain root hair growth rates under oxygen-limiting conditions [80]. Increased ADH activity at powdery mildew infection sites could, therefore, also contribute to prolonged survival of infected host cells (Figure 3).

Maintenance of photosynthesis in non-infected tissues could help to supply pathogens with sufficient sugars. Healthy leaves of maize plants, infected with the smut fungus *U. maydis*, were found to have higher photosynthesis rates and senesce later than leaves of uninfected plants [81], suggesting a systemic effect of infection. It is unknown if mobile pathogen effectors, hormones or other compounds are directly or indirectly responsible for systemic effects in non-infected host tissues. Also, 'green islands', which are typical of many plant diseases and surround infection sites [82], show prolonged photosynthesis, such as in senescing maize leaves infected with the hemibiotroph *Colletotrichum graminicola* [83] enabling prolonged feeding of the pathogen (Figure 2).

Transporters of other metabolites have also been implicated in pathogen feeding. For instance, the poplar (*Populus trichocarpa*) *PtSultr3;5* gene encoding a sulfate transporter is highly expressed during rust fungus (*Melampsora larici-populina*) infections, although its role in feeding needs to be confirmed [84]. The sulfate transporter gene *SST1* from *Lotus japonicus* is essential for symbiotic nitrogen fixation [85]. Genome data suggest that the downy mildew pathogen of *Arabidopsis* lacks the gene encoding sulfite reductase, an enzyme acting downstream of sulfate reduction in the sulfur assimilation pathway [86]. Similarly, important enzymes involved in inorganic nitrogen metabolism in the nitrate reduction pathway are missing in two groups of obligate biotrophic pathogens: *Arabidopsis* downy mildew and white rust (*Albugo laibachii*) [87] and three powdery mildew species [86, 88]. This would imply that the plant provides these pathogens with other forms of sulfur and nitrogen, possibly in the form of host-derived amino acids. However, so far, there were no reports regarding the involvement of plant amino acid transporters in disease susceptibility, possibly because their reduced activity can have severe pleiotropic effects.

Endoreduplication (see Glossary) in plants cells is another striking alteration in response to pathogen infection. Biotrophs that feed on living host cells are suggested to abuse a regulatory mechanism of the host involved in controlling the ploidy level of cells. *Arabidopsis* cells infected with the powdery mildew fungus *Golovinomyces orontii* showed induced transcription of the *MYB3R4* gene that encodes a transcriptional regulator of endoreduplication. At five days post inoculation with *G. orontii*, mesophyll cells underlying infected epidermal cells showed an increase in ploidy level of up to 64C with a median value of 32C. Interestingly, *myb3r4* mutants do not show a significant increase in the ploidy level of mesophyll cells below infected epidermal cells and have reduced fungal growth [89]. Analysis of additional mutants showing reduced endoreduplication levels suggest that ploidy of mesophyll cells underlying the fungal feeding sites is an important susceptibility determinant of powdery mildew infection [90]. Similarly, nematodes can induce endoreduplication in feeding cells formed in host plant roots [91]. In *Arabidopsis*, overexpression of the cell cycle inhibitor Kip-related protein 4 (*KRP4*) inhibits this endoreduplication and consequently delays root knot nematode development [92]. The increased ploidy levels of host cells infected with powdery mildew or nematodes was shown to lead to higher relative transcript levels of metabolic genes. This phenomenon also occurs in the absence of infection in plant cells with higher ploidy level and high catabolic activity, such as the endosperm and trichomes. This suggests that endoreduplication activates host metabolism to supply the hosted biotrophs with nutrients [93] (Figure 3).

Reducing crop susceptibility

Under conditions of disease pressure, the fitness of susceptible crops is severely affected, resulting in yield reduction or complete crop losses. Breeding for genetic resistance is often the best measure for crop protection because chemical control can have negative environmental effects. However, dominant resistance, governed by single resistance (*R*) genes, is often rapidly overcome by new pathogen races. Resistance mechanisms can also be genetically more complex, based on multiple resistance loci, as recently observed for broad-spectrum downy mildew resistance in *Arabidopsis* C24 [94]. Alternative forms of resistance can be based on inactivating or interfering with host genes that contribute to disease susceptibility. This form of resistance is often recessive in nature. These alternative forms of resistance, also referred to as loss-of-susceptibility forms, have the potential to provide alternative and durable sources of disease resistance in crops [95].

Well-known example of recessive resistance in crop breeding is the use of mutations in the barley *Mildew Resistance Locus O* (*MLO*) gene. Plant homozygous for recessive *mlo* alleles confer broad-spectrum resistance to powdery mildew fungi in barley [96, 97], tomato [98], and *Arabidopsis* [99], and even to the bacterial pathogen *Xanthomonas campestris* in pepper (*Capsicum annuum*) [100]. However, *mlo*-based resistance is most likely caused by derepression of immune responses [101] making it different from the non-immunity related forms described below. In rice, several recessive resistance genes to *Xoo* are known, including rice *xa13*, a non-pathogen-responsive variant of a SWEET gene that is, however, also associated with abnormal pollen development and reduced seed set [67]. The application of SWEET-based loss-of-susceptibility in breeding without fitness penalties could be achieved by using tissue-specific silencing of SWEETs in transgenic rice [102]. A second example is the use of loss-of-susceptibility mutations in the translation initiation factor *eIF4E* and its homologs for resistance to viruses. In *Arabidopsis*, translation initiation factor *eIF(iso)4E*, a homolog of *eIF4E*, is essential for successful infection with the tobacco etch virus. Mutants in *eIF(iso)4E* are resistant to the potyvirus by preventing systemic spread of the virus and, unexpectedly, not by reduced viral translation and replication [103]. Mutations in the *eIF4E* group of genes are now widely used as a source of resistance to potyviruses in crops [104-106].

How can we identify additional host susceptibility genes? One approach is based on exploring natural and induced genetic variation. Mutations in the well-known host susceptibility factors encoding SWEETs and *eIF(iso)4E/G* were isolated in natural populations of rice and pepper (*C. annuum* and *C. chinense*) conferring recessive resistance to *Xoo* and potyviruses,

respectively [67, 68, 106]. Genome-wide association mapping in natural populations is expected to be an additional method of identifying new susceptibility genes. However, dominant race-specific resistance genes present within the host plant species can obstruct this analysis, as shown in *Arabidopsis*, where resistance to downy mildew was strongly associated with *R*-gene clusters, which are known to contain genes controlling immunity to *Hyaloperonospora arabidopsidis* [107]. Recently, naturally occurring and induced mutations in the locus *Rhg4* encoding serine hydroxymethyltransferase (SHMT) were shown to confer soybean resistance to the cyst nematode *Heterodera glycines*. The mutations interfere with the *Rhg4*/SHMT catalytic function in glycine and folate metabolism, suggesting that this host enzyme has a role in providing nutrients to the nematode [108]. Resistance to downy mildew was obtained in *Arabidopsis* mutants with altered amino acid metabolism. The *Arabidopsis dmr1*, *rsp1* and *rsp2* mutants with defective *HOMOSERINE KINASE*, *ASPARTATE KINASE 2* and *DIHYDRODIPICOLINATE SYNTHASE 2*, respectively, show perturbations in Asp-derived amino acid synthesis, such as overaccumulation of homoserine and threonine [109-111]. Potentially, high levels of these amino acids reduce the production of as yet unknown metabolites needed for downy mildew infection.

Host gene expression profiling in pathogen-infected plants is another way of discovering candidate disease susceptibility genes. Comparison of genes expressed in resistant and susceptible *Arabidopsis* accessions infected with *H. arabidopsidis* identified a malectin-like receptor-like kinase gene *IMPAIRED IN OOMYCETE SUSCEPTIBILITY 1*, the mutation of which led to enhanced resistance to downy mildew without signs of constitutive immune responses [112]. However, the role of the gene in disease susceptibility is unclear. Similarly, a set of *Arabidopsis* genes was identified that are specifically induced during infection with *H. arabidopsidis* in susceptible plants and that are known to be induced under abiotic stresses such as drought, salinity, and cold [113].

Host proteins that are targets of pathogen effectors could also be regarded as susceptibility proteins. Protein–protein interaction studies, for example, a recent interactome study of *Arabidopsis* [13], are revealing more and more effector targets and helpers [12]. However, many of the interacting proteins are strongly linked to immunity. Ongoing and future studies are likely to reveal more host proteins and genes that have a role in ‘attracting’, ‘accommodating’ and ‘feeding’ plant pathogens. The identification and functional analysis of these genes and proteins could uncover molecular processes that underlie many non-immunity related aspects of plant disease susceptibility and might provide the basis for novel strategies for disease resistance breeding.

Acknowledgements

The Leverhulme Trust (UK) is acknowledged for supporting D.L.

Outline

Downy mildew diseases are caused by oomycete pathogens belonging to the *Peronosporaceae* family [114] and are recognized as economically important on many crops, including lettuce [115], cucurbits [116], and maize [117]. Plants of the *Brassicaceae* family are also susceptible to downy mildews, e.g. *Arabidopsis thaliana* (*Arabidopsis* hereafter), which is infected by *Hyaloperonospora arabidopsidis* (*Hpa*), formerly known as *Peronospora parasitica* [114]. The *Arabidopsis-Hpa* pathosystem is a powerful model to study resistance and susceptibility to downy mildew and to biotrophic pathogens in general [118]. In *Arabidopsis* accessions, isolated from natural populations, a large number of resistance (*R*) genes have been identified that mediate immunity to specific *Hpa* isolates [107, 118]. In addition, non-*R* gene related forms of resistance to downy mildew were found in *Arabidopsis*, e.g. loss-of-susceptibility of the *downy mildew resistant 1* mutant that does not require the well-known salicylic acid, jasmonic acid and ethylene-dependent pathways regulating *Arabidopsis* immunity [110]. In my research I aimed to find novel genes mediating susceptibility or resistance of *Arabidopsis* to downy mildew. The results of a multidisciplinary approach, involving genetics and proteomics, are presented in this thesis.

Chapter 2 describes the genetic analysis of broad-spectrum resistance (BSR) of the natural *Arabidopsis* accession C24 to *Hpa*. By combining segregation analysis and quantitative trait loci mapping in introgression and recombinant inbred lines, we found that BSR in C24 is based on different combinations of isolate-specific loci.

The complex genetics of resistance of C24 to *Hpa* isolate Waco9 is further described in **Chapter 3**. A population of Waco9-susceptible lines was developed by multiple rounds of backcrossing of the susceptible Col-0 accession to C24. Whole-genome sequencing of 48 lines revealed two major introgressed susceptibility loci of Col-0. The corresponding C24 loci each provided only partial resistance, but interestingly, combined they conferred strong resistance to Waco9. Ongoing fine-mapping and complementation studies are aimed at identifying the causal polymorphisms and genes to understand how the interacting loci contribute to quantitative resistance to *Hpa*.

An alternative approach to find plant genes contributing to susceptibility of natural *Arabidopsis* accessions to *Hpa* is by association mapping and is described in **Chapter 4**. To reduce the effect of isolate-specific resistance loci, >250 natural accessions of *Arabidopsis* were inoculated with a mixture of four *Hpa* isolates. Genome-wide and locus-specific association mapping revealed three candidate loci affecting susceptibility of *Arabidopsis* to multiple downy mildew isolates: *CYTOKININ RESPONSE FACTOR 1* (*CRF1*), *STOMATAL CARPENTER 1* (*SCAP1*), and the *At5g53750/AtMLO11* locus. Functional studies revealed potential roles of the *CRF1* and *SCAP1* genes in susceptibility of *Arabidopsis* to *Hpa*.

To identify *Arabidopsis* proteins in downy mildew-infected cells that play a role in susceptibility, a proteomic approach was undertaken, that is presented in **Chapter 5**. A cell-specific N-glycotagging method was applied using the promoter of the *Arabidopsis* *DOWNY MILDEW RESISTANT 6* (*DMR6*) gene, which is expressed in *Hpa*-infected cells [119], fused to the coding sequence of *COMPLEX GLYCAN LESS 1* (*CGL1*). In transgenic lines of the *cgl1-1* mutant containing this construct, complex N-glycosylation was restored in downy mildew-infected cells. N-glycoproteins of these cells were isolated by immunoprecipitation, and peptides identified and quantified by label-free quantitative mass-spectrometry. This resulted in the identification of 18 candidate disease-related complex N-glycosylated proteins, several of which were found to have a potential role in susceptibility of *Arabidopsis* to *Hpa*.

In the final chapter, the obtained results are discussed in a broader perspective and a reflection is provided on how to identify host genes contributing to downy mildew susceptibility.

Chapter 2

Broad spectrum resistance of Arabidopsis C24 to downy mildew is mediated by different combinations of isolate-specific loci

Dmitry Lapin¹, Rhonda C. Meyer³, Hideki Takahashi⁴, Ulrike Bechtold⁵, Guido Van den Ackerveken^{1,2}

¹ Plant-Microbe Interactions, Department of Biology, Utrecht University, Padualaan 8, 3584 CH Utrecht, The Netherlands

² Centre for BioSystems Genomics, Wageningen, The Netherlands

³ Leibniz Institute of Plant Genetics and Crop Plant Research (IPK), Corrensstraße 3, 06466 Gatersleben, Germany

⁴ Graduate School of Agricultural Science, Tohoku University, 1-1 Tsutsumidori-Amamiyamachi Aoba-ku, 987-8555; Sendai, Miyagi, Japan

⁵ University of Essex, School of Biological Sciences, Wivenhoe Park, Colchester CO4 3SQ, UK

New Phytologist 2012 Dec;196(4):1171-81. doi: 10.1111/j.1469-8137.2012.04344.x.

Summary

Most natural *Arabidopsis thaliana* accessions are susceptible to one or more isolates of the downy mildew pathogen *Hyaloperonospora arabidopsidis* (*Hpa*). However, *Arabidopsis* C24 is resistant to all *Hpa* isolates tested so far. Here we describe the complex genetic basis of broad spectrum resistance in C24. The genetics of C24 resistance to three *Hpa* isolates was analyzed by segregation analysis and quantitative trait loci (QTL) mapping on recombinant inbred and introgression lines. Resistance of C24 to downy mildew was found to be a multigenic trait with complex inheritance. Many identified resistance loci were isolate-specific and located on different chromosomes. Among the C24 resistance QTL, we found dominant, co-dominant and recessive loci. Interestingly, none of the identified loci significantly contributed to resistance against all three tested *Hpa* isolates. Our study demonstrates that broad spectrum resistance of *Arabidopsis* C24 to *Hpa* is based on different combinations of multiple isolate-specific loci. The identified quantitative resistance loci are particularly promising as they provide an important basis for the cloning of susceptibility- and immunity-related genes.

Introduction

Life of plants is associated with diverse microorganisms, several of which can cause plant diseases. Plants resist infection attempts of most microorganisms, and disease can therefore be regarded as exception. This is due to the fact that plants are non-hosts for most microbes either due to basal immune responses or because the plant does not provide an appropriate environment to support pathogen growth and development. This non-host resistance or basic incompatibility is considered the major form of resistance effective against the vast majority of potentially pathogenic microbes [2]. Nevertheless, each plant species can be successfully infected by a limited number of adapted pathogens, and this phenomenon is known as basic compatibility. Within plant species there is variation in susceptibility to pathogens that in many cases is the result of gene-for-gene interaction in which dominant resistance genes (*R*-genes)

of the plant confer resistance to specific pathotypes expressing cognate avirulence genes. Hence, this is isolate-specific resistance. Several mechanisms supported with experimental data have been proposed to explain *R*-gene-mediated resistance, including direct recognition of pathogen proteins by plant receptors, but also indirect recognition as described in the guard and decoy model [120]. At the same time, certain genotypes within a single plant species may evolve resistance to multiple isolates of the same otherwise successful pathogen or even several unrelated adapted pathogenic species. This form of resistance is called broad-spectrum resistance (BSR) [121].

There is no general mechanism underlying BSR in plants, and cloned BSR loci represent different classes of genes. Genetically, mechanisms of BSR can be classified as monogenic or polygenic with complex inheritance and interactions between loci.

In cases of monogenic recessive BSR, plants might lack susceptibility factors which are important for successful pathogen development, thereby leading to a partial or complete incompatibility. For example, rice plants with a mutated promoter of the sugar transporter gene *Xa13* are completely or partially resistant to a wide range of races of bacterial blight disease [65, 122]. The translation initiation factor eIF4E is ultimately required for the infection of potyviruses in many plants, and mutations in the gene are responsible for loss of susceptibility [123]. The gene *Tsn1*, encoding a protein with a nucleotide-binding site and leucine-rich repeats (NBS-LRR), is responsible for the sensitivity of bread wheat to the tan spot and *Stagonospora nodorum* blotch toxin *ToxA*. *tsn1* mutants are non-sensitive to the toxin and therefore resistant to the fungal disease [124].

Also, mutants of negative regulators of immune responses may exhibit recessive non-isolate-specific resistance. For example, recessive mutations in Arabidopsis homologs of the barley gene *Mildew Resistance Locus O* (*MLO*) confer effective resistance against powdery mildew fungus due to hyperaccumulation of indolic secondary metabolites that have antimicrobial activity [101].

BSR can also exhibit dominant expression that is simply inherited. For instance, *Pi9* residing in a cluster of NBS-LRR genes is responsible for the resistance of rice to more than 20 *Magnaporthe grisea* isolates [125]. Another NBS-LRR gene from Arabidopsis *WRR4* confers resistance to several races of white rust on crucifers [126]. The Arabidopsis genes *RPW8.1* and *RPW8.2* encoded R-proteins with transmembrane and coil-coiled domains provide BSR against powdery mildew [127]. Additionally, the dominant *R*-gene *Mi* from tomato confers resistance against several pests such as root-knot nematodes, whiteflies and potato aphids [128-131].

Also, there are examples where the genetics of BSR is not governed by single loci. In many of those cases plants have multiple resistance loci with different race-specificities and therefore the plant gains broad-spectrum resistance. Interestingly, in this situation race-specific resistance loci are shown to have quantitative effects on immunity [132-134].

Thus, in general, BSR is a genetically complex trait that is more complicated to analyze than race-specific resistance. Among plants, *Arabidopsis thaliana* (further referred to as Arabidopsis) is one of the best studied model organisms, for which a wealth of mapping populations are available. These genetic resources, such as panels of natural populations and segregating populations derived from crosses between a pair or multiple inbred lines, greatly facilitate dissecting the genetic basis of complex traits in Arabidopsis. For instance, with recombinant and introgression inbred lines from a cross between Arabidopsis accessions Col-0 and C24, it was found that two major loci contribute to heterosis for multiple metabolic and biomass traits observed in progeny of the two accessions [135]. The available Arabidopsis resources can effectively aid the genetic analysis of BSR to pathogens.

The oomycete pathogen *Hyaloperonospora arabidopsidis* (*Hpa*), previously known as *Peronospora parasitica* and *H. parasitica*, causes downy mildew disease on Arabidopsis. It is a frequently used model system to study susceptibility of plants to biotrophic pathogens. Each Arabidopsis accession is typically susceptible to a number of *Hpa* isolates [107, 136],

and studied incompatible interactions are mostly controlled by *Resistance to Peronospora Parasitica (RPP)* genes, many of which are dominant and isolate-specific. More than 25 loci conferring resistance to diverse *Hpa* isolates have been reported previously [137, 138]. The accession C24 is resistant to all of 23 *Hpa* isolates tested [139] and is, therefore, of particular interest for studying BSR of Arabidopsis to downy mildew.

In the present work, we characterized the genetics of BSR to downy mildew in Arabidopsis C24 and identified multiple loci that contribute quantitatively to resistance. Not a single locus or unique combination of loci confers resistance to three tested downy mildew isolates. Our study highlights that resistance of C24 to *Hpa* appears to be largely isolate-specific, and that different combinations of quantitative and qualitative loci determine BSR.

Materials and Methods

Plant material and growth

Arabidopsis thaliana (referred to as Arabidopsis) recombinant inbred lines derived from the cross Col-0xC24 (RILs), C24 introgression lines in Col-0 background (ILs), genetic map, and the genotype information are described in [140, 141]. Tested lines are designated as in [142] and [135]. Col-0 plants expressing the RCY1 protein tagged with hemagglutinin HA are described in [143], and the *rcy1* mutants in C24 background are described in [144]. Plants were grown at 21°C under long day conditions (16h light/8h dark, light intensity 100 $\mu\text{mol}/\text{m}^2/\text{sec}$).

Hyaloperonospora arabidopsidis (Hpa) infection assays and quantification of the pathogen growth

Hpa isolates Waco9, Emco5, Noco2 and Maks9 were maintained as described previously [109]. All infection assays were performed on eleven-day-old seedlings with a standard inoculum density of 50 conidiospores/ μl . For QTL mapping with the RILs, relative *Hpa* biomass was quantified based on the content of *Hpa* DNA relative to Arabidopsis DNA in the infected plants at 5 days post inoculation (dpi). The quantification was performed using TaqMan® quantitative PCR (qPCR). Sequences of primers for the amplification of *Hpa ACT*, Arabidopsis *ACT2*, the corresponding TaqMan® probes and a protocol for the assay are presented in Supporting Information Table S1 and Notes S1. For the qPCR, MgCl_2 was added to a final concentration of 9.5 mM to TaqMan® Universal PCR Master Mix without AmpErase® UNG (Applied Biosystems). The efficiency of the primers and probe sets was estimated with the dilution series of the total genomic DNA from the non-infected Col-0 plants and spores of *Hpa* Waco9. DNA was isolated from the infected seedlings with the CTAB method [145]. Five microliters of the isolated DNA (1-5 ng/ μl) were added to TaqMan® qPCR (final volume 25 μl). The relative *Hpa* biomass was expressed as C_t value obtained for *Hpa* DNA minus C_t value obtained for Arabidopsis DNA.

The level of resistance of ILs to downy mildew was evaluated with spore counting at 6-8 dpi depending on the isolate. Spore counting was performed on five randomly chosen seedlings per replicate per genotype. Each experiment was repeated at least two times with three replicates in every experiment. The segregation analysis of resistance in populations F2 C24xCol-0 *flc3* and BC1 F1xC24 was performed at 9 dpi to allow full pathogen sporulation. Furthermore, to study the early stages of *Hpa* infection, we performed trypan blue staining [146] and microscopic analysis of infected seedlings at 2 dpi.

Quantitative trait loci (QTL) mapping

QTL mapping was performed on a subset of 75 RILs Col-0xC24 (Supporting Information Notes S2). For the mapping ΔC_t values from the TaqMan® qPCR assays (Supporting Information Table S1, Notes S1) were used as phenotype scores without transformation. The composite interval and multiple QTL mapping procedures implemented in R/qtl were applied to locate resistance loci [147]. Epistatic interactions were examined with both QTLNetwork [148] and

R/qrtl. For the QTL mapping with ILs in the Col-0 background, we used the results of spore counting. The statistical analysis was performed with ANOVA followed by the least significant difference (LSD) test ($p < 0.05$, $n = 3$). The experiment was performed two times; IL QTL were considered significant only if they were significant in each of the independent experiments. The identified QTL were named according to their order on the chromosomes; for example, *qrtl1.2* refers to the second identified QTL on chromosome 1.

Analysis of inheritance mode of the resistance QTL

To determine whether C24 alleles of identified resistance QTL are dominant, co-dominant or recessive, we crossed Col-0 ILs containing resistance QTL from C24 with the Col-0 parent. Hybrids were checked with PCR primers specific for a given QTL (Supporting Information Table S1). Then, spore counting expressed in spores/seedling was performed for the ILs, Col-0 and F1 hybrids. Groups of genotypes with similar spore counts were determined on the basis of Tukey-HSD test ($\alpha = 0.05$, three replicates with five seedlings per replicate). If F1 hybrids were assigned to the same group as Col-0, the corresponding QTL was considered recessive; if the F1 hybrid did not appear in the same groups as the IL and Col-0, the QTL was considered co-dominant; and if F1 hybrids were in the same group as the ILs, the QTL was denoted as dominant. Each experiment was performed two times with three replicates in every experiment.

Expression analysis of *Pathogenesis Related 1 (PR-1)*

In order to measure *PR-1* transcript levels in healthy uninfected leaves, eleven-day-old seedlings were sprayed with demineralized water and put under conditions used for the *Hpa* infection. At three days after the treatment, samples were collected and used for total RNA isolation using RNeasy Plant mini-kit (Qiagen) followed by DNaseI treatment (Fermentas) and cDNA synthesis with oligo(dT)₁₄, RevertAid™ H Minus reverse transcriptase (Fermentas) and RiboLock™ RNase Inhibitor (Fermentas) according to manufactures' instructions. For the normalization of *PR-1* expression data, the reference gene At5g19840 was selected with the RefGenes tool of Genevestigator [149]. Sequences of primers for the quantitative real-time PCR (qRT-PCR) and their efficiency coefficients are presented in Supporting Information Table S1. qRT-PCR was performed with the Power CYBER Green master mix (Applied Biosystems) according to the manufacturer's recommendations. The experiment was performed two times with three replicates per genotype in each experiment. Significance of differences in the *PR-1* expression was assessed with ANOVA ($p < 0.05$).

Results

Arabidopsis C24 shows a hypersensitive response (HR) upon downy mildew infection

Resistant Arabidopsis plants are known to give different immune responses against downy mildew, e.g. HR or trailing necrosis, depending on the strength and timing of the cell death response [118]. We microscopically examined the immune reaction of Arabidopsis C24 to three isolates of *Hpa* Waco9, Noco2 and Emco5 that are all virulent on Arabidopsis Col-0. C24 appeared to develop an HR upon infection with each of the tested isolates, visible as cell death in trypan blue-stained leaves (Fig. 1). The susceptible accession Col-0, on the other hand, showed successful hyphal colonization and haustorium formation and only occasionally plant cell death. The cell death response of C24 to *Hpa* isolates Noco2 and Emco5 was comparable to that of the accession Ws-0 to Noco2 that is determined by the dominant *RPP1* locus [150], and to that of the Arabidopsis accession Ler to Emco5 that is mediated by *RPP8* [151]. In contrast, the *RPP5*-mediated response in the Ler-Noco2 interaction [152] was less severe compared to the reaction of C24 to *Hpa* Noco2. Interestingly, cell death triggered by *Hpa* Waco9 in C24 was less pronounced than in the interactions of C24 with Noco2 and Emco5. The microscopically observed HR caused by the downy mildew isolates Noco2 and Emco5 in Arabidopsis C24 resembles HR in known gene-for-gene interactions, suggesting that C24

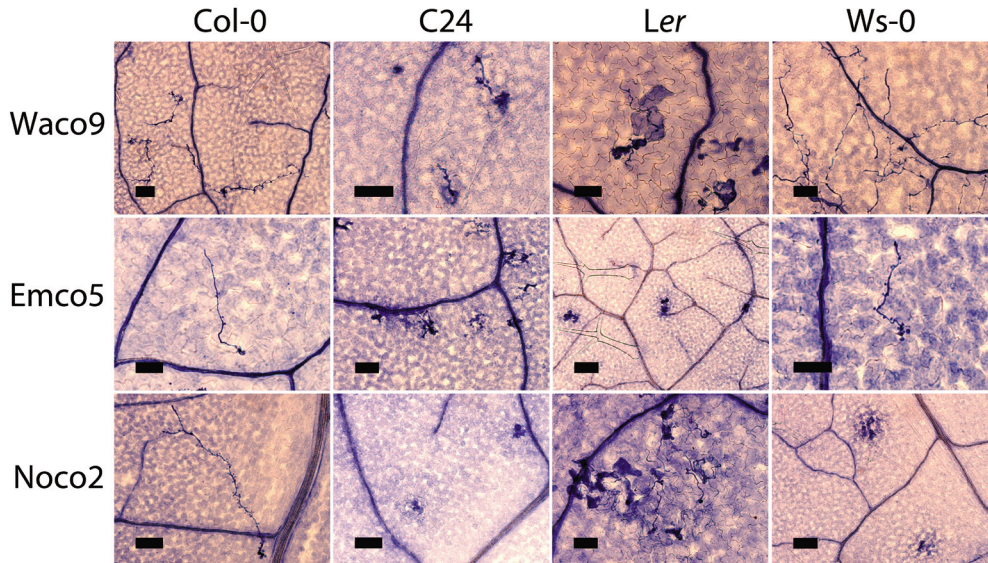


Figure 1. Microscopic analysis of *Hpa* infection on Arabidopsis. Seedlings of accessions Col-0, C24, Ler and Ws-0 were infected with three *Hpa* isolates compatible with Col-0: Waco9, Emco5 and Noco2. The pathogen growth in each interaction at 2 dpi was examined microscopically with trypan blue staining, which allows to discriminate dead cells and oomycete hyphae in the infected leaves (bar=100 μ m). The downy mildew isolates form intercellular hyphae and haustoria in susceptible Col-0 seedlings, and cell death is only occasionally observed. In Arabidopsis C24, HR occurs upon infection with all three tested *Hpa* isolates. Highly localized early cell death is observed when C24 is infected with the downy mildew Noco2 and Emco5. This type of response is similar to immune reactions in the interactions of Ws-0 - Noco2, Ler - Emco5 and Ler - Noco2 triggered by the isolate-specific R-genes *RPP1*, *RPP8* and *RPP5* respectively.

resistance to these isolates may be based on dominant R-genes. The weaker response of C24 to Waco9 might be based on other mechanisms, although it is also associated with cell death.

Resistance of Arabidopsis C24 to *Hpa* is genetically complex

The genetic basis of downy mildew resistance of C24 was analyzed in segregating progenies of crosses with the susceptible accession Col-0. F1 hybrids from the cross C24xCol-0 and the reciprocal cross Col-0xC24 showed an intermediate level of susceptibility to the isolate Waco9, but full resistance to isolates Emco5 and Noco2 (Fig. 2). Since there was no significant difference between F1 plants from the reciprocal crosses, we concluded that resistance of C24 is not differentially affected by cytoplasmic genetic factors but rather depends on nuclear genetic loci, which can be inherited dominantly (to Emco5 and Noco2) or codominantly (to Waco9). Next, the segregation of resistance was analyzed in F2 populations of C24xCol-0 *flc3* and back-cross one progeny (BC1: F1xC24). The Col-0 *flc3* mutant was used to reduce extreme segregation in flowering time that occurs in crosses between C24 and Col-0 [153], and was not different in resistance to *Hpa* compared to the wild type Col-0 (not shown). The segregation ratios of susceptible and resistant seedlings were determined following infection with the three *Hpa* isolates (Table 1). Strikingly, segregation ratios were different for each of the tested isolates (χ^2 -test $p < 0.005$ in all pairwise comparisons for F2 results) implying that C24 resistance is at least partially isolate-specific. If resistance is controlled by a single

dominant locus from C24, it is expected that the ratio of resistant to susceptible plants in F2 populations is 3:1. However, after infection with Emco5 and Waco9 the observed ratio significantly differed from 3:1 ($p < 0.001$ for both isolates) implying that the resistance is not monogenic dominant. At the same time, for Emco5 we did not find susceptible plants in the BC1 population, indicating the presence of at least one completely dominant locus among several resistance loci. The segregation of resistance to Noco2 might be explained by a single completely-dominant *R*-gene although with low confidence ($p = 0.11$) suggesting that several additional small effect loci may condition resistance. Thus, C24 resistance to Waco9 and Emco5 is governed by more than one locus suggesting that in general C24 resistance to downy mildew is multigenic and genetically complex.

Table 1. Segregation analysis of resistance to the downy mildew in F2 and back-cross progeny of Arabidopsis Col-0 *flc3* and C24

<i>Hpa</i> isolate	Population	Sus-ceptible	Resis-tant	Segregation S:R		
				3:1	1:3	1:1
Waco9	F2 C24xCol-0 <i>flc3</i> , N=1142	916	226	$\chi^2=16.5$ $P < 0.0001$	$\chi^2=1856.5$ $P < 0.0001$	-
	BC1 (F1xC24), N=326	72	254	-	-	$\chi^2=165.8$ $P < 0.0001$
Emco5	F2 C24xCol-0 <i>flc3</i> , N=322	52	270	$\chi^2=594.8$ $P < 0.0001$	$\chi^2=13.4$ $P < 0.001$	-
	BC1 (F1xC24), N=99	0	99	-	-	$\chi^2=99.0$ $P < 0.0001$
Noco2	F2 C24xCol-0 <i>flc3</i> , N=317	67	250	$\chi^2=490.5$ $P < 0.0001$	$\chi^2=2.5$ $P = 0.11$	-
	BC1 (F1xC24), N=99	0	99	-	-	$\chi^2=99.0$ $P < 0.0001$

QTL mapping of resistance to *Hpa* Waco9

Unraveling complex traits can be effectively performed by quantitative trait loci (QTL) mapping. As we are particularly interested in the genetics of complex resistance of C24 to downy mildew, we conducted QTL mapping of resistance to the isolate Waco9. For this, we made use of recombinant inbred lines (RILs) derived from a cross between the susceptible parent Col-0 and the resistant parent C24 [141]. The level of susceptibility of 75 RILs to Waco9 was quantified based on the relative *Hpa* DNA content in infected Arabidopsis seedlings with TaqMan® qPCR. The advantage of this method is that it provides a ratio of plant and pathogen DNA from a single reaction thereby reducing technical variation. As a measure of pathogen infection the cycle threshold values for the *ACTIN* genes of *Hpa* and Arabidopsis were subtracted giving a ΔC_t value that was used as input for QTL mapping (Supporting Information Notes S1, Fig. S1). Four loci influencing resistance of C24 to *Hpa* Waco9 were mapped on chromosomes 1, 3 and 5 (Table 2, see Supporting Information Notes S2 for details). These loci had mostly additive effects with a weak interaction between *qt1.2* and *qt3.1* located on chromosomes 1 and 3, respectively (Fig. S3). The C24 alleles of *qt1.1*, *qt3.1* and *qt5.1* contribute positively to resistance with *qt5.1* having the strongest effect. In contrast, the C24 allele of *qt1.2* increased susceptibility of Arabidopsis to Waco9. Together, the four identified

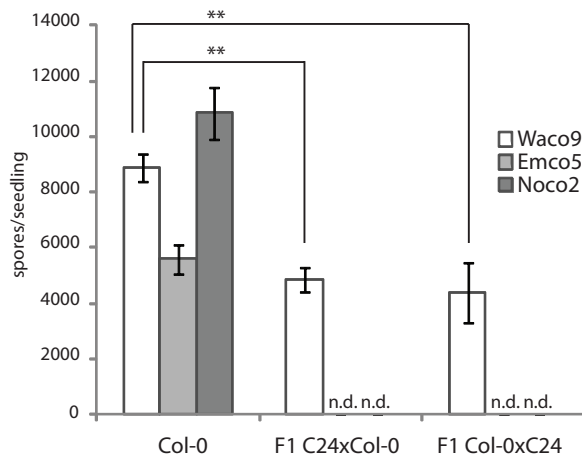


Figure 2. Sporulation of *Hpa* isolates on Col-0 and its F1 hybrids with C24. Susceptible Col-0 and resistant C24 parent and their reciprocal hybrids were inoculated with different downy mildew isolates. The F1 hybrids showed full resistance to the downy mildew Emco5 and Noco2 indicating dominant resistance loci (labeled “n.d.” as spore count was not determined). However, the F1 hybrids were intermediately susceptible to *Hpa* Waco9 (comparison to Col-0: t-test $p < 0.01$ for both reciprocal hybrids, $n = 3$) suggesting that C24 resistance to the isolate is codominant and quantitative. Error bars on the figure represent \pm SD. Each experiment was performed at least two times with three replicates; each replicate included 5 seedlings.

loci explain around 50% of the phenotypic variation in the level of resistance within the subset of RILs. These data confirm that C24 resistance to Waco9 is genetically complex, supporting the results of the segregation analysis in the F2 and BC1 populations.

Table 2. QTL mapping of C24 resistance to isolate Waco9 in the population of Col-0xC24 RILs

QTL*	Location of max LOD, cM	Max LOD	% variance explained	marginal effect/SE**	interval from mapping with RILs, cM
<i>qtl1.1</i>	chr1 9.0	2.4	7.9	3.4	0-17
<i>qtl1.2</i>	chr1 20.4	3.9	13.2	-4.4	17-27
<i>qtl3.1</i>	chr3 38.2	1.9	6.1	2.9	0-50
<i>qtl5.1</i>	chr5 60.1	9.9	41.1	7.8	55-63

*- name of QTL includes number of chromosome and order of the QTL on chromosome (when several QTL present)

** - positive sign indicates that the C24 allele increases resistance

Next, we used 70 lines with introgressions from C24 covering the entire Arabidopsis genome in the Col-0 genetic background (Col-0 ILs) [140] to validate the resistance QTL identified in the RIL population and to find possible additional genetic factors (Table 3, see Supporting Information Notes S3 and Table S4 for details). Resistance of ILs was evaluated by scoring the level of sporulation. None of the Col-0 ILs was as resistant to Waco9 as Arabidopsis accession C24. Three RIL-QTL could be confirmed in the ILs, reinforcing these loci as being

significant. Col-0 IL N 2/13/4, which contains the major QTL *qtl5.1* on chromosome 5, was most resistant to the isolate Waco9, both in cotyledons and first true leaves. ILs with *qtl1.2* were more susceptible to *Hpa* than their parental line Col-0 ($p < 0.05$), while the ILs containing *qtl3.1* were more resistant ($p < 0.05$). Unexpectedly, we could not confirm the effect of *qtl1.1*, as Col-0 ILs with *qtl1.1* from C24 did not show altered resistance phenotypes compared to the parent Col-0. However, an additional line N 29/11/1 was found to be more resistant than the parental accession Col-0 ($p < 0.05$). Line N 29/11/1 contains two introgressions: one introgression corresponds to *qtl1.1* and the second further down on chromosome 1 to the interval 62-83 cM, which we now refer to as *qtl1.3*. Previously, this line was noted to have a severely altered metabolic profile compared to Col-0 and C24 parents [135]. Other tested Col-0 ILs with the C24 allele of *qtl1.3* did not show any resistance to Waco9 in comparison with Col-0, suggesting that resistance of line N 29/11/1 is not determined by effects of the individual QTL *qtl1.1* and *qtl1.3*. Interestingly, with the ILs we identified *qtl4.1* on chromosome 4 (37-56 cM, $p < 0.02$) which appeared to be as effective as *qtl3.1* on chromosome 3, since resistance levels of ILs with *qtl3.1* and *qtl4.1* did not differ significantly ($p > 0.7$). However, in QTL mapping on the RILs *qtl4.1* was not detected as significant. Thus, ILs allowed us to identify more resistance QTL than RILs. We concluded that Arabidopsis C24 contains 4 major loci *qtl1.2*, *qtl3.1*, *qtl4.1* and *qtl5.1* on chromosomes 1, 3, 4 and 5 respectively that contribute to resistance to the downy mildew isolate Waco9.

Table 3. QTL mapping of C24 resistance to the isolate Waco9 in a population of Col-0 ILs

Col-0 IL*	Spore count, 10 ³ spores/ seedling	QTL	Interval from mapping with ILs, cM	Interval from mapping with ILs, bp (TAIR8)
Col-0	4.0	-	-	-
N 29/11/1	0.7 ($p < 0.001$)	<i>qtl1.1</i> **+ <i>qtl1.3</i>	(0-5)+(62-83)	(chr1:0..1189392) + (chr1:18580358..24843636)
N 87/12/10	5.9 ($p < 0.01$)	<i>qtl1.2</i>	20-27	chr1:5855350.. 8168405
N 52/2	1.7 ($p < 0.02$)	<i>qtl3.1</i>	21-33	chr3:6535963..8980078
N 68/5	1.7 ($p < 0.02$)	<i>qtl4.1</i>	38-56	chr4:6810745..10992260
N 2/13/4	0.3 ($p < 0.001$)	<i>qtl5.1</i>	41-63	chr5:11108011..18282539

*- only one line is shown for each QTL; for more details see SI File2

**- effect of *qtl1.1* was significant only in the line N 29/11/1 which contained an additional introgression on chromosome 1, which we named *qtl1.3*

Individual QTL are not responsible for BSR of C24 to *Hpa*

Differences in genetics of C24 resistance to three isolates of *Hpa*, observed in the analysis of F1, F2 and BC1 populations, already indicated that Arabidopsis C24 has isolate-specific immune responses. To analyze this further, Col-0 ILs were screened with *Hpa* isolates Noco2 and Emco5 (Table 4, Supporting Information Table S4). Resistance of the ILs to Emco5 revealed three QTL on chromosomes 3 (*qtl3.1* and *qtl3.2*) and 5 (*qtl5.1*). Only two QTL for

resistance to Noco2 were uncovered on chromosomes 1 (*qt1.4*) and 3 (*qt3.2*). In contrast to infection with Waco9, we did not find alleles of C24 which increase susceptibility to the isolates Emco5 and Noco2, indicating that the small effect *qt1.2* is isolate-specific. In total, we identified six loci that affect resistance to downy mildew. Among all identified loci, we could not find a single locus in C24 that provides resistance to all three tested isolates; *qt3.2* gave full resistance only to the isolates Emco5 and Noco2, but not to Waco9, and *qt5.1* provided resistance to Waco9 and Emco5, but it was not effective against Noco2. Thus, there is no a single locus in C24 that is responsible for BSR to *Hpa*.

Table 4. Downy mildew resistance QTL in Arabidopsis C24

QTL	location, Mbp (TAIR8)	Waco9	Emco5	Noco2	Effect on <i>PR-1</i> expression	Col-0 IL**
<i>qt1.1</i>	chr1, 0-1.2*	R*	C	C	C	N 29/11/1
<i>qt1.2</i>	chr1, 5.9-8.2	S	C	C	C	N 38/6/12/12
<i>qt1.4</i>	chr1, 9.3-13.8	C	C	R	C	N 2/11/6
<i>qt3.1</i>	chr3, 6.5-9.0	R	R	C	C	N 63/14
<i>qt3.2</i>	chr3, 15.7-16.5	C	R	R	C	N 21/3/14
<i>qt4.1</i>	chr4, 6.8-11.0	R	C	C	C	N 68/5
<i>qt5.1</i>	chr5, 11.1-18.2	R	R	C	C	N 2/13/4
	Number of loci	5	3	2	0	-

S – QTL from C24 increases susceptibility (LSD $p < 0.05$); R – QTL from C24 increases resistance (LSD $p < 0.05$); C – line with the QTL is not significantly different from Col-0 in resistance to *Hpa* or expression of *PR-1* (LSD $p > 0.05$)

*- effect of *qt1.1* was significant only in the line N 29/11/1 with an additional introgression *qt1.3*

**- only one IL shown if several ILs contained QTL

C24 resistance to *Hpa* involves recessive, co-dominant and dominant loci

Despite the fact that C24 resistance is overall a dominant or codominant trait based on the analysis of F1 hybrids, some of the individual QTL can be inherited differently. We generated F1 hybrids between Col-0 and Col-0 ILs with partial or complete resistance to different *Hpa* isolates to determine inheritance of individual resistance loci. The level of susceptibility of these hybrids was quantified and compared to Col-0 and parental IL levels (Table 5, Fig. 3). C24 alleles of resistance QTL for Emco5 and Noco2 were either dominant (*qt3.2*) or codominant (*qt1.4* and *qt3.1*). Intriguingly, the dominant *qt3.2* locus conferred full resistance to *Hpa* isolates Emco5 and Noco2 and could contain an *R*-gene that recognizes effector proteins from these downy mildew isolates. In the case of Waco9, only the susceptibility *qt1.2* was found to be dominant as F1 hybrids N 87/12/12xCol-0 were more susceptible than Col-0 but not different from IL N 87/12/12: one could also state that *qt1.2* in Col-0 is a recessive resistance locus. Interestingly, *qt5.1*, conferring resistance to both Emco5 and Waco9, inherited differently depending on the isolate. It provided dominant and complete immunity against Emco5, but was codominant and contributed to resistance quantitatively in case of the isolate Waco9. Two Waco9-specific resistance QTL *qt3.1* and *qt4.1* were recessive. In summary, although the overall resistance of C24 to *Hpa* is either dominant or codominant,

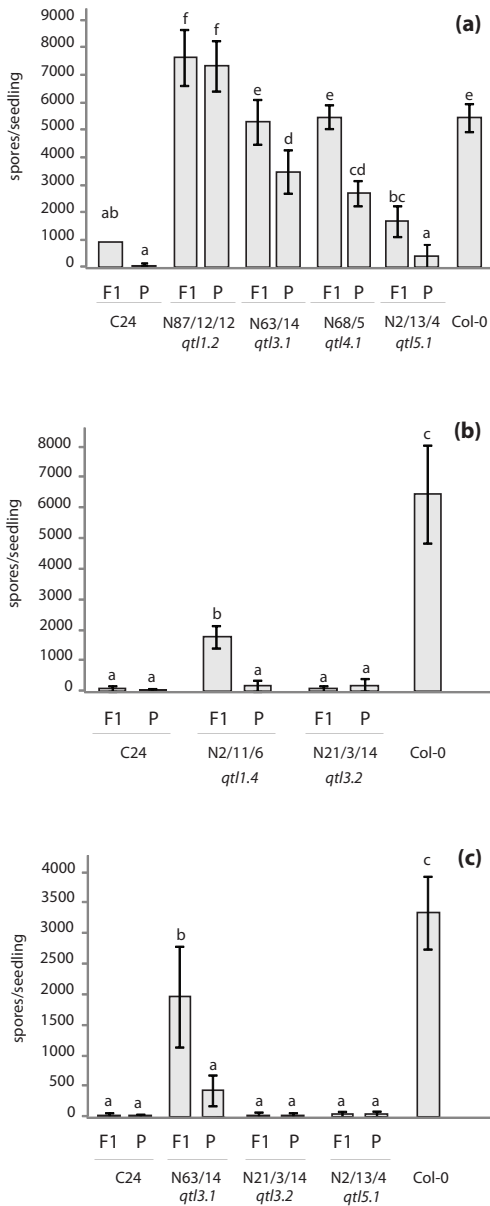


Figure 3. Sporulation of *Hpa* isolates Waco9 (a), Noco2 (b) and Emco5 (c) on F1 hybrids between Col-0 and ILs. To determine how individual resistance QTLs are inherited, F1 hybrids from crosses between Col-0 and ILs harboring a resistance QTL were tested with different *Hpa* isolates. Spore counting for downy mildew Waco9 (a) revealed that the major *qtl5.1* (line N 2/13/4) is codominant as the corresponding F1 hybrid showed an intermediate level of susceptibility compared to the parental IL (Tukey-HSD test $p=0.06$) and Col-0 ($p<0.001$). Other Waco9 resistance QTLs, *qtl3.1* and *qtl4.1*, are inherited recessively since the F1 hybrids with ILs N 63/14 and N 68/5 were as susceptible as Col-0, but less resistant than the ILs ($p<0.01$ for both lines). C24 allele of *qtl1.2* was dominant, because F1 N 87/12/12xCol-0 differed from Col-0 ($p<0.001$) but not from IL containing the QTL. In contrast to Waco9 situation, Noco2 (b) and Emco5 (c) resistance QTLs were either dominant or codominant but not recessive. F1 hybrids between Col-0 and IL N 21/3/14 conferring major Emco5 and Noco2 *qtl3.2* were fully resistant in contrary with susceptible parent Col-0. Similarly, *qtl5.1* gave full resistance against Emco5 in F1 N 2/13/4xCol-0. At the same time, Emco5 *qtl3.1* (IL N 63/14) and Noco2-specific *qtl1.4* (IL N 2/11/6) were clearly co-dominant since the corresponding F1 hybrids were significantly different in spore count from Col-0 ($p<0.001$ for both crosses) and ILs ($p<0.01$ for both crosses). Error bars on the figure represent \pm SD. Statistical analysis of the spore count was performed with ANOVA and Tukey-HSD test ($\alpha=0.05$; $n=3$; two independent experiments with three replicates each).

the effects of individual resistance loci can be different: dominant (*qtl3.2*, *qtl5.1*), codominant (*qtl1.4*, *qtl3.1*, *qtl5.1*) or even recessive (*qtl3.1*, *qtl4.1*).

Resistance conferred by *qtl5.1* is not caused by *RCY1*

The major QTL on chromosome 5 *qtl5.1* was found to be responsible for resistance to the *Hpa* isolates Waco9, Emco5 (Table 4) and Maks9 (data not shown). This QTL in C24 contains the *RCY1* locus, which was previously reported as a dominant *R*-gene underlying resistance of

C24 to *Cucumber mosaic virus* yellow strain [CMV(Y)] [154]. Besides this, the *RCY1* gene is allelic to *RPP8* (At5g43470) that confers resistance to *Hpa* Emco5 in *Arabidopsis* accession Ler [151]. Therefore we checked whether *RCY1* underlies the major QTL on chromosome 5. An *Arabidopsis* Col-0 transgenic line expressing *RCY1* and resistant to CMV(Y) (line #12) [143] was as susceptible to the tested downy mildew isolates Waco9, Emco5 and Noco2 as the Col-0 control (Fig. 4a). The expression of *RCY1* in transgenic plants was confirmed by western blot analysis (Supporting Information Fig. S4). In addition, we compared resistance of F1 hybrids between Col-0, C24 and several *rcy1* mutants in the C24 background [144]. If *RCY1* confers resistance to *Hpa*, F1s C24xCol-0 should be more resistant than F1 hybrids between Col-0 and *rcy1* mutants. However, it appeared that the F1 hybrids are equally susceptible to the isolate Waco9 (Fig. 4b). These results demonstrate that *RCY1* is not responsible for downy mildew resistance of C24.

Elevated expression of *PR-1* in C24 is not linked to downy mildew resistance

Previously, it was reported that C24 accumulates increased levels of salicylic acid [142, 155], the defense hormone required to establish immune responses against biotrophic pathogens [156]. In addition, C24 was shown to have high levels of the SA-responsive marker gene *Pathogenesis Related 1* (*PR-1*, At2g14610) [155]. To determine if the elevated expression of *PR-1* is linked to downy mildew resistance of C24, we checked if any of the Col-0 ILs with introgressed resistance QTL showed elevated levels of *PR-1* expression in healthy uninfected seedlings. Intriguingly, the expression of *PR-1* in the ILs was not significantly different from Col-0 (Table 4, Supporting Information Fig. S5, $p > 0.25$), whereas C24 had higher *PR-1*

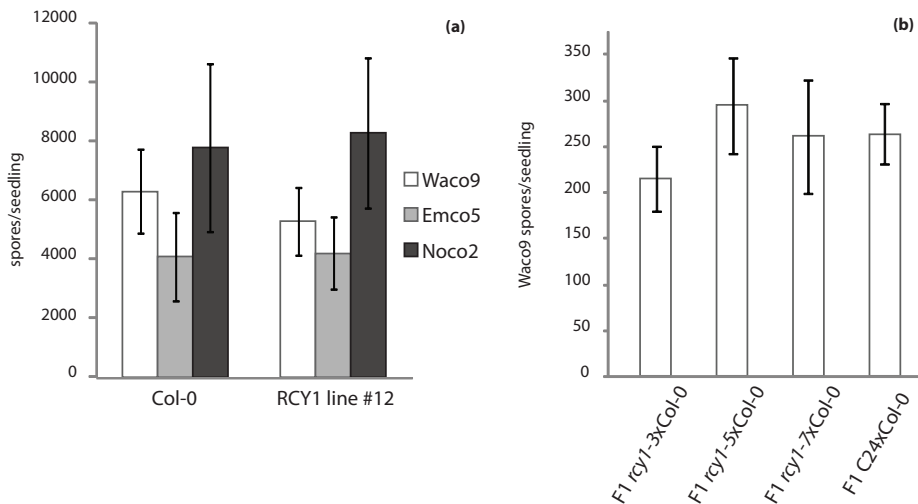


Figure 4. Sporulation of *Hpa* isolates on *Col-0* plants expressing *RCY1* gene (a), and F1 hybrids of *rcy1* mutants and *Col-0* (b). *qt15.1* is a major Waco9 and Emco5 resistance QTL, harboring *RCY1* locus which confers resistance of C24 to cucumber mosaic virus Y and is homologues to *Hpa* resistance gene *RPP8*. (a) Transgenic *Arabidopsis* *Col-0* plants expressing C24 *RCY1* gene were inoculated with three downy mildew isolates. The transgenic plants appeared to be as susceptible as wild type *Col-0* (t-test $p > 0.2$ for all *Hpa* isolates). (b) Three independent EMS mutants of *RCY1* in C24 background *rcy1-3*, *rcy1-5*, and *rcy1-7*, impaired in the virus resistance, were crossed with *Col-0*. The hybrids F1 did not differ in resistance from F1 C24xCol-0 (ANOVA $p = 0.30$), that provides evidence that *RCY1* does not underlie C24 resistance *qt15.1*. Error bars on the figure represent ± one standard deviation. Statistical analysis was performed with ANOVA ($p < 0.05$, $n = 3$) for two independent experiments with three replicates each and five seedlings per replicate.

expression levels compared to all tested lines-test $p < 0.001$). Thus, even though individual identified QTL significantly contribute to downy mildew resistance, they do not affect *PR-1* expression in Col-0 ILs. Increased expression of *PR-1* in Arabidopsis C24 is therefore not directly linked to resistance against *Hpa*.

Table 5. Inheritance of the C24 resistance QTL

QTL	location, Mbp (TAIR8)	Waco9	Emco5	Noco2	Col-0 IL
<i>qtl1.2</i>	chr1, 5.9-8.2	dominant	n.a.	n.a.	N 87/12/12
<i>qtl1.4</i>	chr1, 9.3-13.8	n.a.	n.a.	codominant	N 2/11/6
<i>qtl3.1</i>	chr3, 6.5-9.0	recessive	codominant	n.a.	N 63/14
<i>qtl3.2</i>	chr3, 15.7-16.5	n.a.	dominant	dominant	N 21/3/14
<i>qtl4.1</i>	chr4, 6.8-11.0	recessive	n.a.	n.a.	N 68/5
<i>qtl5.1</i>	chr5, 11.1-18.2	codominant	dominant	n.a.	N 2/13/4

n.a. – not applicable

Discussion

Arabidopsis C24 is resistant to all tested isolates of the downy mildew *Hpa* [139]. This accession was reported to have elevated levels of SA, hydrogen peroxide and expression of defense-related genes [142, 155]. However, downy mildew resistance is not directly caused by the elevation in SA levels and SA-induced gene expression, since (i) *PR-1* expression, which is a marker of SA-dependent defense pathways, is not linked to *Hpa* resistance QTL, (ii) downy mildew resistance QTL, except for *qtl1.3* detected only in one IL N 29/11/1, did not overlap with QTL responsible for the accumulation of signal molecules SA and glycerol-3-phosphate in C24 [142], which are important for the establishment of systemic acquired resistance [157], (iii) there are no *Hpa* broad-resistance QTL in C24 which one would expect in the case of unspecific activation of immune responses, and (iv) F2 plants C24xCol-0 *flc3* resistant to downy mildew did not show any growth abnormalities, which in some cases are characteristic to plants with constitutive activation of defense, for instance in the case of hybrid necrosis [158]. Thus, there is no evidence that BSR of Arabidopsis C24 is caused by constitutively high defense responses. Furthermore, it is known that Arabidopsis accessions may have different transcriptional responsiveness to exogenous application of SA [159], but yet the responsiveness *per se* does not determine resistance against downy mildew. For instance, the accession Mt-0 was shown to be hyper-SA-responsive, however it does not confer BSR to downy mildew [107]. Similarly, the accession Bur-0 has higher SA-induced *PR-1* expression compared to Col-0 [160], but it is still susceptible to multiple *Hpa* isolates [107, 136].

Our study is the first example of genetically characterized multigenic BSR in Arabidopsis, which led to the identification of seven resistance QTL against the downy mildew *Hpa* in a single Arabidopsis accession C24. Most of the loci identified in our study appeared to confer resistance against *Hpa* in a quantitative manner, and only two loci *qtl3.2* (to Emco5 and Noco2) and *qtl5.1* (to Emco5) were qualitative and completely dominant. A combination of both quantitative and qualitative isolate-specific resistance mechanisms was found in a study on the Arabidopsis-*Hpa* interactions [136] and other pathosystems [161]. The importance of the combination of qualitative and quantitative resistance was demonstrated in a study on the resistance-breaking capacity of Potato virus Y (PVY) in pepper, where the strong effect *R*-gene *PVR2³* was not overcome by PVY when it was combined with smaller-effect resistance

QTL, but it was overcome in the *PVR2*³-only situation [162].

Our results show that downy mildew resistance loci in C24 can be dominant, codominant and recessive. Genetically-controlled resistance in many previously studied interactions between *Arabidopsis* and downy mildew is mediated by dominant *R*-genes with NBS-LRR domains [138]. We cannot exclude that a classical *R*-gene confers resistance in a codominant manner, e.g. when one copy of the *R*-gene leads to pathogen detection and defense activation to a level that is not sufficient to induce a strong immune response. This could be due to dosage of the *R*-protein, epistasis by modifiers at other genetic loci in the plant genome, or effectors of the pathogen that suppress the immunity. There are also examples of recessive forms of *Hpa* resistance, e.g. mutants *downy mildew resistant 1* and *6* [109, 110, 119], *rar1 suppressors 1* and *2* [111]. The corresponding wild type genes (that might be considered susceptibility genes) encode for proteins with predicted metabolic activities. Future cloning of the genes underlying some of the C24 QTL will reveal the mechanisms of resistance and might explain their mode of inheritance.

In addition to BSR against downy mildew, caused by the oomycete pathogen *Hpa*, *Arabidopsis* C24 has complex resistance to the powdery mildew fungus *Golovinomyces orontii* [163], dominant resistance mediated by the *RCY1* gene effective against CMV(Y) [154], and dominant resistance to *Pseudomonas syringae* pv. *tomato* DC3000 (unpublished data from our lab). Resistance of C24 to a surprisingly broad spectrum of biotrophic and hemibiotrophic pathogens raises questions about evolution of C24 defense mechanisms. The so-called evolved recycling polymorphism model [164] suggests that in plant populations there is extensive proliferation of resistance genes, and, as a result, a pool of constantly appearing “unused” resistance specificities is always present. BSR of C24 could be the result of such proliferated new resistance specificities

Our study demonstrates that BSR of C24 to downy mildew is compound and depends on combinations of isolate-specific loci; some of the loci contribute to the resistance against only one of three isolates, but others confer resistance to two *Hpa* isolates. This is not unique to C24 as similar mechanisms were found in other pathosystems, such as rice - fungal blast disease [133], *Medicago truncatula* - oomycete pathogen *Aphanomyces euteiches* [134], pepper – potyviruses [165], bread wheat – tan spot disease [166], barley – powdery mildew [167], potato – late blight disease [168]. In these examples, as well as in our study, there was at least one QTL which conferred resistance to several pathogen isolates, but these broad-resistance QTL were found in combinations with other isolate-specific QTL. Unfortunately, in the mentioned studies the identified multiple QTL were not cloned. The *Arabidopsis* C24 – downy mildew pathosystem allows a detailed genetic and genomic analysis of complex BSR in plants.

Ongoing fine-mapping and cloning of the identified *Hpa* resistance QTL in *Arabidopsis* C24 is expected to lead to the cloning of susceptibility- and immunity-related genes that will improve our understanding of the molecular mechanisms and evolution of complex resistance in plants.

Acknowledgments

This project was made possible with a Technology Transfer Award of The Leverhulme Trust (UK) to G.V.d.A. R.C.M. acknowledges the support of the Deutsche Forschungsgemeinschaft (SPP1149).

Supporting Information

Table S1. Primers and probes used in the study

Name of the sequence	5'->3'	Comment
Probe_HpACT	CGCGATTGTGCGTTTGGATCT	6FAM->BHQ1, E=97% (r2>0.999)
Probe_AtACT2	AGGTCGTTGCACCACCTGAAAGG	YAKIMA YELLOW->BHQ1, E=93% (r2>0.999)
HpACT_Fw	GTGTCGCACACTGTACCCATTAT	-
HpACT_Rv	ATCTTCATCATGTAGTCGGTCAAGT	-
AtACT2_AT3G18780_Fw	AATCACAGCACTTGCACCA	-
AtACT2_AT3G18780_Rv	GAGGGAAGCAAGAATGGAAC	-
At5g19840_Fw	TCTTAACGCTGGTGATGCAG	E=101% (r2>0.998)
At5g19840_Rv	TCCATGTGTTCCAGGCATGTT	
PR-1_Fw	GGTCCACCATTGTTACACCT	E=100% (r2>0.999)
PR-1_Rv	GAACACGTGCAATGGAGTTT	
F21B7_Fw	TCACGTGTTTGTGGGTCAAT	indel marker for <i>qt1.1</i>
F21B7_Rv	ATTGTGCGTGGCCTTTTATAG	
F20D23/T13M22_Fw	TCTCCGCATCTTGATCATTG	indel marker for <i>qt1.2</i>
F20D23/T13M22_Rv	CGCAAAAAGCTGAAGAACAA	
F16M22_Fw	AAGAGCATAAGGAGCTCATGAAA	indel marker for <i>qt1.3</i>
F16M22_Rv	TCAGTTAGTGCCTTGTTCTTGG	
ciw12_Fw	AGGTTTTATTGCTTTTCACA	indel marker for <i>qt1.4</i>
ciw12_Rv	CTTTCAAAAAGCACATCACA	
MOB24_Fw	TTTAAACCGGCGAACTCTGA	indel marker for <i>qt1.3</i>
MOB24_Rv	TGTGCATCATCCGAGGTAAA	
T10D7_Fw	AAAAACAAAATAATCTCACGGTTT	indel marker for <i>qt1.3.2</i>
T10D7_Rv	CTCCATTATTCCATGCATTTTT	
FCAALL_Fw	TTGCTTGCTCTCAACGCTTA	indel marker for <i>qt1.4</i>
FCAALL_Rv	GCCGTGGCGTAGTAGTTTGT	
MQD19_Fw	AACCCTACAAAACCCCAAAA	indel marker for <i>qt1.5.1</i>
MQD19_Rv	CGATGATCACAGTAACGATTATCC	

Notes S1. Optimization and conditions for TaqMan® based *Hpa* quantification in *Arabidopsis*

TaqMan® qPCR for quantification of *Hpa* and *Arabidopsis* DNA in a single tube was performed on ABI 7900HT Fast Real-Time PCR System instrument with the following conditions: 95°C for 10 min followed by amplification 40 steps 95°C – 10 sec 60°C – 1 min. Master mix is presented in SI Table 2.

Table S2. Master mix for TaqMan® based quantification of *Hpa* growth in Arabidopsis

component	final concentration	concentration of stock	in 25 ul
mQ			2.75
TaqMan® Universal PCR Master Mix without AmpErase® UNG	1x	2x	12.5
Actin primers mix	300 nM	10 uM each	0.75
Actin probe mix (in TE)	200 nM	10 uM each	0.5
MgCl ₂	3.5 mM	25 mM	3.5
sample DNA in mQ	varies	up to 10 ng/ul	5
total	-	-	25

Detection of the fluorescent signal was done with filters for 6-FAM and VIC (for YAKIMA-YELLOW). Since we used BHQ1 quencher to reduce background fluorescence from the probes (SI Table1), 'no quencher' setting was applied instead of the default TAM quencher. During optimization we tried a range of MgCl₂ concentrations from 1.5 to 9.5 mM. The highest efficiency for each primer-probe combination was achieved with the concentration 9.5 mM, therefore this concentration was used later. Then, with these PCR conditions we tested efficiency of the assay with different amount of DNA per reaction (SI Figure 1). The signal could be detected with 25-50 pg of downy mildew and Arabidopsis DNA in a reaction. The highest amount of DNA was around 70 ng per reaction and we did not observe signs of the reaction inhibition. Therefore routinely DNA concentration of the samples was not measured. Efficiency of the *Hpa* reaction (probe+2 primers) was 97%, for Arabidopsis 93%. In case of multiplexing when the concentration of *Hpa* DNA changed but the concentration of the Arabidopsis DNA remained constant, the efficiency of the *Hpa* probe reached 110% (r²=0.999) (SI Figure 1).

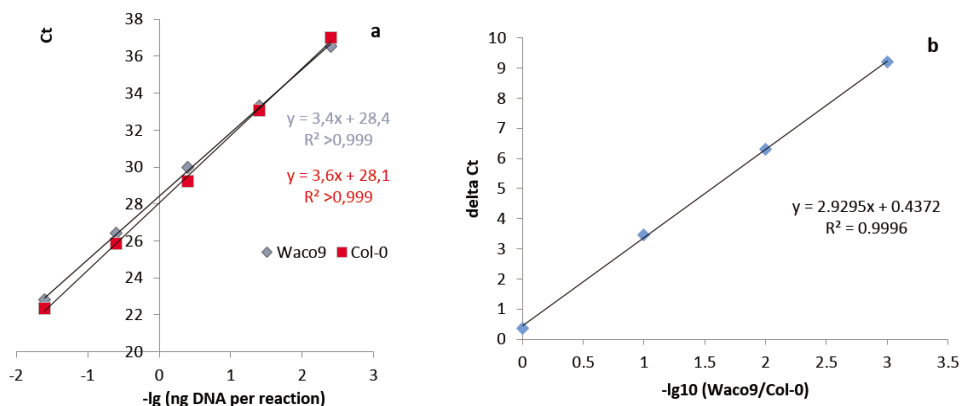


Figure S1. Optimization of the TaqMan® assay for quantification of *Hpa* growth on Arabidopsis. (a) *Hpa* actin probe, labeled with the reporter dye 6-FAM and a quencher of Black Hole type (BHQ1), had efficiency 97% (r²>0.999) in the reaction only with *Hpa* Waco9 spore DNA (blue line). Arabidopsis ACT2 probe, labeled with YAKIMA YELLOW as a reporter dye and BHQ1 as a quencher, had slightly lower efficiency 93% (r²>0.999) in the reaction only with Arabidopsis Col-0 DNA (red line). (b) When the concentration of *Hpa* was changed while keeping Arabidopsis constant, efficiency reached level of 110% (r²>0.999), that is suitable for the practical application.

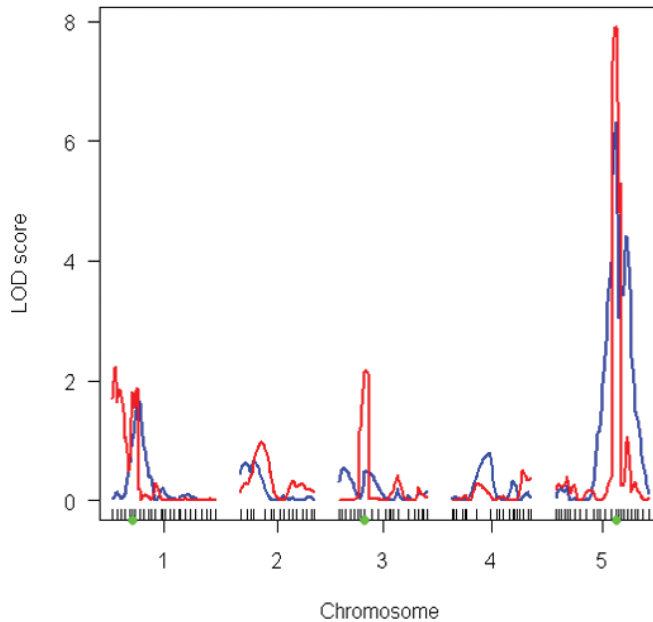


Figure S2. LOD profile of interval mapping of C24 resistance in RILs Col-0xC24. Standard interval mapping (blue line) identified only one significant QTL on chromosome 5 between markers V.102 and V.104 (1.5-drop-off interval) with max LOD=6.3 at V.103a ($p < 0.004$). Composite interval mapping (red line) with three covariates (green dots) selected by forward approach identified several additional QTLs. Positions of 4 peaks with the highest LOD scores were used to refine their positions and get estimates of explained variance and support intervals with multiple QTL mapping functions such as *refineqtl()*, *fitqtl()* and *lodint()*.

Notes S2. QTL mapping in a population of RILs Col-0xC24

QTL mapping of C24 resistance to downy mildew Waco9 was performed in R/qtl software [147] with ΔC_t values from the TaqMan® assay as input in a population of 75 RIL Col-0xC24. Standard interval mapping revealed one significant QTL on chromosome 5 with double peak (SI Figure 2).

In composite interval mapping we did not confirm presence of the second peak at *qtl5.1*. Instead, we could find three additional QTL on chromosomes 1 and 3. Positions of all 4 QTLs were refined with *refineqtl()* method, and effects of these QTL with refined positions were estimated with *fitqtl()* function. 1.5-drop-off support intervals were determined with *lodint()* (Table S3).

Table S3. Estimates of QTL effects

QTL	before refining QTL positions					after refining QTL positions				support interval, cM
	QTL position	LOD	% var	F-test p-value	QTL position	LOD	% var	F-test p-value		
<i>qtl1.1</i>	1@4.7	0.41	1.6	0.176	1@9.0	2.4	7.9	0.001	0-17	
<i>qtl1.2</i>	1@22.8	2.6	10.7	<0.001	1@20.4	3.9	13.2	<0.001	17-27	
<i>qtl3.1</i>	3@24.9	1.5	6.2	0.010	3@38.2	1.9	6.1	0.004	0-50	
<i>qtl5.1</i>	5@54.8	5.7	26.4	<0.001	5@60.1	9.9	41.1	<0.001	55-63	

To check for the possible interactions between identified loci, we used *fitqtl()* function allowing interactions between QTLs. The lowest p-value, though not significant ($p=0.09$), was found for interaction between *qtl1.2* and *qtl3.1* (Figure S3). Analysis with QTLNetwork software [148] confirmed the presence of the interaction with slightly higher significance ($p=0.02$).

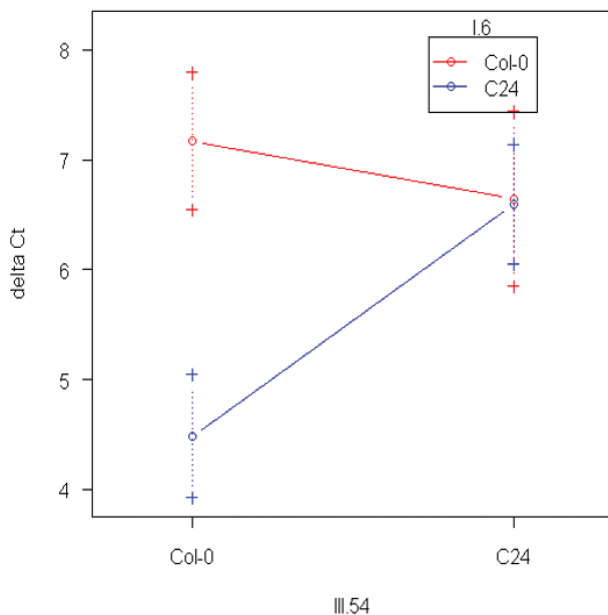


Figure S3. Interaction plot for *qtl1.2* and *qtl3.1*. The interaction between *qtl1.2* (LOD peak at marker I.6) and *qtl3.1* (peak at III.54), examined with *fitqtl()* method, appeared to be not significant ($p=0.09$), however, it indicated presence of small epistatic effects. In the interaction plot, RILs with genotype Col*qtl1.2* C24*qtl3.1* are expected to have higher C_t value (to be more resistant) than it was observed in case of only-additively acting QTL, i.e. the red and blue lines should be parallel. Instead, plants with genotypes Col*qtl1.2* C24*qtl3.1* and C24*qtl1.2* C24*qtl3.1* had similar levels of susceptibility to downy mildew. Although in case of a strong interaction, one would expect that the red and blue line cross each other.

QTL mapping of C24 resistance to several downy mildew isolates in the population of Col-0 ILs

Table S4. Results of mapping of C24 resistance and susceptibility loci in the population of Col-0 ILs

QTL	Col-0 IL	Spore count, spores/seedling			Significance of difference between Col-0 and IL (LSD-test p-value)			Remark
		Waco9	Emco5	Noco2	Waco9	Emco5	Noco2	
qt1.1	N 29/6/3	5296	3522	3833	ns	ns	ns	
	N 32/1/2	4444	2911	2189	ns	ns	ns	
qt1.2	N 2/11/6	4925	2966	155	ns	ns	0.00	contains qt1.4
	N 87/12/10	4161	3022	255	0.00	ns	0.00	
	N 87/12/12	3685	2700	133	0.02	ns	0.00	
	N 38/6/12/12	3657	3422	2755	0.02	ns	ns	
	N 38/6/12/14	5009	3311	3022	0.00	ns	ns	
	N 38/6/8/5	3895	3711	2800	0.01	ns	ns	
	N 54/7/10/5	4409	3755	2966	0.00	ns	ns	
	N 54/7/4/8	4074	3333	2766	ns	ns	ns	
	N 54/7/5/5	4295	not tested	not tested	0.00	NA	NA	
	N 87/2/7/8	5259	not tested	not tested	ns	NA	NA	
qt1.3	N 21/6/7	4259	not tested	not tested	ns	NA	NA	
	N 42/2/7	5370	3100	2166	ns	ns	ns	
	N 74/4/8	5148	not tested	not tested	ns	NA	NA	
qt1.1+								
qt1.3	N 29/11/1	703	2111	2611	0.00	ns	ns	
qt1.4	N 2/11/6	4925	2966	155	ns	ns	0.00	contains qt1.3.2
qt1.3.1	N 52/2	1740	44	55	0.02	0.00	0.00	
	N 63/14	1925	426	3088	0.03	0.00	ns	
qt1.3.2	N 67/5	3555	0.1	77	ns	0.00	0.00	
	N 21/3/14	3814	55	44	ns	0.00	0.00	
qt1.4.1	N 68/5	1666	2477	1833	0.02	ns	ns	
qt1.5.1	N 2/13/4	333	411	2400	0.00	0.00	ns	
	Col-0	4074	3233	3150	NA	NA	NA	
	Col-0	1571 [§]	3333 [@]	NA	NA	NA	NA	
	Col-0	5333 [%]	NA	NA	NA	NA	NA	

*results of the LSD test are presented only for one of several independent experiments

**Although IL N 2/11/6 and N 87/2/7/8 contain qt1.2, they were not more susceptible to Waco9 in any of the experiments

***ns – not significant (LSD $p > 0.05$); NA – line was not tested

****experiments with Waco9 and most of IL containing *qtl1.2* were performed at 5 dpi in order to see differences between the ILs and Col-0 more clearly; line N87/12/10 was included in the screen at 6 dpi as well and the corresponding p-value is presented in the main text Table 3.

\$ Col-0 value corresponds to ILs in the green cells; the experiment with Waco9 was performed at 5 dpi

% Col-0 value corresponds to ILs in yellow cells (Waco9)

@ Col-0 value corresponds to ILs in the green cells (Emco5)

Effect of *RCY1* on resistance of Arabidopsis C24 against downy mildew

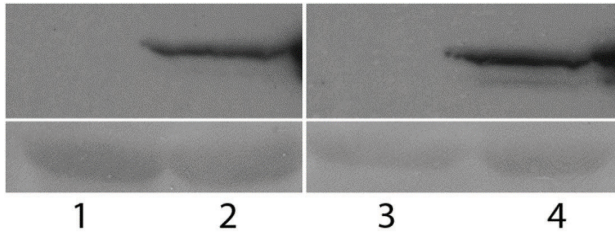


Figure S4. HA-tagged *RCY1* is expressed in the tested Col-0 transgenic line #12. Wild type plants Col-0 mock-treated (lane 1) and infected (lane 3) with Waco9 do not show any signal on the western blot. The transgenic line #12 expressing *RCY1* tagged with HA has detectable level of *RCY1* expression with (lane 2) and without (lane 4) infection.

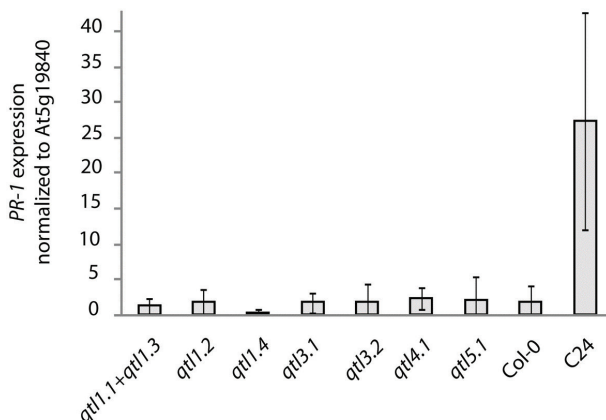


Figure S5. Expression of *PR-1* in non-infected but water-sprayed Col-0, C24 and ILs. To estimate whether increased expression of *PR-1* in non-infected C24 has an effect on downy mildew, we measured *PR-1* expression in Col-0 ILs which contained C24 resistance QTLs and compared these levels to Col-0. It appeared that none of the tested ILs had elevation in *PR-1* compared to Col-0 (LSD $p > 0.25$, $n = 6$) demonstrating that the increased *PR-1* expression is not linked to downy mildew resistance in C24. Error bars on the figure represent \pm one standard deviation. The experiment was performed two times with three replicates in each experiment.

Chapter 3

Two interacting downy mildew resistance loci in the Arabidopsis accession C24 revealed by whole genome sequencing of backcross lines

Dmitry Lapin¹, Isaac Nijman², Ewart de Bruijn², Edwin Cuppen^{2,3}, Guido Van den Ackerveken¹

¹ – Plant-Microbe Interactions, Department of Biology, Faculty of Science, Utrecht University, Utrecht, The Netherlands

² - Hubrecht Institute, Utrecht, The Netherlands

³ - Department of Medical Genetics, University Medical Center Utrecht, Utrecht, The Netherlands

Abstract

Resistance of plants to infectious diseases can be a complex trait controlled by several genetic loci. Arabidopsis accession C24 has broad-spectrum resistance to downy mildew caused by the biotrophic oomycete pathogen *Hyaloperonospora arabidopsidis* (*Hpa*). Different combinations of multiple isolate-specific loci mediate this resistance. Interestingly, the immune response of C24 to *Hpa* isolate Waco9 is quantitative, a form of resistance that is still poorly understood. The goal of this study was to find the major C24 loci controlling this quantitative resistance. For that, we developed a population of partially susceptible C24 backcross lines with introgressed loci from the susceptible accession Col-0. These lines were analyzed by whole genome sequencing revealing two loss-of-resistance loci. Next, analysis of F2 segregants and introgression lines confirmed that these two loci correspond to the previously identified *qtl1.3* and *qtl5.1*. We demonstrate that these loci interact to confer full resistance of Arabidopsis C24 to *Hpa*. Our results reveal a genetic mechanism that could underlie other examples of quantitative disease resistance of plants.

Introduction

Pathogenic microorganisms interfere with host plant processes affecting many physiological functions contributing to disease. However, innate immunity of plants restricts pathogen growth and development. Although single-gene based mechanisms of plant disease resistance are well known and studied [5, 120], frequently resistance in natural populations is a multigenic trait. There are many examples where genetic mapping of resistance in different plant species against diseases caused by biotrophic, hemibiotrophic or necrotrophic pathogens typically revealed 2-3 major loci [169, 170]. Notably, even in the case of single-locus based resistance, several tightly linked genes might be responsible for plant immunity. For instance, the nematode resistance locus *Rhg1* in soybean includes tandem repeats of three genes, and the three genes all contribute to confer soybean immunity [171].

Genetic mapping of multigenic traits is often performed in bi-parental mapping populations, e.g. populations of di-haploids, recombinant inbred lines (RILs), introgression lines (ILs), backcross (BC) and F2 and F3 segregating families derived from crosses of two parents that differ in phenotypic trait of interest. These methods are successfully used in different plant species to estimate the number of loci involved, their approximate location, and interactions between them. Unfortunately, low mapping resolution achieved with these populations

does not allow identifying the underlying genes. To overcome the problem of low resolution mapping, advanced generation intercross mapping populations could be used as well. In *Arabidopsis thaliana* (further referred to as *Arabidopsis*) multiparental advanced generation intercross (MAGIC) lines were obtained by crossing 19 founder natural accessions with each other followed by intercrossing of the obtained progeny for several generations. According to simulation studies, these MAGIC lines are expected to provide a mapping resolution of around 300 kb that corresponds to 50-100 genes in *Arabidopsis* [172]. Higher resolution mapping was achieved in the nested association mapping (NAM) panel of maize. The NAM population consists of 25 RIL sets of 200 lines each derived from crosses of 25 diverse maize accessions with the reference line B73 [173]. This population was used to identify candidate genes linked to and associated with resistance to the northern and southern leaf blight disease in maize [174, 175]. Mapping with association panels of natural accessions enables high-resolution mapping of QTL too, e.g. up to individual genes in the case of *Arabidopsis* [176] or even to polymorphisms within a gene in maize [177, 178]. For example, a maize association mapping panel consisting of 253 inbred lines allowed the identification of alleles of a glutathione S-transferase gene associated with moderate levels of resistance to three leaf fungal pathogens [177]. Combinations of different mapping procedures are frequently used in QTL mapping. For instance, susceptibility of wheat to the necrotrophic fungi *Stagonospora nodorum* and *Pyrenophora tritici-repentis* caused by plant sensitivity to the toxin ToxA was first fine-mapped to a region of ~ 350 kb; this region was predicted to have six genes, and candidate-gene association mapping in a set of varieties further identified the *Tsn1* gene which encodes for a nucleotide binding site – leucine-rich repeat (NB-LRR) domain containing kinase [124, 166].

Whole-genome sequencing (WGS) and the availability of algorithms for sequence data analysis now provide excellent opportunities for gene mapping. One of the straightforward applications is gene mapping in mutagenized populations. The frequently used mutagen ethyl methanesulfonate (EMS) mainly leads to G/C-to-A/T transitions in DNA (>99% in *Arabidopsis*), which might cause alteration in phenotypic traits of interest [179, 180]. Identification of a causal mutation could be achieved by crossing mutants with a non-mutagenized line, selecting individuals with the mutant phenotype from the segregating population, their sequencing, and selecting EMS-induced mutations shared by the selected mutants [181-183]. WGS-based gene mapping was also applied to identify intervals with candidate genes underlying phenotypic variation among natural accessions of animal and plant species, e.g. in fruit flies [184] and rice [185]. One of the mapping approaches is based on backcrossing with selection in each BC generation. For example, the fruit fly species *Drosophila simulans* and *D. sechellia* have different food preferences: morinda fruits are toxic for the first species but represent a suitable feeding substrate for *D. sechellia*. By backcrossing *D. sechellia* to *D. simulans* for fifteen generations and selecting for morinda-lovers in each BC, the chromosome segments of *D. sechellia* responsible for the dietary preference were introgressed into the *D. simulans* genetic background. These introgressions were further identified by WGS and silencing of individual genes revealed the underlying genetic loci [184].

The genetically tractable model plant *Arabidopsis* [186] is widely used to study plant immunity and susceptibility to pathogen infection. In particular, the interaction with the biotrophic oomycete pathogen *Hyaloperonospora arabidopsidis* (*Hpa*), causing downy mildew, is a powerful pathosystem to study plant resistance and susceptibility to diseases [118]. Natural *Arabidopsis* accessions are typically susceptible to a number of downy mildew isolates [136], however, accession C24 is immune against all tested isolates of *Hpa* [139]. Previously, using QTL mapping, we showed that broad-spectrum resistance of C24 against downy mildew is multigenic and mediated by different combinations of isolate-specific resistance loci. Importantly, resistance of C24 to the downy mildew isolate Waco9 is influenced by six different loci, and not a single of these loci confers full resistance [94]. The aim of this study was to identify and fine-map the major C24 loci that control quantitative resistance to the *Hpa* isolate

Waco9.

For fine-mapping of the C24 resistance QTLs, we developed independent BC5 lines of C24 with introduced susceptibility loci from accession Col-0. In every BC generation, for each independent BC population we selected a seedling susceptible to Waco9 and backcrossed it again to C24. WGS of the resultant susceptible BC5 lines revealed two major resistance loci on chromosomes 1 and 5. Analysis of ILs and their hybrids confirmed that, whereas individually each locus only provides partial resistance, the combined C24 loci confer strong resistance to *Hpa* isolate Waco9. Our data demonstrate that epistasis, or genetic interaction, between the two C24 alleles provides a strong quantitative form of resistance, and ongoing fine-mapping and further functional analysis of causal genes might explain the molecular basis of genetic interactions contributing to disease resistance in other plant species.

Materials and methods

Plant material and growth

Arabidopsis thaliana (L.) Heyhn (referred to as *Arabidopsis*) mutant *flc3* in the Col-0 background was obtained from dr. M. Proveniers (Molecular Plant Physiology group, Utrecht University). C24 introgression lines in Col-0 background (referred to as Col-0 ILs), Col-0 introgression lines in C24 background (referred to as C24 ILs), and their genotype information were described previously [140, 141]; the lines were provided by dr. R.C. Meyer (IPK, Gatersleben, Germany). Correspondence between IL codes used in the current study and in the studies [142] and [135] is as follows: Col-0 IL N17 is N 29/11/1, Col-0 IL N38 is N 2/13/4, Col-0 IL N41 is N 21/6/7, C24 IL M02 is M 31/8, C24 IL M54 is M 37/7/1/6. Plants were grown at 21°C under long day conditions (16h light/8h dark, light intensity 100 $\mu\text{mol}/\text{m}^2/\text{sec}$).

Downy mildew infection assays and quantification

The downy mildew *Hyaloperonospora arabidopsidis* (Gäum.) Göker, Riethm., Voglmayr, Weiss & Oberw. (*Hpa*) isolate Waco9 was maintained as described previously [109]. All infection assays were performed on eleven-day-old seedlings at 16°C under short day conditions (9h light/15h dark, light intensity 100 $\mu\text{mol}/\text{m}^2/\text{sec}$, relative humidity 100%) with a standard inoculum density of 50 conidiospores/ μl . The level of resistance of different genotypes was estimated by counting spores and expressed as number of spores per mg of fresh weight. Each experiment was repeated at least two times with at least three replicates per genotype. For the segregation analysis in a F2 population C24xCol-0 *flc3*, seedlings were scored resistant if they did not have a single conidiophore on their true leaves and cotyledons up to 9 days post inoculation (dpi), otherwise they were scored susceptible. For the backcross populations, seedlings were scored resistant if they contained no conidiophores on their true leaves or cotyledons at 8 dpi.

Development of backcross (BC) lines

The resistant parent C24 was used a maternal plant to prevent occurrence of susceptible BC plants due to self-pollination. As a donor of susceptibility, the Col-0 *flc3* mutant was utilized instead of the wild type Col-0 to eliminate appearance of late-flowering plants [187]. Fifty BC1 seedlings susceptible at 5 to 8 dpi from the segregating BC1 population C24x(C24xCol-0 *flc3*) were backcrossed to C24. Our previous QTL mapping study showed that C24 resistance against Waco9 is linked to five independent loci [94], therefore the chance of finding plants heterozygous for all five loci is $(\frac{1}{2})^5=0.03$, giving $150 \times 0.03 \approx 5$ susceptible seedlings in a population of 150 BC plants. Therefore, for each BC line in each round of BC, a minimum 150 hybrids seeds were derived from crosses with C24. The level of susceptibility and the number of susceptible plants in the BC populations was reducing from one BC generation to another, therefore an additional set of BC lines was developed. Additional 67 susceptible plants were selected from several BC2F2 or C24xBC2F2 populations (SI Figure 2).

DNA isolation

Approximately 100 mg of leaves and shoots of a single plant from each BC5 line was ground in liquid nitrogen and used for a two-step DNA isolation. In the first step, DNA was isolated with the CTAB-based method without RNase A treatment [145]. The pellet was then dissolved in milliQ water (10 MΩxcm) and used for a subsequent purification step using the DNeasy Plant mini-kit (Qiagen, Hilden, Germany). Concentration and quality of DNA was estimated with the standard spectrophotometric A260 method. Measured concentration, size and integrity of the isolated DNA was examined on 0.7% agarose gel (A9539, Sigma-Aldrich, MO, USA). The final pooled DNA sample included 150 ng of DNA from each of 48 individual BC5 lines. F2 plants and other hybrids and lines were routinely genotyped on DNA isolated with the sucrose method [188].

SOLiD library preparation and sequencing

Preparation of SOLiD libraries was performed as described previously [189]. The derived library was sequenced on the AB/SOLiD sequencer (Life Technologies, UK) with V3 chemistry according to the manufacturer protocol to produce 50 bp reads.

Filtering of the sequence data and alignment to the reference Arabidopsis genome

SOLiD sequence data analysis, alignment of sequences to the Arabidopsis genome (TAIR10), SNP and indel calling was performed as described in [190]. Raw and analyzed sequence data are available upon request.

Localization of putative C24 resistance loci based on sequence data

For analysis of the sequencing data only SNP calls with coverage ≥ 80 and $\leq 250x$ were considered (median coverage 136x). To determine chromosome regions with a percentage of non-reference reads (PNR) significantly different from the average chromosome level, a method similar to the sliding window approach used by Earley and Jones [184] was employed. With this method, bins of 1000 adjacent SNPs were selected and a Wilcoxon test was applied to determine whether the PNR level in each bin is different from the PNR of 1000 randomly selected SNPs on a given chromosome. The obtained p-values were adjusted with the false discovery rate method [191] (FDR adjusted p-values are called q-values). Since q-values are dependent on a control sample of SNPs randomly selected across a chromosome, this test was performed with 100 different random control samples. A mean of the $-\log(q)$ values for every SNP bin was then used as an indicator of whether this SNP bin was selected during BC. In the second test to infer the intervals of the resistance loci more precisely, a region containing SNP bins with $q < 0.001$ as determined with the first test was divided on overlapping bins of 1000 SNPs (step 50 SNPs). Then a Wilcoxon test with FDR correction was performed to check the significance of difference in PNR levels between all these bins. After such 2D scan neighboring bins with non-significant differences in PNR levels were considered as one introgression block (in general $q > 0.001$). The analysis was performed in the R environment [192]. Graphical visualization was done with the packages lattice [193] and gplots [194].

Validation of WGS-identified loci

Inferred borders of the C24 loss-of-resistance loci on chromosomes 1 and 5 were used as guides for developing markers and for further validation of candidate loci by genotyping of each BC5 line individually. Indel and SNP markers were developed based on sequence alignments from our sequence data, the MSQT database [195] and a published reference-guided C24 genome assembly [196]. Generally, genotyping with SNP markers was performed with high-resolution melting curve analysis on the LightScanner® (Biofire, Utah, USA) (for details check SI Note 1, SI Table 2). Details on the used genetic markers are presented in SI Table 1. Based on the genotyping data, the percentage of C24 alleles in the population of 48 BC5 lines was

calculated for each tested polymorphic position. Primers sequences and other information for centromeric and pericentromeric markers on different chromosomes are shown in SI Table 1.

Results

Identification of two major resistance QTL by whole-genome sequencing of BC lines

To find the major QTL responsible for resistance of Arabidopsis C24 to the downy mildew isolate Waco9, we applied a backcross (BC) approach coupled to high-throughput whole genome sequencing (Figure 1). For this, we crossed the resistant accession C24 with the Col-0 *flc3* mutant, which is susceptible to *Hpa* Waco9. We used the *flc3* mutant to eliminate late-flowering plants that segregate in a cross between C24 and Col-0 due to presence of the functional alleles of *FLOWERING LOCUS C* and *FRIGIDA* in Col-0 and C24, respectively [187]. Susceptibility of the *flc3* mutant to *Hpa* Waco9 did not significantly differ from that of the wild type Col-0 (t-test $p=0.21$, SI Figure 1a), nor did the *FLC3* locus co-segregate with resistance to Waco9 in a F2 population derived from a C24xCol-0 *flc3* cross (χ^2 -test $p=0.28$, 51 fully resistant seedlings). Thus, the *flc3* mutation was not expected to affect results of the BC mapping approach. C24xCol-0 *flc3* F1 hybrids were intermediately susceptible to the

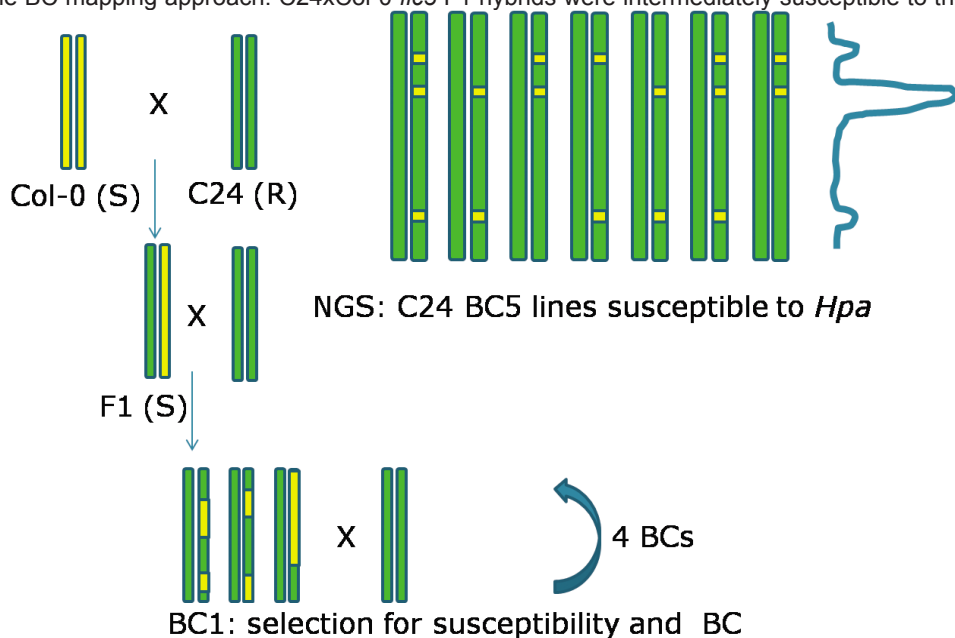


Figure 1. Backcross (BC) approach for mapping of C24 resistance loci. Arabidopsis Col-0 is susceptible to *Hpa* isolate Waco9, and the accession C24 has several loci responsible for its full resistance to this pathogen. For fine-mapping of the C24 resistance loci, we aimed to develop multiple independent BC lines in C24 background with introduced susceptibility loci from Col-0. For that in each BC generation, we selected a seedling which was susceptible to Waco9 and cross again back to C24. The 48 susceptible BC5 lines were used for whole genome sequencing in order to identify the introduced susceptibility loci. In our mapping approach, resistance loci of C24 were expected to be heterozygous for Col-0 alleles in all or majority of BC5 plants, but other loci on the genome - mostly homozygous for C24 alleles. Thus, at the resistance loci percentage of C24 sequence reads should be 50%, and at other loci, not linked to resistance, the background level of PNR - close to 100% ($(1/2)5 \times 100\% = 3\%$).

Hpa isolate Waco9 (SI Figure 1b). The incomplete dominance of C24 resistance loci enables selection for susceptibility when the loci are heterozygous. The F1 hybrids were backcrossed to the resistant C24 parent resulting in a BC1 population segregating for susceptibility to *Hpa* Waco9. We selected 50 susceptible BC1 plants and crossed them again to C24. Backcrosses and selection for susceptibility were performed in each subsequent BC generation until we obtained BC5 lines that were partially susceptible to *Hpa* Waco9. Additional 67 lines were selected from BC2F2 and BC3 generations and further backcrossed to the BC5 generation to increase the total number of individual susceptible BC5 lines (SI Figure 2). In total, 48 BC5

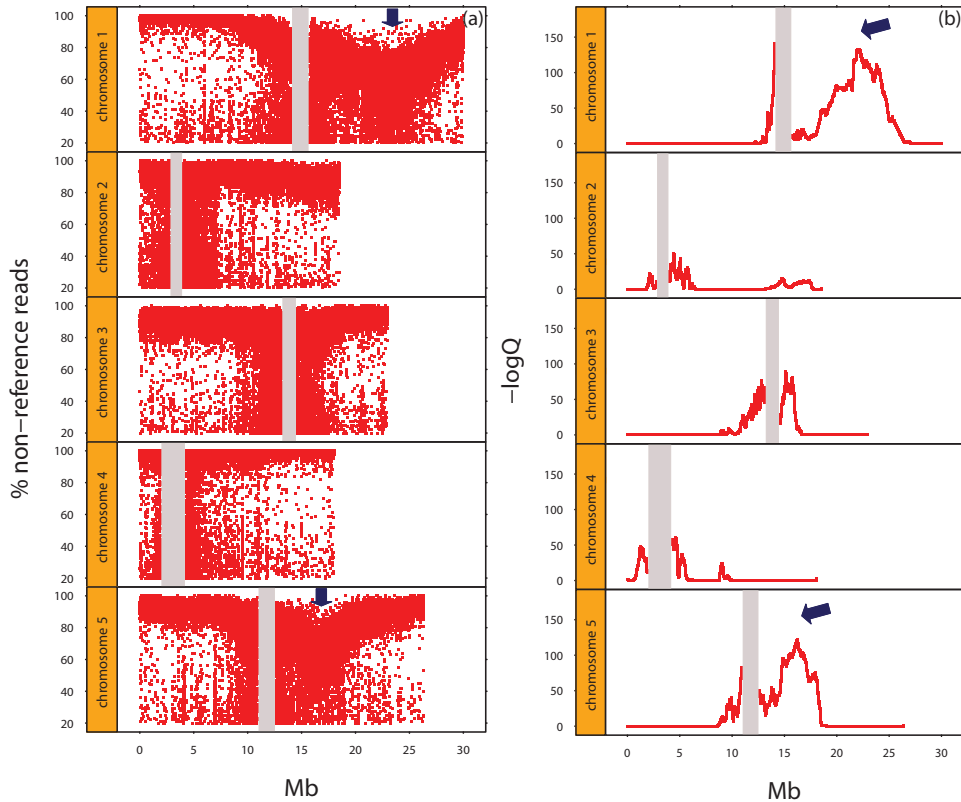


Figure 2. Identification of heterozygous loss-of-resistance loci in the C24 backcross 5 (BC5) lines. (a) After quality control, sequence reads from the whole genome sequencing of C24 BC5 were aligned to the Col-0 reference genome. At each single nucleotide polymorphism (SNP) position with coverage 80-250x, percentage of non-reference reads (PNR) was calculated and plotted across all chromosomes. Two regions with reduced average PNR levels were detected on chromosomes 1 and 5 (vertical arrows) suggesting presence of resistance loci. (b) Results of the statistical analysis of the PNR values plotted on the panel (a). Locations of the putative resistance loci were roughly estimated via sliding window approach described by Earley and Jones (2011) [184] with modifications. The $-\log_{10}$ of the false discovery rate q shows how significantly the average PNR level in a bin of 1000 adjacent SNPs differs from the average PNR level on a given chromosome. Grey bars on each chromosome correspond to the genetically determined borders of centromeres (SI Table 3 based on [198]). The most significant deviation of local PNR values from the average on a chromosome was found around all centromeres and on the lower arm of chromosomes 1 (ca. 12.9-26.4 Mb) and 5 (ca. 8.8-18.5 Mb) ($q < 0.001$).

lines were generated that had lost full resistance to the downy mildew isolate Waco9. Next, we pooled equal amounts of DNA isolated from each of the 48 BC5 lines, prepared a sequencing library, and performed whole genome sequencing using AB/SOLiD technology. After stringent quality control, more than 4×10^8 sequence reads of ~50 nucleotides long were aligned to the Col-0 reference genome (version TAIR10 [197]) corresponding to a mean coverage of 173 fold. From the aligned sequences, we inferred the percentage of reference and non-reference reads at each detected single nucleotide polymorphism (SNP) locus with a coverage of 80 to 250 fold (Figure 2a). As the sequenced DNA was obtained from BC5 plants, the percentage of non-reference reads (PNR) is expected to be $(\frac{1}{2})^6 \times 100\% = 98.5\%$ for non-selected loci, i.e. those that do not affect susceptibility. Selection for loss of susceptibility would result in a reduction of the PNR at the contributing loci. A strong reduction in the PNR was observed on the lower arms of the chromosomes 1 and 5, suggesting that heterozygosity at two loci in C24 is sufficient to lose full resistance to the isolate Waco9 (Figure 2a). The PNR was also strongly reduced in centromeric and pericentromeric regions of all five chromosomes, possibly as a result of the incorrect alignment of reads to repeats in these regions. To test this idea, we genotyped the 48 sequenced BC5 plants for a marker in the centromeric region of chromosome 4 (SI Note 2). The percentage of C24 alleles at this position was determined to be 98%, suggesting that the reduction in PNR at the centromeric and pericentromeric regions is indeed an artifact. Genotyping of the 48 lines with markers for the pericentromeric regions of chromosomes 1 and 5 showed a PNR of ~87% that might be caused by linkage to the potential major loss-of-resistance loci on the lower arms of these chromosomes (SI Note 2). Our analysis, therefore, indicates that heterozygosity at the two loci on chromosomes 1 and 5, i.e. the presence of the Col-0 alleles, resulted in loss of resistance of the BC5 lines. To determine the chromosomal position of the two identified loci with more precision, we analyzed the sequence mapping results using a modified sliding window-based procedure [184]. Briefly, the entire chromosome was divided into overlapping bins of 1000 adjacent SNPs, and for each bin the PNR level was compared to the PNR of 1000 randomly sampled SNPs on that chromosome. If a locus is selected during backcrossing or linked to the locus under selection, one expects that the mean PNR for this locus is lower than the mean PNR for the entire chromosome. Significant reduction of PNR (using a Wilcoxon test) was confirmed at the loci on the lower arms of the chromosomes 1 (ca. 12.9-26.4 Mb) and 5 (ca. 8.8-18.5 Mb) (false discovery rate $q < 0.001$) (Figure 2b). Although the significance test helped to identify intervals with reduced PNR, it did not allow the selection of the smallest introgressed region shared by the sequenced BC5 lines within these intervals. Therefore, we performed an additional analysis specifically for the intervals on the lower arms of chromosomes 1 and 5 found in the first analysis. In this additional analysis, the significance of differences in the PNR between all pairs of SNP bins within the indicated intervals is determined, and not between the bins and the mean chromosomal PNR level. Adjacent bins with non-significantly different PNR values are suggested to belong to one introgression block in our BC5 lines (Figure 3, dash lines on the lower panels). The smallest introgressed block shared by the BC5 lines was positioned in the intervals 21.89-23.66 Mb on chromosome 1 and 15.56-17.32 Mb on chromosome 5 ($q > 0.001$). The inferred locations of the candidate Col-0 susceptibility loci on chromosomes 1 and 5 were refined by genotyping each of the 48 BC5 lines individually with a set of SNP and indel markers for the defined intervals. Based on the obtained genotype data we calculated the percentage of C24 alleles (SI Note 2, blue dots on Figure 3), and markers flanking intervals with minimal level of C24 alleles were considered as borders of the heterozygous loss-of-resistance loci. With this method, the candidate loci could be mapped to the intervals 22,265-23,083 kb and 16,406-16,994 kb on chromosomes 1 and 5, respectively (shown as blue bars in Figure 3). When all BC5 lines would be heterozygous for the loss-of-resistance loci the percentage of C24 alleles would be exactly 50%. The actual percentage of C24 alleles at the loss-of-resistance locus on chromosome 1 was 64.6%, whereas on chromosome 5 - 70.8%

(SI Note 2, SI Table 1) indicating that not all BC5 lines were heterozygous at these loci. The majority (44 of 48) of BC5 lines contained at least one heterozygous loss-of-resistance locus on chromosomes 1 or 5 (Table 1). Four lines were homozygous for C24 alleles at both loss-of-resistance loci suggesting that other loci influence the susceptibility phenotype. This is not unexpected since we previously showed that C24 resistance to Waco9 is affected by at least five independent loci [94]. Overall, we conclude that two major candidate loci determine susceptibility of the analyzed BC5 lines that were derived from backcrossing the susceptible

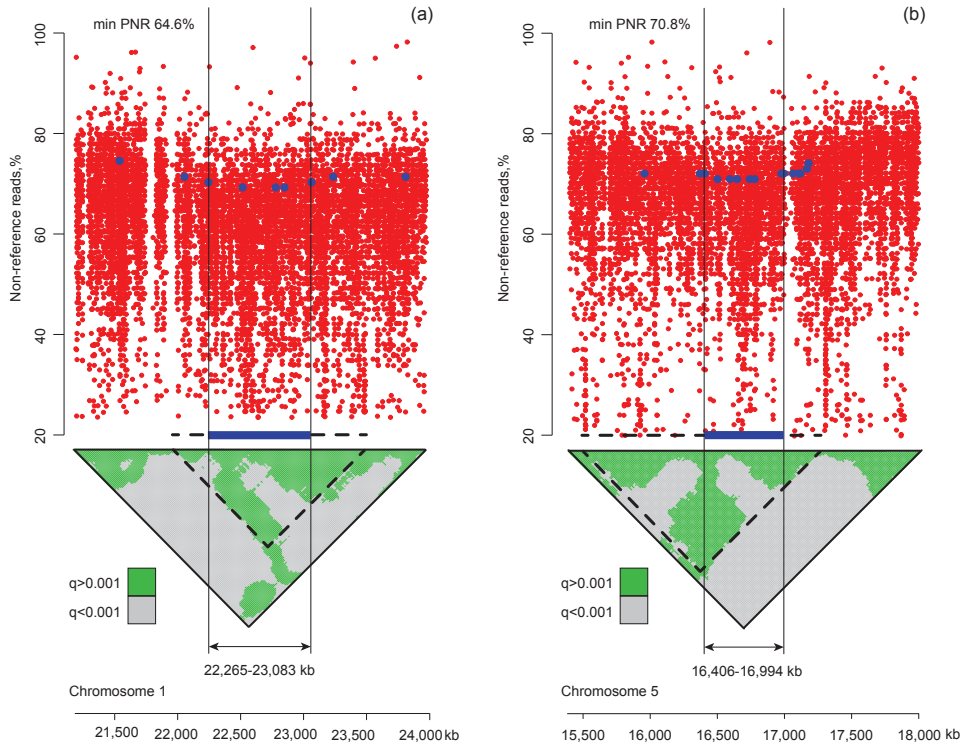


Figure 3. Localization of the loss-of-resistance loci and validation of the inferred intervals on the chromosomes 1 (a) and 5 (b). Intervals for the loss-of-resistance loci on chromosomes 1 (ca. 12.9–26.4 Mb) and 5 (ca. 8.8–18.5 Mb) were analyzed to infer location of the loci more precisely. Raw PNR values for individual SNPs within ca. 2.7 Mb intervals with maximum $-\log_{10} q$ values from the first analysis (Figure 2b) are plotted in red on upper panels of (a) and (b). PNR levels in the bins of 1000 adjacent SNPs were compared with each other within the intervals 12.9–26.4 Mb (chromosome 1) and 8.8–18.5 Mb (chromosome 5), and bins with non-significant differences in the PNR levels were considered as a single Col-0 introgression block ($-\log_{10} q \leq 3$, blocks are shown in green). Based on these criteria, the smallest introgressed regions with the minimal average PNR corresponding to the loss-of-resistance loci were found to be in the intervals 21.89–23.66 Mb on chromosome 1 and 15.56–17.32 Mb on chromosome 5 (dash lines on the lower panels). The inferred intervals were checked by genotyping the backcross 5 (BC5) lines with a set of SNP and indel markers. Actual PNR values were calculated as $100 - [\# \text{heterozygous lines} / (\# \text{lines} \times 2)] \times 100\%$, and they are shown as blue dots on the upper panels. The minimal PNR for the loss-of-resistance locus on chromosome 1 was 64.6% and for the chromosome 5 locus – 70.8%. Markers surrounding intervals with minimal PNR values, 22,265–23,083 kb and 16,406–16,994 kb on chromosomes 1 and 5 respectively (shown as blue thick bars), were regarded as borders of the heterozygous loss-of-resistance loci.

accession Col-0 *flc3* to the recurrent resistant accession C24.

Table 1. Allelic combinations at the loss-of-resistance loci in the population of C24 BC5 lines

Genotype at the loss-of-resistance locus on chromosome 1	Genotype at the loss-of-resistance locus on chromosome 5	Number of C24 BC5 lines
C24/Col-0	C24/Col-0	18
C24/Col-0	C24/C24	16
C24/C24	C24/Col-0	10
C24/C24	C24/C24	4

The identified C24 loci correspond to *qtl1.3* and *qtl5.1* and represent major resistance QTL

The two major loss-of-resistance loci identified with BC mapping appeared to overlap with two C24 QTLs, *qtl1.3* and *qtl5.1*, revealed by QTL mapping with ILs and RILs and conferring resistance to Waco9 [94]. It suggests that *qtl1.3* and *qtl5.1* are major C24 resistance loci. It was expected for *qtl5.1* since the C24 allele of this locus provided the highest level of quantitative resistance in Col-0 ILs, however the effect of *qtl1.3* was not significantly different from effects of two other Waco9-specific resistance loci *qtl3.1* and *qtl4.1* [94]. To validate that *qtl1.3* and *qtl5.1* are major C24 resistance loci, an independent genetic analysis was performed on a segregating F2 population from a C24xCol-0 *flc3* cross. We genotyped 87 F2 individuals fully resistant to the isolate Waco9 with polymorphic markers linked to the six previously mapped C24 resistance QTLs [94], including *qtl1.3* and *qtl5.1* (Table 2). There was strong linkage of *qtl1.3* and *qtl5.1* with resistance (χ^2 -test $p < 10^{-9}$, Table 2) showing that these are indeed the major C24 loci contributing to resistance to isolate Waco9. Notably, these loci appeared to overlap with the loss-of-resistance loci mapped with the BC approach. Of the remaining loci, one locus, *qtl3.1*, also showed linkage to resistance although much weaker compared to *qtl1.3* and *qtl5.1* (χ^2 -test $p = 0.003$, Table 2). Lines with C24 introgressions in the Col-0 background at both *qtl1.3* and *qtl5.1* were generated by crossing ILs N17 and N41 (both have *qtl1.3*) with IL N38 (*qtl5.1*). Also, Col-0 introgressions of *qtl1.3* and *qtl5.1* were combined in the C24 background by crossing IL M54 (*qtl1.3*) and IL M02 (*qtl5.1*). The two Col-0 lines with the double introgression of *qtl1.3* and *qtl5.1* (F3 N41xN38 C10 and F3 N38xN17 95-1) showed a high level of resistance to Waco9, similar to the resistant accession C24 (Figure 4), demonstrating that the C24 alleles at *qtl1.3* and *qtl5.1* in Col-0 are sufficient to confer strong resistance to Waco9. The resistance of the double introgression lines is stronger than that of the parental lines with the single introgressions (Figure 4), suggesting that the C24 alleles at the two loci can function additively by regulating two independent resistance mechanisms or act epistatically by enhancing each other's effect. The line A23 with *qtl1.3* and *qtl5.1* from Col-0 in the C24 background was susceptible to downy mildew although it did not reach the level of susceptibility of Col-0 (Tukey HSD $p = 0.06$, Figure 4). In contrast, the parental IL M02 (*qtl5.1*) and IL M54 (*qtl1.3*) had a strong level of resistance to *Hpa* Waco9 (Figure 4), suggesting that the Col-0 alleles of *qtl1.3* and *qtl5.1* genetically interact to confer susceptibility. Alternatively, the removal of one C24 QTL is not sufficient to significantly compromise resistance. Multiple lines of evidence, obtained from genetic analyses of BC5, F2 and double ILs, show that *qtl1.3* and *qtl5.1* are the major C24 resistance QTL against downy mildew isolate Waco9 that together confer strong quantitative resistance to this *Hpa* isolate.

Table 2. Linkage of C24 resistance QTL to full resistance in a F2 population C24xCol-0 *flc3*

Resistance locus	Allele enhancing resistance	# plants homozygous for Col-0 allele	# heterozygous plants Col-0/C24	# plants homozygous for C24 allele	Deviation from the segregation 1:2:1
<i>qtl1.1</i> (N=80)	C24	20	47	13	$\chi^2=3.68$, $p=0.16$
<i>qtl1.2</i> (N=83)	Col-0	22	44	17	$\chi^2=0.90$, $p=0.64$
<i>qtl1.3</i> (N=87)	C24	11	23	53	$\chi^2=59.88$, $p=10^{-13}$
<i>qtl3.1</i> (N=83)	C24	15	34	34	$\chi^2=11.41$, $p=0.003$
<i>qtl4.1</i> (N=86)	C24	18	38	30	$\chi^2=4.51$, $p=0.105$
<i>qtl5.1</i> (N=86)	C24	9	31	46	$\chi^2=38.54$, $p=10^{-9}$

***qtl1.3* is a partially dominant C24 resistance locus**

Previously we showed that the C24 allele of *qtl5.1* confers partially dominant resistance to Waco9, since the F1 hybrid N38xCol-0 was intermediately susceptible to the *Hpa* isolate compared to the parents IL N38 and Col-0 [94]. To test how *qtl1.3* is inherited, we scored the resistance of the F1 hybrid between Col-0 IL N41 (C24 *qtl1.3*) and Col-0 (Figure 5). The F1 hybrids had significantly higher sporulation levels than IL N41 but less than Col-0 (Sidak test $p<0.05$ for both comparisons) clearly demonstrating that the C24 allele of *qtl1.3* confers partially dominant resistance to the downy mildew isolate Waco9.

The intensity of sporulation of the F1 hybrid N41xN38 (both *qtl1.3* and *qtl5.1* are heterozygous) was not significantly different from the most resistant parent IL N38 (Sidak test $p=0.88$, Figure 5). Accordingly, the F1 hybrids between IL M54 and M02 heterozygous for *qtl1.3* and *qtl5.1* in the C24 background had a very low level of sporulation similar to the parental lines M54 and M02 (Figure 5). It suggests that plants heterozygous for the two partially dominant loci *qtl1.3* and *qtl5.1* are still able to mediate high but not complete immunity to *Hpa* Waco9 allowing for low sporulation levels. The conclusion that C24 resistance is compromised when *qtl1.3* or *qtl5.1* are heterozygous is also supported by the observation on the BC5 lines. Among the 48 BC5 lines, which were selected as partially susceptible to *Hpa* Waco9, we found 18 lines with both heterozygous *qtl1.3* and *qtl5.1* as well as 16 lines heterozygous *qtl1.3* but homozygous for C24 alleles at *qtl5.1* and ten BC5 lines heterozygous *qtl5.1* but homozygous for C24 alleles at *qtl1.3* (Table 1)

Discussion

Broad-spectrum resistance of Arabidopsis C24 to downy mildew is a multigenic trait, and some of the resistance loci confer full dominant resistance to *Hpa* isolates Emco5 and Noco2. In contrast, resistance of C24 to the isolate Waco9 does not involve single dominant loci but rather five QTLs that contribute to full immunity [94]. Here, we applied a BC approach to fine-map the major C24 loci mediating quantitative resistance to Waco9. The susceptible Arabidopsis accession Col-0 was backcrossed to C24 to eliminate the resistance loci, and a

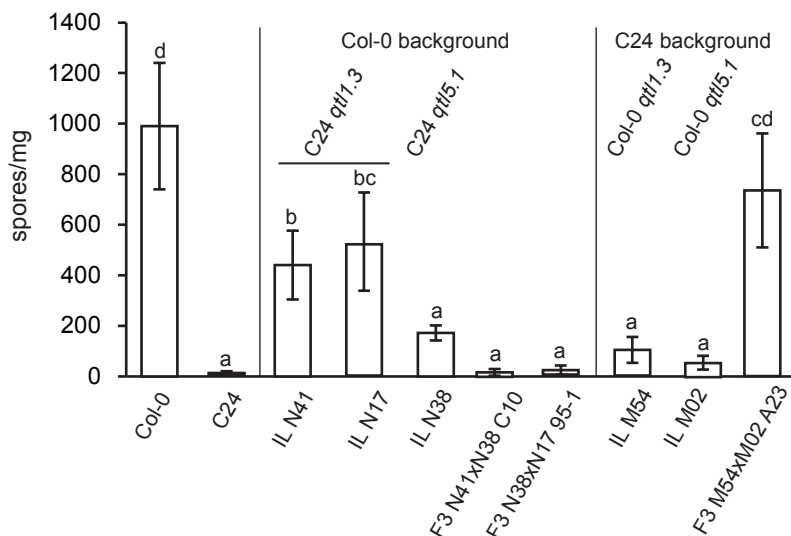


Figure 4. Resistance of Arabidopsis accessions C24, Col-0 and introgression lines with C24 and Col-0 alleles of *qt1.3* and *qt1.5.1* to the downy mildew *Hpa* Waco9 at 6 days post inoculation. Col-0 ILs N41 and N17 containing C24 introgression of *qt1.3* show partial resistance to downy mildew compared to Col-0. Similarly, Col-0 IL N38 with C24 *qt1.5.1* is partially resistant to *Hpa* Waco9 compared to the background parental line Col-0. The lines F3 N41xN38 C10 and F4 N38xN17 #95-1 have both *qt1.3* and *qt1.5.1* and are completely resistant to *Hpa*, however few conidiophores were occasionally observed. C24 ILs M54 and M02 have Col-0 introgressions at *qt1.3* and *qt1.5.1* respectively. These lines show full resistance with occasionally observed weak sporulation, in contrast to the fully resistant parental accession C24. However, the line F3 M54xM02 A23 with both *qt1.3* and *qt1.5.1* eliminated from the C24 genome is susceptible to the isolate Waco9; differences in *Hpa* susceptibility between Col-0 and F3 M54xM02 A23 are only nominally significant (Tukey HSD test, $p=0.06$). Significance of differences in the level of sporulation among lines was estimated with mixed ANOVA and Tukey HSD post-hoc test based on results of two independent experiments ($n=6$, $\alpha=0.05$). Letters indicate homogenous sets of genotypes as determined with Tukey HSD test ($\alpha=0.05$). Error bars represent \pm SE.

set of 48 susceptible BC5 lines was sequenced to identify the introgressed Col-0 susceptibility loci. WGS of the BC lines enabled the identification of two major loci of around 550-800 kb in size corresponding to the previously identified *qt1.3* and *qt1.5.1*. Combination of C24 alleles at these loci in the Col-0 background conferred near-complete resistance to the isolate Waco9. Similarly, introgression of the Col-0 loci *qt1.3* and *qt1.5.1* in the C24 background rendered plants susceptible to this isolate. Thus, our BC approach coupled to WGS revealed the combination of *qt1.3* and *qt1.5.1* as being the major contributor to quantitative resistance of C24 to *Hpa* Waco9.

Advantages of the BC mapping

The backcross mapping with selection for susceptibility in each generation has several advantages. Firstly, recombination events occurring on every chromosome accumulate over several backcross generations that allows for higher mapping resolution compared to mapping populations of the same size not derived by multiple backcrossing or intercrossing (e.g. F2, RILs). The resolution obtained in the BC5 generation is comparable to that of multiparental advanced intercrossed populations, which provide support intervals of several

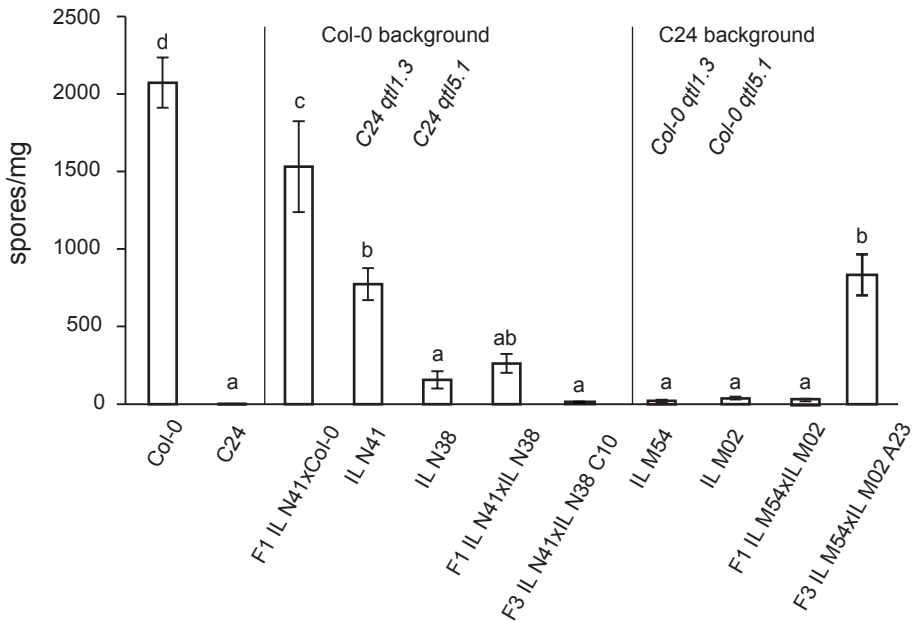


Figure 5. Resistance of Arabidopsis Col-0, C24, introgression lines (IL) in Col-0 background (IL N41, IL N38), IL in C24 background (IL M54, IL M02) and their F1 hybrids to the downy mildew pathogen *Hpa Waco9* at 7 days post inoculation. IL N41 with C24 allele of *qtl1.3* in Col-0 background shows significantly lower level of sporulation compared to Col-0, however the hybrid F1 IL N41xCol-0 has level of susceptibility intermediate between Col-0 and IL N41. The F1 hybrid between IL N41 and IL N38 (C24 *qtl5.1* in Col-0 background) demonstrates level of susceptibility similar to IL N38. IL M54 and M02 with Col-0 alleles of *qtl1.3* and *qtl5.1* in C24 background and their F1 hybrid M54xM02 have weak occasional sporulation of *Hpa Waco9*. Significance of differences between genotypes was estimated with mixed ANOVA followed by t-test with Sidak correction for multiple testing based on combined results of three experiments (n=6, $\alpha=0.05$).

hundred kb to several Mb [172, 199]. Secondly, effects of introgressed loci are tested multiple times since screening for the susceptibility phenotype is applied in each BC generation thereby enabling selection of major QTLs with reproducible effects on the phenotype. Thirdly, after detecting major loci enriched during backcrossing and selection for susceptibility, the backcross lines can be used to develop introgression lines for the QTLs of interest by selfing the advanced generation BC lines. Finally, populations derived by selfing of selected BC lines could be used to find recombinants in the mapping interval to further narrow-down the mapping intervals. Nevertheless, there are also disadvantages to the applied BC mapping method. Development of BC mapping populations is time- and labor-intensive. Also, the developed BC population is unlikely to be used to map other traits and cannot be maintained as an immortal inbred population. Based on our results and experience with the backcross approach we now suggest an optimal procedure for mapping complex multigenic traits in self-pollinating plants like Arabidopsis. It includes 3-4 rounds of backcrossing with selection for a given phenotype in each generation and identification of introgressed QTLs by WGS. After WGS, selected heterozygous BC lines containing loci of interest are selfed to obtain homozygous ILs with introgressed multiple QTLs. The same population after selfing can be used to select recombinants for QTLs of interest and perform further fine-mapping (SI Figure 3). Also, barcoding of sequencing libraries from different BC lines would provide significant WGS information, so that reads can be traced back to every individual BC line. This will then

allow straightforward detection of introgressed loci through counting of BC lines heterozygous at any given locus.

qtl1.3* and *qtl5.1* interact to confer strong resistance of C24 to *Hpa Waco9

In this study, we show that *qtl1.3* and *qtl5.1* in *Arabidopsis* C24 are major loci for quantitative resistance to downy mildew isolate *Waco9*. However, the C24 alleles of *qtl1.3* and *qtl5.1* individually only gave partial resistance, in contrast to the near-complete resistance observed when C24 alleles of the two loci are combined in Col-0. These findings suggest an interaction, or epistasis, between the two resistance loci. Gene interaction is a well-known biological phenomenon that is broadly understood as the dependency of gene expression on the genetic background. Epistatic interactions have been observed in quantitative disease resistance in natural plant populations [169, 170], however, the molecular mechanisms of the genetic interactions remain poorly understood. Several mechanisms are proposed to explain different cases of interaction between two genetic loci found in studies of yeasts, worms, mammals, and plants: (i) molecular recognition as in the case of hybrid necrosis, (ii) functional redundancy between genes, (iii) buffering between functional modules and pathways when, for example, genes encoding chaperones influence expression and penetrance of mutations, (iv) positive interaction in linear pathways, and (v) non-linear regulatory relationships. Finally, physical, chemical or developmental constraints may complicate quantitative measurement of phenotypic traits and thereby lead to erroneous declaration of epistasis [200]. Since individually *qtl1.3* and *qtl5.1* from *Arabidopsis* C24 confer only partial resistance in Col-0, it is likely that *qtl1.3* and *qtl5.1* function redundantly during the immune response of C24 to *Hpa Waco9*. Also, one QTL might be able to positively regulate expression of another, or even both QTLs could positively regulate each other. Ongoing fine-mapping and cloning of these C24 QTLs for resistance to *Hpa Waco9* is expected to reveal the molecular mechanism involved in quantitative resistance of *Arabidopsis* to downy mildew.

Acknowledgements

This project was made possible with a Technology Transfer Award of The Leverhulme Trust (UK) to G.V.d.A.

Supporting information

SI Table 1. Information on markers used in the study

Application of the marker	Name of the marker	Forward primer sequence (5'→3')	Reverse primer sequence (5'→3')	Type of marker***	Notes*
Validation of borders for C24 resistance locus on chromosome 1**	At1g60430	GGTGGCGATTC TCATGATCT	TCATGAACGTG- GTCGTCCTA	indel	PNR=65.6%
	At1g61890	CCATATTCGGG GAAACAAA	AGCCGCTTTT- GAAGCAATAA	indel	PNR=64.5%
	chr1_block25	GACCAAATGGAT- GAAAGAGCA	TGGTCGTTACAT- GGGTTTCA	indel	PNR=64.5%
	At1g62380	GTC AAGTTTCAGC- CCAAGGA	AGAAAGTCTC- TACGGCTGCTG	SNP	PNR=65.6%
Validation of borders for C24 resistance locus on chromosome 5**	At5g40940	CACCTTCTTCTTCTTG TTCTCCA	G G A T T G C T - GTTTCATGGCTTT	indel	PNR=71.9%
	At5g41250	TGTGTTCTTGAACAG- GAACTGAAT	C A C C G - GAATCTCCTA- CAACAA	indel	PNR=70.8%
	At5g41910	AGGGTTTTGAATCAC- GGAAA	G C G C C T G T - GATCTTCTTCTC	indel	PNR=70.8%
	At5g42500	CGATCATAATCACGC- CAAAA	TCTCCGGTGA- CAAACCTACC	SNP	PNR=71.9%
Checking linkage between centromeric and pericentromeric regions and C24 resistance	chr1_13Mb	A A C C C A T - CAAAATCTCTGTCTCA	GCTTGAGAGAAT- GAGGAGAAGAA	indel	PNR=87.8%
	chr4_2Mb	ATG A A G C A A A T G - GAGATGGA	AATGTGATTTGG- GGATTTGG	indel	PNR=98.9%
	chr5_10Mb	TGGCTCATGTTGAT- CAAGTACA	TGTTCTCTCCAT- CAGAGCATTG	indel	PNR=86.4%

Checking co-segregation between resistance and QTL in the population F2 C24x-Col-0 <i>flc3</i>	F6F3	GAGCTGAATCAG-GTTTTTCTCA	TTCTCAAC-GAACTCTTTTAA-ACCA	indel	<i>qtl1.1</i>
	F20D23 / T13M22	TCTCCGCATCTTGAT-CATTG	CGCAAAAAGCT-GAAGAACAA	indel	<i>qtl1.2</i>
	F16M22	AAGAGCATAAG-GAGCTCATGAAA	TCAGTTAGTG-CCTTGTCTCTGG	indel	<i>qtl1.3</i>
	MOB24	TTTAAACCGGC-GAACTCTGA	TGTGCATCATC-CGAGGTAAA	indel	<i>qtl3.1</i>
	FCAALL	TTGCTTGCTCTCAAC-GCTTA	GCCGTGGCG-TAGTAGTTTGT	indel	<i>qtl4.1</i>
	MQD19	AACCCTACAAAAAC-CCCAAAA	CGATGATCACAG-TAACGATTATCC	indel	<i>qtl5.1</i>
Selection of double ILS	chr1_block21	AAATTCACCATACGC-GTCCT	TCCAATTCTTG-CAAGGTGAA	indel	-
	chr1_block26	CGACATCTTCTGAT-GTGATAC	GGGAGCGTATTG-GCTCTCTT	indel	
	MQD19mod	C G A A A A C -CATATTTCTGAGCA	TGTCCAAGCAAT-TCCACAAA	indel	
	chr5_15957	ACATAGACATAGC-CGATCTCATTA	TCACACTAGCT-CAAACAAGTTC-TATT	indel	

*PNR="percentage of non-reference reads"

**only markers determining left and right borders of the locus are presented

***indel markers are PCR-based markers with difference in C24 and Col-0 DNA bands larger than 5 bp, separation of the PCR products typically on 3-4% agarose gel; genotyping with SNP markers is performed with high-resolution melting curve analysis (HRMA) with LightScanner® (Biofire, Utah, USA); protocol for HRMA is described in SI Note 1.

SI Table 2. Master mix for PCR before HRMA

Component	Final concentration
5x Phire® Hot StartII buffer	1x
dNTPs	200 nM each
Primers	250 nM each
DNA	~10 ng
Phire® Hot StartII polymerase	0.1 u
LC Green® Plus+	1x
mQ	to the final volume 10 µl

SI Table 3. Genetically determined borders of centromeres (based on [198])

chromosome	5' marker	3' marker	5' border BAC	3' border BAC	5' coordinate of the 5' BAC (TAIR10), bp	3' coordinate of the 3' BAC (TAIR10), bp	Marker in our study*
1	T22C23-t7	T3P8-sp6	F28L22	F5A13	14,083,487	15,697,825	chr1_13Mb
4	T24H24.3	F13H14-t7	T24H24	F28D6	1,913,792	4,263,015	chr4_2Mb
5	F13K20-t7	CUE1	F3F24	F19N2	10,927,735	12,662,612	chr5_10Mb

* sequences of the indel markers are presented in the SI Table 1

SI Note 1

Protocol for high-resolution melting curve analysis (HRMA) with the LightScanner®

HRMA is based on detecting differences between the melting curves of PCR products with different nucleotide sequence; in our lab, visualization of the melting process is achieved by using the fluorescent dye LC Green® Plus+ (Biofire, Utah, USA) which binds to the double-stranded PCR product. During melting of the PCR product, the dye is released reducing overall level of fluorescence. Fluorescence acquisition, analysis of melting profiles and genotype calling is performed with LightScanner® and software supplied with the scanner (Biofire, Utah, USA). Typically, primers were designed with Primer3 web application v. 0.4.0 [201] to amplify 50-120 bp product with SNP located in the middle of the amplified sequence. Annealing temperature (typically it is around 62°C) was selected based on the T_m's calculations recommended for amplification with Phire® Hot Start II polymerase (F122L, Thermo Fisher Scientific, MA, USA) (<http://www.thermoscientificbio.com/webtools/tmc/>). Components of the master mix are presented in the SI Table 2.

The reaction was covered with 20 µl mineral oil (M5904 or M8410, Sigma-Aldrich, MO, USA) to prevent evaporation of the PCR mix during amplification and the melting curve analysis. Conditions for PCR were as follows: 98°C – 30", 40-45 x (98°C – 5", Ta – 10", 72°C – 10"), 72°C – 1', 2 x (98°C – 30", 25°C – 30"). HRMA analysis was performed on the LightScanner® (Biofire, Utah, USA) according to the supplier recommendations (BIOKÉ, Leiden, The Netherlands). If differences between genotypes homozygous for SNP were not detected by HRMA, PCR product for a sample was mixed with PCR product for a reference (typically, Arabidopsis Col-0), heteroduplexes were formed again 2 x (98°C – 30", 25°C – 30"), and then the mixed PCR product was melted again; PCR products with heterozygous SNP normally have a melting profile different from a PCR product with homozygous SNP that allows genotyping of homozygous forms [202].

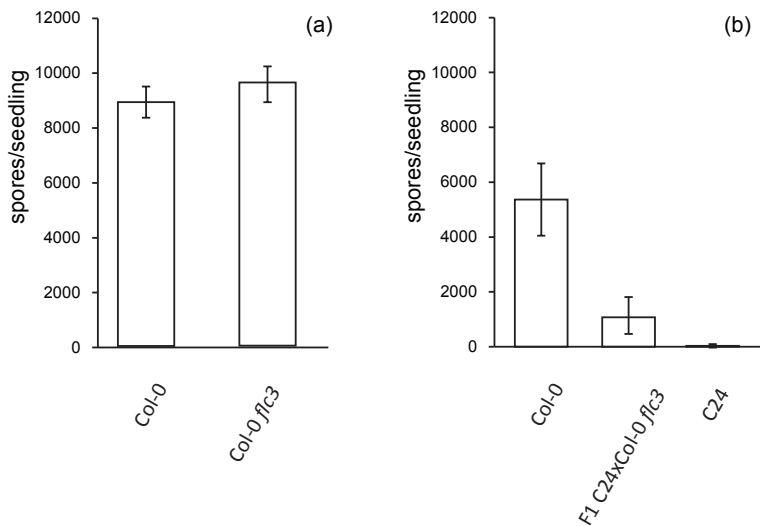
For HRMA, plant total genomic DNA was isolated with the CTAB method [145] or a column-based isolation method in GenElute™ Plant Genomic DNA Miniprep Kit (G2N70, Sigma-Aldrich, MO, USA) according to the manufacturer recommendations.

SI Note 2

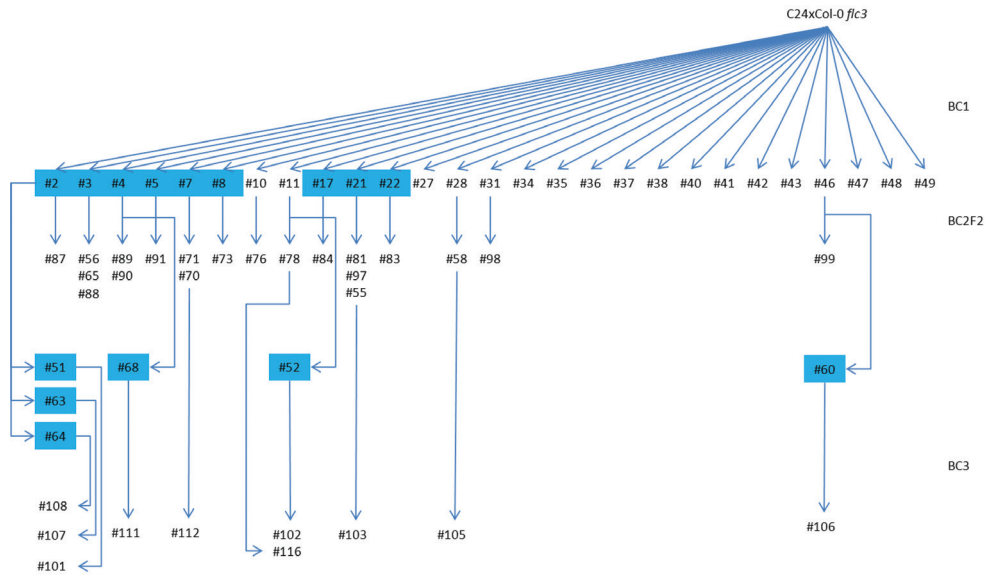
Validation of chromosome regions with reduced PNR levels, as revealed from the BC method

The analysis of sequence data for the BC5 population suggested presence of candidate resistance loci on intervals 21.9-23.2 Mb and 15.7-17.3 Mb of chromosomes 1 and 5 respectively (TAIR10 coordinates). Based on these proposed intervals we designed several SNP and indel markers inside and outside of the intervals. Markers which point to the left and right borders of the intervals are shown in SI Table 1. The 48 BC5 lines were genotyped for these markers, and PNR for each marker position was calculated as $PNR(\%) = 100 - \frac{\# \text{heterozygous lines}}{\# \text{lines} \times 2} \times 100\%$. Physical location of markers flanking intervals with minimal PNR

for the candidate resistance loci was considered as the interval for the resistance loci. We could conclude that candidate resistance loci selected during the BC scheme are located in the intervals 22,265-23,083 kb and 16,406-16,994 kb on chromosomes 1 and 5 respectively. Since in the analysis of BC sequence data, we observed reduction of PNR levels at chromosome regions around centromeres, it was decided to validate whether indeed these chromosome regions have PNR levels lower than expected 97%. For that, we genotyped 45 BC5 lines with indel markers for regions linked to genetically determined centromeres (around 1 Mb for chromosomes 1 and 5) or at the centromere (chromosome 4) (SI Table 4). For chromosome 4, PNR at the centromere was 98.9% (SI Table 1) suggesting that high variation in PNR level for SNPs detected at the centromeric and pericentromeric regions of chromosome 4 from sequencing data is likely caused by the technical challenges of sequence alignment at these positions but does not reflect reality. For chromosomes 1 and 5, instead of ~97% we observed PNR of around 87% that might be attributed to the genetic linkage between centromeres and the resistance loci *qtl1.3* and *qtl5.1*.



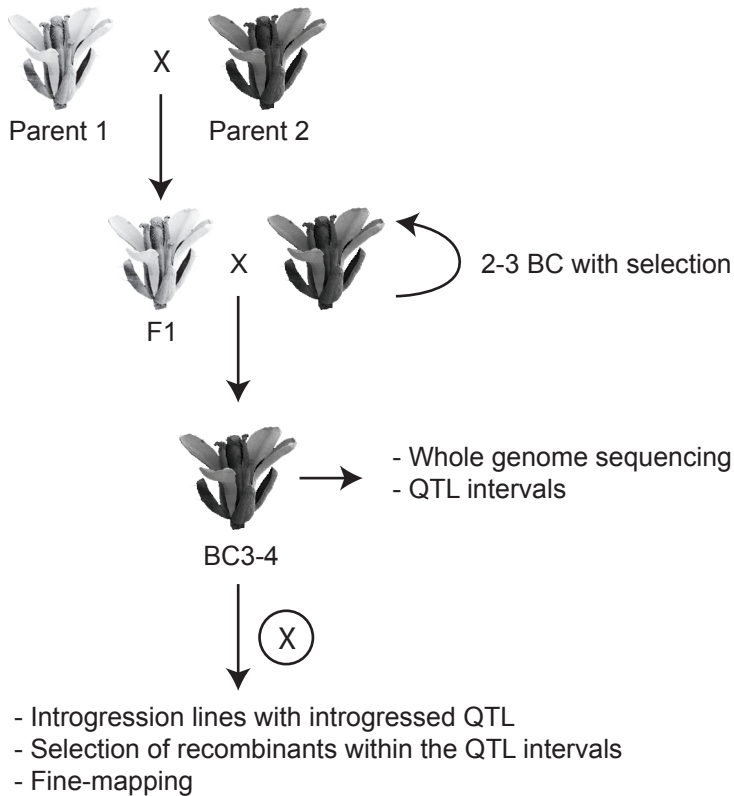
SI Figure 1. Resistance of Arabidopsis accessions Col-0 *flc3*, C24 and the hybrid F1 C24x-Col-0 *flc3* to *Hpa* isolate Waco9. (a) Col-0 and the *flc3* mutant in Col-0 background have similar levels of susceptibility to Waco9 (t-test $p=0.21$, $n=3$). (b) Arabidopsis C24 is resistant to *Hpa* Waco9, however Col-0 shows high level of susceptibility to *Hpa*. The hybrid F1 C24xCol-0 *flc3* is susceptible to *Hpa* Waco9, although less than the wild type Col-0 (t-test $p<0.01$, $n=3$). Error bars represent \pm SD. The experiments were repeated two times with similar results.



In total, 48 BC5 used for sequencing of 117 lines initiated at different steps of the BC procedure

 the line did not have susceptible seedlings in BC5

SI Figure 2. Development of susceptible Arabidopsis C24 backcross (BC) lines for fine-mapping of C24 resistance loci by whole genome sequencing. Initially, 50 independent BC1 lines from a cross C24x(F1C24xCol-0 *flc3*) were selected for susceptibility and crossed back to C24. However, already in the BC2 generation we could find susceptible seedlings only for 29 lines. Therefore, it was decided to select additional 50 susceptible seedlings from 14 BC2F2 populations and continue backcrossing. Furthermore, we selected additional 17 susceptible seedlings from BC3 (C24xBC2F2) populations, and continued the scheme. In total, we attempted to develop 117 BC lines, however susceptible seedlings were found only in 48 BC5 lines. Thus, the lines are not completely independent and have different degree of relatedness.



SI Figure 3. Proposed scheme for the efficient fine-mapping of quantitative trait loci (QTL) in natural accessions. Two inbred lines Parent 1 and Parent 2 with contrasting values of a phenotypic trait (e.g. resistance) are crossed to obtain F1 hybrids. The F1 plant is crossed back with the recurrent resistant Parent 2 which has a recessive or partially dominant trait. In the BC1, only susceptible progeny is selected and crossed to the Parent 2. BC3-4 lines are used for whole genome sequencing and finding QTL intervals. The BC3-4 lines with desired introgressions are selfed to fix the introgression and derive stable introgression lines. The same selfed BC populations are used to select for recombinants and further fine-mapping.

Chapter 4

Association mapping reveals a potential role for CYTOKININ RESPONSE FACTOR 1 in *Arabidopsis* susceptibility to downy mildew

Dmitry Lapin¹, Tracy Raines², Silvia Coolen¹, Richard Hickman¹, Marcel Van Verk¹, Saskia Van Wees¹, Guido Van den Ackerveken¹

¹ – Plant-Microbe Interactions group, Department of Biology, Faculty of Science, Utrecht University, Padualaan 8, 3584 CH Utrecht, The Netherlands

² - Department of Biology, University of North Carolina, Chapel Hill, North Carolina, United States of America

Abstract

Many known forms of natural resistance of *Arabidopsis thaliana* to downy mildew are controlled by *R*-genes coding for nucleotide binding site leucine-rich repeat proteins. These genes mediate immunity to one or several isolates of the downy mildew *Hyaloperonospora arabidopsidis* (*Hpa*). In addition, other forms of resistance, effective against all *Hpa* isolates, have been identified in mutant screens. However, very little is known about the genetic mechanisms contributing to natural non-isolate specific resistance to downy mildew. We, therefore, performed association mapping of *Arabidopsis* resistance/susceptibility to a mixture of four *Hpa* isolates. This approach revealed three candidate loci including *CYTOKININ RESPONSE FACTOR 1* (*CRF1*). Tomato and tobacco *CRF1* orthologs are known to affect plant immunity to bacterial pathogens. Our results show that higher level of *CRF1* mRNA in natural *Arabidopsis* accessions is correlated with enhanced susceptibility to the mixed *Hpa* infection. In addition, a knock-out mutant for *CRF2*, a close paralog of *CRF1*, demonstrated reduced sporulation of downy mildew. It indicates that *CRF1* and *CRF2* might positively regulate *Arabidopsis* susceptibility to *Hpa*.

Introduction

Plants are exposed to pathogenic microorganisms in natural and agricultural ecosystems and can be severely affected when successfully infected. The plant immune system, however, prevents most microorganisms from infecting by a range of defensive mechanisms. An important first layer of inducible defenses is triggered by recognition of conserved microbe-associated molecular patterns (MAMPs) such as bacterial flagellin or fungal chitin leading to MAMP-triggered immunity (MTI). However, adapted microbes use effector proteins to suppress the recognition of MAMPs allowing further establishment of the symbiotic interaction [203, 204]. To stop pathogen development, plants evolved a second layer of immunity relying, amongst others, on proteins with nucleotide binding and leucine-rich repeats domains (NLRs) which recognize pathogen effectors directly or sense manipulation of the plant immune system [120]. This recongnition leads to transcriptional reprogramming that is an essential part of the immune response resulting in resistance [205-208]. This second layer of defense is called effector-triggered immunity (ETI). Molecular signaling pathways and responses significantly overlap during MTI and ETI. Both immunity mechanisms involve production of reactive oxygen and nitrogen species [209, 210], and the activation of mitogen activated protein kinases MPK3 and MPK6 [211]. Also, both PTI induced by the MAMP flg22 and ETI triggered by the AvrRpt2

effector depend on the production of salicylic acid (SA), jasmonic acid (JA), the regulator of ethylene-induced immune responses *ETHYLENE* (ET) *INSENSITIVE 2* (*EIN2*) and the lipase-like protein *PHYTOALEXIN DEFICIENT 4* (*PAD4*) [212]. It is suggested that ETI is based on more robust and stronger activation of the defense-related pathways compared to MTI [213]. Significant overlap in molecular signatures of activated immune systems was found in different plant lineages [3, 4]. Experiments with transfer of immune receptors between different groups of flowering plants also suggest that molecular signaling pathways during MTI and ETI are similar among these plants. For instance, activity of the *ELONGATION FACTOR Tu RECEPTOR* (*EFR*) from *Arabidopsis thaliana* (*Arabidopsis* hereafter) responsible for sensing elongation factor Tu, which is a bacterial MAMP, and rice *FLAGELLIN INSENSITIVE 2* (*OsFLS2*) was preserved when these MAMP receptors were transferred between families of flowering plants [214, 215]. Similarly, heterologous expression of the barley NLR gene *MLA1*, which confers isolate-specific resistance to the powdery mildew fungus *Blumeria graminis* f. sp. *hordei* containing the cognate AVR_A effector, mediated isolate-specific resistance to the barley powdery mildew in an immuno-compromised *Arabidopsis* mutant [216]. These experiments clearly demonstrate that molecular MTI and ETI pathways downstream of pathogen recognition are significantly preserved in monocots and dicots. Evolutionary conservation of MTI and ETI and their convergence on the same signaling pathways suggests that genetic variation at the loci regulating the core plant immune system may affect resistance to unrelated pathogens or multiple isolates of the same pathogen, referred to as broad-spectrum resistance (BSR) [121]. Therefore, studies on genetic variation affecting the core plant immune system can lead to the identification of new components and mechanisms of BSR.

In addition to MTI and ETI, resistance of plants can be achieved via non-immunity related mechanisms, e.g. when plants do not support development of pathogen ([217], Chapter 1 of this thesis). For example, resistance to potyviruses in multiple plant species is caused by loss-of-function mutations in the plant translation initiation factor *eIF4E* and its homologs [106] that likely supports successful systemic spread of the viruses, as it was shown for tobacco etch virus infection in *Arabidopsis* [103]. Non-immunity related mechanisms of plant resistance can point to host processes supporting basic pathogen physiology. Therefore, genetic variation at plant susceptibility loci might affect the conserved aspects of pathogens development and, thus, lead to BSR.

Components of plant resistance mechanisms interact with each other so that gain of resistance to one pathogen can occur on the expense of enhanced susceptibility to another one. For example, barley *mlo* mutants with non-isolate specific resistance to the powdery mildew fungus *Blumeria graminis* f.sp. *hordei* show increased susceptibility to the hemibiotrophic fungus *Magnaporthe oryzae* [218, 219]. Also the *Arabidopsis* mutant *resurrection 1* (*rst1*) shows both increased resistance to the necrotroph *Botrytis cinerea* and enhanced susceptibility to the powdery mildew fungus *Golovinomyces cichoracearum* due to constitutive activation of JA-dependent defense reactions but suppression of SA-dependent immunity [220]. SA- and JA-induced signaling pathways, which positively regulate resistance against biotrophic and necrotrophic pathogens respectively, are well known to negatively affect each other [221]. These cross-talk mechanisms are manipulated by pathogens to increase plant susceptibility. The bacterial pathogen *Pseudomonas syringae* pv. *tomato* DC3000 (*Pst* DC3000) produces coronatine, a functional mimic of JA that negatively affects SA accumulation that is important for the immune response to biotrophic pathogens [7].

A well-studied biotrophic pathogen of *Arabidopsis* is the oomycete *Hyaloperonospora arabidopsidis* (*Hpa*), the causal agent of downy mildew [118]. Research on natural variation in *Arabidopsis* for resistance to downy mildew revealed multiple Toll-Interleukin receptor (TIR) and coil-coiled (CC) domains-containing NLRs that control resistance to specific *Hpa* isolates. For example, *Arabidopsis* Nd-0 contains the CC-NLR gene *RPP13* (for *RECOGNITION OF PERONOSPORA PARASITICA 13*) that specifically mediates resistance to *Hpa* isolates with the effector *ATR13* (*ARABIDOPSIS THALIANA RECOGNISED 13*) [222, 223]. Interestingly,

several natural *Arabidopsis* accessions have BSR to *Hpa*, however for the majority of these accessions genetic mechanisms of BSR are unknown. Previously, BSR of *Arabidopsis* C24 to downy mildew was shown to be mediated by different combinations of isolate-specific resistance loci [94].

To learn more about mechanisms regulating BSR of *Arabidopsis* to *Hpa* in nature, we looked for genetic variation in natural *Arabidopsis* populations associated with resistance to several downy mildew isolates. We expected that this genetic variation points to processes downstream of recognition of individual *Hpa* isolates or *Arabidopsis* loss-of-susceptibility loci. We inoculated >250 natural accessions from the core HapMap population [224, 225] with four *Hpa* isolates simultaneously. We applied both genome-wide (GWA) and locus-specific association mapping to identify candidate resistance loci. Three candidate loci, namely At5g53750...At5g53760/MILDEW LOCUS O 11 (*MLO11*), *STOMATAL CARPENTER 1* (*SCAP1*) and *CYTOKININ RESPONSE FACTOR 1* (*CRF1*), were found to be associated with susceptibility to the mixed *Hpa* infection. The *scap1* mutant and *SCAP1* RNAi silencing line showed reduced susceptibility to *Hpa* indicating that *Arabidopsis SCAP1* contributes to successful sporulation of downy mildew. Analysis of mutants suggested that the predicted APETALA 2/ETHYLENE RESPONSE FACTOR (AP2/ERF) TF gene *CRF1* and its close paralog *CRF2* regulate *Arabidopsis* susceptibility to *Hpa*. Further ongoing characterization of *CRF1* and *CRF2* might unravel novel mechanisms of *Arabidopsis* susceptibility to *Hpa*.

Materials and methods

Plant material and growth conditions

The mutants *mlo11-4*, *mlo11-4/14*, *mlo4/11-4/14*, *mlo11-5*, *mlo11-6*, *mlo11-3* [226], GABI_068G09 (*crf1-1*), SAIL_371_D04 (*crf2-2*) [227] and SAIL_1151_G06 (for the At5g53750 locus) were obtained from NASC [228, 229]. Primers for PCR-confirmation of T-DNA insertions were designed with the iSect tool [228]. Plants were grown at 21°C under long day (16h light/8h dark, light intensity 100-150 µmol/m²/sec) or short day conditions (10h light/14h dark, light intensity 100 µmol/m²/sec). To generate transgenic plants over-expressing *CRF1*, the coding sequence was amplified and cloned into the pK7FWG2 vector [230]. This placed *CRF1* under the control of the CaMV 35S promoter and fused it to the *GFP* gene (resulting in a C-terminal GFP tag). Transgenic plants were generated by the floral-dip method [231]. T1 lines were selected by plating surface sterilized seeds on 1x Murashige and Skoog (MS) agar with 1% sucrose containing 50 µg/ml kanamycin. Single copy transgene lines were obtained by observing the segregation ratios of the T2 lines and selecting lines exhibiting the Mendelian 3:1 ratio. For MeJA assays on plates, seedlings of Col-0, *crf1-1* and *CRF1* OX#1 lines were grown on 1x MS medium supplemented with 1% sucrose. Methyl jasmonate (MeJA) (M1068, TCI Europe N.V., Zwijndrecht, Belgium) was dissolved in 96% ethanol and added to the cooled medium to a final concentration 75 µM; the same volume of ethanol was added to medium in a control experiment. Trypan blue staining to reveal plant cell death in leaves of 3-4 week-old plants was done as described previously [146].

Downy mildew infection assays and quantification

The downy mildew *Hyaloperonospora arabidopsidis* (Gäum.) Göker, Riethm., Voglmayr, Weiss & Oberw. (*Hpa*) isolates Waco9, Noco2, Emco5 and Cala2 were maintained as described previously [109]. All infection assays were performed on eleven-day-old seedlings at 16°C under short day conditions (9h light/15h dark, light intensity 100 µmol/m²/sec, relative humidity 100%). For screening resistance of 259 HapMap *Arabidopsis* accessions to the mixed *Hpa* infection, inoculi of the four individual downy mildew isolates (50 conidiospores/µl) were mixed in a ratio 1:1:1:1. Resistance phenotypes were scored visually at seven days post inoculation (dpi) with a four-level scoring system: 1 - no sporulation; 2 - <15% of seedlings are sporulating; 3 - 15-80% of seedlings are sporulating; 4 - >80% of seedlings are

intensively sporulating. A resistance score was given for each Arabidopsis accession based on 20-40 seedlings per experiment. The experiment was performed twice, and the average resistance score of each Arabidopsis line was used as the phenotype for further analysis. All other infection assays were done with a single isolate Waco9 (50 conidiospores/ μ l) and levels of susceptibility were quantified by spore counting at 5-7 dpi. For experiments with the cytokinin 6-benzylaminopurine (6-BAP), plants were pre-treated with the hormone 48 hours before *Hpa* inoculation as previously described [232]. Treatment with MeJA (100 μ M of MeJA in water with 0.002% Silwet L77 (Van Meeuwen Chemicals BV, Weesp, the Netherlands)) was performed every day for five or three days or one day before *Hpa* inoculation; mock treatment included water with 0.002% Silwet L77. For the pre-treatment, solutions for MeJA and mock treatment were sprayed on seedlings in separate trays, and the trays were immediately closed and placed back to the long-day growth chamber. Statistical analysis was performed with IBM SPSS Statistics 20.

Association mapping

Broad-sense heritability (H^2) was calculated based on the variance components from ANOVA (IBM SPSS Statistics 20) $H^2 = V_G / (V_G + V_E / N)$, where V_G and V_E is variance of the susceptibility scores between and within accessions respectively and N is a number of biological replicates. Genome-wide association (GWA) mapping was performed with Kruskal-Wallis test in the GWAPP tool [233]. For GWA analysis, susceptibility scores of Arabidopsis after mixed *Hpa* inoculation in the 1-4 scale were transformed into binary scores: if the susceptibility score was < 1.5 the accession was considered resistant (on the binary scale, score 0) otherwise the line was considered susceptible (on the binary scale, score 1). Candidate loci were declared at SNPs with $-\log_{10}(P) \geq 5$, left and right borders of a candidate locus were located at most distant SNPs showing linkage disequilibrium (LD) $r^2 \geq 0.3$ with the most significant SNP.

For the locus specific association mapping, sequences from 142 natural Arabidopsis accessions were downloaded from the 1001 Genome project (<http://signal.salk.edu/atg1001/3.0/gebrowser.php>). The derived multiple alignments of candidate regions were used to identify polymorphic loci. Only polymorphic loci with a minor allele frequency (MAF) $> 5\%$ were utilized for the locus-specific association mapping with the Kruskal-Wallis test. For the *CRF1* locus, mapping was also performed using the EMMA package [234] with correction for the population structure based on the kinship matrix calculated from all polymorphic loci in the locus. False discovery rate correction was applied to the raw p-values to correct for multiple testing [191]. Locus-specific association mapping was implemented in the R environment [192]. Conversion between nucleotide sequence formats was done with Jalview [235].

Linkage disequilibrium (r^2) between $\sim 10\%$ of SNPs used for the locus-specific association mapping at three candidate loci *At5g53750...MLO11*, *CRF1* and *SCAP1* (MAF $> 5\%$) was calculated with TASSEL [236]. The LD decay plot was obtained by plotting r^2 values versus distance between corresponding SNPs with a hexagon binning procedure implemented in the *hexbin* package [237]. r^2 values were fitted against the distance between SNPs (r^2 -distance) using the R function *loess()* for local polynomial regression fitting with the smoothing value span=0.4 [192].

Quantification of CYTOKININ RESPONSE FACTOR 1 (CRF1) mRNA levels

For the analysis of *CRF1* mRNA levels in different Arabidopsis accessions (SI Table 6), eleven-day-old seedlings were sprayed with water and placed in the growth chamber for *Hpa* infection assays; three days later around 100 mg of seedlings from each accession was collected. Total RNA was isolated with the Spectrum™ Plant Total RNA Kit (Sigma, St. Louis, MO, USA). The isolated RNA was treated with DNase I, RNase-free (Thermo Scientific, Waltham, MA, USA), and the first DNA strand was synthesized with RevertAid H Minus Reverse Transcriptase (Thermo Scientific, Waltham, MA, USA). All these procedures were performed according to the manufacturers' recommendations. Primers for the quantitative real-time (qRT) PCR

are shown in the SI Table 5. For qRT-PCR, we used SYBR® Green PCR Master Mix (Life Technologies Corporation, Carlsbad, CA, USA). The *CRF1* and *PR-1* mRNA levels were normalized to the Arabidopsis reference gene *ACTIN2* (SI Table 4) with the $2^{-\Delta C_t}$ method.

Measurement of chlorophyll and anthocyanin levels in seedlings

To measure chlorophyll and anthocyanin, a previously described method [238] was slightly modified. Briefly, 10-30 mg of seedlings without roots were ground in 1 ml of MeOH with 1% HCl and incubated overnight at 4°C or for two hours at room temperature. Absorbance at 530 and 657 nm corresponding to absorbance of anthocyanin and chlorophyll was measured for their quantification and normalized to the fresh weight of ground plant material.

Results

Association mapping of Arabidopsis resistance/susceptibility to downy mildew

Previously it was shown that resistance of Arabidopsis to individual *Hpa* isolates is mainly controlled by *R*-genes encoding NLR proteins [138]. By inoculating the multiple Arabidopsis accessions with a mix of spores of different downy mildew isolates at the same time, we expected to reduce the effect of isolate-specific resistance loci and evaluate non-isolate specific susceptibility of Arabidopsis accessions to *Hpa*. We performed simultaneous inoculation of 259 Arabidopsis accessions from the core HapMap collection with a mixture of conidiospores from four *Hpa* isolates: Waco9, Emco5, Noco2, and Cala2 that are known to be recognized

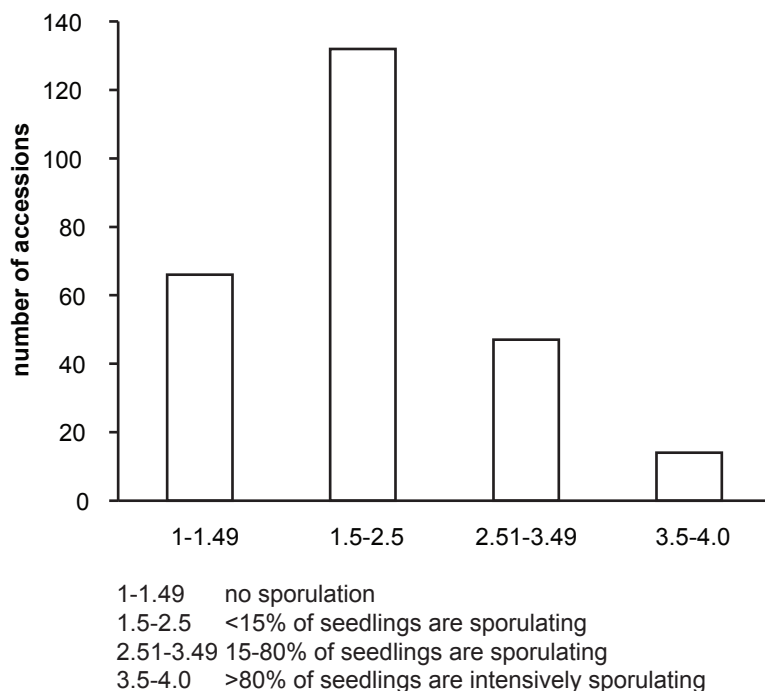


Figure 1. Distribution of 259 natural Arabidopsis accessions from the HapMap collection in phenotypic classes after mixed infection with several isolates of the downy mildew *Hpa*. The disease severity was scored at 7 days after inoculation based a four-level scoring system, where fully-resistant accessions without sporulation have a score 1, and intensively sporulating accessions have a score 4. Three quarters of the tested Arabidopsis accessions are found to be susceptible to the mixed *Hpa* infection.

by different *RPP* loci. The majority of the tested accessions (75% or 193 accessions) were susceptible to the mixed infection, and 66 genotypes were either fully resistant or slightly susceptible showing sparse sporulation on a few seedlings (Figure 1, SI Table 1). We checked how susceptibility of *Arabidopsis* to individual isolates relates to susceptibility to the infection with a mixture of *Hpa* isolates. More than 50 accessions from our screen were previously tested for resistance to several individual *Hpa* isolates including Noco2, Emco5 [107] and Cala2 [136]. We additionally tested resistance of these accessions to the *Hpa* isolate Waco9 (SI Table 2). Although correlation was found between susceptibility to the mixed infection and infection with individual isolates (Spearman's correlation coefficient $\rho \leq 0.46$, $p = 0.14 \dots 0.01$, SI Table 3), the strongest correlation was found between *Arabidopsis* susceptibility to mixed infection and the susceptibility score calculated as a mean of susceptibility scores after *Arabidopsis* infection with the four individual isolates Waco9, Emco5, Noco2 and Cala2 ($\rho = 0.65$, $p < 10^{-4}$, SI Table 3). This suggests that in the case of mixed infection defense against incompatible isolate(s) did not substantially affect susceptibility to the compatible isolate(s). The broad-sense heritability (H^2) of the susceptibility after the mixed infection in the tested *Arabidopsis* population was 0.83 indicating a strong contribution of genetic factors to the observed variation that could potentially be mapped with association mapping. All accessions with a mean susceptibility score < 1.5 were considered resistant and accessions with the score ≥ 1.5 – susceptible. GWA mapping with 242 accessions on the derived binary phenotypic data revealed fourteen candidate loci associated with susceptibility to *Hpa* ($-\log_{10}p \geq 5$, SI Figure 1). GWA run with untransformed data produced lower $-\log_{10}p$ values (not shown). To independently validate identified associations between SNPs and susceptibility to *Hpa*, we performed locus-specific association mapping using sequences available for 142 *Arabidopsis* accessions. Alignment of the complete sequences from different accessions provides more polymorphic markers compared to SNP data present in the GWAPP tool that could, therefore, increase resolution of mapping. In the locus-specific association mapping, we used 142 accessions instead of 242 accessions in GWA mapping. The lower number of accessions could reduce power of the locus-specific association mapping to detect significant associations. Thus, if a candidate locus is found as associated in genome-wide mapping but not in the locus-specific mapping procedure, it is likely that it is false positive or has weak additive effect which is difficult to validate experimentally. On the other hand, if a locus found in the genome-wide mapping was confirmed in the locus-specific association mapping, one has higher confidence that this locus is indeed associated with susceptibility. Also, for the locus-specific association mapping, we used susceptibility scores on the scale 1 to 4 in contrast to the binary scores in GWA scan to eliminate the effect of scoring system on our mapping results. For the locus-specific association mapping, a haploblock with SNPs associated in GWA ($-\log_{10}p \geq 5$) was considered as a candidate locus, i.e. borders of the candidate locus were defined as SNPs located up- and downstream of SNP, most significantly associated in GWA, and showing linkage disequilibrium (LD) with this significantly associated SNP ($r^2 = 0.3$ cut-off, GWAPP tool). Out of fourteen candidate loci revealed in the GWA, only three loci were associated with resistance to *Hpa* in this locus-specific association mapping (SI Figure 2, the cut-off value $-\log_{10}p = 4.0$, Kruskal-Wallis test): the interval At5g53750..At5g53760/AtMLO11 (Kruskal-Wallis test, $-\log_{10}p = 4.95$, FDR=0.0003), the locus At5g65590/SCAP1 (Kruskal-Wallis test, $-\log_{10}p = 4.79$, FDR=0.0595), and the locus At4g11130..At4g11140/CRF1 (Kruskal-Wallis test, $-\log_{10}p = 4.27$, FDR=0.1642; EMMA, $-\log_{10}p = 4.57$, FDR=0.2414). With marker data used for the locus-specific association mapping, we calculated extent of LD (measured as r^2) for these three loci in the population of 142 *Arabidopsis* accessions to estimate resolution of the locus-specific mapping (SI Figure 3). Average fitted r^2 value dropped approximately 2.5 times from 0.16 to 0.06 on the 5 kb interval between markers that is similar to previous estimates of LD decay in *Arabidopsis* [239]. Thus, application of locus-specific association mapping based on sequencing information confirmed several loci identified in our GWA screen resulting in a mapping resolution of several kilobase pairs that could facilitate the identification of causal polymorphisms.

Functional analysis of *CYTOKININ RESPONSE FACTOR 1* and *STOMATAL CARPENTER 1*

To verify whether the identified loci contribute to downy mildew susceptibility in Arabidopsis, we tested mutants and overexpression lines for the associated genes. MILDEW LOCUS O 11 (*MLO11*) belongs to a family of transmembrane proteins similar to the barley *MLO*, and barley *mlo* mutants confer broad-spectrum resistance to the powdery mildew fungus [97]. In Arabidopsis, the triple mutant *mlo2/6/12* is also resistant to the powdery mildew *Golovinomyces orontii* but not to the downy mildew *Hpa* [99]. We checked whether mutations in *MLO11* and its close paralogs *MLO4* and *MLO14* affect Arabidopsis resistance to *Hpa*. Several *mlo11* mutants, the triple mutant *mlo4/11/14* and the double mutant *mlo11/14* were not different in the level of sporulation of *Hpa* Waco9 from the wild type Col-0 (not shown). The gene At5g65590 known as *STOMATAL CARPENTER 1* (*SCAP1*) encodes for the plant-specific Dof-type transcription factor (TF) essential for the development of guard cells in stomata [240]. The *scap1* mutant and the RNAi silenced line RNA #8-2 showed slightly reduced susceptibility to *Hpa* Waco9 compared to the wild type Col-0 (Tukey HSD $p=0.01$ and $p=0.04$ respectively, Figure 2). These data further indicate a role of the GWA-identified *SCAP1* gene in the infection of Arabidopsis by downy mildew.

CYTOKININ RESPONSE FACTOR 1 (*CRF1*) is a member of the CRF clade within the family of AP2/ERF TFs. Experiments with overexpression of *CRF1* orthologs from tomato and tobacco suggest that these proteins affect plant immune responses [241, 242], however a role of Arabidopsis *CRF1* in susceptibility to downy mildew is unknown, and we, therefore, further focused our study on the *CRF1* gene. The Arabidopsis *crf1-1* mutant did not show a significantly altered level of sporulation compared to Col-0 (Figure 3b). In contrast, a *CRF1* overexpression line (OX #1) was significantly more resistant to downy mildew compared to the wild type (t-test, $p<0.05$, Figure 3a). Several additional independent T4 *CRF1* OX lines showed slightly elevated resistance, although not significant compared to Col-0 (Figure 3c, t-test $p=0.17\dots0.52$). We noticed that leaves of all 3-4 week-old uninfected *CRF1* overexpression lines grown under both short and long-day conditions displayed elevated cell death, visible as trypan blue stained patches that was not observed in the wild type Col-0 and the *crf1-1* mutant (Figure 3d). In addition, the plants of the overexpression lines showed reduced rosette growth and were chlorotic (Figure 3d) indicating that *CRF1* overexpression

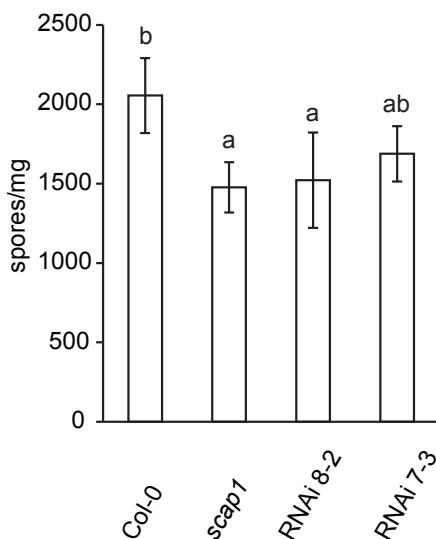


Figure 2. Sporulation of the downy mildew *Hpa* isolate Waco9 at 6 days post inoculation on the *SCAP1* RNAi silenced lines RNAi 8-2, RNAi 7-3 and the *scap1* mutant. The mutant *scap1* and the RNAi silencing line RNAi 8-2 showed slightly reduced levels of *Hpa* sporulation ($p=0.01$ and $p=0.04$ respectively) compared to the wild type Col-0. Results of three independent experiments were analyzed with mixed ANOVA followed by Tukey HSD post-hoc test. Letters indicate homogeneous subsets of genotypes at $\alpha=0.05$ ($n=8$). Error bars represent \pm SE.

leads to spontaneous cell death and retardation of *Arabidopsis* growth. The OX#1 line that shows partial resistance to *Hpa* had the similar extent of cell death patches as the other OX lines, indicating that cell death in the uninfected leaves of *CRF1* overexpression lines does not correlate with resistance to *Hpa*.

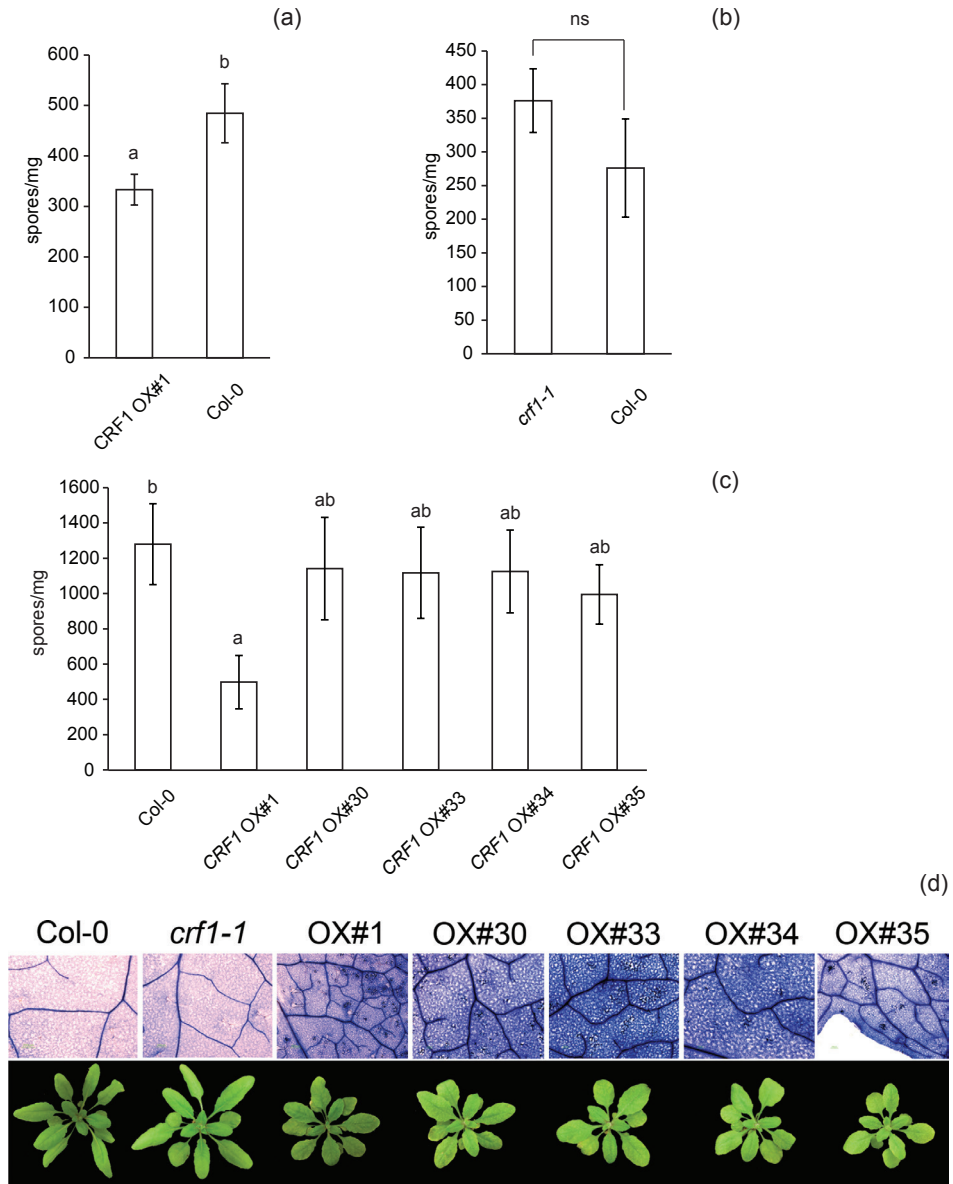


Figure 3. Resistance of Col-0, *crf1-1* and *CRF1* overexpression lines to downy mildew. (a and b) The homozygous T4 *CRF1* overexpression line OX#1 supported lower sporulation level of the downy mildew isolate Waco9 at 5 days post inoculation (dpi) as compared to the wild type Col-0 (t-test, $p < 0.05$, $n = 3$, experiment was repeated twice), however differences

***CRF1* is not required for cytokinin-induced susceptibility and resistance of Arabidopsis to downy mildew**

Cytokinins (CKs) are known to have either positive or negative effect on Arabidopsis resistance to downy mildew at higher or lower concentrations, respectively [232]. We hypothesized that effect of CKs on Arabidopsis susceptibility to *Hpa* involves *CRF1* that is known to translocate to the nucleus after CK treatment [227]. The wild-type Col-0, the *crf1-1* mutant and *CRF1* OX#1 plants were inoculated with *Hpa* isolate Waco9 after treatment with 6-BAP, which is a commonly used CK (Figure 4). At a concentration of 100 μ M, the CK treatment induced resistance to *Hpa* in wild type Col-0 plants. Similarly to the wild type Col-0, the CK treatment induced resistance in both the *CRF1* OX#1 and *crf1-1* lines, and the level of resistance between the genotypes was not significantly different (mixed ANOVA, t-test $p > 0.05$, Sidak correction). At a much lower concentration of 100 nM, 6-BAP treatment caused enhanced susceptibility of the wild type Col-0 plants. Also the *CRF1* OX#1 and *crf1-1* plants were more susceptible to isolate Waco9 than the mock control. Again, we did not find significant differences between lines in the level of susceptibility after pretreatment with 100 nM 6-BAP (mixed ANOVA, t-test $p > 0.05$, Sidak correction). Therefore, *CRF1* is likely not required for CK-induced resistance or susceptibility of Arabidopsis to *Hpa*.

Susceptibility to *Hpa* positively correlates with *CRF1* mRNA levels

In the locus-specific association mapping for the *CRF1* locus, the most significant associations with the level of susceptibility were not found in the protein coding sequence but in the up- and downstream sequences (SI Figure 4a). Analysis of a multiple alignment of *CRF1* upstream sequences obtained from the 1001 Genome browser showed that a large 2.5-3.0 kb region on chromosome 4 is poorly assembled or missing in multiple Arabidopsis accessions with enhanced susceptibility to mixed infection. We sequenced the region with potential insertion/deletion (indel) mutations in four resistant and nine susceptible accessions (SI Note 1). It appeared that the four resistant accessions with phenotypic score 1.0 have a ~230 bp insertion that is absent in most of the susceptible accessions (SI Figure 4b, indel 1 locus). At the same time, nine susceptible accessions with the phenotypic score ≥ 3 had a ~300 bp insertion that was absent in the reference line Col-0 and all four resistant accessions (SI Figure 4b, indel 2 locus). To verify whether these two rearrangements are found within the poorly aligned or missing region upstream of *CRF1* in other Arabidopsis accessions, we picked 21 additional accessions with or without potential rearrangement relative to Col-0 reference genome as indicated by data in 1001 Genome browser; then the accessions were genotyped using primers spanning indels 1 and 2 loci (SI Table 5, SI Figure 5). In total, all fifteen tested resistant accessions had an insertion at the indel 2 (similarly to the susceptible reference Col-0) and fourteen of them had a deletion at the indel 1. On the other hand, among nineteen susceptible accessions, seventeen (except for Col-0 and Utrecht) had a deletion at the indel 2 and but did contain insertion of variable size at the indel 1 (SI Figure

Figure 3 (continuation) in the spore count were not significant between the *crf1-1* mutant and Col-0 (t-test, $p > 0.05$, $n = 3$, the experiment was repeated three times). (c) Sporulation of Waco9 on several independent *CRF1* overexpression lines at 6 dpi. The T4 *CRF1* OX lines ##30, 33, 34 and 35 did not show consistently elevated resistance to *Hpa* visible as reduced spore count compared to the wild type Col-0, in contrast to the OX#1 line (mixed ANOVA, Bonferroni test $p = 1.0$, $n \geq 7$). For panels a, b and c, different letters mark significant differences in the genotype means ($\alpha = 0.05$). Error bars represent \pm SD. (d) Trypan blue staining of leaves from 3-4 weeks-old plants grown under short day condition. Dead cells are visible as patches with intensive blue staining. The wild type Col-0 and the *crf1-1* mutant do not have visible symptoms of cell death, however leaves of *CRF1* overexpression lines have signs of spontaneous cell death. This occasional cell death is readily observed as necrotic spots on the edges of mature leaves from the overexpression lines grown under both short- and long-day conditions (not shown).

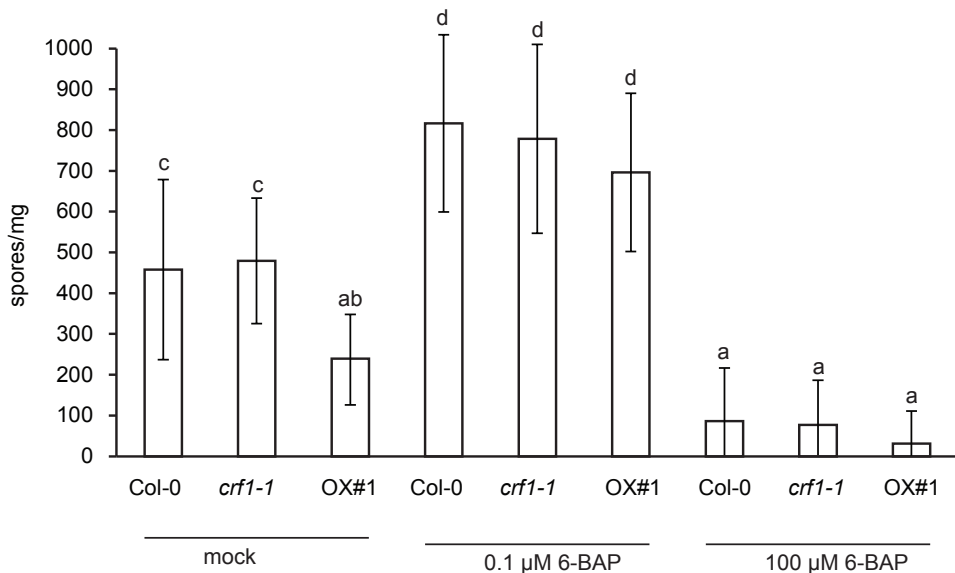


Figure 4. Effect of *CYTOKININ RESPONSE FACTOR 1* (*CRF1*) on cytokinin (CK)-induced resistance or susceptibility of Arabidopsis to the downy mildew *Hpa* Waco9. The commonly used CK, 6-benzylaminopurine (6-BAP), was applied 48 hours before *Hpa* inoculation. At the concentration 100 μM, pretreatment with 6-BAP led to a strong reduction of sporulation in all tested lines (Sidak test, $p < 0.05$). In contrast, at the low concentration, CK treatment enhanced sporulation of *Hpa* in all lines (Sidak test, $p < 0.05$). Results of four independent experiments were combined and analyzed with mixed ANOVA considering an experiment as a random factor, post-hoc t-test p-values were corrected for multiple testing through the Sidak correction ($n \geq 9$). Error bars represent \pm SD.

5). Thus, among 34 genotyped Arabidopsis accessions, enhanced susceptibility to mixed *Hpa* infection is associated with an insertion at the indel 1 and a deletion at the indel 2 loci in the *CRF1* upstream region. Given that in the population of 142 Arabidopsis accessions the most significant associations were found in the *CRF1* up- and downstream regions and not in the *CRF1* protein coding sequence, it is possible that susceptibility to *Hpa* is associated with different levels of the *CRF1* transcription in resistant and susceptible accessions. To test that, we determined the level of *CRF1* mRNA in uninfected seedlings of the genotyped 34 Arabidopsis accessions with or without insertions at the indel 1 and indel 2 loci (Figure 5). In the uninfected seedlings grown under conditions used for the *Hpa* infection assays *CRF1* mRNA levels positively correlated with susceptibility of different Arabidopsis accessions (Figure 5a, $\rho = -0.495$ between Δ Ct values and susceptibility score, $p = 0.008$) suggesting that *CRF1* negatively regulates Arabidopsis resistance to *Hpa*. Also, accessions with a deletion at the indel 2 in the *CRF1* upstream region, which was associated with enhanced susceptibility to the mixed infection, had significantly higher level of *CRF1* mRNA (Figure 5b, two-tailed t-test, $p = 0.003$).

Does *CRF1* have a role in jasmonate-induced susceptibility to downy mildew?

To identify gene regulatory networks controlling defense signaling pathways in Arabidopsis, a large-scale transcriptome profiling experiment was initiated in which four-week-old Col-0 plants were treated with MeJA, SA and the combination of the two hormones in a time-course of 16 hours with fifteen time points. The genome-wide abundance of transcripts was determined with RNAseq (Van Verk *et al.* in preparation). In this experiment, *CRF1* was transcriptionally

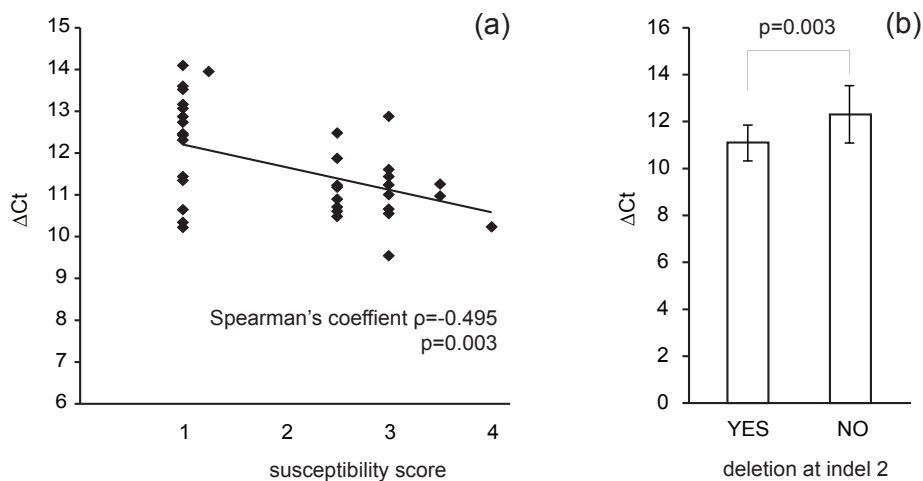


Figure 5. CYTOKININ RESPONSE FACTOR 1 (*CRF1*) mRNA levels in natural *Arabidopsis thaliana* accessions. *CRF1* mRNA relative to the *ACTIN2* reference gene was measured in non-infected seedlings of 34 *Arabidopsis* accessions with different levels of susceptibility to the mixed inoculation with the downy mildew *Hpa*. (a) The phenotype score 1 corresponds to full resistance, and 4 to full susceptibility. Levels of susceptibility positively correlated with the level of *CRF1* expression (Spearman's rank correlation coefficient $\rho = -0.495$ $p = 0.003$ between the phenotype score and $\Delta Ct = Ct_{CRF1} - Ct_{ACT2}$). (b) *Arabidopsis* accessions with the deletion in the indel 2 locus in the *CRF1* promoter had a higher average level of *CRF1* mRNA (or lower ΔCt) compared to the average level for accessions without this deletion (two-tailed t-test $p = 0.003$). Error bars represent $\pm SD$. Accessions were treated as technical replicates. The experiment was performed three times with similar results.

induced more than 2 times in the first hour after methyl jasmonate (MeJA) treatment, and *CRF1* was co-regulated with a cluster of genes with significantly overrepresented JA-related gene ontology terms (SI Figure 6, $p < 10^{-4}$, Bonferroni correction, Van Verk *et al.* in preparation). These observations prompted us to investigate the effect of *CRF1* on jasmonate signaling in *Arabidopsis*. Treatment of *Arabidopsis* seedlings with MeJA causes accumulation of anthocyanin, inhibition of primary root growth and chlorosis. We tested if the *CRF1* OX line #1 and the *crf1-1* mutant show altered responses to this hormone compared to the wild type Col-0 (Figure 6). As expected, MeJA treatment led to reduced primary root growth and increased anthocyanin levels in all tested lines (Figure 6a and 6b). Differences between Col-0, *CRF1* OX#1 and *crf1-1* within treatments were not significant except for slightly higher level of anthocyanin in *crf1-1* after MeJA treatment compared to *CRF1* OX#1 (Tukey HSD, $p = 0.01$). The three tested lines also had decrease in chlorophyll content in response to MeJA treatment (Figure 6c). Interestingly, seedlings of the *CRF1* OX line #1 were more chlorotic as compared to the *crf1-1* mutant and the wild type Col-0 (Tukey HSD, $p < 0.05$). Based on these results, we hypothesized that *CRF1* influences resistance to *Hpa* by affecting jasmonate signaling in *Arabidopsis*. To test this idea, we checked whether MeJA treatment is able to alter resistance of *Arabidopsis* to *Hpa* and whether this involves *CRF1*. The mutant *crf1-1* and the wild type Col-0 seedlings were pretreated with 100 μM MeJA five, three or one consecutive days before *Hpa* inoculation and checked for differences in sporulation at 5 dpi (Figure 7). All MeJA treatments enhanced susceptibility of both Col-0 and *crf1-1* to Waco9 compared to the mock-treated seedlings, however differences between the genotypes were not significant (Tukey HSD, $p < 0.05$). These results show that MeJA enhances susceptibility of *Arabidopsis* to *Hpa* however there is no evidence for a role of *CRF1* in this process.

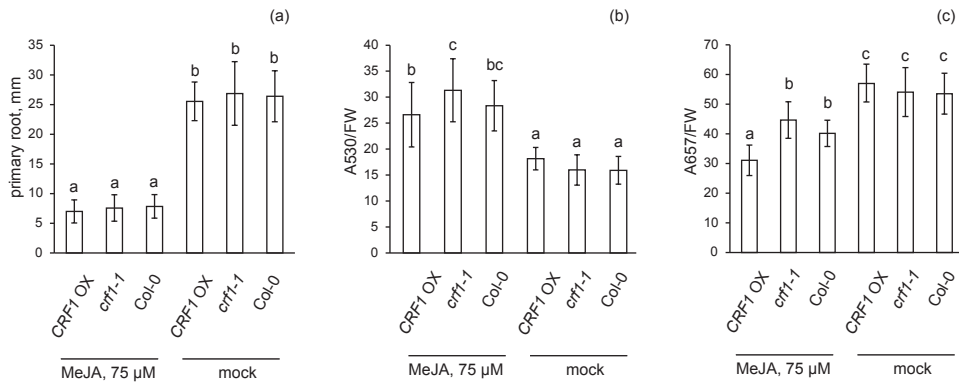


Figure 6. Responses of mutant *crf1-1*, *CRF1* overexpression line OX#1 and the wild type Col-0 seedlings grown for 8 days on MS plates containing methyl jasmonate (MeJA) at a concentration 75 μM compared to control plates without MeJA. (a) Primary root growth was significantly reduced in all tested lines following MeJA treatment compared to the mock-treated seedlings (Tukey HSD, $\alpha=0.05$). (b) Anthocyanin, measured as absorbance of plant extracts at 530 nm, was significantly increased in Col-0, *crf1-1* and *CRF1* OX#1 plants and differences between the lines were not significant (Tukey HSD, $\alpha=0.05$). (c) Chlorophyll levels, measured as absorbance of plant extracts at 657 nm, were reduced in all seedlings grown on the MeJA supplemented plates. Measured chlorophyll content was lower in the *CRF1* OX#1 line compared to Col-0 and the *crf1-1* mutant (Tukey HSD $p<0.001$). Results of three independent experiments were combined and analyzed with mixed ANOVA followed by Tukey HSD test ($\alpha=0.05$, $n=9$). Error bars represent \pm SD.

Arabidopsis *crf2-2* shows enhanced resistance to *Hpa*

CRF1 has a close homolog in the Arabidopsis genome, *CRF2* [227] that might have a similar activity as *CRF1* in Arabidopsis susceptibility to *Hpa*. Therefore the *crf2-2* mutant was tested for susceptibility to the downy mildew Waco9. The mutant showed reduced sporulation of *Hpa* compared to the wild type Col-0 (Figure 8, Bonferroni test, $p=0.004$) suggesting that *CRF2* plays a role in Arabidopsis susceptibility to downy mildew. According to publicly available microarray data visualized with Genevestigator [243], *CRF2* shows more dynamic transcriptional changes compared to *CRF1* during different biotic stresses, after treatment with elicitors/MAMPs, and following hormone treatment (SI Figure 7a). Notably, *CRF2* mRNA levels are reduced after inoculation with biotrophic and hemibiotrophic pathogens, e.g. downy and powdery mildews, *Pst* DC3000. Also SA application reduced *CRF2* mRNA levels, which was confirmed in the RNA-seq experiment (Van verk *et al.*, in preparation, SI Figure 7b). *CRF2* is transcriptionally induced after treatment with MeJA and infection with the necrotroph *Alternaria brassicicola* (SI Figure 6a), however in the RNA-seq experiment, *CRF2* did not show transient accumulation of transcripts following the MeJA treatment (SI Figure 7b). Thus, *CRF2* might be functioning redundantly with *CRF1* in the MeJA-induced susceptibility of Arabidopsis to downy mildew. Currently, we generating a *crf1-1/crf2-2* double mutant to be tested for susceptibility to downy mildew after treatment with MeJA.

Discussion

Naturally occurring BSR of Arabidopsis to downy mildew was found in several Arabidopsis accessions such as C24 and RLD [139]. Our previous study on the genetic analysis of C24 resistance to several *Hpa* isolates revealed that C24 BSR is not controlled by a single locus; instead, different combinations of isolate-specific resistance loci are responsible for that [94].

In this study we aimed to identify novel genetic loci that contribute to natural Arabidopsis resistance to downy mildew in the non-isolate specific manner. It is known from previous work that resistance of natural Arabidopsis accessions is strongly associated with gene clusters containing genes mediating isolate-specific resistance [107, 138]. These resistance loci mask the effects of putative BSR loci. Therefore, we decided to perform association mapping of susceptibility to simultaneous infection with four downy mildew isolates in >250 Arabidopsis accessions of the core HapMap population. In our screen, the accession is expected to be resistant if it has a BSR or a loss-of-susceptibility locus or if it has multiple independent loci conferring resistance to all tested isolates separately. Also the level of susceptibility of Arabidopsis accessions could be influenced by isolate-specific resistance genes, i.e. two accessions can be different in susceptibility to mixed *Hpa* infection due to different number of isolate-specific resistance loci and not due to variation at BSR or susceptibility loci. Thus, isolate-specific resistance genes could reduce the power of our approach to detect BSR or susceptibility loci by elevating phenotypic variation within different genotype groups and increase the number of false negatives. Therefore, we used less stringent significance thresholds compared to thresholds derived from FDR or Bonferroni correction. Interaction of plants with a compatible or incompatible pathogen is known to affect defense response to subsequent infection with another pathogen. This phenomenon is referred to as induced inaccessibility or accessibility. An example of induced accessibility follows the successful establishment of haustoria by compatible powdery mildew isolates in oat and barley that suppresses cell death induced by the incompatible isolates in previously infected

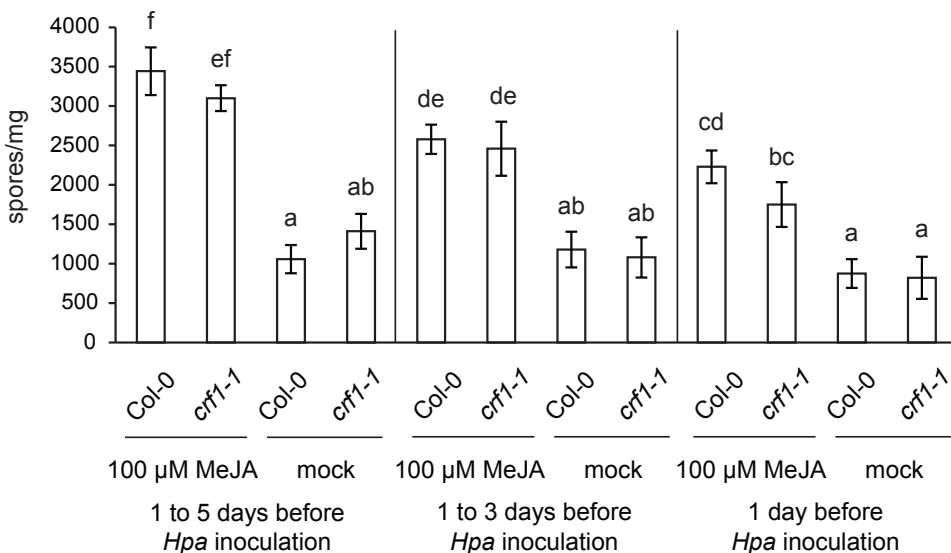


Figure 7. Sporulation of the downy mildew *Hpa* Waco9 on Arabidopsis wild type Col-0 and the *crf1-1* mutant after methyl jasmonate (MeJA) and mock treatment. Seedlings of the Col-0 and *crf1-1* lines were sprayed for five, three or one days with 100 μ M MeJA before *Hpa* inoculation. Under all variants of MeJA treatment, level of *Hpa* Waco9 sporulation was significantly increased in Col-0 plants compared to mock treatment. Treatment of Col-0 seedlings with MeJA for five days prior *Hpa* inoculation resulted in higher spore counts compared to Col-0 seedlings pretreated only for one day. The *crf1-1* mutant also supported higher sporulation in all cases of pretreatment with MeJA compared to mock-treated plants. Results of five independent experiments were combined and analyzed with mixed ANOVA followed by Tukey HSD test at $\alpha=0.05$ ($n=10$). Genotypes and treatments with significantly different means are marked with different letters. Error bars represent \pm SEM.

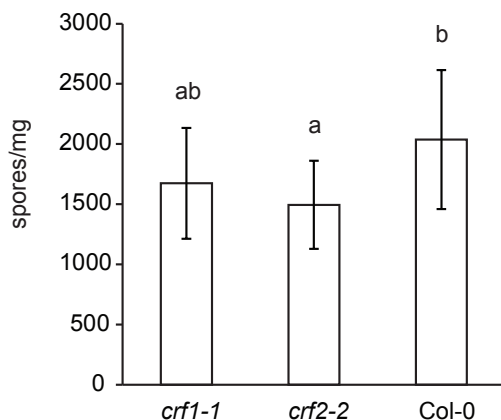


Figure 8. Sporulation of *Hpa* Waco9 on the Arabidopsis wild type Col-0 and the mutants *crf1-1* and *crf2-2*. Susceptibility of the *crf1-1* mutant was not significantly affected as compared to Col-0, however the *crf2-2* mutant was significantly more resistant to *Hpa* relative to Col-0 ($p=0.004$). Results of five independent experiments were combined and analyzed with mixed ANOVA and Bonferroni post-hoc test ($\alpha=0.05$, $n=15$). Genotypes with significantly different means are flagged with different letters. Error bars represent \pm SD.

epidermal cells or in adjacent epidermal cells. Conversely, in both oat and barley infection with incompatible powdery isolates reduced penetration efficiency and increased cell death frequency upon subsequent infection with compatible isolates [244, 245]. Induced local resistance (inaccessibility) was also found after infection with a virulent pathogen, e.g. in the interaction of barley with the compatible rust fungus *Puccinia hordei* that reduced susceptibility to a subsequent infection with the compatible powdery mildew fungus *Blumeria graminis* [246]. In addition to the local effects, incompatible interactions with avirulent pathogens can lead to enhanced resistance to virulent pathogens in systemic plant organs, which is called systemic acquired resistance. In contrast to situations where plants are exposed to consecutive infection with compatible and incompatible pathogens, available experimental data suggest that simultaneous infection with compatible and incompatible pathogens does not affect resistance of plants to the individual ones. It was reported that in poplar growth of compatible and incompatible *Melampsora* rust fungi in the case of mixed infection did not significantly differ from growth of these rusts in individual inoculations [247]. Similarly, transcriptional response of poplar plants to the mixed infection could be explained as a sum of transcriptional responses to individual infections suggesting minimal interaction between resistance pathways against these pathogens [248]. To our knowledge, the effect of simultaneous infection with compatible and incompatible isolates has not been reported for *Hpa*. We found that susceptibility of Arabidopsis accessions to mixed infection was positively correlated with susceptibility to individual *Hpa* isolate Emco5, Noco2, Waco9 and Cala2 ($p=0.314..0.464$, $p=0.14..0.005$), however the correlation was much stronger with the average susceptibility score for these isolates ($p=0.649$, $p<10^{-4}$). These findings indicate that in Arabidopsis during mixed *Hpa* infection there is no preference either for induced accessibility or inaccessibility. Association mapping of Arabidopsis susceptibility to mixed downy infection revealed three candidate loci: At5g53750...*MLO11*, *SCAP1* and *CRF1*. The function of these genes in Arabidopsis disease resistance or susceptibility has not been reported so far. The *scap1* mutant and the silencing line RNAi 8-2 were slightly more resistant to downy mildew compared to the wild type Col-0. *SCAP1* was recently shown to regulate development of guard cells via transcriptional activation of *MYB60* and *GORK* encoding TF and K^+ -channel proteins, respectively. In addition, the *scap1* mutation suppresses demethylesterification of pectin in the walls of guard cells that likely results in increased elasticity of cell walls [240]. Given that *SCAP1* is expressed not only in the guard cells [240], it is plausible that modification of cell walls in leaf mesophyll of the mutant affects the *Hpa* infection process. Besides that, it cannot be excluded that *SCAP1* is required for successful infection of Arabidopsis by downy mildew. We focused our study on the role of *CRF1* in Arabidopsis susceptibility to downy mildew. This gene encodes for a TF belonging to the group VI ERFs with the predicted AP2 repressor domain [249]. The *CRF1* ortholog of tomato, *Pti6*, interacts in the yeast-two-hybrid system

with the Pto kinase of tomato, and positive effect of Pto on *PR*-genes expression in transgenic tobacco is suggested to be mediated by Pti6 homologs [250]. Both Tsi1, the CRF1 orthologous protein in tobacco, and Pti6 bind to the GCC-box found in promoters of *PR*-genes [241, 242, 250]. The GCC-box is found in promoter elements of *PR*-genes and is important for JA-induced *PDF1.2* expression [251] and SA-mediated negative regulation of JA-induced *PDF1.2* expression in Arabidopsis [252]. These findings suggest that *CRF1* of Arabidopsis might also affect Arabidopsis resistance.

We found that enhanced susceptibility of Arabidopsis to mixed infection with *Hpa* is associated with polymorphisms in the *CRF1* upstream sequence but not with polymorphisms in the protein coding sequence. Analysis of *CRF1* mRNA levels in different Arabidopsis accessions demonstrated that lower abundance of *CRF1* transcripts in uninfected seedlings positively correlated with partial or complete resistance to *Hpa* and presence of deletion and insertion at the indel 1 and 2 loci respectively in the *CRF1* promoter element suggesting that polymorphisms in the upstream sequence in susceptible Arabidopsis accessions lead to derepression of *CRF1* transcription. Even though the *crf1-1* knockout mutant did not show altered resistance phenotype to *Hpa* Waco9 compared to the wild type Col-0, the *crf2-2* mutant was less susceptible to the downy mildew isolate Waco9. We hypothesize that *CRF1* and *CRF2* have overlapping functions in negative regulation of Arabidopsis resistance to *Hpa* and future testing of the double mutant may reveal the function of *CRF1/CRF2* during infection with downy mildew.

Of the Arabidopsis *CRF1* overexpression lines tested, only one showed elevated resistance to *Hpa* at the seedling stage. The effect of *CRF1* overexpression on resistance of plants to pathogens is not understood. Indeed, overexpression of *Tsi1* in tobacco leads to enhanced resistance to *Pseudomonas syringae* pv. *tabaci* [241]. In contrast, overexpression of tomato *Pti6* in Arabidopsis did not result in elevated resistance to the powdery mildew *G. orontii* and to *Pst* [242]. In this study we observed that 3-4 week-old Arabidopsis plants from *CRF1* overexpression lines displayed spontaneous cell death suggesting that *CRF1* overexpression can also lead to perturbation of the Arabidopsis immune network resulting in cell death not considerably affecting pathogen resistance.

We observed that *CRF1* is quickly and transiently induced after MeJA treatment and co-regulated with a cluster of genes associated with JA-related GO terms. Interestingly, the *CRF1* overexpression line with elevated resistance to *Hpa* showed a lower chlorophyll level after growing on MeJA plates compared to the wild type and the *crf1-1* mutant suggesting that *CRF1* might play a role in Arabidopsis response to MeJA. Overexpression of tomato *Pti6* in Arabidopsis leads to higher *PDF1.2* transcript levels indicating activation of *ERF1*-branch of MeJA-induced pathway [242]. Interestingly, we observed that MeJA treatment makes Arabidopsis Col-0 seedlings more susceptible to *Hpa* indicating that the MeJA-pathway negatively affects Arabidopsis resistance to *Hpa*. In our experiments, the *crf1-1* mutant was not impaired in MeJA-induced susceptibility when MeJA was applied before *Hpa* inoculation. Given that the Arabidopsis *crf2-2* mutant was significantly more resistant to *Hpa*, it is important to check whether the *crf1-1/crf2-2* double mutant is defective in MeJA-induced susceptibility to *Hpa*.

In summary, association mapping of Arabidopsis susceptibility to mixed infection with several downy mildew isolates identified three novel loci affecting Arabidopsis-*Hpa* interaction. Future studies will reveal the potential role and mechanism by which these host genes affect susceptibility and resistance to downy mildew

Acknowledgements

The authors thank prof. Koh Iba (Kyushu University, Japan) for seeds of the *scap1* mutant and the RNAi silencing lines ## 7-3 and 8-2.

SI Note 1 is available as a separate file on the enclosed CD

Supporting information

SI Table 1. *Arabidopsis thaliana* accessions of the HapMap population tested for susceptibility to the mixed infection with the four *Hpa* isolates Waco9, Cala2, Emco5 and Noco2.

Accession	Name	Susceptibility score*	Accession	Name	Susceptibility score*
CS22689	RRS-10	2	CS28779	Tscha-1	1
CS28007	Aa-0	3	CS28780	Tsu-0	3
CS28014	Amel-1	2.5	CS28786	Ty-0	3
CS28018	Ang-0	3	CS28787	Uk-1	2.75
CS28049	Ann-1	3	CS28788	Uk-2	3
CS28053	Ba-1	3	CS28795	Utrecht	3.5
CS28063	Be-1	2.5	CS28804	Wa-1	1
CS28097	Bs-2	2.5	CS28808	Wag-3	1
CS28099	Bsch-0	1	CS28810	Wag-5	2.5
CS28108	Bu-8	1	CS28822	Wl-0	2.5
CS28128	Ca-0	2.5	CS28823	Ws	3.5
CS28133	Cha-0	3	CS28833	Wt-3	3.5
CS28135	Chat-1	1.5	CS28847	Zu-1	1
CS28140	CIBC2	2	CS28848	Ors-1	1
CS28141	CIBC4	2.5	CS28849	Ors-2	1
CS28142	CIBC5	1	CS76083	11ME1.32	2.5
CS28163	Co-2	1.75	CS76085	328PNA054	1
CS28181	Cold Spring Harbor Lab-5	2	CS76087	Ag-0	1.5
CS28193	Com-1	2.5	CS76088	Alc-0	3
CS28200	Da-0	3	CS76091	An-1	2.5
CS28201	Da(1)-12	2.5	CS76092	App1-16	2.5
CS28202	Db-0	1	CS76093	Ba1-2	1
CS28208	Di-1	1	CS76094	Bay-0	1
CS28210	Do-0	1.25	CS76096	Bg2	1.5
CS28214	Dra-2	1.5	CS76097	Bla-1	2
CS28217	Ede-1	3	CS76098	Blh-1	1
CS28236	Ep-0	1	CS76099	Bor-1	1.5
CS28243	Est-0	1	CS76100	Bor-4	1
CS28252	Fi-1	1	CS76101	Br-0	1.5
CS28268	Fr-4	1.5	CS76102	Bro1-6	2.5
CS28277	Ge-1	2	CS76103	Bu-0	3
CS28279	Gel-1	2.5	CS76104	BUI	3
CS28280	Gie-0	2	CS76105	Bur-0	2.5
CS28282	G ⁿ -0 = Gö-0	2	CS76106	C24	1

CS28326	Gr-5	1	CS76108	CAM-61	1.5
CS28332	Gü-1	1.5	CS76109	Can-0	2
CS28345	Hh-0	1	CS76110	Cen-0	3
CS28350	Hn-0	1	CS76111	CIBC17	2
CS28369	Jl-3	1	CS76112	CLE-6	3.5
CS28373	Jm-1	1	CS76113	Col-0	3
CS28382	Kelsterbach -2	1	CS76114	Ct-1	1.5
CS28394	Kl-5	2.5	CS76115	CUR-3	1.5
CS28395	Kn-0	1	CS76116	Cvi-0	3.25
CS28419	Kr-0	2	CS76119	DralV1-14	2
CS28420	Kro-0	1.5	CS76120	DralV1-5	1
CS28423	Krot-2	1.5	CS76122	DralV6-16	2.5
CS28454	Li-3	2.5	CS76123	DralV6-35	1
CS28457	Li-5:2	1.5	CS76124	Duk	3
CS28459	Li-6	2	CS76125	Eden-2	2.5
CS28461	Li-7	3.5	CS76126	Edi-0	2
CS28492	Mh-0	2.5	CS76127	Est-1	1
CS28495	Mnz-0	1.5	CS76128	Fab-4	1
CS28513	N7	3.25	CS76129	Fei-0	1.75
CS28550	NFC20	2	CS76132	Fja1-5	1.5
CS28564	No-0	3	CS76133	Ga-0	1
CS28573	Nw-0	2	CS76134	Gd-1	2
CS28575	Nw-2	3	CS76136	Goettingen-7	3
CS28580	Ob-1	3.5	CS76137	Gr-1	3
CS28583	Old-1	3	CS76139	Gy-0	1
CS28587	Or-0	4	CS76140	Hi-0	1
CS28595	Pa-2	2	CS76141	Hod	1
CS28613	PHW-13	2.5	CS76143	Hovdala-2	3.5
CS28620	PHW-20	1	CS76144	HR5	2
CS28622	PHW-22	2.5	CS76145	Hs-0	3.5
CS28628	PHW-28	1	CS76146	HSm	1.5
CS28633	PHW-33	2	CS76148	JEA	2.5
CS28640	Pla-0	2	CS76149	Ka-0	1
CS28645	Pn-0	2.75	CS76150	Kas-2	2
CS28650	Pog-0	2	CS76151	KBS-Mac-8	1.5
CS28685	Rhen-1	2.5	CS76152	Kelsterbach -4	2.5
CS28720	S96	1	CS76153	Kin-0	2.75
CS28724	Sapporo-0	2	CS76154	Knox-18	1
CS28725	Sav-0	3.5	CS76156	Kulturen-1	1.5
CS28729	Sei-0	1.75	CS76157	LAC-3	1

CS28734	Sh-0	3	CS76158	LAC-5	2.5
CS28739	Si-0	2.5	CS76159	Lc-0	2.5
CS28758	Tha-1	3	CS76160	LDV-14	2
CS28760	Tiv-1	1	CS76161	LDV-25	1.5
CS76162	LDV-34	2.5	CS76269	Udu1-34	1
CS76163	LDV-58	4	CS76272	UKID37	2
CS76164	Ler-1	2	CS76273	UKID48	2
CS76165	LI-OF-095	1.5	CS76274	UKID80	1.5
CS76166	Liarum	3	CS76275	UKNW06-059	2
CS76168	Lip-0	2	CS76276	UKNW06-060	1.5
CS76171	PHW-33	3	CS76281	UKSE06-192	1
CS76172	LL-0	3	CS76282	UKSE06-272	2
CS76173	Lm-2	2.5	CS76284	UKSE06-349	3
CS76174	Lom1-1	1.5	CS76285	UKSE06-351	1
CS76175	Lov-5	2	CS76289	UKSE06-482	3
CS76176	Lp2-2	1.5	CS76293	UII2-3	3.25
CS76177	Lp2-6	2	CS76296	Uod-7	1
CS76179	Lz-0	1	CS76297	Van-0	2.75
CS76181	MIB-15	3	CS76299	VOU-1	2
CS76183	MIB-28	2.5	CS76300	VOU-2	1
CS76184	MIB-84	2.5	CS76301	Wei-0	2.5
CS76185	MNF-Che-2	2	CS76302	Wii-1	1
CS76187	MNF-Pot-48	2	CS76303	Ws-0	1.5
CS76188	MNF-Pot-68	2.5	CS76304	Wt-5	1.75
CS76190	Mr-0	2	CS76305	Yo-0	2.5
CS76191	Mrk-0	4	CS76306	Zdr-6	1
CS76192	Mt-0	1.5	CS76307	Zdrl2-24	2
CS76193	Mz-0	1.5	CS76263	TOU-I-17	3
CS76194	N13	1.5	CS76266	TOU-J-3	2.5
CS76195	Na-1	3	CS76267	TOU-K-3	1.5
CS76197	Nd-1	3	CS76268	Ts-1	1.5
CS76198	NFA-10	2			
CS76199	NFA-8	2			
CS76200	Omo2-1	1.5			
CS76202	Ost-0	1			
CS76203	Oy-0	1.5			
CS76204	Pa-1	1			
CS76206	PAR-4	3			
CS76208	Paw-3	1			
CS76210	Per-1	1			

CS76211	Petergof	1	CS76253	TOU-A1-116	3
CS76213	Pna-17	1	CS76254	TOU-A1-12	1
CS76214	Pro-0	2.75	CS76255	TOU-A1-43	1.5
CS76215	Pu2-23	1.5	CS76256	TOU-A1-62	1.5
CS76216	Ra-0	3	CS76257	TOU-A1-67	1.5
CS76217	Rak-2	1	CS76258	TOU-A1-96	2.5
CS76218	Rennes-1	1	CS76259	TOU-C-3	3
CS76220	Rmx-A180	3	CS76260	TOU-E-11	2.5
CS76221	ROM-1	2.5	CS76261	TOU-H-12	2.5
CS76222	Rsch-4	2.5	CS76262	TOU-H-13	3
CS76223	Sanna-2	2.5			
CS76224	Sap-0	2.5			
CS76225	Sav-1	1			
CS76226	Se-0	1			
CS76227	Sha	1			
CS76228	SLSP-30	2.5			
CS76230	Sq-8	2			
CS76231	St-0	2.5			
CS76232	Ste-3	1			
CS76233	T1040	1			
CS76239	T540	1.5			
CS76240	T620	1.5			
CS76242	Ta-0	1			
CS76243	Tad01	3			
CS76244	Tamm-2	2			
CS76245	TDr-1	2			
CS76247	TDr-18	2			
CS76249	TDr-8	4			
CS76251	Tottarp-2	3.5			
CS76252	TOU-A1-115	2			

* - Susceptibility score: 1 - no sporulation; 2 - <15% of seedlings are sporulating plants; 3 – 15-80% of seedlings are sporulating; 4 - >80% of seedlings are intensively sporulating

SI Table 2. Susceptibility of *Arabidopsis thaliana* accessions to the *Hpa* isolate Waco9

Name	Susceptibility*	Name	Susceptibility*
Ag-0	0	Pro-0	1
An-1	1	Pu2-23	1
Bay-0	1	Ra-0	1
Bor-1	0	Rmx-A180	1
Bor-4	0.5	RRS-10	0.5
Br-0	0.5	Se-0	0
Bur-0	0	Sq-8	1
C24	0	Tamm-2	1
CIBC17	1	Ts-1	0
CIBC5	0	Ull2-3	1
Col-0	1	Uod-7	0
Ct-1	0	Van-0	1
Eden-2	1	Wa-1	0
Edi-0	1	Wei-0	0.5
Est-1	1	Ws-0	1
Fei-0	0	Wt-5	1
Ga-0	0	Yo-0	1
Gy-0	0	Zdr-6	1
HR5	0	Omo2-1	0
Kin-0	0	Pna-17	0
Knox-18	1	Mr-0	1
Ler-1	0	Mt-0	1
LL-0	1	Mz-0	0
Lov-5	1	NFA-10	1
Lp2-2	0	NFA-8	1
Lp2-6	1		
Lz-0	0		

* - Susceptibility score: 0 – full resistance, 0.5 – few sporulating conidiophores observed, 1 – majority or all seedlings accession are susceptible

SI Table 3. Correlation between susceptibility of *Arabidopsis thaliana* accessions to infection with individual and mixed downy mildew isolates

<i>Hpa</i> isolate	Spearman's rank correlation coefficient ρ	Bonferroni corrected p-value	Number of accessions
Emco5 [§]	0.353	0.040*	56
Noco2 [§]	0.354	0.040*	56
Waco9 ^{§§}	0.464	0.005**	51
Cala2 ^{§§§}	0.314	0.14	49
Average resistance score for the isolates Emco5, Noco2, Waco9	0.649	<0.001***	45

Flags for the significance levels of the ρ correlation coefficient: * - $p=0.05..0.01$, ** - $p=0.01..0.001$, *** - $p<0.001$

[§] - susceptibility scores were taken from [107]

^{§§} - susceptibility was scored in this study (experiment was performed once)

^{§§§} - susceptibility scores were taken from [136]

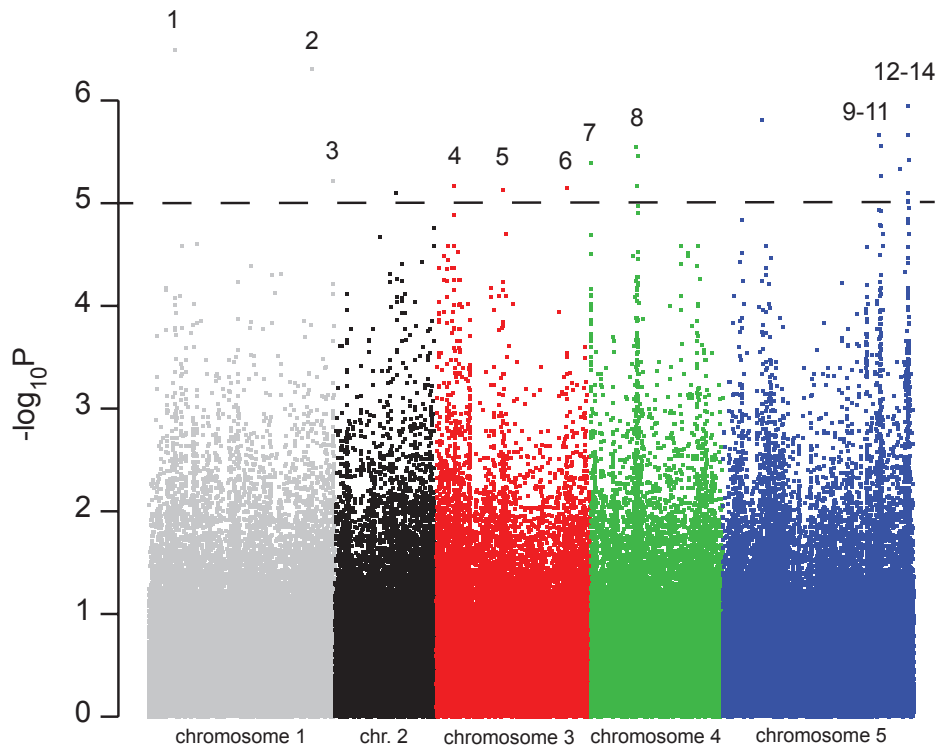
SI Table 4. Sequences of primers used in this study

Primer name	5'->3' sequence	Application
GABI_068G09_LP	TCCTTACGCAACAGATTCGTC	Genotyping of the <i>crf1-1</i> mutant
GABI_068G09_RP	CGTGAGACAACACGTGATACG	
GABI kat LB	ATATTGACCATCATACTCATTGC	
CRF2OX_Fw	caccATGGAAGCGGAGAAG	Genotyping of the <i>crf2-2</i> mutant
CRF2OX_open_Rv	AACAGCTAAAAGAGGATCCG	
SAIL LB2	GCTTCCTATTATATCTTCCCAAATTAC-CAATACA	
SAIL-1151-G06_LP	TTTAGTCCGTTTTCCACATGCC	Genotyping of SAIL-1151-G06
SAIL-1151-G06_RP	GGAGGAGGAAGTGAATGGAAC	
LBb1.3	ATTTTGCCGATTTCCGGAAC	
CRF1_expr2_Fw	CCGGTTTCTGTTCTCGAATC	Relative quantification of <i>CRF1</i> mRNA levels with qRT-PCR
CRF1_expr2_Rv	CGGCTCCTTTTAAACCACAA	
ACT2_Fw	AATCACAGCACTTGCACCA	
ACT2_Rv	GAGGGAAGCAAGAATGGAAC	
CRF1_indel_Fw	TGGAGGATGCGGTTTTAGTC	Confirmation of the presence of deletion in the <i>CRF1</i> promoter of different <i>Arabidopsis</i> accessions
CRF1_indel_Rv	CAAACACGGTCCACGTTAAA	
CRF1_4Fw	TCGACTTGTGTGCTTTTTAACG	
CRF1_5Rv	TCACGAAGAACTTTGAAAACC	
CRF1_6Fw	TTTAGTACTTATCTTAGCCGATTGGA	
CRF1_6Rv	CCAAAAGAGATGTTGGCAGA	

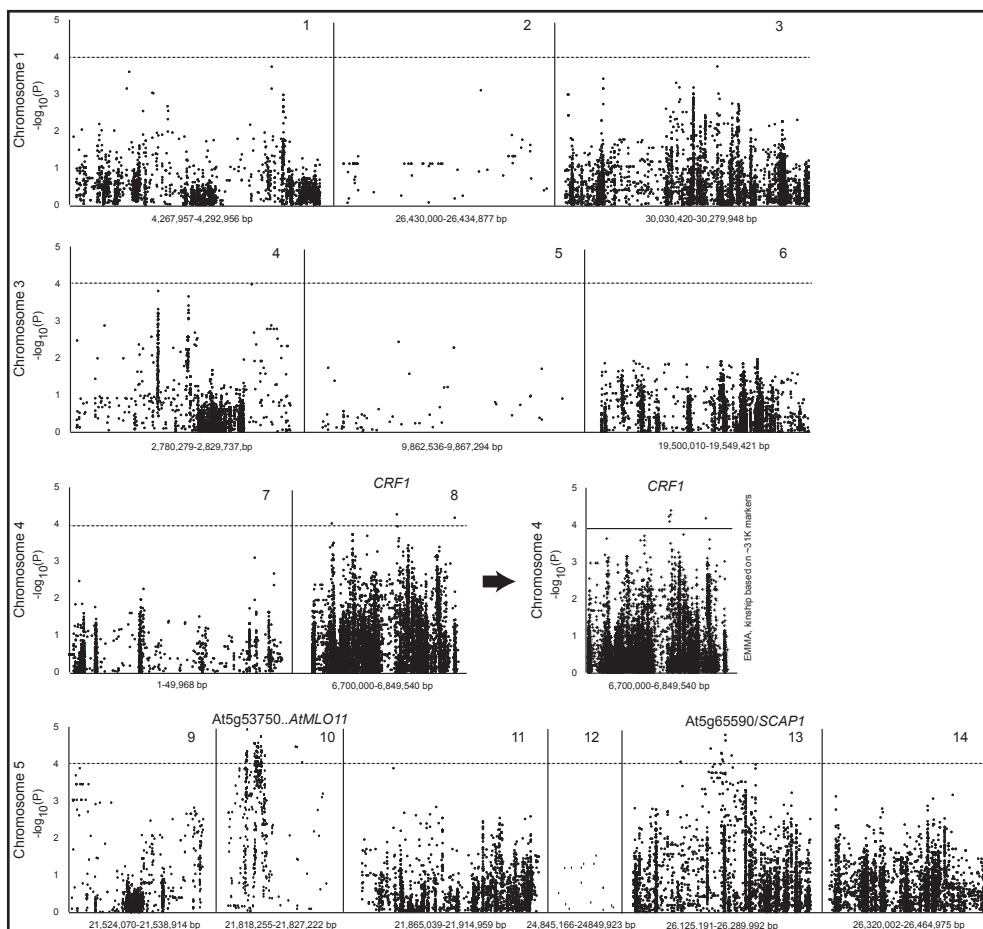
SI Table 5. List of Arabidopsis accessions used for the analysis of *CYTOKININ RESPONSE FACTOR 1* mRNA levels.

Accession	Deletion at the indel 1 locus	Deletion at the indel 2 locus	Susceptibility to mixed downy mildew infection*
Bay-0	YES	NO	1
Blh-1	YES	NO	1
Bsch-0	YES	NO	1
C24	NO	NO	1
Col-0	YES	NO	3
Do-0	YES	NO	1.25
Est-1	YES	NO	1
Ga-0	YES	NO	1
Gy-0	YES	NO	1
Hi-0	YES	NO	1
Hn-0	YES	NO	1
Kn-0	YES	NO	1
Per-1	YES	NO	1
Rak-2	YES	NO	1
Rennes-1	YES	NO	1
Wil-1	YES	NO	1
Aa-0	NO	YES	3
Alc-0	NO	YES	3
Ba-1	NO	YES	3
Bu-0	NO	YES	3
Ca-0	NO	YES	2.5
Eden-2	NO	YES	2.5
Gel-1	NO	YES	2.5
Hovdala-2	NO	YES	3.5
KI-5	NO	YES	2.5
Liarum	NO	YES	3
Lm-2	NO	YES	2.5
Rhen-1	NO	YES	2.5
Sanna-2	NO	YES	2.5
St-0	NO	YES	2.5
T-Dr8	NO	YES	4
Tha-1	NO	YES	3
Ty-0	NO	YES	3
Utrecht	YES	NO	3.5

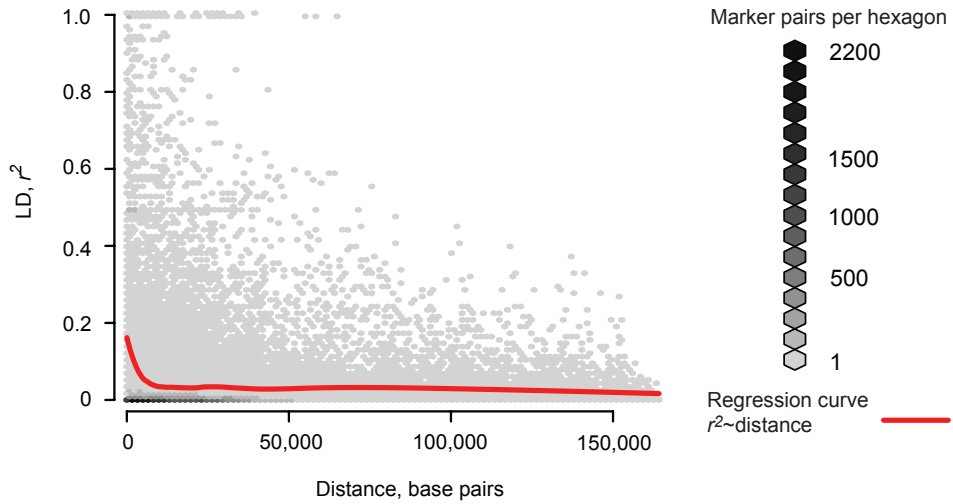
* - susceptibility scores are reproduced from the SI Table 1.



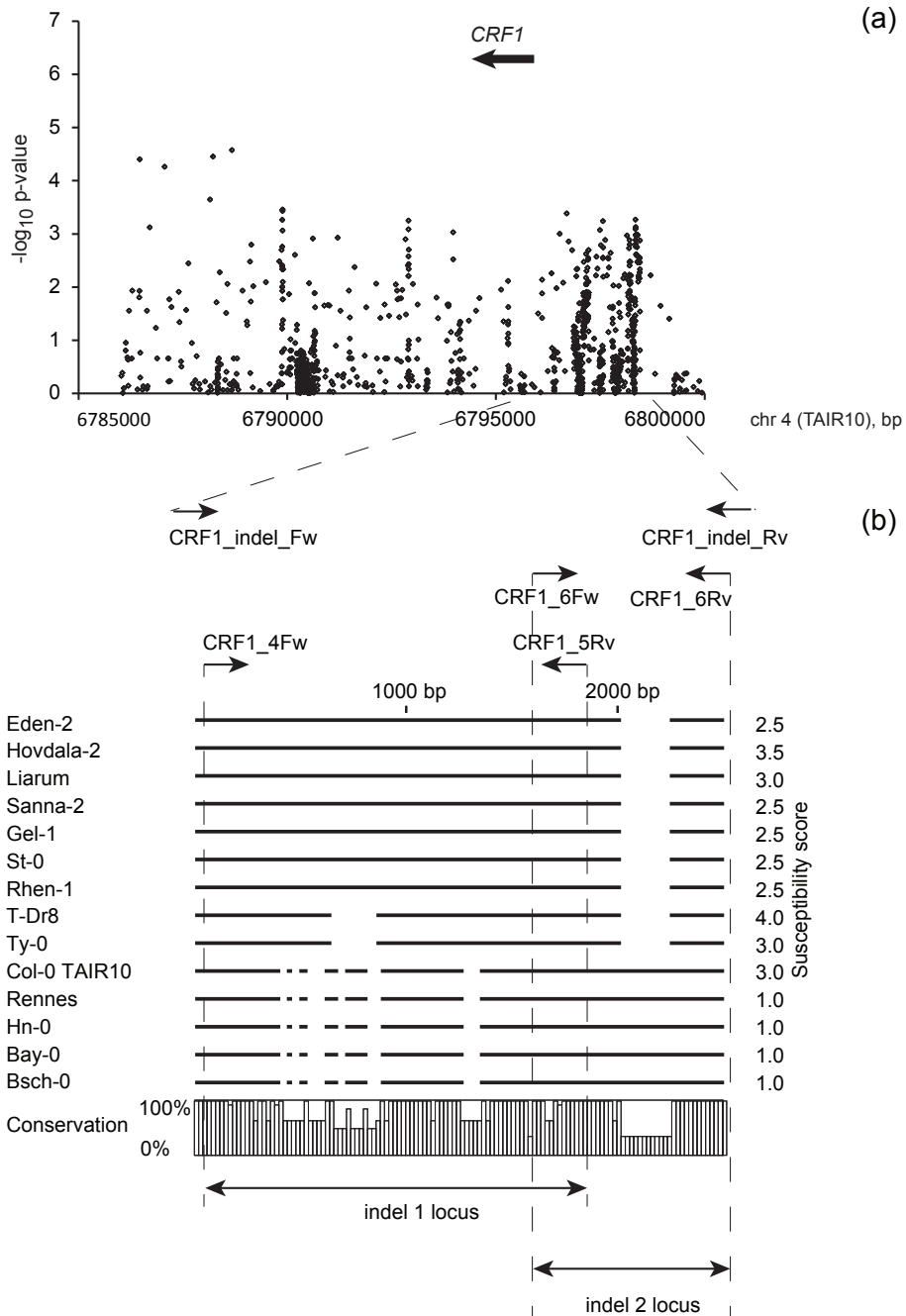
SI Figure 1. Manhattan plot of the genome-wide association (GWA) mapping results for susceptibility of *Arabidopsis* to the mixed infection with four isolates of the downy mildew *Hpa*. Association between a single nucleotide polymorphism (SNP) and susceptibility was determined with the Kruskal-Wallis test (GWAPP tool), and the corresponding $-\log_{10}(P)$ values are plotted on all five *Arabidopsis* chromosomes shown in different colors. SNPs with scores above the arbitrary threshold $-\log_{10}(P)=5$ (Kruskal-Wallis test, GWAPP tool) were considered as strongly associated with the susceptibility phenotype. Candidate loci used further for the locus-specific association mapping are labeled with numbers corresponding to the numbers on SI Figure 2.



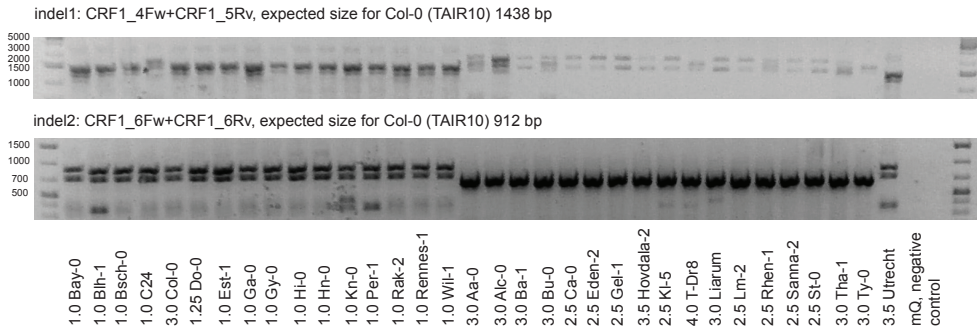
SI Figure 2. Locus-specific association mapping for the candidate loci found to be associated with Arabidopsis resistance to the mixed infection with the downy mildew *Hpa* in the genome-wide association mapping (Kruskal-Wallis test $-\log_{10}\{p\text{-value}\} \geq 5$). The number on top of each locus corresponds to a locus number on the SI Figure 1. Most of the candidate loci did not show strong association with resistance to *Hpa* (Kruskal-Wallis test $-\log_{10}\{p\text{-value}\} < 4$). However, the loci At5g53750..AtMLO11 and At5g65590/SCAP1 were significantly associated with this phenotype (Kruskal-Wallis test, $-\log_{10}\{p\text{-value}\} > 4$, FDR < 0.05). The locus At4g11130..At4g11140/CRF1 was also nominally associated with resistance to mixed *Hpa* infection (Kruskal-Wallis test, $-\log_{10}p = 4.27$, FDR = 0.1642; EMMA, $-\log_{10}p = 4.57$, FDR = 0.2414).



SI Figure 3. Decay of linkage disequilibrium (r^2) with the distance between markers on the intervals used for locus-specific association mapping of *At5g53750..MILDEW LOCUS O 11*, *CYTOKININ RESPONSE FACTOR 1* and *STOMATAL CARPENTER 1*. Marker pairs with similar r^2 and distance values were grouped with the hexagon binning algorithm. Intensity of grey within each bin (hexagon) reflects number of marker pairs in this bin. The red regression curve depicts relationship between the linkage disequilibrium and distance between markers.

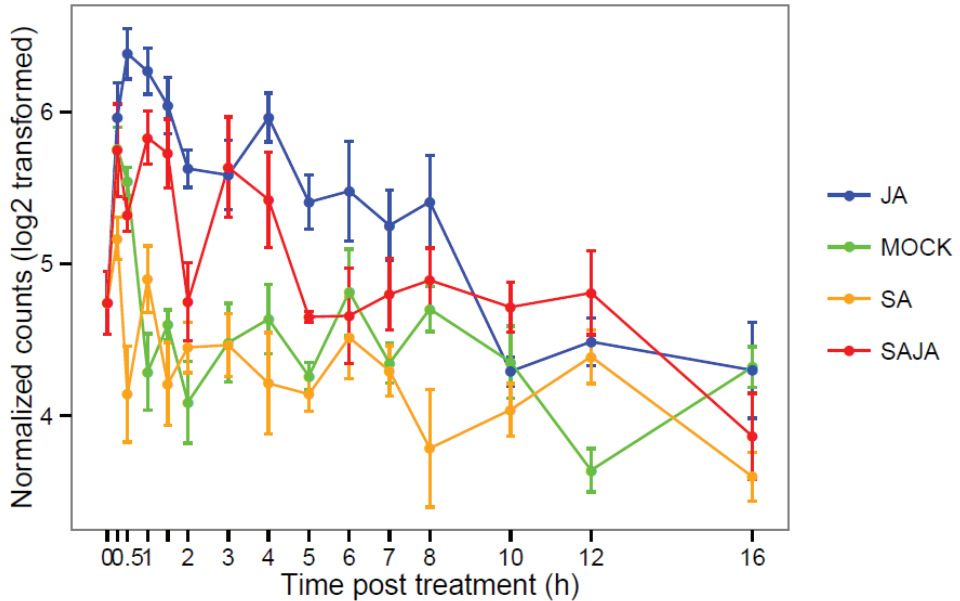


SI Figure 4. (a) Association between polymorphisms within and around the *CYTOKININ RESPONSE FACTOR 1* locus and resistance to *Hpa*. Each dots shows the significance of association of polymorphic positions as determined with the K-method of mapping in the population of 142 *Arabidopsis* accessions. Most of the significant associations were found within the ca. 3 kb *CRF1* upstream region (cut-off at $-\log_{10}\{p\text{-value}\} > 2.3$, $FDR < 5\%$).



SI Figure 5. Agarose gel with amplicons spanning the indel 1 and indel 2 loci in different Arabidopsis accessions. Upper panel: the indel 1 locus is amplified with the primer combination CRF1_4Fw and CRF1_5Rv. The expected amplicon size in Col-0 accession is 1438 bp. Fifteen resistant accessions have the amplicon smaller than amplicons from susceptible accessions. Lower panel: the indel 2 locus is amplified with the primer combination CRF1_6Fw and CRF1_6Rv. Seventeen susceptible have ca. 200 bp deletion relative to the reference Col-0 and resistant accessions. The number in front of the accession name represents the susceptibility score.

SI Figure 4 (continuation): (b) Schematic representation of multiple alignment of the CRF1 upstream region from SI thirteen Arabidopsis accessions associated with susceptibility to mixed *Hpa* infection. Nine susceptible accessions have deletion shown as indel 2 on the figure, and four resistant accessions have deletion in the region labeled as indel 1 relative to the nine susceptible accessions. Arrows labeled as CRF1_indel_Fw, CRF1_indel_Rv, CRF1_4Fw, CRF1_5Rv, CRF1_6Fw and CRF1_6Rv indicate location of primers used to amplify the aligned region and validate the indel mutations in other accessions.



GO:0009694 jasmonic acid metabolic process $p=9.96e-16$
 GO:0009753 response to jasmonic acid stimulus $p=4.32e-15$
 GO:0009725 response to hormone stimulus $p=2.01e-07$
 GO:0009611 response to wounding $p=7.66e-07$
 GO:0009719 response to endogenous stimulus $p=1.19e-06$
 GO:1901700 response to oxygen-containing compound $p=2.46e-06$
 GO:0080086 stamen filament development $p=4.01e-05$
 GO:0009695 jasmonic acid biosynthetic process $p=4.56e-05$

SI Figure 6. Dynamics of *CYTOKININ RESPONSE FACTOR 1 (CRF1)* mRNA levels following treatment of the wild type *Arabidopsis Col-0* plants with salicylic acid (SA) at the concentration 1 mM, methyl jasmonate (MeJA) at the concentration 100 μ M and the combined SA/MeJA treatment. *CRF1* transcripts are quickly induced after MeJA and combined SA/MeJA treatment, however they drop to a level of mock treatment at 10 hours after MeJA and at 6 hours after the combined SA/MeJA treatment. SA treatment did not raise *CRF1* mRNA levels at the tested time points. Below the graph the gene ontology (GO) terms are indicated that are overrepresented in the set of *CRF1* co-regulated genes.

Pseudomonas syringae, non-adapted pathogens *Phytophthora infestans* and *Blumeria graminis*. Similarly, *CRF2* mRNA levels were reduced following the treatment with elicitors such as elf18, elf26 and hairpin Z and pep2. Notably, *CRF2* was slightly transcriptionally upregulated after exposure to the volatiles from *Stenotrophomonas* and *Serratia* rhizobacteria that induce hydrogen peroxide accumulation in *Arabidopsis*. Also, *CRF2* mRNA accumulated treatment with the cytokinin zeatin. Finally, *CRF2* mRNA levels were increased 1 hour after methyl jasmonate application but decreased in the salicylic acid treated plants. (b) Dynamics of *CRF2* mRNA levels following treatment of the wild type *Arabidopsis* Col-0 plants with SA at the concentration 1 mM, MeJA at the concentration 100 μ M and the combined SA/MeJA treatment. *CRF2* mRNA levels expressed as normalized RNA-seq counts are strongly reduced after treatment with SA and SA/MeJA. MeJA treatment did not substantially affect levels of *CRF2* mRNA except for time points at 2-4 and 12 hours following MeJA application.

Chapter 5

Disease-related N-glycoproteins of Arabidopsis infected by downy mildew

Dmitry Lapin¹, Wei Song^{2,3}, Jan Cordewener³, Alexander van der Krol², Antoine America³, Guido Van den Ackerveken¹

¹ – Plant-Microbe Interactions, Utrecht University, Padualaan 8, 3584 CH, Utrecht, The Netherlands

² – Plant Physiology, Wageningen University and Research center, Droevendaalsesteeg 1, 6708 PB, Wageningen, The Netherlands

³ – Applied Genomics and Proteomics, Plant Research International, Droevendaalsesteeg 1, 6708 PB, Wageningen, The Netherlands

In preparation

Abstract

The pathogen *Hyaloperonospora arabidopsidis* (*Hpa*), causing downy mildew in *Arabidopsis*, grows inside host tissues and forms specialized infection structures in plant cells, called haustoria. Local host responses to pathogens contribute to susceptibility or resistance to infection. However, responses of *Arabidopsis* in cells invaded by *Hpa* haustoria are poorly studied. Therefore, we aimed to identify host disease-related proteins in *Hpa*-infected cells. For this, cell-specific N-glycotagging was deployed to specifically tag proteins with complex N-glycans in infected *Arabidopsis* cells. Immunoprecipitation-based enrichment of tagged proteins followed by label-free quantitative proteomic analysis revealed 18 candidate disease-related complex N-glycosylated proteins. The *IMPAIRED IN OOMYCETE SUSCEPTIBILITY 1* (*IOS1*) gene, encoding one of the identified proteins, was previously shown to be transcriptionally activated specifically in the downy mildew infected cells and important for successful pathogen development, providing an important proof-of-principle of our method. Analysis of publicly available microarray data indicated that the majority of genes encoding the identified proteins are differentially expressed during pathogen infection suggesting their putative involvement in *Arabidopsis* disease susceptibility. Analysis of susceptibility of mutants for the identified genes revealed a potential important role of *PLASMODESMATA GERMIN LIKE PROTEIN 1* and *SUBTILASE 3.5* in *Arabidopsis* susceptibility to *Hpa*. Functional analysis of the identified disease-related *Arabidopsis* proteins will further improve our understanding of the host processes affected in downy mildew-infected cells.

Introduction

The inability of plants to mount proper immune responses can be one of the causes of infectious diseases. Also, plant susceptibility factors can promote disease development by attracting pathogens, stimulating their germination and penetration, facilitating establishment of infectious structures inside infected host cells, and providing nutrition [217]. Pathogen infection causes changes in systemic uninfected plant tissues, e.g. in photosynthetic activity [81, 253] or by priming for defense responses [254]. Local immune responses of plants to pathogens can stop pathogen infection and often involves a hypersensitive response at the

penetration site or invaded host cells [255] and a balanced immune response in the adjacent uninfected cells [256, 257]. Non-immunity related host responses of pathogen-infected and surrounding cells, e.g. endoreduplication [89] and increase in alcohol dehydrogenase activity [76], are also important for successful infection by certain pathogens. Many biotrophic and hemibiotrophic fungal and oomycete pathogens form specialized structures, called haustoria, which penetrate through the plant cell wall but remain separated from the host cell cytoplasm by the invaginated plant plasma membrane [22]. That points to the importance of local plant responses during the infection process. Haustoria were shown to be a site of translocation of pathogen effector molecules [51-53, 258] and to play a role in nutrient uptake [34, 259]. Therefore, studying of host infection-related processes at the level of single cells containing pathogen haustoria is essential for understanding local plant responses to infection.

Several approaches have been developed to study local cell-type specific processes in plants. They include mechanical separation of selected cell types, e.g. by laser capture microdissection (LCM), fluorescence activated cell sorting and isolation of tagged nuclei from specific cell types [260]. In studies of plant-microbe and plant-nematode interactions, LCM or shearing-off root hairs was used to obtain samples enriched in infected cells. In these studies, RNA from these tissues was analyzed by DNA microarrays or quantitative real-time polymerase chain reaction to identify genes abundantly transcribed or induced in infected plant cells [261, 262]. However, protein levels are well-known to be regulated not only at the level of transcription but also at the post-transcriptional levels. Therefore, proteome analysis of infected cells is a critical step in understanding plant responses to pathogen infection.

Downy mildew of *Arabidopsis thaliana* (hereafter *Arabidopsis*) is caused by the obligate biotrophic oomycete pathogen *Hyaloperonospora arabidopsidis* (*Hpa*). The interaction between these two well-studied organisms is a frequently used model to elucidate mechanisms of disease susceptibility and resistance in plants [118]. *Hpa* grows intercellularly and forms haustoria in adjacent plant cells. However, virtually nothing is known about molecular events that occur inside *Arabidopsis* cells invaded by this oomycete pathogen.

Characterization of cell type-specific proteomes is challenging and depends on the efficiency of the methodology to isolate specific cell types. So far, such analyses were performed in systems for which it is possible, yet challenging, to isolate sufficient amounts of pure and uniform cell populations, e.g. root hairs, trichomes, pollen grains and tubes, egg cells, nitrogen fixing nodules [263-265], S-cells located between phloem and endodermis [266], and root cells [267]. Plant cell type-specific proteome profiling during interactions with pathogenic microorganisms, however, has not been reported so far to our knowledge. Another obstacle in the analysis of cell type-specific proteomes is the complexity of proteins in samples and the dynamic range in protein concentrations that complicates detection of low-abundant proteins. One of the solutions, extensive peptide separation prior to mass spectrometry (MS), makes analyses very time-consuming and costly thus limiting the number of tested samples [268]. Another solution is enriching a sub-fraction of the proteome by focusing on proteins with specific post-translational modifications, e.g. glycoproteins.

N-glycosylation of proteins is a posttranslational modification comprising binding of a sugar moiety (glycosyl group) to asparagine (N) residues within the NxS/T amino acid sequence. N-glycans of plants can be divided into high-mannose and complex glycans. Synthesis of high-mannose type glycans and their attachment to N residues occurs in the endoplasmic reticulum (ER), whereas complex N-glycans are built up in the Golgi complex through further modification of high-mannose type glycans [269]. Transfer of N-acetylglucosamin (NAcGlc) groups by the NAcGlc transferase I (GnTI) is a key step in the synthesis on complex N-glycans. The *complex glycan less 1-1* (*cg11-1*) mutant of *Arabidopsis* does not produce complex N-glycans under normal growth conditions due to introduction of an additional N-glycosylation site in the mutant GnTI protein that traps GnTI in the ER. Notably, the *Arabidopsis cg11* mutants do not show visible changes in plant growth [270-272]. GnTI activity enables all subsequent modifications of N-glycans including transfer of core β 1,3 fucose and β 1,2 xylose groups. The

last two groups are not essential for the synthesis of complex N-glycans in plants [273], but they are commonly found in plant N-glycans [274, 275]. Plant complex N-glycosylated proteins (CNGPs) can be efficiently detected with polyclonal antibodies raised against horseradish peroxidase. These polyclonal antibodies consist of two main fractions: one reacting to the core β 1,3 fucose group and another to the core β 1,2 xylose [274].

To identify proteins in downy mildew-infected cells of Arabidopsis, we applied cell-specific N-glycotagging followed by label-free quantitative liquid chromatography (LC) MS analysis. N-glycotagging is based on the restoration of complex N-glycosylation in Arabidopsis cells containing downy mildew haustoria. Previously, we identified the Arabidopsis *DOWNY MILDEW RESISTANT 6 (DMR6)* gene that is strongly activated in plant cells invaginated by haustoria of *Hpa* but not in neighboring uninfected cells [119]. In this study, the promoter of *DMR6* was fused to the coding sequence of *GnTI* and transformed into the *cg1-1* mutant background to achieve accumulation of CNGPs specifically in downy mildew-infected cells. Using immunoprecipitation (IP), we enriched protein samples for CNGPs and analyzed them by LC-MS. Our glycotagging approach revealed 18 candidate CNGPs related to downy mildew infection of Arabidopsis cells. Differential expression of the majority of these genes during infection of Arabidopsis with different pathogens suggests that the identified CNGPs might play a role in disease susceptibility. This is further supported by fact that two of the CNGPs were previously implicated in Arabidopsis susceptibility to pathogens, including *Hpa*. Finally, by analyzing resistance of mutant lines, we found *PLASMODESMATA GERMIN LIKE PROTEIN1* and *SUBTILASE 3.5* to be novel players in Arabidopsis susceptibility to downy mildew.

Materials and methods

Plant material and growth conditions

Arabidopsis thaliana (L.) Heyhn (referred to as Arabidopsis) mutants in Col-0 background were obtained from NASC. Primers for T-DNA insertion mutant genotyping were designed with iSect tool [228] and are listed in SI Table 1. Names of the T-DNA insertion mutants for each gene are listed in the Table 2. The previously described single *pdglp1*, *pdglp2* and double *pdglp1/2* mutants and the *pPDGLP1:PDGLP1-GFP* line were provided by prof. dr. W. Lucas (UC Davis, USA). The *ios1-1* mutant and *35S:IOS1* lines were obtained from dr. H. Keller (INRA, Antibes, France). The T-DNA insertion mutant SALK_085226 was provided by prof. dr. T. Nürnberger (University of Tübingen, Germany). Plants were grown at 21°C under long day conditions (16h light/8h dark, light intensity 100 μ mol/m²/sec).

Cloning and preparation of transgenic plants

The binary vectors containing *pDMR6:GnTI* and *pDMR6:GUS* were constructed via three-way MultiSite Gateway® recombination cloning procedure (Life Technologies, UK). The 2420 bp region immediately upstream of *DMR6* start codon in Col-0 (TAIR9) was PCR amplified and cloned into the pGEM-T/pDONR™ P4-P1R with Gateway® BP clonase® II Enzyme mix (Life Technologies, UK). Primer sequences are shown in the SI Table 1. The donor vector pGENTR221 (created by V. Jansweijer, Plant Developmental Biology, Wageningen University, the Netherlands) with *GnTI* coding sequence (AT4G38240), pGEM-T® Easy/pDONR221 with β -glucuronidase (*GUS*) coding sequences, pGEM-T/ENT R2R3 with *nos* terminator, pGreenII 0125/pDEST-R4R3 and pGEM-T/ pDONR™ P4-P1R were kindly provided by dr. Renzé Heidstra (Plant Developmental Biology, Wageningen University, the Netherlands) [276]. The promoter, protein coding sequences and terminator were recombined into pGreenII 0125/pDEST-R4R3 with Gateway® LR clonase® II Enzyme mix (Life Technologies, UK). The sequence-verified *pDMR6:GnTI* and *pDMR6:GUS* constructs were transformed into the *cg1-1* mutant background via floral-dip transformation [277] using the *Agrobacterium tumefaciens* strain C58C1. Transgenic plants were selected on the MS medium containing 100 nM norflurazon. Experiments were performed on non-segregating T3 plants.

Downy mildew infection assays

The downy mildew *Hyaloperonospora arabidopsidis* (Gäum.) Göker, Riethm., Voglmayr, Weiss & Oberw. (*Hpa*) isolate Waco9 was maintained as described previously [109]. All infection assays were performed on eleven-day-old seedlings at 16°C under short day conditions (9h light/15h dark, light intensity 100 $\mu\text{mol}/\text{m}^2/\text{sec}$, relative humidity 100%) with a standard inoculum density of 50 conidiospores/ μl . Intensity of sporulation was determined by spore counting at 6-7 days post inoculation and expressed in spores/mg of fresh seedling weight.

Whole-mount β -Glucuronidase (GUS) activity assays and trypan blue staining

At three days post inoculation either with *Hpa* or water as mock treatment, seedlings with the *pDMR6:GUS* construct in *cg1-1* background were subjected to the whole-mount β -Glucuronidase (GUS) staining as described previously [278] using Magenta GlcA substrate (M1412, Duchefa Biochemie B.V., The Netherlands). *Hpa* hyphae inside the GUS-stained seedlings were visualized with trypan blue staining [119].

Detection of CNGPs with western blotting

The detection of complex N-glycosylated proteins was performed by western blotting on nitrocellulose membranes (RPN303D, Amersham Hybond-ECL, GE Healthcare, UK) with rabbit anti-horse-radish peroxidase (HRP) antibody as a primary antibody (P7899, Sigma-Aldrich, MO, USA or 323-005-021, Jackson ImmunoResearch Laboratories, PA, USA) in 1:2000 dilution and anti-rabbit HRP-linked IgG (#7074, Cell Signaling Technology, MA, USA) as a secondary antibody in 1:10000 dilution. Detection of the HRP activity was done with the SuperSignal® West Pico Chemiluminescent substrate (#34087, Thermo Fisher Scientific, MA, USA).

Collection of plant material and isolation of CNGPs by immunoprecipitation

Cotyledons of seedlings from four different genotype-treatment combinations (*cg1-1* infected, *cg1-1* mock treated, *cg1-1* with *pDMR6:GnT1* infected and *cg1-1* with *pDMR6:GnT1* mock treated) were collected at 5 days after *Hpa* Waco9 or mock inoculation, and immediately frozen in liquid nitrogen. Each sample contained around 400 mg of cotyledons. Samples were collected in five independent experiments each considered as a biological replicate. The property of the anti-HRP antibodies to react with plant CNGPs was utilized to isolate the proteins by immunoprecipitation (IP). IP was performed with the Pierce® Crosslink Immunoprecipitation kit (Thermo Fisher Scientific, MA, USA). Briefly, the IP procedure includes binding of antibodies to agarose beads, cross-linking of bound antibodies to the beads, incubation of the beads with total extract of cotyledons, and elution of bound proteins. The default kit protocol was modified to obtain higher IP yields. The detailed optimized protocol can be found in SI Note 1. Eluates of the first four IPs for each sample were combined. Isolated proteins were precipitated before the tryptic digestion using RCI and II reagents from RC DC™ protein assay with co-precipitants (500-0122, Bio-Rad, CA, USA).

Liquid chromatography – mass spectrometry (LC-MS)

Sample preparation, including tryptic digests, orthogonal LC, MS/MS and MS^E, alignment of chromatograms, peak detection and selection were performed essentially as described previously [279]. To match peptide quantitation and identification results from both MS/MS and MS^E analyses, a recently developed bioinformatics pipeline (America A. *et al.*, in preparation) was deployed.

Filtering criteria for the selection of candidate CNGPs

Peptides uniquely matching a single Arabidopsis protein were used in the selection procedure. Abundance of each protein in samples was calculated as the mean normalized abundance

of all peptides uniquely matching to the protein. All missing values and null abundances were substituted with a low random value between 1 and 10. Statistical analysis was performed on the \log_2 -transformed protein abundance values. The protein was included in the list of candidate CNGLPs if its abundance was significantly higher in the *pDMR6:GnTI* infected samples compared to other samples (one-tail t-test assuming non-equal variance, false discovery rate <5%) [191].

Gene ontology (GO) terms enrichment analysis

GO terms counts for the set of candidate CNGLPs and the entire Arabidopsis genome (TAIR10) were obtained from the TAIR database [197]. Then, significance of enrichment was assessed

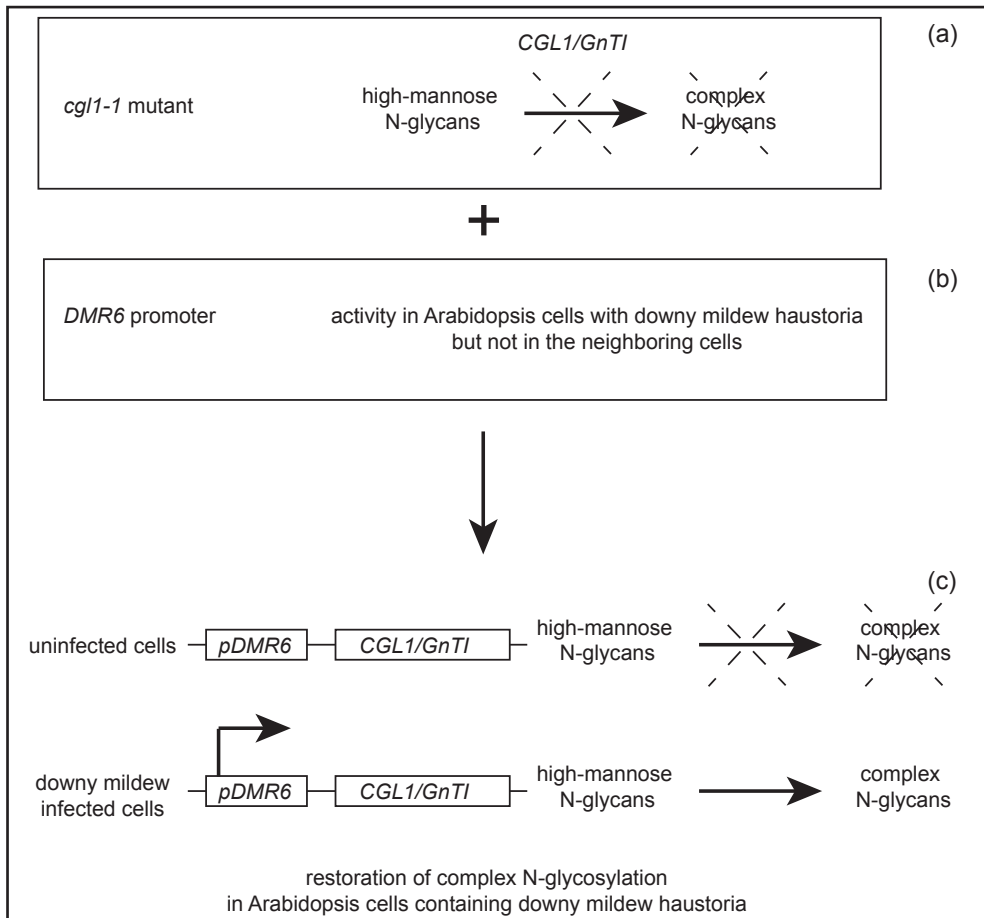


Figure 1. N-glycotagging approach to identify disease-related complex N-glycoproteins of Arabidopsis. (a) Maturation of high-mannose N-glycans into complex N-glycans is initiated by the N-acetylglucosamine transferase I (GnTI). The Arabidopsis mutant *complex glycan less 1-1* (*cgl1-1*) with a mutated *GnTI* gene is impaired in complex N-glycosylation. (b) The *DOWNY MILDEW RESISTANT 6* promoter is activated in Arabidopsis cells containing haustoria of *Hpa* but not in the neighboring cells. (c) The wild type *CGL1/GnTI* gene was fused to the *DMR6* promoter sequence, and the construct was transformed into the *cgl1-1* mutant background. Infection with *Hpa* is expected to restore complex N-glycosylation specifically in Arabidopsis cells containing *Hpa* haustoria.

with the Fisher's exact test following Bonferroni correction for multiple testing.

Identification of consensus N-glycosylation sites and predicted signal peptides

Consensus N-glycosylation sites (including subsequence NPS/T) and signal peptides were identified with the servers NetNGlyc1.0 [280] and SignalP4.1 [243, 281].

Cluster analysis of expression profiles for genes encoding potential CNGPs

Microarray-based gene expression data for Arabidopsis were derived from Genevestigator [243]. Genes were clustered based on the hierarchical clustering procedure (Pearson correlation coefficient, average linkage) and heat plots were generated with the MeV software [282] using the \log_2 transformed gene expression values of infected Arabidopsis tissues relative to mock treatment.

Results

N-glycotagging approach to identify disease-related proteins of Arabidopsis

A cell-specific N-glycotagging approach was designed to identify Arabidopsis proteins present in cells infected with downy mildew. The procedure is based on the restoration of complex N-glycosylation specifically in host cells containing *Hpa* haustoria but not in neighboring cells (Figure 1). For this, we deployed a promoter of the disease-related gene *DMR6* that is activated in *Hpa*-infected cells but not in the adjacent host cells [119]. By fusing the *DMR6* promoter to the coding sequence of *GnTI* and transforming this construct into the *cgl1-1* mutant, which is impaired in CNGPs biosynthesis [270], complex N-glycosylation would be specifically restored in downy mildew-infected cells.

Complex glycosylation induced in downy mildew-infected Arabidopsis cells

To check whether expression of *DMR6* is specific to downy mildew-infected cells in the *cgl1-1* mutant, we transformed the mutant with a *pDMR6:GUS* construct and checked the spatial pattern of *DMR6* promoter activity in downy mildew-infected and mock-treated seedlings by β -glucuronidase (GUS) staining (SI Figure 1). GUS activity was observed in host cells containing *Hpa* haustoria but not in the adjacent cells in both true leaves and cotyledons (SI Figure 1 a and b) demonstrating that the 2.4 kb *DMR6* promoter present in the T-DNA construct is activated in the *Hpa*-infected cells of the Col-0 *cgl1-1* mutant, similar to what has been previously observed in Arabidopsis *Ler eds1-2* plants [119]. Cotyledons of mock-treated seedlings did not show visible GUS activity, however, young true leaves and stem apices of mock-treated plants showed GUS activity indicating that the *DMR6* promoter is active in these tissues (SI Figure 1 c). These observations made us decide to use cotyledons for the proposed N-glycotagging approach due to the low background level of the *DMR6* promoter in mock-treated plants.

Next, we checked whether activation of the *DMR6* promoter also leads to accumulation of CNGPs in the *cgl1-1* seedlings carrying the *pDMR6:GnTI* construct that contains the identical promoter fragment as used in *pDMR6:GUS*. Presence of CNGPs in total extracts of the wild type Col-0, the *cgl1-1* mutant and the *pDMR6:GnTI* plants (*cgl1-1* background) was examined by western blot analysis with anti-HRP antibodies reacting to complex N-glycans (Figure 2). As expected, mock-treated seedlings of the *cgl1-1* mutant showed no detectable signal, indicating that no CNGPs are present. Also, proteins of *cgl1-1* seedlings infected with *Hpa* did not react with anti-HRP antibodies clearly showing that the downy mildew pathogen does not produce CNGPs with the core β 1,3 fucose and β 1,2 xylose groups. It also implies that all changes in the complex N-glycoproteome, detected by the anti-HRP antibodies, are those of the Arabidopsis host. Proteins from wild type Col-0 plants reacted strongly with anti-HRP antibodies demonstrating the feasibility of IP-based enrichment of CNGPs. We detected anti-HRP signals in extracts from whole aboveground parts of mock-treated seedlings with the *pDMR6:GnTI* construct (T3 line #16-4), but only very weak signal in extracts of cotyledons.

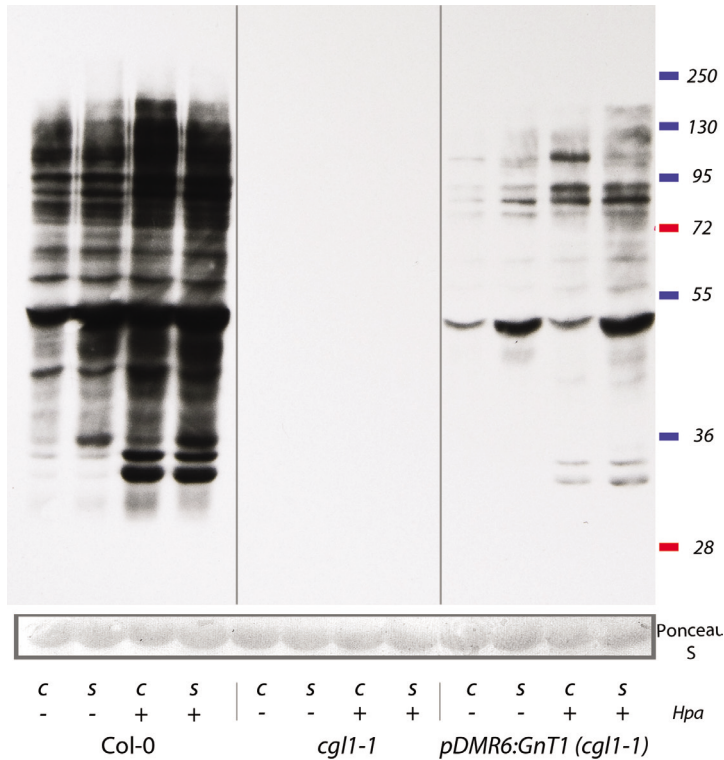


Figure 2. Western blot analysis of complex N-glycosylated proteins (CNGPs) in the wild type Arabidopsis Col-0, *complex glycan less 1-1 (cgl1-1)* mutant, and the glycotagging line *pDMR6:GnT1 (cgl1-1)* background) #16-4. Complex N-glycans can be detected on western blots with anti-HRP antibodies. Proteins from the whole aboveground part (labeled as 's') of Col-0 mock-treated seedlings give a strong signal corresponding to complex N-glycans attached to the proteins. In contrast, whole aboveground parts of the *cgl1-1* mutant with or without *Hyaloperonospora arabidopsidis (Hpa)* infection do not have detectable levels of CNGPs demonstrated by the absence of anti-HRP signal. Infection of Col-0 seedlings with *Hpa* changed the CNGP profile in the entire aboveground part, in particular the accumulation of two apparent CNGP bands in the 28-36 kDa range. In the mock-treated *pDMR6:GnT1* seedlings, very weak signal was detected in extracts from cotyledons (denoted as 'c'), in contrast to that of the whole aboveground part with stronger anti-HRP signal. Following *Hpa* infection, protein bands reacting with anti-HRP antibodies were found in both cotyledons and whole aboveground part including the bands in the range 28-36 kDa.

This is consistent with our observation that cotyledons of the *pDMR6:GUS* line have a very low background *DMR6* promoter activity compared to true leaves and stem apices. Infected cotyledons did show a clear accumulation of CNGPs including prominent bands in the 28-36 kDa range. These bands were also detected in extracts of whole aboveground parts of infected Col-0 seedlings suggesting that the use of cotyledons for N-glycotagging did not introduce substantial bias toward cotyledon-specific proteins. Therefore, cotyledons of *Hpa*-infected *pDMR6:GnT1* seedlings were used for the isolation of CNGPs to identify disease-related proteins.

MS-based identification of 18 candidate CNGPs from downy mildew-infected cells

For N-glycotagging of Arabidopsis proteins expressed in cells containing *Hpa* haustoria,

we inoculated eleven-day-old seedlings of the *cg1-1* transgenic line #16-4, containing the *pDMR6:GnTI* construct, and the untransformed *cg1-1* mutant with *Hpa* spores or water as a mock-treatment (SI Figure 2 a). Isolation of CNGPs in plants is not trivial; so far, no methods were reported to efficiently and specifically isolate such proteins. Since Arabidopsis CNGPs can be efficiently detected with anti-HRP antibodies (Figure 2), we used these antibodies to immunoprecipitate CNGPs. Details of the optimized IP protocol are described in the Material and methods section and SI Note 1. Briefly, anti-HRP antibodies were covalently bound to agarose beads, and used for several consecutive rounds of IP with total extracts from cotyledons of the mock- and *Hpa*-treated *cg1-1* and *pDMR6:GnTI* seedlings (the unbound fraction after one IP was used as input for the next round of IP with the same beads reconstituted after elution). Eluates containing CNGPs from four IP rounds for each sample were combined for subsequent analysis (SI Figure 2 b).

Following IP, proteins were precipitated from the eluates, digested with trypsin and subjected to two-dimensional (2D) LC-MS analysis in MS^E and DDA modes (SI Figure 2 c). Combining these two modes allows label-free relative quantitation and sequencing of the detected peptides [268]. 2D-fractionation of peptides, by reversed-phase separation using discontinuous and continuous acetonitrile gradients at high (dimension 1) and low pH (dimension 2), reduces the complexity of the peptide mixture and thus enables a better detection of low-abundant peptides by MS. After the second separation, peptides eluting from the column were online injected into the Synapt Q-TOF MS for MS^E runs (Waters Corporation, MA, USA). Based on the analysis of the MS^E data, we prepared an include list with 15424 peaks showing significantly different volume (peak area) in at least one of the samples (ANOVA, $p < 0.05$). Peptides corresponding to the peaks of the include list were subjected to the MS/MS analysis on the Orbitrap XL (Thermo Scientific, MA, USA) to determine the amino acid sequences of individual peptides. Finally, results of DDA and MS^E procedures were matched using a recently developed bioinformatics pipeline implemented on the Galaxy server (America A. *et al.*, in preparation) (SI Figure 2 d). Of all peaks from the include list, identification results of MS/MS and MS^E, and quantitation results from MS^E were matched for a total of 5903 peaks. Average normalized abundances of all matched peptides were similar across all samples (SI Figure 3 a) suggesting that equal amounts of proteins were isolated by IP from the different samples. This was rather unexpected as the IP was specifically aimed at isolating CNGPs that are clearly induced in *Hpa*-infected *pDMR6:GnTI* samples (Figure 2). Also, the ratios of the intensity of matched peaks of *Hpa*-infected compared to mock-treated cotyledons between *cg1-1* and *pDMR6:GnTI* samples showed a low but significant correlation ($r^2 = 0.12$, $p < 0.001$, SI Figure 3 b). Principal component analysis (PCA) of the normalized peak intensities (SI Figure 3 c) showed that the largest difference in the four samples was between mock-treated and infected samples suggesting that *Hpa* treatment had a stronger effect than genotype. Importantly, adding PC3 to the analysis, as shown in the biplot for the principle components PC2 and PC3 (SI Figure 3 d), resulted in a clear separation between all four groups of samples demonstrating that there is specific enrichment observed of peptides in eluates of *pDMR6:GnTI* cotyledons infected with *Hpa*. These peptides are expected to correspond to candidate CNGPs, therefore we focused our further analysis on those peptides.

To select candidate disease-related CNGPs in our dataset, we first determined the relative abundance of all detected proteins by calculating the average normalized abundance of all peptides uniquely matching to given Arabidopsis proteins. Since CNGPs are enriched in the *pDMR6:GnTI* cotyledons infected with *Hpa* (Figure 2), candidate CNGPs were selected to have higher relative abundance in samples from *pDMR6:GnTI* cotyledons infected with *Hpa* compared to the other three samples: *pDMR6:GnTI* mock, *cg1-1* mock, and *cg1-1* downy mildew-inoculated (t-test, FDR < 0.05). Based on this criterion, we identified 18 candidate CNGPs (Table 1, SI Note 2). On average, each of the 18 identified Arabidopsis proteins was supported by 4.6 unique peptides and had a mean coverage of 12.1%. All identified proteins appeared to contain at least one consensus N-glycosylation site NxS/T further indicating

that these proteins could indeed be N-glycosylated. Complex N-glycosylation implies that the proteins carry signal peptides or signal anchors that target them to the ER and Golgi complex. Consistently, we found that 16 out of candidate CNGPs have a predicted N-terminal signal peptide (Table 1). Enrichment analysis of gene ontology (GO) terms also pointed to an overrepresentation of proteins associated with the cell component GO categories “extracellular” and “cell wall” (SI Table 1, Fisher’s exact test, Bonferroni corrected $p < 0.05$) suggesting that the set of candidate CNGPs is indeed enriched for secreted proteins. Furthermore, the list of 18 identified proteins was enriched for the GO category “response to abiotic and biotic stimulus” (SI Table 1, Fisher’s exact test, Bonferroni corrected $p = 0.017$). Fourteen genes encoding the candidate CNGPs were transcriptionally induced after *Arabidopsis* infection with compatible and incompatible *Hpa* isolates, the bacterial pathogen *Pseudomonas syringae* pv. *tomato* DC3000 or after treatment with fungal, oomycete and bacterial elicitors (SI Figure 4, SI Table 3). At the same time, three genes, At1g01980 (FAD-binding Berberine family protein), At4g28940 (phosphorylase) and At5g49760 (kinase-like protein), were not induced in these analyzed microarray experiments suggesting the differential abundance of the corresponding proteins is regulated post-transcriptionally. Thus, the 18 identified proteins are associated with *Arabidopsis* responses to infection and disease.

Table 1. Identified candidate complex N-glycosylated proteins

Arabidopsis protein accession	Number of supporting peptides	Protein coverage, %	Number of potential N-glycosylation sites ¹	Predicted signal peptide (Y-score) ²	Gene description	Bonferroni corrected t-test p-value ³	Mean normalized abundance in pDMR6:GnTI infected cotyledons
AT1G01980.1	1	3.7	7	YES (0.85)	FAD-binding Berberine family protein	<0.001	712.37
AT1G02360.1	4	12.9	3	YES (0.81)	Chitinase family protein	<0.001	454.46
AT1G09560.1	3	10.0	1	YES (0.84)	PDGLP1 germin-like protein 5	<0.01	110.52
AT1G26380.1	9	14.2	10	YES (0.79)	FAD-binding Berberine family protein	0.02	198.18
AT1G32940.1	11	18.5	12	YES (0.87)	ATSBT3.5 Subtilase family protein	<0.0001	122.29
AT1G32960.1	8	12.6	9	YES (0.81)	ATSBT3.3 Subtilase family protein	<0.01	165.58
AT1G51800.1	1	1.2	19	YES (0.82)	Leucine-rich repeat protein kinase family protein	<0.0001	164.33

AT1G61360.1	1	1.0	16	YES (0.83)	S-locus lectin protein kinase family protein	<0.0001	204.37
AT2G19190.1	1	1.4	12	YES (0.71)	FRK1 FLG22-induced receptor-like kinase 1	<0.0001	162.36
AT2G38255.1	1	5.1	4	NO (0.10)	Protein of Unknown Function	<0.0001	125.00
AT3G22060.1	12	27.0	1	YES (0.68)	Receptor-like protein kinase-related family protein	0.04	511.64
AT3G54420.1	1	4.4	4	YES (0.81)	ATCHITIV homolog of carrot EP3-3 chitinase	<0.001	183.05
AT4G28940.1	4	18.4	3	YES (0.57)	Phosphorylase superfamily protein	<0.0001	86.85
AT5G03610.1	6	15.9	3	YES (0.69)	Acyhydrolase superfamily protein	0.01	324.62
AT5G06320.1	4	15.6	4	NO (0.11)	NHL3 NDR1/HIN1-like 3	<0.0001	279.49
AT5G18470.1	7	18.2	9	YES (0.87)	Curculin-like (mannose-binding) lectin family protein	<0.0001	49.71
AT5G39580.1	8	36.4	2	YES (0.87)	Peroxidase superfamily protein	<0.01	251.79
AT5G49760.1	1	0.9	17	YES (0.89)	Leucine-rich repeat protein kinase family protein	<0.0001	321.38

¹ – number of NxS/T subsequences where x is any amino acid except for P

² – predicted with the SignalP4.1 server using default settings

³ – one-tailed t-test for the difference in mean protein abundance in the pDMR6::GnTI infected cotyledons and in *cgl1-1* mock treated, *cgl1-1* infected, *pDMR6::GnTI* mock inoculated cotyledons treated as one group.

The *plasmodesmata germin-like protein 1* mutant is recued susceptible to *Hpa*

N-glycotagging identified 18 candidate CNGPs associated with downy mildew infection in Arabidopsis. To gain insight into the function of these proteins during the host-*Hpa* interaction, we tested whether the level of susceptibility of mutants corresponding to these genes encoding the candidate CNGPs is altered compared to the wild type. The *IMPAIRED IN OOMYCETE SUSCEPTIBILITY 1 (IOS1)* gene encoding one of the candidate CNGPs was previously described to be downy mildew-induced, and the *ios1-1* mutant had reduced susceptibility to the compatible *Hpa* isolate Wela [112]. We checked the level of susceptibility

for 22 T-DNA insertion lines to *Hpa* (SI Table 2). The majority of the tested mutants did not show altered sporulation levels compared to wild type plants upon infection with the compatible *Hpa* isolate Waco9 (Figure 3a, Bonferroni test $p > 0.05$) except for a few mutants. The mutant *SAIL_400_F09* for *SUBTILASE3.5* (*ATSBT3.5*), which encodes unknown subtilase family protein, demonstrated slightly increased sporulation of Waco9 (Figure 3a, $p = 0.001$) suggesting that *ATSBT3.5* positively contributes to Arabidopsis immunity to downy mildew. A mutant for the *PLASMODESMATA GERMIN-LIKE PROTEIN 1* (*PDGLP1*), *pdg1p1*, was slightly less susceptible to *Hpa* Waco9 than the wild type Col-0 (Figure 3b, Tukey HSD $p < 0.05$). Notably, the mutant of the *PDGLP1* paralog, *pdg1p2*, was also less susceptible to Waco9. Unexpectedly, level of sporulation of the double *pdg1p1 pdg1p2* mutant was not different from that of single mutants ($p > 0.05$). These results show that the mutations do not affect Arabidopsis susceptibility additively suggesting that *PDGLP1* and *PDGLP2* do not have redundant roles in the Arabidopsis-*Hpa* interaction. Thus, in addition to the previously reported reduced susceptible mutant *ios1-1*, the mutants analysis indicates that two Arabidopsis genes, *ATSBT3.5* and *PDGLP1*, encoding candidate CNGPs, affect Arabidopsis interaction with downy mildew.

Discussion

An N-glycotagging approach was developed to identify host disease-related CNGPs in Arabidopsis cells containing haustoria of the downy mildew pathogen *Hpa*. Identification of proteins in these particular cells can aid in understanding the molecular processes occurring in the host plant during downy mildew infection. To our knowledge, there are no reports about targeted identification of host proteins present in cells in immediate contact with pathogenic fungi or oomycetes. The N-glycotagging approach described here is based on the restoration

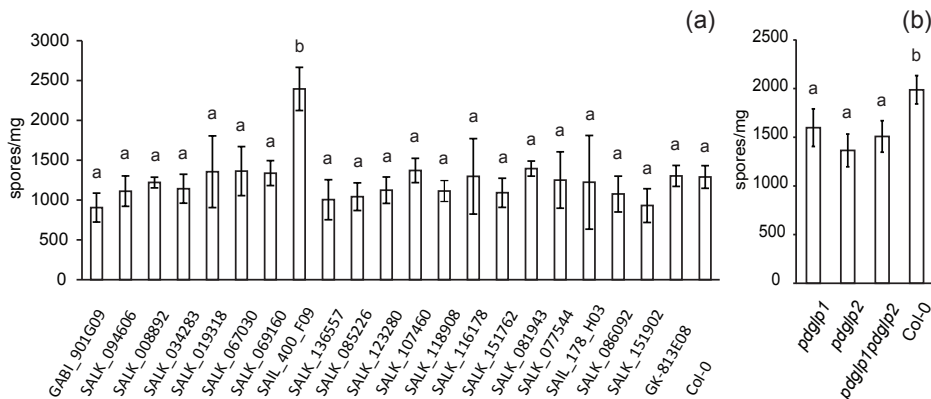


Figure 3. Sporulation of *Hpa* Waco9 on Arabidopsis mutants corresponding to genes encoding candidate complex N-glycoproteins. (a) The majority of mutant lines have similar levels of susceptibility to Waco9, reflected by a spore count, as the wild type Col-0, however the mutant line *SAIL_400_F09* (for the *ATSBT3.5* gene) has significantly increased sporulation compared to the wild type at 7 days post inoculation (dpi) ($p = 0.001$). The experiment was performed three times with two replicates each. A Bonferroni post-hoc test was performed on means of the three experiments ($n = 3$). Error bars represent \pm SD. Letters above bars label groups of the homogenous sets of genotypes ($\alpha = 0.05$). (b) The single *pdg1p1*, *pdg1p2* and double *pdg1p1 pdg1p2* mutants show slightly reduced spore counts of the *Hpa* isolate Waco9 at 6 dpi compared to the wild type Col-0 ($p < 0.05$). The experiment was performed three times and combined results of three experiments were analyzed with mixed ANOVA followed by the Tukey HSD test. Letters indicate homogenous subsets of genotypes ($\alpha = 0.05$). Error bars represent \pm SEM.

of complex N-glycosylation in specific cell types of the *Arabidopsis cgl1-1* mutant by expressing the *GnTI* gene under a pathogen-responsive promoter [283]. For this we used the promoter of the *DMR6* gene that is expressed specifically in *Arabidopsis* cells invaded by *Hpa* haustoria but not in neighboring host cells. Activation of the *DMR6* promoter after infection would induce complex N-glycosylation mediated by the GnTI enzyme in the infected cells. Although the procedure seems straightforward, identification of proteins tagged with complex N-glycans in specific cell types is problematic due to difficulties in efficient isolation of CNGPs.

To isolate CNGPs, we considered using plant L-lectins for affinity purification, however, to our knowledge, there are no lectins with established specificity to plant CNGPs. Wheat germ agglutinin, which is frequently used for the isolation of glycosylated proteins, is not suitable for plant complex N-glycans since its binding is inhibited by the core β 1,3 fucose group [284]. A chemical, hydrazide-based, approach to enrich samples for peptides from CNGPs is also based on affinity purification. First, glycopeptides are oxidized and subsequently bound to hydrazide beads. Then bound glycopeptides are released by treatment with peptide-N-glycosidases (PNGases) F and A [285]. PNGase F treatment releases peptides bound to high-mannose N-glycans, and PNGase A works on both high-mannose and complex N-glycopeptides [286]. Unfortunately, PNGase A treatment is not efficient in glycopeptide extracts of *Arabidopsis* so that the amount of peptides released from hydrazide beads is rather low, non-quantitative and not sensitive enough [283]. In this work, we used an IP-based method to isolate CNGPs. Anti-HRP antibodies, which react to the core β 1,3 fucose and β 1,2 xylose specifically present on plant CNGPs, were covalently bound to the agarose beads, and then several consecutive IPs were performed on the same material to maximize CNGPs recovery and enrichment. Despite all attempts, we could not immunoprecipitate all detectable CNGPs from wild type Col-0 seedlings. However, the IP procedure with four consecutive incubations was efficient in isolation of all detectable CNGPs from the mix of wild type and *cgl1-1* total extracts in the ratio 1:10 and 1:100 (data not shown). Therefore, IP of CNGPs with anti-HRP antibodies is suitable for experiments with tissue-specific profiling since one expects cell-specific tagging only in the a small fraction of cells infected with *Hpa*. The identified candidate CNGPs have at least one consensus N-glycosylation site NxS/T and the majority of them have an N-terminal signal peptide further supporting that these proteins can be complex N-glycosylated. Three proteins, RLK At3g22060, RLK At5g49760 and NHL3, were also found to be complex N-glycosylated in an independent analysis with the hydrazide-based affinity purification (Wei S. *et al.*, in press). Thus, our IP-based procedure for CNGPs enrichment is suitable for the N-glycotagging. Infection of wild type *Arabidopsis* Col-0 seedlings with *Hpa* led to the appearance of two prominent CNGPs bands in the 28-36 kDa range. Several of the 18 identified candidate CNGPs have a predicted size lower than 36 kDa (including signal peptide): two chitinases At1g02360 and At3g54420, PDGLP1, RLK At3g22060, NHL3 and the peroxidase-like protein At5g39580. The chitinase At1g02360 and RLK At3g22060 appear as most abundant in the MS analysis suggesting that these proteins match to the prominent 28-36 kDa proteins induced by *Hpa* infection and detected on western blot.

Previous proteomics studies of interactions between plants and pathogenic microbes focused on the identification of either pathogen proteins or host proteins in whole infected organs. Results of these investigations showed that pathogen attack causes significant changes in the plant proteome and physiology: accumulation of pathogenesis-related proteins, increase in the abundance of proteins related to secondary metabolism (e.g. phenylpropanoid pathway), antioxidant enzymes and posttranslational protein modifications (e.g. phosphorylation) [287]. We aimed to identify disease-related proteins of *Arabidopsis* present in downy mildew-infected cells using N-glycotagging. GO term enrichment analysis showed a clear association of the identified set of CNGPs with “response to biotic and abiotic stimuli” (SI Table 3) indicating that these proteins are disease-related. Also, genes coding for fourteen of the eighteen candidate CNGPs identified with our N-glycotagging approach appeared to be transcriptionally induced at least two fold after infection with compatible or incompatible

bacterial, fungal or oomycete pathogens (SI Figure 4) further supporting that the identified proteins are disease-related. Genes encoding some of the candidate CNGPs were previously found in analyses of Arabidopsis responses to pathogens and microbe-associated molecular patterns (MAMPs) or constitutive activation of defense including the marker gene to study early defense signaling in Arabidopsis *FLAGELLIN INDUCED RECEPTOR-LIKE KINASE 1* [288], the S-locus lectin protein kinase gene At1g61360 [289] and *ATSBT3.3* encoding a subtilase family protein [290]. Also, transcription of the chitinase encoding gene At1g02360 was found to be significantly induced after infection with the downy mildew *Hpa* [112]. Finally, some of the identified candidate CNGPs were previously implicated in Arabidopsis responses to infection, e.g. *NHL3*, a homolog of the well-known regulator of Arabidopsis plant immunity *NDR1*, that is suggested to play a positive role in Arabidopsis immunity. *NHL3* mRNA levels are strongly increased after infection with avirulent *Pst* DC3000 and its overexpression leads to elevated resistance of Arabidopsis to virulent *Pst* [291, 292]. Another candidate CNGP, the predicted malectin-like receptor like kinase *IOS1*, is also involved in Arabidopsis susceptibility to *Hpa* since the *IOS1* gene is transcriptionally induced specifically in Arabidopsis cells that are in immediate contact with *Hpa* hyphae, and the *ios1-1* mutant has a lower susceptibility to *Hpa* compared to the wild type [112]. This provides a proof-of-principle that our N-glycotagging approach can reveal disease-related proteins in *Hpa*-infected cells.

To reveal a role for CNGP genes other than *IOS1* in Arabidopsis susceptibility to downy mildew, we tested whether Col-0 mutants with T-DNA insertions in genes encoding the identified candidate CNGPs show altered sporulation levels after infection with the compatible *Hpa* isolate Waco9. The *sbt3.5* mutant was more susceptible to infection compared to the wild type Col-0 indicating a positive role of SBT3.5 protein in Arabidopsis immunity to *Hpa*. Subtilases are serine proteases, however the exact function of SBT3.5 is unknown. Also, the *pdglp1* mutant was slightly more resistant to the compatible *Hpa* isolate than the wild type Col-0. To check for redundancy the *pdglp2* and *pdglp1_pdglp2* mutants were tested and showed reduced susceptibility similar to that of the *pdglp1* mutant. This suggests that the two proteins act non-additive and possibly are active in the same pathway. Overexpression of *PDGLP1* and *PDGLP2* changes Arabidopsis root architecture, i.e. increased lateral root formation and shortened main roots of seedlings, possibly as a result of altering nutrient translocation through plasmodesmata. However, the single and double mutants do not show visible changes in root architecture. Role of the *PDGLP* genes in Arabidopsis susceptibility to diseases has not been reported so far [293]. It is tempting to speculate that the mutations change cell-to-cell communication in the mesophyll of leaves infected with downy mildew that results in reduced susceptibility to *Hpa*. Potentially, the plasmodesmata localized *PDGLP1* and *PDGLP2* proteins [293] mediate translocation of nutrient to the infection site or *Hpa* effectors into cells adjacent to the cells with haustoria. The identified CNGP genes that are involved in the infection process will be further studies to reveal the mechanisms by which they contribute to disease.

Acknowledgements

The proteomic analysis was supported by Centre for BioSystems Genomics (CBSG) (Proteomics Hotel project TD8-15). The Leverhulme Trust is acknowledged for supporting DL. We also thank R.W. Dekter for preparing the *pDMR6:GnTI* and *pDMR6:GUS* constructs used in this study, dr. Harald Keller (INRA, Antibes, France) for seeds of the *ios1-1* mutant and prof. dr. W. Lucas (UC Davis, USA) for seeds of the *pdglp1*, *pdglp2*, *pdglp1/2* mutant lines.

Supporting information

SI Table 1. Primers used in this study

Primer name	5'-3' sequence
FattB4-pDMR6	GGGGACAACCTTTGTATAGAAAAGTTGCAgccccgtatttggatagaa
RattB1-pDMR6	GGGGACTGCTTTTTTGTACAAAATTGAttgatgtcagaaaattgaagaagaa
SAIL_178_H03_LP	TCCTTGCAATAAGGCTAGGG
SAIL_178_H03_RP	TCGGACATATCGACGGTAATG
SALK_081943_LP	ACGCCATTGATGATCAACTTC
SALK_081943_RP	GGTCCAATTCAACTATCGTGG
SALK_116178_LP	GTTCCACCTGGCTTAGGATTC
SALK_116178_RP	GGCTCAGATTTACACGAGAC
GK-813E08_LP	GCTAGTCCGGAGAATCCAATC
GK-813E08_RP	CTCAGGTTACTCTCTGTGGCG
SAIL_400_F09_LP	TTTAAATGGGCCTTAAATCCG
SAIL_400_F09_RP	CCAAGTTCGAGTTGTAGCGAG
SALK_086092_LP	TCACACACACCTTGTCTTTGC
SALK_086092_RP	AAAACGCATGCGAACATTTAC
SALK_107460_LP	CTTGGGGAGGAAGAAAAGATG
SALK_107460_RP	GAGGACCTAACTCGATGTCCC
GABI_901G09_LP	ATGAAGAACAATGCCACCAAG
GABI_901G09_RP	CGTAGCCCAATCAATCTCAAG
SALK_085226_LP	TCCCGTACATGAAACGAGTTC
SALK_085226_RP	TAAACGTGTCCGGTACCTAC
SALK_094606_LP	AAGTCGCGTTAAAGTATCCCC
SALK_094606_RP	TTTTACGCAAATGGTTGAAGG
SALK_067030_LP	AAAGGGATAGTCTTGAAGGGC
SALK_067030_RP	TCATTCCACATCTTTAAGCG
SALK_069160_LP	TCCTTGAAAACCTTTGTAACCCC
SALK_069160_RP	GAGGACTAATTCATCCGGAG
SALK_151902_LP	TTTACCGTCGCAACAGTTAGG
SALK_151902_RP	TTAAAACGCATCGTTTGGTTC
SALK_123280_LP	CAAAATGTTGACTCCCACCA
SALK_123280_RP	CACACTCCAAAGCACCGTTA
SALK_136557_LP	TGATGCATACATGCATGTTCTC
SALK_136557_RP	GACAACCACTTCTCGTCAAGG
SALK_008892_LP	TAAAAGTCTTCTTGAACCCG
SALK_008892_RP	TTGACAAACAAATAGTACAAATTCCAG
SALK_019318_LP	TTCGTCAAGATTCCACTGGAC
SALK_019318_RP	TTTCCATTTTCCACACCAGTC

SALK_034283_LP	TCCATTGTTTCGTC AAGATTCC
SALK_034283_RP	TTTCCATTTTCCACAC CAGATC
SALK_151762_LP	TCGGCAATCTTTGTATT CGAC
SALK_151762_RP	TGCACTGCATGGTTTATT GTC
SALK_118908_LP	TCGATTGGATTGGACAAGA AG
SALK_118908_RP	GATGTGTTAGGTTGCAA ACCC
SALK_077544_LP	GCTCGTGATCGTGAGAA ACTC
SALK_077544_RP	TCGAAAAACTCCGAGT GATTG
LBb1.3	ATTTTGCCGATTTCGGA AC
SAIL LB2	GCTTCCTATTATATCTT CCCAAATTACCAATACA
pAC161 o8409	ATATTGACCATCATACTC ATTGC

SI Table 2. T-DNA insertion mutants used in this study

Arabidopsis gene model	T-DNA line (location of the insertion)
AT1G01980	SAIL_178_H03 (exon)
AT1G02360	SALK_081943 (exon); SALK_116178 (exon)
AT1G09560	<i>pdgfp1</i> (exon)
AT1G26380	GK-813E08 (exon)
AT1G32940	SAIL_400_F09 (intron)
AT1G32960	SALK_086092 (exon); SALK_107460 (exon)
AT1G51800	<i>ios1-1</i> (exon)
AT1G61360	GABI_901G09 (intron)
AT2G19190	SALK_085226 (exon)
AT2G38255	SALK_094606 (exon); SALK_067030 (exon); SALK_069160 (exon)
AT3G22060	SALK_151902 (intron)
AT3G54420	SALK_123280 (exon); SALK_136557 (3'-UTR)
AT4G28940	SALK_008892 (intron)
AT5G18470	SALK_019318 (5'-UTR); SALK_034283 (5'-UTR)
AT5G39580	SALK_151762 (exon)
AT5G49760	SALK_118908 (exon); SALK_077544 (exon)

SI Table 3. Gene ontology categories enriched in the candidate CNGPs set (Fisher's exact test $p < 0.05$)

Gene ontology category		Fisher's test p-value, Bonferroni corrected
Biological process	response to abiotic or biotic stimulus	0.017
Cellular component	cell wall	0.000
	extracellular	0.017

SI Table 4. Peptide sequences and their matched normalized abundances (.csv file in the enclosed CD)

SI Table 5. List of microarray studies used for the expression analysis of genes encoding candidate complex N-glycosylated proteins

Text on the SI Figure 4	ID in GEO, NASC arrays or ArrayExpress databases
<i>Botrytis cinerea</i>	GSE5684
<i>Rhizoctonia solani</i> AG2-1 isolate	GSE26206
<i>Phytophthora infestans</i> 12 h	GSE5616
<i>Phytophthora parasitica</i> 10.5 h	GSE20226
<i>Blumeria graminis</i>	GSE12856
<i>Golovinomyces orontii</i> , 96 h	GSE5686
<i>Golovinomyces cichoracearum</i>	GSE26679
<i>Fusarium oxysporum</i>	GSE15236
<i>Hpa</i> compatible 8+24 hpi	GSE21076
<i>Hpa</i> compatible 12 hpi	GSE22274
<i>Hpa</i> compatible 2 dpi	
<i>Hpa</i> compatible 3 dpi	
<i>Hpa</i> compatible 4 dpi	GSE22274
<i>Hpa</i> compatible 4+6 dpi	GSE21076
<i>Hpa</i> compatible 6 dpi	GSE22274
<i>Hpa</i> incompatible 12 hpi	GSE22274
<i>Hpa</i> incompatible 3 dpi	GSE14946
<i>Hpa</i> incompatible 4 dpi	GSE22274
<i>Hpa</i> incompatible 6 dpi	
<i>Pst</i> DC3000 <i>avrRPM1</i> , 24 h	
<i>Pst</i> DC3000 2 hpi	NASCArrays-120
<i>Pst</i> DC3000 24 hpi	
<i>Pst</i> DC3000 <i>hrpC</i> - 2 hpi	
<i>Pst</i> DC3000 <i>hrpC</i> - 24 hpi	
<i>Xanthomonas campestris</i>	
	GSE9674

DFPM	GSE28800
fumonisin B1	NASCARRAYS-77
elf26 1 hpi	E-MEXP-547
flg22 4 hpi	GSE5615
NPP1 4 hpi	
lipopolysaccharides 4 hpi	
lipopolysaccharides 3 hpi	E-NASC-76
chitin	GSE2538
ABA 3 hpi	NASCArrays-176
ACC 3 hpi	NASCArrays-172
BL 3 hpi	NASCArrays-178
GA3 3 hppi	NASCArrays-177
IAA 3 hpi	NASCArrays-175
MeJA 3 hpi	NASCArrays-174
zeatin 3 hpi	NASCArrays-173
SA 4 hpi	E-TABM-51
SA 28 hpi	
SA 52 hpi	
SA 6 hpi	GSE34047
glycerol-3-phosphate	GSE26973
anoxia	GSE16222
cold stress	NASCARRAYS-138
drought stress	NASCARRAYS-141
hypoxia	GSE9719
osmotic stress	NASCARRAYS-139
oxidative stress	NASCARRAYS-143
salt stress	NASCARRAYS-140
wounding	NASCArrays-145

SI Note 1. Detailed protocol for the immunoprecipitation of complex N-glycosylated proteins in Arabidopsis

Protocol for immunoprecipitation (IP) of complex N-glycosylated proteins from total plant extract (based on the protocol from the Pierce® Crosslink Immunoprecipitation kit (Thermo Fisher Scientific, Waltham, MA, USA))

For the IP of complex N-glycosylated proteins from around 400 mg of Arabidopsis cotyledons, we have used 800 µl of extraction buffer, 100 µl of control beads slurry, 40 µl of antibody beads slurry, 100 µg of unconjugated rabbit α-horseradish peroxidase (HRP) antibodies (323-005-021, Jackson ImmunoResearch Laboratories, PA, USA).

Buffers:

Coupling buffer/Washing buffer (provided with the kit)

NaCl 150 mM, Na phosphate (?) 10 mM pH7.2

Conditioning buffer (provided with the kit)

neutral pH

Elution buffer (provided with the kit)

pH2.8; contains primary amine

TBS/Washing buffer (provided with the kit)

Tris-HCl 25 mM, NaCl 150 mM, pH7.2

Extraction buffer (not provided)

Tris-HCl 50 mM pH7.5, NaCl 150 mM, EDTA 5 mM, Triton X-100 1%, Brij-58 1%, Glycerol 5%, plant protease inhibitor cocktail (P9599, 1:100 dilution, Sigma-Aldrich, MO, USA)

Unless specified, all centrifugation steps are performed at +4°C with the speed 1000xg. All buffers and solutions (except for those based on DMF/DMSO) are pre-cooled on ice.

- I. Preparation of beads cross-linked with antibodies
 1. prepare 1x coupling buffer, keep on ice
 2. add 40 µl of slurry per IP in each column
 3. wash beads with 400 µl of 1x coupling buffer in each column separately, centrifuge 1 min
 4. prepare antibodies for coupling to the beads (SI Table 5)
 5. combine the prepared antibody mix with all beads in one tube, incubate beads with antibodies at room temperature for 1.5 hours with continuous rotation
 6. washing away unbound antibodies
 - i. load the incubated slurry in separate columns, centrifuge for 1 min; **retain flow-through to check antibody binding**
 - ii. wash beads with 200 µl 1x coupling buffer in each column separately, centrifuge for 1 min
 - iii. wash beads with 600 µl 1x coupling buffer in each column separately, centrifuge for 1 min; repeat this step
 7. crosslinking (**protect from light**)
 - i. combine all washed beads in one tube (use a part of coupling buffer and mQ from the mixture in SI Table 2)
 - ii. add 217 µl of DMF to one aliquot of DSS; dissolve by pipeting
 - iii. take 100 µl of the stock solution of DSS (25 mM), add 900 µl of DMF to prepare 2.5 mM solution; prepare mixture for crosslinking (SI Table 6) and mix it with beads
 8. incubate at room temperature for 45 min with continuous rotation
 9. washing after cross-linking
 - i. load the incubated slurry in separate columns, centrifuge for 1 min, discard flow-through
 - ii. wash beads with 100 µl of elution buffer to each column, centrifuge for 1 min, **retain flow-through to check crosslinking**
 - iii. wash beads with 200 µl of elution buffer to each column, centrifuge for 1 min, discard flow-through; repeat this step
 - iv. wash beads with 400 µl of elution buffer to each column, centrifuge for 1 min, discard flow-through; repeat this step
 - v. storage in the extraction buffer (overnight) at +4°C
- II. Protein isolation and preparation of pre-cleared lysate
 1. mix 400 mg of grinded cotyledons and 800 µl of extraction buffer; incubate 45 min on ice; vortex every 5 min

2. centrifuge to remove debris 1 min >12,000xg, pipet the cleared lysate into a new tube and repeat this step until the lysate is free of debris
 3. prepare control beads
 - i. load 100 μ l of the control beads slurry onto a column for washing
 - ii. centrifuge for 1 min, discard flow-through
 - iii. wash beads with 100 μ l of 1x coupling buffer, centrifuge for 1 min, discard flow-through
 4. load 700 μ l of lysate onto the columns with the prepared control beads
 5. incubate beads at +4°C for 2.5 hours with continuous rotation
 6. centrifuge for >12,000xg 5 min to remove the control beads, repeat this step; discard control beads
- III. Immunoprecipitation itself
1. centrifuge the prepared crosslinked beads for 1 min after o/n storage, discard the flow-through
 2. wash the crosslinked beads with 400 μ l of the extraction buffer, centrifuge for 1 min, discard the flow-through
 3. load the pre-cleared lysate on the crosslinked beads
 4. Incubate samples with the crosslinked beads at 4°C with continuous rotation; each sample was subjected to five IP rounds with the same cross-linked beads, the first incubation was overnight, second – 3-4 hours, third – overnight, forth – 3-4 hours, and fifth – overnight
- IV. Washing and elution of the immunoprecipitated proteins
1. Centrifuge columns with the incubated samples 1000xg 1 min, retain the flow-through for the next round of IP
 2. Wash beads in 400 μ l of 1xTBS, centrifuge 1000xg 1 min, discard flow-through (in total four washes)
 3. Incubate beads with 170 μ l of the elution buffer for 15 min at 4°C, , centrifuge 1000xg 1 min, collect samples in silanized tubes
 4. reconstitute beads
 - i. wash with 200 μ l of 1x coupling buffer, centrifuge 1000xg 1 min, discard the flow-through
 - ii. wash with 400 μ l of extraction buffer, centrifuge 1000xg 1 min, discard the flow-through, repeat this step
 5. go to step III.2

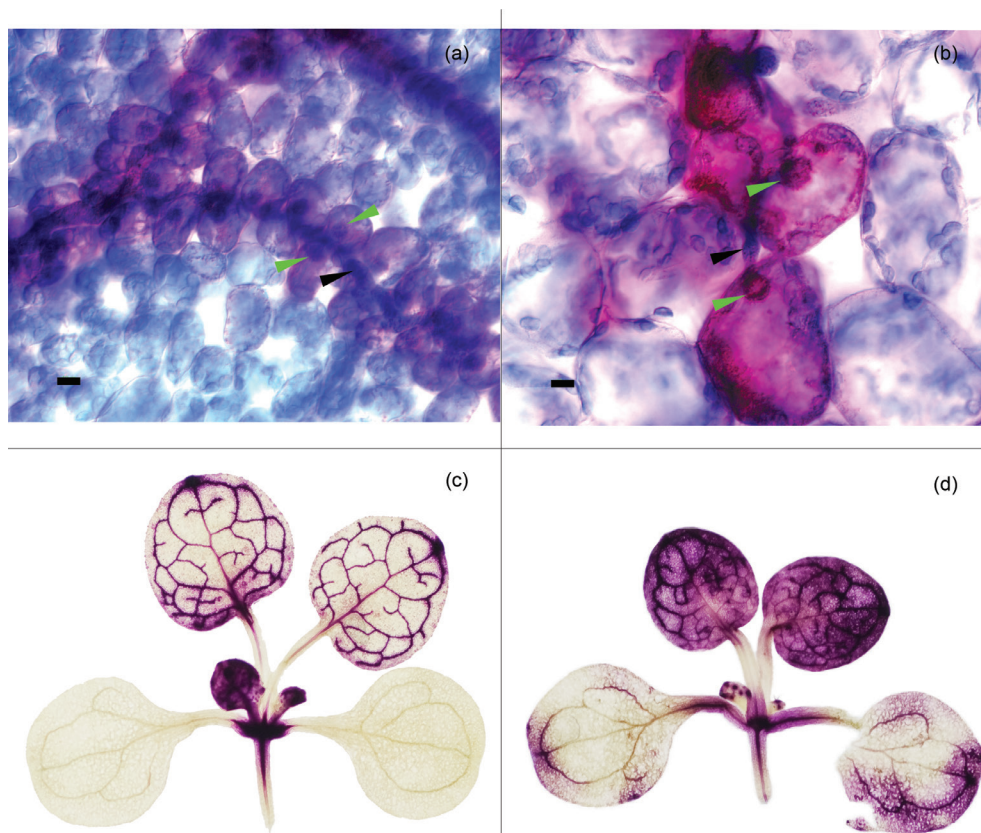
SI Table 5. Components of the coupling solution with anti-HRP antibodies

Component	volume per IP, μ l
anti-HRP 2,4 mg/ml	42
mQ	53
20x coupling buffer	5
total	100

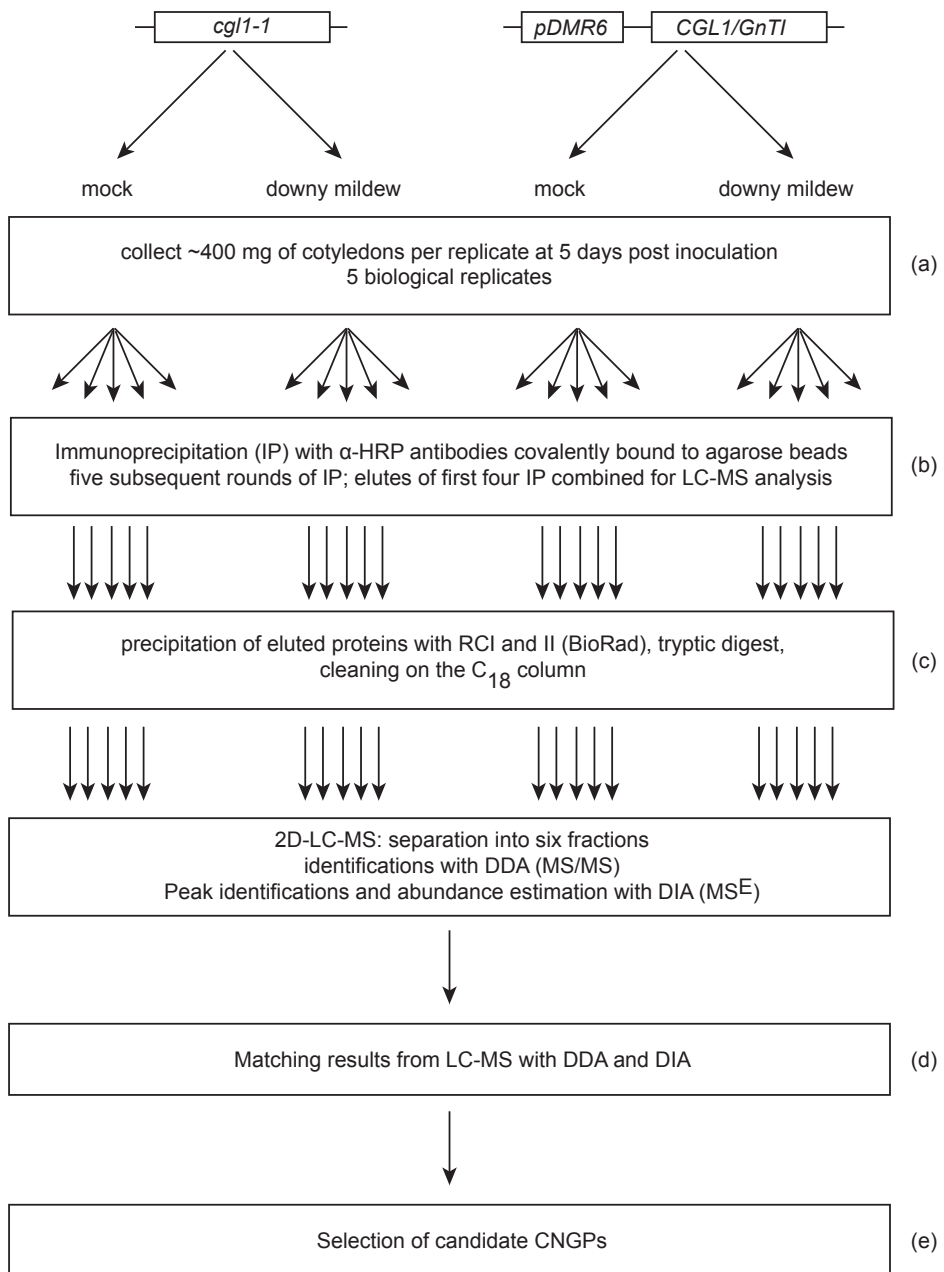
SI Table 6. Components of solution for crosslinking of anti-HRP to beads

Component	volume per IP, μ l
DSS 2.5 mM	18
mQ	77
20x coupling buffer	5
total	100

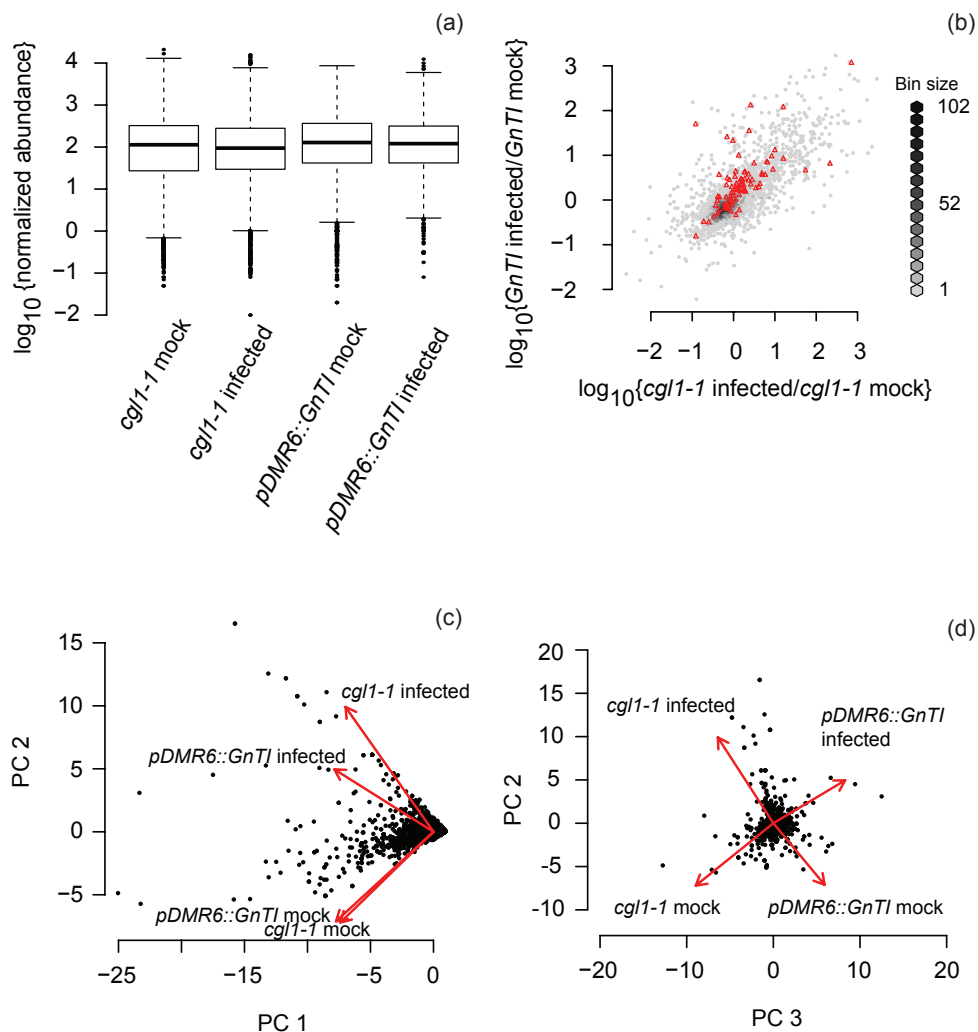
SI Note 2. Arabidopsis candidate complex N-glycosylated proteins identified in this study (available as a separate file on the enclosed CD)



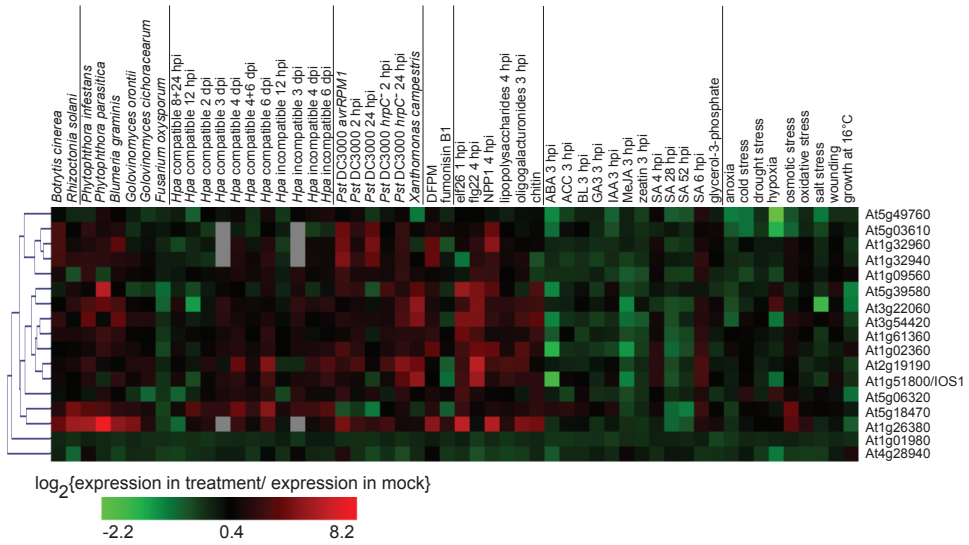
SI Figure 1. β -glucuronidase (GUS) and trypan blue staining of *Arabidopsis complex glycan less 1-1* (*cgl1-1*) seedlings carrying the *pDMR6:GUS* construct and infected with *Hpa*. In young true leaves (a) and cotyledons (b), GUS-activity tracked with Magenta GlcA substrate was found in host cells which are in direct contact with the *Hpa* hyphae (black arrows) and contain pathogen haustoria (green arrows) visible as dark-blue structures after trypan blue staining (scale bar 10 μ m). (c) As a result of GUS-activity, magenta stain was observed in the apex and true leaves but not cotyledons of mock-treated *pDMR6:GnTI* seedlings. (d) After *Hpa* infection, intensive magenta staining indicative of the *DMR6* promoter activity was detected in cotyledons, apex and true leaves.



SI Figure 2. High-level workflow of sample preparation and analysis during N-glycotagging of disease-related proteins of Arabidopsis.



SI Figure 3. Overview of results from LC-MS/MS and MS^E analysis. (a) Boxplot of \log_{10} -transformed normalized abundances of 5903 peptides detected with LC-MS/MS and MS^E analysis in cotyledons of *complex glycan less 1-1* (*cg1-1*) and *pDMR6::GnTI* (*cg1-1* background) seedlings either treated with water (mock) or infected with *Hyaloperonospora arabidopsidis* (*Hpa*). (b) \log_{10} -transformed changes of peptide intensities in *cg1-1* cotyledons with or without *Hpa* infection relative to those in *pDMR6::GnTI* cotyledons. Hexagon binning algorithm was applied to group peptides located in close proximity on the biplot (size of bins is indicated in legend). Red dots show peptides matched to candidate complex N-glycosylated proteins (c, d) Biplot of results from principal component analysis of normalized abundance of identified 5903 peptides. Red arrows indicate loadings of each sample into the principal components (PCs). PC1 and PC2 separate samples into mock- and *Hpa*-treated, however, PC2 and PC3 could separate all four sample based on their genotype and treatment.



SI Figure 4. Clustering of expression profiles of genes encoding the identified candidate complex N-glycosylated proteins under different biotic and abiotic stresses. Only data from the microarray experiments with wild type plants were considered except for interactions with *Hyaloperonospora arabidopsidis* (*Hpa*) where data for the *rpp4* mutant was also used. Studies describing the microarray experiments are listed in the SI Table 5. Abbreviations: *Pst* DC3000 – *Pseudomonas syringae* pv. *tomato* DC3000, DFPM - [5-(3,4-dichlorophenyl)furan-2-yl]-piperidine-1-ylmethanethione, NPP1 - NECROSIS-INDUCING PHYTOPHTHORA PROTEIN 1, ABA – abscisic acid, ACC – 1-aminocyclopropane-1-carboxylic acid, BL – brassinolide, GAA3 – gibberellic acid, IAA – indole-3-acetic acid, MeJA – methyl jasmonate, SA – salicylic acid.

Chapter 6: General discussion

Downy mildews cause destructive diseases in many crops, e.g. lettuce [115] and cucumber [116]. The model plant species *Arabidopsis thaliana* (*Arabidopsis* hereafter) is also susceptible to downy mildew caused by the oomycete pathogen *Hyaloperonospora arabidopsidis* (*Hpa*). This pathosystem is a model to study susceptibility of plants to downy mildews and other biotrophic pathogens [118]. Host processes affecting susceptibility of plants to biotrophic and hemibiotrophic pathogens can be broadly divided into immunity- and non-immunity related ones. In many cases, immunity is based on detection of microbe-associated molecular patterns (MAMPs) and effector proteins associated with pathogen growth that leads to the activation of plant defense responses [5, 120]. Non-immunity related mechanisms of resistance can be mediated by loss-of-susceptibility factors in a host plant. Susceptibility factors such as components of root exudates, waxes and cuticle can attract and stimulate pathogen development. Furthermore, susceptibility genes can facilitate the establishment of pathogen infection structures in plant cells and the provision of nutrients at the infection site [217]. The research described in this thesis was aimed at the identification of novel *Arabidopsis* genes and proteins affecting its susceptibility to downy mildew via immunity or non-immunity related pathways. For that, a multidisciplinary approach combining genetic and proteomic methods was undertaken.

Broad-spectrum and quantitative resistance of Arabidopsis C24 to downy mildew

Natural *Arabidopsis* accessions are typically susceptible to a number of *Hpa* isolates but resistant to others. In different natural accessions, resistance was mapped to 27 *RPP* loci (for *RESISTANCE TO PERONOSPORA PARASITICA*) on all five *Arabidopsis* chromosomes. The cloned loci, *RPP1*, *RPP2*, *RPP5* (*RPP4*), *RPP8* and *RPP13* (*RPP11*), include genes conferring qualitative resistance to different *Hpa* isolates and encoding proteins with nucleotide-binding domain and leucine-rich repeats (NLR) [118, 138]. However, extensive phenotypic analysis of interactions between different *Arabidopsis* accessions and five downy mildew isolates revealed the prevalence of partial, or quantitative, resistance. Moreover, this analysis also showed that cotyledons of many *Arabidopsis* accessions, 4 to 12% depending on the *Hpa* isolate, are more susceptible than true leaves [136]. In addition, age-related resistance to *Hpa* was found in *Arabidopsis* populations. For example, the accession Col-0 has age-related resistance, i.e. plants of this genotype are susceptible at the seedling stage but become fully resistant to *Hpa* isolate Emco5 at the adult stage (4-5 week-old). This resistance was mapped to a major locus on chromosome 5 and a minor locus on the chromosome 2 [294] demonstrating the presence of multigenetic developmental stage-related mechanisms of *Arabidopsis* resistance to *Hpa*. Thus, in addition to qualitative strong resistance, *Arabidopsis* accessions frequently have quantitative multigenic resistance modified by the plant age.

Most of the *Arabidopsis* accessions are susceptible to *Hpa*, e.g. around 88% of accessions (73 out of 83) were susceptible to at least one of the five tested *Hpa* isolates [136]. Notably, the accession C24 has broad-spectrum resistance (BSR) to downy mildew [139], for which the underlying genetics was unknown. To study BSR in more details, we performed quantitative trait loci (QTL) mapping and segregation analysis of C24 resistance to three isolates of *Hpa*. C24 resistance to these isolates appeared to be multigenic and mediated by different combinations of isolate-specific loci. Interestingly, all identified C24 loci contributing to resistance to *Hpa* isolate Waco9 were responsible only for partial reduction of the pathogen sporulation [94]. Partial quantitative *Arabidopsis* resistance to *Hpa* has not been studied as extensively as qualitative resistance and, therefore, we further focused our analysis on the quantitative resistance of C24 to Waco9. In general, histochemical analyses of interactions between biotrophic or hemibiotrophic pathogens and plants with quantitative resistance show that it frequently displays typical hallmarks of immune responses, e.g. elevated lignification

and increased accumulation of phenolic compounds at infection sites, extended patches of chlorosis and/or of cell death around infection sites, and accelerated senescence. However, this form of resistance can also be associated with reduced pathogen growth without signs of plant cell death in surrounding tissues: reduced penetration and entry rates, aborted haustorium formation, restricted intercellular growth of pathogens leading to prolonged latent period of infection [295-299]. Preliminary microscopic analysis of Col-0 introgression lines with two major C24 quantitative resistance loci *qtl1.3* and *qtl5.1*, which affect Waco9 sporulation, suggests that resistance controlled by *qtl1.3* involves abundant Arabidopsis cell death occurring along *Hpa* hyphae that likely limits level of Waco9 sporulation. In contrast, *qtl5.1* seems to mediate resistance to Waco9 by reducing intensity of hyphal growth and only partially elevating cell death around growing hyphae.

Many loci conferring partial resistance to pathogens have been identified and described in literature. They encode different classes of proteins: from transporters [300, 301], proteins with kinase domains [296, 302, 303], NLR proteins [304-306], germin-like proteins [307], enzymes involved in thiamine, auxin and jasmonate biosynthesis [303, 308] and transcription factor [303] to unknown proline-rich protein [309]. Given that cloned quantitative resistance genes encode different types of proteins, diverse and unrelated molecular mechanisms might regulate this form of resistance [161]. Thus, pathogens are less likely to overcome resistance mediated by quantitative loci and, therefore, pyramiding quantitative resistance loci might be powerful and lead to more durable forms of disease resistance. So far, results of ongoing fine-mapping of the two major partial resistance loci *qtl1.3* and *qtl5.1* in Arabidopsis C24 point to loci including NLR genes. In addition to the major loci *qtl1.3* and *qtl5.1*, quantitative C24 resistance to Waco9 is affected by at least three additional minor loci *qtl1.2*, *qtl3.1* and *qtl4.1*. Of these, *qtl1.2* is a unique locus since its C24 allele increases susceptibility rather than resistance specifically to the isolate Waco9 [94]. Unfortunately, attempts to fine-map this locus to a single gene failed suggesting that it consists of several tightly linked genes. However, there is no evidence that the quantitative effect of *qtl1.2* on Arabidopsis susceptibility is mediated by *R*-genes making *qtl1.2* interesting for further investigation. Quantitative resistance to *Hpa* mediated by different loci in Arabidopsis C24 could be used to further characterize mechanisms of quantitative resistance of plants, in particular of susceptible crop species, to downy mildews.

Arabidopsis C24 is known not only because of BSR to downy mildew. This accession confers complex multigenic resistance to several powdery mildew fungi infecting Arabidopsis [163], dominant *R*-gene-based resistance to cucumber mosaic virus Y (CMV(Y)) [144, 154] and dominant resistance to *Pseudomonas syringae* pv. *tomato* (*Pst*) DC3000 [94]. This accession also has higher levels of the plant defense hormone salicylic acid (SA) and hydrogen peroxide compared to the Arabidopsis accession Col-0 [155]. In addition to many disease resistance traits, C24 has exceptional tolerance to drought [155] and submergence [310]. Increased resistance of plants is sometimes associated with early senescence, reduced seed set and compromised tolerance to abiotic stresses (de Vos *et al.*, in press). For instance, in the natural Arabidopsis accession Est-1, a hyperactive allele of *ACCELERATED CELL DEATH 6* (*ACD6*) contributes to elevated resistance to *Pst* DC3000, powdery and downy mildews and is associated with abundant necrotic lesions and reduced dry weight of plants [311]. Arabidopsis C24 retains an unusual combination of resistance to biotic and abiotic stresses that might be useful in the development of crop varieties combining different quality traits.

Role of jasmonates in susceptibility of plants to biotrophic and hemibiotrophic pathogens

To identify genes that quantitatively affect Arabidopsis interaction with downy mildew in non-isolate-specific manner, we performed association mapping of susceptibility of Arabidopsis accessions from the core HapMap population following infection with a mix of four *Hpa* isolates. This mapping approach revealed that variation at the *CYTOKININ RESPONSE FACTOR1* (*CRF1*) locus affects the interaction with *Hpa*. Higher *CRF1* mRNA levels were

correlated with higher levels of susceptibility in 34 *Arabidopsis* accessions indicating that *CRF1* could negatively regulate resistance to *Hpa*. We observed that after treatment with different concentrations of cytokinin the *crf1-1* mutant showed altered susceptibility to *Hpa* to an extent similar to the wild type Col-0 suggesting that *CRF1* does not play a significant role in cytokinin-induced changes of *Arabidopsis* susceptibility to *Hpa*. Instead, *CRF1* was transiently induced at the transcriptional level after methyl jasmonate (MeJA) treatment and was found to be coexpressed with a cluster of genes associated with JA-related gene ontology terms (see chapter 4) suggesting a role of *CRF1* in the JA-signaling pathway. Notably, we found that pretreatment of *Arabidopsis* seedlings with MeJA enhances susceptibility to downy mildew but the effect of *CRF1* alone on the MeJA-induced susceptibility was not evident. In contrast to SA, which positively regulates immunity of *Arabidopsis* to *Hpa* [312], the effect of MeJA on susceptibility to downy mildew is not well established. Consistent with our findings, the *coi1* mutant that is JA insensitive showed enhanced resistance to *Hpa* Noco2 indicating that the JA-pathway negatively affects resistance to downy mildew. However, in the same study treatment of infected plants with MeJA vapour led to reduced sporulation levels [313]. Possibly, opposite effects of MeJA treatment on *Arabidopsis* susceptibility to downy mildew infection in the mentioned study and in our experiments could be caused by differences in the method of MeJA application, concentration of the compound or the use of different compatible *Hpa* isolates. Recently, it was reported that the *Hpa* effector HaRxL44 binds to the Med19a component of the *Arabidopsis* mediator complex to induce transcription of genes responsive to MeJA suggesting that *Hpa* manipulates JA-signaling pathway to promote *Arabidopsis* susceptibility [314]. Jasmonates can enhance susceptibility of plants to different hemibiotrophic pathogens. Coronatine, a structural and functional mimic of jasmonic acid produced by the bacterial pathogen *Pst* DC3000, activates the expression of the *Arabidopsis* *MYC2* gene in a *CORONATINE-INSENSITIVE 1 (COI1)* dependent manner. This induces the expression of three genes encoding NAC TFs that negatively regulate the accumulation of SA and attenuate activation of SA-dependent immune responses effective against *Pst* DC3000. Thus, the pathogen hijacks the MeJA-signaling pathway to negatively affect the SA-pathway [7]. Similarly, successful infection of *Arabidopsis* by the hemibiotrophic fungus *Fusarium graminearum* is strongly dependent on an intact JA-biosynthetic and signaling pathway that likely delays *NPR1*-regulated immune responses [315]. Another mechanism by which MeJA promotes susceptibility also involving *COI1* and *MYC2* was found in the interaction of the hemibiotrophic fungus *F. oxysporum* with *Arabidopsis*. However, the enhanced resistance of the *coi1* mutant was independent of SA accumulation suggesting that the positive effect of the MeJA-signaling pathway on susceptibility to *F. oxysporum* does not rely on negative regulation of the SA-pathway [316]. Finally, it is plausible that JA leads to destabilization of NLRs in a *COI1*-dependent manner as *coi1* mutants show elevated accumulation of these proteins [317].

In addition to the positive role of jasmonates in susceptibility to certain (hemi-)biotrophic pathogens, it was found that it can also increase resistance to other (hemi-)biotrophs. Firstly, jasmonic acid is known to exert an antimicrobial activity by reducing spore germination of *Magnaporthe oryzae* [318], appressorium formation and penetration of *Blumeria graminis* [319], and mycelial growth of *Phytophthora infestans* [320]. In addition to the antimicrobial activity, there are examples of jasmonates positively regulating plant defense to (hemi-) biotrophic pathogens. Mutants of *Arabidopsis* and tomato defective in JA-biosynthesis show enhanced susceptibility to the powdery mildew fungus *Golovinomyces cichoracearum* [321] and the oomycete *Phytophthora infestans* [322]. In line with these findings, natural variation at the JA-biosynthetic gene *AOS2* underlies quantitative resistance to *P. infestans* and functionally more active alleles of *AOS2* correlate with higher level of resistance suggesting that efficient JA-biosynthesis is required for defense to this hemibiotroph [308]. Similarly, MeJA treatment induced resistance to the powdery mildew fungi *Erysiphe necator*, *G. cichoracearum* and *Blumeria graminis* in grapevine [323], *Arabidopsis* [313] and barley [324], respectively.

Unfortunately, the mechanisms of the negative effects of MeJA on susceptibility to biotrophs and hemibiotrophs are largely unknown except that JAs play a role in the establishment of systemic resistance [325]. Potentially, application of MeJA leads to the accumulation of antimicrobial metabolites that might be effective against (hemi-)biotrophs [326]. Further studies on the molecular mechanisms of MeJA-induced susceptibility in the Arabidopsis-downy mildew interaction might reveal why MeJA has different effects on plant susceptibility to unrelated (hemi-)biotrophs.

Processes occurring in Arabidopsis cells invaded with downy mildew haustoria

Downy mildew pathogens form specialized infection structures, haustoria, which penetrate through the plant cell wall but remain separated from the host cytoplasmic membrane. Similar structures are also found in different unrelated biotrophic and hemibiotrophic pathogens that points to their importance in pathogenesis [22]. Indeed, haustoria are likely to play a role in nutrient transport to biotrophic fungi [34, 327], and the secretion of effector molecules from both fungi and oomycetes into infected host plant cells occurs at least partially through foci of effector accumulation at haustoria [51-53, 258, 328]. Thus, it is important to understand processes in the host cells that are invaginated by pathogen haustoria as it can improve our understanding of plant disease susceptibility.

Arabidopsis subcellular responses to *Hpa* infection were intensively studied with microscopy methods. Aggregation of cytoplasm was observed at the site of young developing haustoria. Membranes of endoplasmic reticulum (ER) and bodies of Golgi complex (GC) appeared to localize close to the developing haustoria. Also markers of early and late endosomal compartments were localized around *Hpa* haustoria and actively moved throughout the infected plant cell toward and away from haustoria proving extensive membrane trafficking at the infection site. Treatment of infected cells with brefeldin A, an inhibitor of endocytic recycling, led to the accumulation of endosomes demonstrating that infected Arabidopsis cells actively endocytose [35, 329]. Given that lipid rafts-mediated endocytosis was shown to be important for the translocation of fungal and oomycete effectors into plant cells [54], active endocytosis in *Hpa*-infected host cells could play a role in *Hpa* effector translocation. Also, one can speculate that endocytosis in infected Arabidopsis cells might deliver *Hpa*-associated molecules which help Arabidopsis to sense the presence of the pathogen and adjust the strength of immune responses. In addition to aggregation of plant cytoplasm around haustoria, the tonoplast was found to surround *Hpa* haustoria [329]. Notably, it had abundant invaginations in the infected cells resembling bulbs in the vacuoles of uninfected plant cells [330]. Unfortunately, roles of these invaginations or bulbs are unknown, but it was suggested that they could function in autophagy, serve as reservoir of membrane material, or work as miniature factories with hydrolytic activities [331]. Next to the active rearrangement of membranes in *Hpa*-infected cells, the Arabidopsis nucleus moves towards haustoria and is found in close proximity with them [35, 329]. However, not all host cellular compartments are pulled towards the haustorium penetration site in infected cells. The majority of plasma membrane markers are excluded from the Arabidopsis membrane surrounding haustoria, i.e. extrahaustorial membrane (EHM) [35, 329]. Thus, host plasma membranes, as well as vacuoles and cytoplasm of *Hpa*-infected cells, undergo significant alterations at the site of haustoria development.

The processes described for Arabidopsis cells invaginated by *Hpa* haustoria are similar to those observed in the Arabidopsis-powdery mildew interactions. Arabidopsis epidermal cells infected with the powdery mildew *G. cichoracearum* also show aggregation of ER and GC components close to the EHM, surrounding of pathogen haustoria by tonoplast, movement of nuclei towards haustoria and exclusion of the majority of plasma membrane markers from EHM. Remarkably, nuclei of the powdery mildew-infected Arabidopsis epidermal cells were approximately twice larger than nuclei of uninfected epidermal cells [36]. In contrast, for *Hpa*-infected mesophyll cells of Arabidopsis an increase in nucleus size has not been reported.

Substantial metabolic changes are likely to occur in *Hpa*-infected Arabidopsis cells. *DOWNY*

MILDEW RESISTANT 6 (DMR6) gene of *Arabidopsis* is expressed during *Hpa* infection specifically in the downy mildew-infected cells and encodes for a putative 2-oxoglutarate Fe(II)-dependent oxygenase of yet unknown substrate specificity. Enhanced *DMR6* expression leads to negative regulation of defense locally in the infected cells [119] suggesting it is essential for successful *Hpa* development. Similarly, repression of SA-dependent defense reactions specifically in infected and adjacent plant cells was found in the *Ustilago maydis* – *Zea mays* interaction, where the pathogen effector Cmu1, functional chorismate mutase with virulence function, was localized only to the infected and adjacent maize cells [61]. Compatible interactions between *Arabidopsis* and *Hpa* were studied on the level transcription [113]. *TREHALOSE-6-PHOSPHATE PHOSPHATASE J (TPPJ)* was highly induced in this interaction, and promoter-GUS fusions show that the gene is active in the downy mildew infected cells of *Arabidopsis* (unpublished data). TPPs dephosphorylate trehalose-6-phosphate into trehalose that functions as a reserve carbon source and protects cell components during dehydration, hypoxia and nutrient starvation [332]. Potentially, elevated expression of *Arabidopsis TPPJ* helps *Hpa* to prolong survival and feeding on the infected *Arabidopsis* cells.

To gain more insight into subcellular responses of *Arabidopsis* to *Hpa* infection, we deployed an N-glycotagging approach. In this approach, the *DMR6* promoter, activated in the *Hpa*-infected but not surrounding cells [119], was fused to a *COMPLEX GLYCAN LESS* coding sequence, and the construct was transformed into the *cg1-1* mutant, which does not form complex N-glycans [270]. Infection with *Hpa* resulted in the restoration of complex N-glycosylation in the infected cells, and the glycoproteins were enriched and further analyzed by mass-spectrometry methods (chapter 5). Using this method, we identified 18 *Arabidopsis* candidate disease-related proteins from diverse classes and expressed in *Hpa*-infected cells: receptor-like and leucine-rich repeat kinases, chitinases, a germin-like protein, homolog of NON-RACE-SPECIFIC DISEASE RESISTANCE1 (NDR1), FAD-binding Berberine family proteins, phosphorylase, lectin, peroxidase, acylhydrolase, and subtilases. The gene encoding one of the identified leucine-rich repeat proteins IMPAIRED IN OOMYCETE SUSCEPTIBILITY 1 (IOS1) is specifically expressed in downy mildew-infected cells of *Arabidopsis* and positively regulates susceptibility to *Hpa* via yet unknown mechanism [112]. *Arabidopsis* germin-like protein PDGLP1, also identified in our proteomic study, was previously suggested to play a role in symplastic transport of nutrients in roots [293] indicating that this protein might be involved in nutrient transport in the *Hpa*-infected cells. Given that PDGLP1 is localized to plasmodesmata [293], and plasmodesmata are likely to play a role in effector translocation from rice and maize cells infected with *Magnaporthe oryzae* [52] and *U. maydis* [61] respectively into neighboring cells, it is tempting to speculate that PDGLP1 could be involved in the cell-to-cell transport of *Hpa* effector proteins. Further functional characterization of the identified disease-related *Arabidopsis* proteins expressed in the *Hpa*-infected cells and their paralogs seems important to study host processes in downy mildew infected cells.

Systems approaches to study susceptibility and quantitative resistance of *Arabidopsis* to downy mildew

The interaction between *Arabidopsis* and downy mildew is a complex process regulated by a wide range of biotic and abiotic factors. Transcriptional profiling of compatible *Arabidopsis*-*Hpa* interaction revealed an overrepresentation of abscisic acid responsive genes induced by osmotic, cold and drought stresses [113] implying that these stresses could influence the outcome of the interaction. In addition, recent studies demonstrated that *Arabidopsis* immune responses to downy mildew are partially controlled by the two close homologs *CIRCADIAN CLOCK ASSOCIATED1 (CCA1)* and *LATE ELONGATED HYPOCOTYL (LHY)*, well-known regulators of the circadian clock in *Arabidopsis*. Strikingly, the level of susceptibility to downy mildew appeared to be dependent on time of the spore inoculation [333, 334] clearly showing that the *Arabidopsis*-*Hpa* interaction is modulated by circadian rhythms. Finally, fertilization of pearl millet with urea was reported to reduce severity of the downy mildew disease in fields

[335], and thus, complex downy mildew disease management can benefit from our detailed understanding of the role of plant nutrition in disease development. Genetic and genomic resources for *Arabidopsis* offer excellent opportunities to investigate interactions of plants with downy mildews in a context of different environmental conditions.

One of the ways to change *Arabidopsis* susceptibility to *Hpa* is by modification of host plant metabolism to starve the pathogen. Systems biology approaches might be instrumental to study nutrition of *Hpa*. The genome of *Hpa* lacks several genes encoding key enzymes involved in sulfate and nitrate reduction [86]. In a recent large-scale study, loss-of-function mutations in genes from different regulatory and metabolic pathways in *Escherichia coli* were shown to increase fitness of bacteria under nutrient deprivation. Flux balance analysis of metabolic capacities suggested key enzymes whose mutations lead to higher growth rates of bacteria under starvation conditions, and the predictions were validated experimentally [336]. Thus, loss of key metabolic enzymes by *Hpa* could be due to starvation of the pathogen and not due to the abundance of nutrients during infection in *Arabidopsis*. Following this hypothesis, it might be possible to predict a 'diet' provided by *Arabidopsis* that shaped *Hpa*'s genome and metabolism and, consequently, to identify host genes affecting biosynthesis of these compounds *in planta* that could help to reduce plant susceptibility to downy mildews.

Systems biology could also be powerful in the identification of *Arabidopsis* genes quantitatively restricting *Hpa* growth. In a high-resolution temporal transcriptomic analysis of *Arabidopsis* responses to *Botrytis cinerea* infection, expression profiles of clusters of genes differentially regulated during *Botrytis* infection and dynamics of the pathogen growth were modeled to infer a causal structure identification network. One gene cluster appeared to be located upstream of the pathogen growth in the inferred network, and the TGA3 transcription factor present in this upstream cluster was proved as an essential regulator of *Arabidopsis* resistance to *Botrytis* [337]. Similar high-resolution time-course analysis would be useful to study *Arabidopsis* regulatory networks underlying its quantitative resistance to *Hpa*.

Finally, collecting results of association and linkage mapping studies of *Arabidopsis* susceptibility to diseases in one repository could be essential for the prioritization of *Arabidopsis* genetic pathways detected with systems biology approaches for further functional studies. I strongly believe that an integrated systems-level view on this interaction will result in better understanding of the downy mildew infection process in plants and provide more sustainable and reliable solutions to combat this disease in crops.

References

- 1 Boller, T. and Felix, G. (2009) A renaissance of elicitors: perception of microbe-associated molecular patterns and danger signals by pattern-recognition receptors. *Annu. Rev. Plant. Biol.* 60, 379-406. DOI: 10.1146/annurev.arplant.57.032905.105346
- 2 Nurnberger, T. and Lipka, V. (2005) Non-host resistance in plants: new insights into an old phenomenon. *Mol. Plant. Pathol.* 6, 335-345. DOI: 10.1111/j.1364-3703.2005.00279.x
- 3 Weinberger, F. (2007) Pathogen-induced defense and innate immunity in macroalgae. *Biol. Bull.* 213, 290-302
- 4 Ponce de Leon, I. and Montesano, M. (2013) Activation of Defense Mechanisms against Pathogens in Mosses and Flowering Plants. *Int. J. Mol. Sci.* 14, 3178-3200. DOI: 10.3390/ijms14023178
- 5 Jones, J.D.G. and Dangl, J.L. (2006) The plant immune system. *Nature* 444, 323-329
- 6 Pel, M.J. and Pieterse, C.M. (2013) Microbial recognition and evasion of host immunity. *J. Exp. Bot.* 64, 1237-1248. DOI: 10.1093/jxb/ers262
- 7 Zheng, X.Y. *et al.* (2012) Coronatine promotes *Pseudomonas syringae* virulence in plants by activating a signaling cascade that inhibits salicylic acid accumulation. *Cell. Host Microbe* 11, 587-596. DOI: 10.1016/j.chom.2012.04.014
- 8 Cornelis, G.R. (2006) The type III secretion injectisome. *Nat. Rev. Microbiol.* 4, 811-825. DOI: 10.1038/nrmicro1526
- 9 Tampakaki, A.P. *et al.* (2010) Playing the "Harp": evolution of our understanding of hrp/hrc genes. *Annu. Rev. Phytopathol.* 48, 347-370. DOI: 10.1146/annurev-phyto-073009-114407
- 10 Panstruga, R. and Dodds, P.N. (2009) Terrific Protein Traffic: The Mystery of Effector Protein Delivery by Filamentous Plant Pathogens. *Science* 324, 748-750. DOI: 10.1126/science.1171652
- 11 Stassen, J.H. and Van den Ackerveken, G. (2011) How do oomycete effectors interfere with plant life? *Curr. Opin. Plant Biol.* 14, 407-414. DOI: 10.1016/j.pbi.2011.05.002
- 12 Win, J. *et al.* (2012) Effector Biology of Plant-Associated Organisms: Concepts and Perspectives. *Cold Spring Harb. Symp. Quant. Biol.* DOI: 10.1101/sqb.2012.77.015933
- 13 Mukhtar, M.S. *et al.* (2011) Independently evolved virulence effectors converge onto hubs in a plant immune system network. *Science* 333, 596-601. DOI: 10.1126/science.1203659
- 14 O'Connell, R.J. *et al.* (2012) Lifestyle transitions in plant pathogenic *Colletotrichum* fungi deciphered by genome and transcriptome analyses. *Nat. Genet.* 44, 1060-1065. DOI: 10.1038/ng.2372
- 15 Morris, P.F. and W. (1992) Chemoattraction of zoospores of the soybean pathogen, *Phytophthora sojae*, by isoflavones. *Physiol. Mol. Plant Pathol.* 40, 17-22
- 16 Ruan, Y. and K. (1995) Flavonoids Stimulate Spore Germination in *Fusarium solani* Pathogenic on Legumes in a Manner sensitive to inhibitors of cAMP-Dependent Protein Kinase. *Mol. Plant-Microbe Interact.* 8, 929-938
- 17 Kolattukudy, P.E. *et al.* (1995) Surface signaling in pathogenesis. *Proc. Natl. Acad. Sci. U. S. A.* 92,

- 18 Dor, E. *et al.* (2011) The synthetic strigolactone GR24 influences the growth pattern of phytopathogenic fungi. *Planta* 234, 419-27. DOI: 10.1007/s00425-011-1452-6
- 19 Hansjakob, a. *et al.* (2011) Wax matters: absence of very-long-chain aldehydes from the leaf cuticular wax of the *glossy11* mutant of maize compromises the prepenetration processes of *Blumeria graminis*. *Plant Pathol.* 60, 1151-1161. DOI: 10.1111/j.1365-3059.2011.02467.x
- 20 Uppalapati, S.R. *et al.* (2012) Loss of abaxial leaf epicuticular wax in *Medicago truncatula irg1/palm1* mutants results in reduced spore differentiation of anthracnose and nonhost rust pathogens. *Plant Cell* 24, 353-70. DOI: 10.1105/tpc.111.093104
- 21 Hansjakob, A. *et al.* (2010) Very-long-chain aldehydes promote in vitro prepenetration processes of *Blumeria graminis* in a dose- and chain length-dependent manner. *The New Phytologist* 188, 1039-54. DOI: 10.1111/j.1469-8137.2010.03419.x
- 22 Kemen, E. and Jones, J.D.G. (2012) Obligate biotroph parasitism: can we link genomes to life-styles? *Trends Plant Sci.* 17, 448-457. DOI: 10.1016/j.tplants.2012.04.005
- 23 Agrios, G. (2005) Glossary. In *Plant Pathology, 5th ed.*, pp. 889, Elsevier
- 24 Taiz, L. and Zeiger, E. (2010) Topic 13.1: Cutin, Waxes, and Suberin. *Plant Physiology, Fifth Edition Online*. <http://5e.plantphys.net/Article.Php?ch=13&id=434> 2013
- 25 De Veylder, L. *et al.* (2011) Molecular control and function of endoreplication in development and physiology. *Trends Plant Sci.* 16, 624-634. DOI: 10.1016/j.tplants.2011.07.001
- 26 Assmann, S. (2002) Heterotrimeric and unconventional GTP binding proteins in plant cell signaling. *Plant Cell* 14, S355-S373. DOI: 10.1105/tpc.001792
- 27 Yang, Z. (2002) Small GTPases: Versatile signaling switches in plants. *Plant Cell* 14, S375-S388. DOI: 10.1105/tpc.001065
- 28 Agrios, G. (2005) Glossary. In *Plant Pathology, 5th ed.*, pp. 895, Elsevier
- 29 Wang, Y. *et al.* (2013) A novel Arabidopsis-oomycete pathosystem: differential interactions with *Phytophthora capsici* reveal a role for camalexin, indole glucosinolates and salicylic acid in defence. *Plant, Cell Environ.* 36, 1192-1203. DOI: 10.1111/pce.12052
- 30 Agrios, G. (2005) Glossary. In *Plant Pathology, 5th ed.*, pp. 892, Elsevier
- 31 Ruyter-Spira, C. *et al.* (2013) The biology of strigolactones. *Trends Plant Sci.* 18, 72-83. DOI: 10.1016/j.tplants.2012.10.003
- 32 Wang, E. *et al.* (2012) A Common Signaling Process that Promotes Mycorrhizal and Oomycete Colonization of Plants. *Current Biology* 22, 2242-2246. DOI: 10.1016/j.cub.2012.09.043
- 33 Mendoza-Mendoza, A. *et al.* (2009) Physical-chemical plant-derived signals induce differentiation in *Ustilago maydis*. *Mol. Microbiol.* 71, 895-911. DOI: 10.1111/j.1365-2958.2008.06567.x
- 34 Voegelé, R.T. *et al.* (2001) The role of haustoria in sugar supply during infection of broad bean by the rust fungus *Uromyces fabae*. *Proc. Natl. Acad. Sci. U. S. A.* 98, 8133-8138. DOI: 10.1073/pnas.131186798

- 35 Lu, Y.J. *et al.* (2012) Patterns of plant subcellular responses to successful oomycete infections reveal differences in host cell reprogramming and endocytic trafficking. *Cell. Microbiol.* 14, 682-697. DOI: 10.1111/j.1462-5822.2012.01751.x
- 36 Koh, S. *et al.* (2005) *Arabidopsis thaliana* subcellular responses to compatible *Erysiphe cichoracearum* infections. *Plant J.* 44, 516-529. DOI: 10.1111/j.1365-313X.2005.02545.x
- 37 Craddock, C. *et al.* (2012) New insights into Rho signaling from plant ROP/Rac GTPases. *Trends Cell Biol.* 22, 492-501. DOI: 10.1016/j.tcb.2012.05.002
- 38 Chen, L. *et al.* (2010) Analysis of the Rac/Rop small GTPase family in rice: expression, subcellular localization and role in disease resistance. *Plant Cell Physiol.* 51, 585-95. DOI: 10.1093/pcp/pcq024
- 39 Poraty, L. *et al.* (2013) The Arabidopsis ROP GTPase AtROP6 functions in developmental and pathogen response pathways. *Plant Physiol.* DOI: 10.1104/pp.112.213165
- 40 Pathuri, I.P. *et al.* (2009) Ectopic expression of barley constitutively activated ROPs supports susceptibility to powdery mildew and bacterial wildfire in tobacco. *Eur. J. Plant Pathol.* 125, 317-327. DOI: 10.1007/s10658-009-9484-5
- 41 Hoefle, C. *et al.* (2011) A barley ROP GTPase ACTIVATING PROTEIN associates with microtubules and regulates entry of the barley powdery mildew fungus into leaf epidermal cells. *Plant Cell* 23, 2422-39. DOI: 10.1105/tpc.110.082131
- 42 Schultheiss, H. *et al.* (2008) Barley RIC171 interacts with RACB in planta and supports entry of the powdery mildew fungus. *Cell. Microbiol.* 10, 1815-26. DOI: 10.1111/j.1462-5822.2008.01167.x
- 43 Schultheiss, H. *et al.* (2003) Functional analysis of barley RAC/ROP G-protein family members in susceptibility to the powdery mildew fungus. *The Plant Journal* 36, 589-601. DOI: 10.1046/j.1365-313X.2003.01905.x
- 44 Kessler, S.a. *et al.* (2010) Conserved molecular components for pollen tube reception and fungal invasion. *Science* 330, 968-71. DOI: 10.1126/science.1195211
- 45 Duan, Q. *et al.* (2010) FERONIA receptor-like kinase regulates RHO GTPase signaling of root hair development. *Proc. Natl. Acad. Sci. U. S. A.* 107, 17821-6. DOI: 10.1073/pnas.1005366107
- 46 Molendijk, A.J. *et al.* (2001) Arabidopsis thaliana Rop GTPases are localized to tips of root hairs and control polar growth. *EMBO J.* 20, 2779-2788. DOI: 10.1093/emboj/20.11.2779
- 47 Venus, Y. and Oelmuller, R. (2012) Arabidopsis ROP1 and ROP6 Influence Germination Time, Root Morphology, the Formation of F-Actin Bundles, and Symbiotic Fungal Interactions. *Mol. Plant.* . DOI: 10.1093/mp/sss101
- 48 Ke, D. *et al.* (2012) The small GTPase ROP6 interacts with NFR5 and is involved in nodule formation in *Lotus japonicus*. *Plant Physiol.* 159, 131-143. DOI: 10.1104/pp.112.197269
- 49 Genre, A. *et al.* (2008) Prepenetration apparatus assembly precedes and predicts the colonization patterns of arbuscular mycorrhizal fungi within the root cortex of both *Medicago truncatula* and *Daucus carota*. *Plant Cell* 20, 1407-20. DOI: 10.1105/tpc.108.059014
- 50 Genre, A. *et al.* (2005) Arbuscular mycorrhizal fungi elicit a novel intracellular apparatus in *Medicago truncatula* root epidermal cells before infection. *Plant Cell* 17, 3489-3499. DOI: 10.1105/tpc.105.035410

- 51 Kemen, E. *et al.* (2005) Identification of a protein from rust fungi transferred from haustoria into infected plant cells. *Mol. Plant Microbe Interact.* 18, 1130-1139. DOI: 10.1094/MPMI-18-1130
- 52 Khang, C.H. *et al.* (2010) Translocation of *Magnaporthe oryzae* effectors into rice cells and their subsequent cell-to-cell movement. *Plant Cell* 22, 1388-1403. DOI: 10.1105/tpc.109.069666
- 53 Kleemann, J. *et al.* (2012) Sequential Delivery of Host-Induced Virulence Effectors by Appressoria and Intracellular Hyphae of the Phytopathogen *Colletotrichum higginsianum*. *PLoS Pathog* 8, e1002643
- 54 Kale, S.D. *et al.* (2010) External Lipid PI3P Mediates Entry of Eukaryotic Pathogen Effectors into Plant and Animal Host Cells. *Cell* 142, 284-295. DOI: 10.1016/j.cell.2010.06.008
- 55 Rafiqi, M. *et al.* (2010) Internalization of flax rust avirulence proteins into flax and tobacco cells can occur in the absence of the pathogen. *Plant Cell* 22, 2017-2032. DOI: 10.1105/tpc.109.072983
- 56 Tyler, B.M. *et al.* (2013) Microbe-Independent Entry of Oomycete RxLR Effectors and Fungal RxLR-Like Effectors Into Plant and Animal Cells Is Specific and Reproducible. *Molecular Plant-Microbe Interactions : MPMI* 26, 611-616. DOI: 10.1094/MPMI-02-13-0051-IA
- 57 Sun, F. *et al.* (2013) Structural basis for interactions of the *Phytophthora sojae* RxLR effector Avh5 with phosphatidylinositol 3-phosphate and for host cell entry. *Mol. Plant Microbe Interact.* 26, 330-344. DOI: 10.1094/MPMI-07-12-0184-R
- 58 Jiang, R.H.Y. *et al.* (2013) Eukaryotic virulence determinants utilize phosphoinositides at the ER and host cell surface. *Trends Microbiol.* 21, 145-156. DOI: 10.1016/j.tim.2012.12.004
- 59 Wawra, S. *et al.* (2013) *In Vitro* Translocation Experiments with RxLR-Reporter Fusion Proteins of Avr1b from *Phytophthora sojae* and AVR3a from *Phytophthora infestans* Fail to Demonstrate Specific Autonomous Uptake in Plant and Animal Cells. *Molecular Plant-Microbe Interactions : MPMI* 26, 528-536. DOI: 10.1094/MPMI-08-12-0200-R
- 60 Gan, P.H. *et al.* (2010) Lipid binding activities of flax rust AvrM and AvrL567 effectors. *Plant. Signal. Behav.* 5, 1272-1275. DOI: 10.4161/psb.5.10.13013
- 61 Djamei, A. *et al.* (2011) Metabolic priming by a secreted fungal effector. *Nature* 478, 395-398. DOI: 10.1038/nature10454
- 62 Berger, S. *et al.* (2007) Plant physiology meets phytopathology: plant primary metabolism and plant-pathogen interactions. *Journal of Experimental Botany* 58, 4019-4026. DOI: 10.1093/jxb/erm298
- 63 Aoki, N. *et al.* (2012) Sucrose Transport in Higher Plants: From Source to Sink. In (Eaton-Rye, J. J., *et al.*, ed), pp. 703-729, Springer Netherlands
- 64 Chen, L.Q. *et al.* (2012) Sucrose efflux mediated by SWEET proteins as a key step for phloem transport. *Science* 335, 207-211. DOI: 10.1126/science.1213351
- 65 Chen, L.Q. *et al.* (2010) Sugar transporters for intercellular exchange and nutrition of pathogens. *Nature* 468, 527-532. DOI: 10.1038/nature09606
- 66 Hayes, M.A. *et al.* (2010) Involvement of abscisic acid in the coordinated regulation of a stress-inducible hexose transporter (*VvHT5*) and a cell wall invertase in grapevine in response to biotrophic fungal infection. *Plant Physiol.* 153, 211-221. DOI: 10.1104/pp.110.154765
- 67 Chu, Z. *et al.* (2006) Promoter mutations of an essential gene for pollen development result in

disease resistance in rice. *Genes Dev.* 20, 1250-1255. DOI: 10.1101/gad.1416306

68 Antony, G. *et al.* (2010) Rice *xa13* Recessive Resistance to Bacterial Blight Is Defeated by Induction of the Disease Susceptibility Gene Os-11N3. *The Plant Cell* 22, 3864-3876. DOI: 10.1105/tpc.110.078964

69 Yuan, M. *et al.* (2010) The bacterial pathogen *Xanthomonas oryzae* overcomes rice defenses by regulating host copper redistribution. *Plant Cell* 22, 3164-3176. DOI: 10.1105/tpc.110.078022

70 Kocal, N. *et al.* (2008) Cell wall-bound invertase limits sucrose export and is involved in symptom development and inhibition of photosynthesis during compatible interaction between tomato and *Xanthomonas campestris* pv. *vesicatoria*. *Plant Physiol.* 148, 1523-1536. DOI: 10.1104/pp.108.127977

71 Siemens, J. *et al.* (2011) Extracellular invertase is involved in the regulation of clubroot disease in *Arabidopsis thaliana*. *Mol. Plant. Pathol.* 12, 247-262. DOI: 10.1111/j.1364-3703.2010.00667.x

72 Bonfig, K.B. *et al.* (2010) Post-Translational Derepression of Invertase Activity in Source Leaves via Down-Regulation of Invertase Inhibitor Expression Is Part of the Plant Defense Response. *Mol. Plant.* 3, 1037-1048. DOI: 10.1093/mp/ssq053

73 Sonnewald, S. *et al.* (2012) Regulation of cell wall-bound invertase in pepper leaves by *Xanthomonas campestris* pv. *vesicatoria* type three effectors. *PLoS One* 7, e51763. DOI: 10.1371/journal.pone.0051763

74 White, J. *et al.* (2007) Nutrient sharing between symbionts. *Plant Physiol.* 144, 604-14. DOI: 10.1104/pp.107.097741

75 Antoun, H. *et al.* (1984) Utilization of the tricarboxylic acid cycle intermediates and symbiotic effectiveness in *Rhizobium meliloti*. *Plant Soil* 77, 29-38. DOI: 10.1007/BF02182809

76 Pathuri, I.P. *et al.* (2011) Alcohol dehydrogenase 1 of barley modulates susceptibility to the parasitic fungus *Blumeria graminis* f.sp. *hordei*. *J. Exp. Bot.* 62, 3449-3457. DOI: 10.1093/jxb/err017

77 Tesniere, C. *et al.* (2006) Effects of genetic manipulation of alcohol dehydrogenase levels on the response to stress and the synthesis of secondary metabolites in grapevine leaves. *J. Exp. Bot.* 57, 91-99. DOI: 10.1093/jxb/erj007

78 Andrews, D.L. *et al.* (1993) Hypoxic and Anoxic Induction of Alcohol Dehydrogenase in Roots and Shoots of Seedlings of *Zea mays* (ADH Transcripts and Enzyme Activity). *Plant Physiol.* 101, 407-414

79 Peng, H.P. *et al.* (2001) Signaling events in the hypoxic induction of alcohol dehydrogenase gene in *Arabidopsis*. *Plant Physiol.* 126, 742-749

80 Shiao, T.L. *et al.* (2002) Overexpression of alcohol dehydrogenase or pyruvate decarboxylase improves growth of hairy roots at reduced oxygen concentrations. *Biotechnol. Bioeng.* 77, 455-461

81 Horst, R.J. *et al.* (2010) *Ustilago maydis* infection strongly alters organic nitrogen allocation in maize and stimulates productivity of systemic source leaves. *Plant Physiol.* 152, 293-308. DOI: 10.1104/pp.109.147702

82 Walters, D.R. *et al.* (2008) Are green islands red herrings? Significance of green islands in plant interactions with pathogens and pests. *Biol. Rev.* 83, 79-102. DOI: 10.1111/j.1469-185X.2007.00033.x

83 Behr, M. *et al.* (2010) The hemibiotroph *Colletotrichum graminicola* locally induces photosyn-

thetically active green islands but globally accelerates senescence on aging maize leaves. *Molecular Plant-Microbe Interactions : MPMI* 23, 879-92. DOI: 10.1094/MPMI-23-7-0879

84 Petre, B. *et al.* (2012) RNA-Seq of early-infected poplar leaves by the rust pathogen *Melampsora larici-populina* uncovers *PtSultr3;5*, a fungal-induced host sulfate transporter. *PLoS One* 7, e44408-e44408. DOI: 10.1371/journal.pone.0044408

85 Krusell, L. *et al.* (2005) The sulfate transporter SST1 is crucial for symbiotic nitrogen fixation in *Lotus japonicus* root nodules. *Plant Cell* 17, 1625-1636. DOI: 10.1105/tpc.104.030106

86 Baxter, L. *et al.* (2010) Signatures of adaptation to obligate biotrophy in the *Hyaloperonospora arabidopsidis* genome. *Science* 330, 1549-1551. DOI: 10.1126/science.1195203

87 Kemen, E. *et al.* (2011) Gene Gain and Loss during Evolution of Obligate Parasitism in the White Rust Pathogen of *Arabidopsis thaliana*. *PLoS. Biol.* 9, e1001094. DOI: 10.1371/journal.pbio.1001094

88 Spanu, P.D. *et al.* (2010) Genome expansion and gene loss in powdery mildew fungi reveal tradeoffs in extreme parasitism. *Science* 330, 1543-1546. DOI: 10.1126/science.1194573

89 Chandran, D. *et al.* (2010) Laser microdissection of Arabidopsis cells at the powdery mildew infection site reveals site-specific processes and regulators. *Proc. Natl. Acad. Sci. U. S. A.* 107, 460-5. DOI: 10.1073/pnas.0912492107

90 Chandran, D. *et al.* (2013) Host ploidy underlying the fungal feeding site is a determinant of powdery mildew growth and reproduction. *Mol. Plant Microbe Interact.* DOI: 10.1094/MPMI-10-12-0254-R

91 de Almeida Engler, J. and Gheysen, G. (2013) Nematode-induced endoreduplication in plant host cells: why and how? *Mol. Plant Microbe Interact.* 26, 17-24. DOI: 10.1094/MPMI-05-12-0128-CR

92 Vieira, P. *et al.* (2012) Whole-mount confocal imaging of nuclei in giant feeding cells induced by root-knot nematodes in Arabidopsis. *The New Phytologist* 195, 488-96. DOI: 10.1111/j.1469-8137.2012.04175.x

93 Wildermuth, M.C. (2010) Modulation of host nuclear ploidy: a common plant biotroph mechanism. *Curr. Opin. Plant Biol.* 13, 449-458. DOI: 10.1016/j.pbi.2010.05.005; 10.1016/j.pbi.2010.05.005

94 Lapin, D. *et al.* (2012) Broad-spectrum resistance of Arabidopsis C24 to downy mildew is mediated by different combinations of isolate-specific loci. *New Phytol.* 196, 1171-1181. DOI: 10.1111/j.1469-8137.2012.04344.x

95 Pavan, S. *et al.* (2010) Loss of susceptibility as a novel breeding strategy for durable and broad-spectrum resistance. *Molecular Breeding : New Strategies in Plant Improvement* 25, 1-12. DOI: 10.1007/s11032-009-9323-6

96 Jorgensen, J. (1992) Discovery, Characterization and Exploitation of *Mlo* Powdery Mildew Resistance in Barley. *Euphytica* 63, 141-152

97 Buschges, R. *et al.* (1997) The barley *Mlo* gene: a novel control element of plant pathogen resistance. *Cell* 88, 695-705

98 Bai, Y. *et al.* (2008) Naturally occurring broad-spectrum powdery mildew resistance in a Central American tomato accession is caused by loss of *mlo* function. *Mol. Plant Microbe Interact.* 21, 30-39. DOI: 10.1094/MPMI-21-1-0030

- 99 Consonni, C. *et al.* (2006) Conserved requirement for a plant host cell protein in powdery mildew pathogenesis. *Nat. Genet.* 38, 716-720. DOI: 10.1038/ng1806
- 100 Kim, D.S. and Hwang, B.K. (2012) The pepper *MLO* gene, *CaMLO2*, is involved in the susceptibility cell-death response and bacterial and oomycete proliferation. *Plant J.* 72, 843-55. DOI: 10.1111/tj.12003
- 101 Consonni, C. *et al.* (2010) Tryptophan-derived metabolites are required for antifungal defense in the Arabidopsis *mlo2* mutant. *Plant Physiol.* 152, 1544-1561. DOI: 10.1104/pp.109.147660
- 102 Li, C. *et al.* (2012) Gene silencing using the recessive rice bacterial blight resistance gene *xa13* as a new paradigm in plant breeding. *Plant Cell Rep.* 31, 851-862. DOI: 10.1007/s00299-011-1206-8
- 103 Contreras-Paredes, C.A. *et al.* (2013) The Absence of Eukaryotic Initiation Factor eIF(iso)4E Affects the Systemic Spread of a Tobacco etch virus Isolate in *Arabidopsis thaliana*. *Mol. Plant Microbe Interact.* 26, 461-470. DOI: 10.1094/MPMI-09-12-0225-R
- 104 Cavatorta, J. *et al.* (2011) Engineering virus resistance using a modified potato gene. *Plant. Biotechnol. J.* 9, 1014-1021. DOI: 10.1111/j.1467-7652.2011.00622.x
- 105 Ruffel, S. *et al.* (2002) A natural recessive resistance gene against potato virus Y in pepper corresponds to the eukaryotic initiation factor 4E (eIF4E). *Plant J.* 32, 1067-1075
- 106 Wang, A. and Krishnaswamy, S. (2012) Eukaryotic translation initiation factor 4E-mediated recessive resistance to plant viruses and its utility in crop improvement. *Mol. Plant Pathol.* 13, 795-803. DOI: 10.1111/j.1364-3703.2012.00791.x
- 107 Nemri, A. *et al.* (2010) Genome-wide survey of Arabidopsis natural variation in downy mildew resistance using combined association and linkage mapping. *Proc. Natl. Acad. Sci. U. S. A.* 107, 10302-10307. DOI: 10.1073/pnas.0913160107
- 108 Liu, S. *et al.* (2012) A soybean cyst nematode resistance gene points to a new mechanism of plant resistance to pathogens. *Nature* 492, 256-260. DOI: 10.1038/nature11651; 10.1038/nature11651
- 109 Van Damme, M. *et al.* (2005) Identification of Arabidopsis loci required for susceptibility to the downy mildew pathogen *Hyaloperonospora parasitica*. *Mol. Plant Microbe Interact.* 18, 583-592. DOI: 10.1094/MPMI-18-0583
- 110 van Damme, M. *et al.* (2009) Downy Mildew Resistance in Arabidopsis by Mutation of *HOMO-SERINE KINASE*. *The Plant Cell* 21, 2179-2189. DOI: 10.1105/tpc.109.066811
- 111 Stuttmann, J. *et al.* (2011) Perturbation of Arabidopsis amino acid metabolism causes incompatibility with the adapted biotrophic pathogen *Hyaloperonospora arabidopsidis*. *Plant Cell* 23, 2788-2803. DOI: 10.1105/tpc.111.087684
- 112 Hok, S. *et al.* (2011) An Arabidopsis (malectin-like) leucine-rich repeat receptor-like kinase contributes to downy mildew disease. *Plant. Cell. Environ.* 34, 1944-1957. DOI: 10.1111/j.1365-3040.2011.02390.x
- 113 Huibers, R.P. *et al.* (2009) Disease-specific expression of host genes during downy mildew infection of Arabidopsis. *Mol. Plant Microbe Interact.* 22, 1104-1115. DOI: 10.1094/MPMI-22-9-1104
- 114 Thines, M. *et al.* (2009) Taxonomy and Phylogeny of the Downy Mildews (*Peronosporaceae*). In *Oomycete Genetics and Genomics*, pp. 47-75, John Wiley & Sons, Inc.

- 115 Michelmore, R. and Wong, J. (2008) Classical and molecular genetics of *Bremia lactucae*, cause of lettuce downy mildew. *Eur. J. Plant Pathol.* 122, 19-30. DOI: 10.1007/s10658-008-9305-2
- 116 Lebeda, A. and Cohen, Y. (2011) Cucurbit downy mildew (*Pseudoperonospora cubensis*)-biology, ecology, epidemiology, host-pathogen interaction and control. *Eur. J. Plant Pathol.* 129, 157-192. DOI: 10.1007/s10658-010-9658-1
- 117 Lukman, R. *et al.* (2013) Unraveling the Genetic Diversity of Maize Downy Mildew in Indonesia. *J Plant Pathol Microb* 2, 162
- 118 Coates, M.E. and Beynon, J.L. (2010) *Hyaloperonospora arabidopsidis* as a pathogen model. *Annu. Rev. Phytopathol.* 48, 329-345. DOI: 10.1146/annurev-phyto-080508-094422
- 119 van Damme, M. *et al.* (2008) Arabidopsis *DMR6* encodes a putative 2OG-Fe(II) oxygenase that is defense-associated but required for susceptibility to downy mildew. *Plant J.* 54, 785-793. DOI: 10.1111/j.1365-313X.2008.03427.x
- 120 van der Hoorn, R.A.L. and Kamoun, S. (2008) From Guard to Decoy: A New Model for Perception of Plant Pathogen Effectors. *The Plant Cell* 20, 2009-2017. DOI: 10.1105/tpc.108.060194
- 121 Kou, Y. and Wang, S. (2010) Broad-spectrum and durability: understanding of quantitative disease resistance. *Curr. Opin. Plant Biol.* 13, 181-185. DOI: 10.1016/j.pbi.2009.12.010
- 122 Yang, B. *et al.* (2006) *Os8N3* is a host disease-susceptibility gene for bacterial blight of rice. *Proc. Natl. Acad. Sci. U. S. A.* 103, 10503-10508. DOI: 10.1073/pnas.0604088103
- 123 Robaglia, C. and Caranta, C. (2006) Translation initiation factors: a weak link in plant RNA virus infection. *Trends Plant Sci.* 11, 40-45. DOI: 10.1016/j.tplants.2005.11.004
- 124 Faris, J.D. *et al.* (2010) A unique wheat disease resistance-like gene governs effector-triggered susceptibility to necrotrophic pathogens. *Proc. Natl. Acad. Sci. U. S. A.* 107, 13544-13549. DOI: 10.1073/pnas.1004090107
- 125 Qu, S. *et al.* (2006) The broad-spectrum blast resistance gene *Pi9* encodes a nucleotide-binding site-leucine-rich repeat protein and is a member of a multigene family in rice. *Genetics* 172, 1901-1914. DOI: 10.1534/genetics.105.044891
- 126 Borhan, M.H. *et al.* (2008) *WRR4* encodes a TIR-NB-LRR protein that confers broad-spectrum white rust resistance in *Arabidopsis thaliana* to four physiological races of *Albugo candida*. *Mol. Plant Microbe Interact.* 21, 757-768. DOI: 10.1094/MPMI-21-6-0757
- 127 Xiao, S. *et al.* (2001) Broad-spectrum mildew resistance in *Arabidopsis thaliana* mediated by *RPW8*. *Science* 291, 118-120. DOI: 10.1126/science.291.5501.118
- 128 Nombela, G. *et al.* (2003) The root-knot nematode resistance gene *Mi-1.2* of tomato is responsible for resistance against the whitefly *Bemisia tabaci*. *Mol. Plant Microbe Interact.* 16, 645-649. DOI: 10.1094/MPMI.2003.16.7.645
- 129 Vos[dagger], P. *et al.* (1998) The tomato *Mi-1* gene confers resistance to both root-knot nematodes and potato aphids. *Nat Biotech* 16, 1365-1369
- 130 Rossi, M. *et al.* (1998) The nematode resistance gene *Mi* of tomato confers resistance against the potato aphid. *Proc. Natl. Acad. Sci. U. S. A.* 95, 9750-9754. DOI: 10.1073/pnas.95.17.9750

- 131 Milligan, S.B. *et al.* (1998) The Root Knot Nematode Resistance Gene *Mi* from Tomato Is a Member of the Leucine Zipper, Nucleotide Binding, Leucine-Rich Repeat Family of Plant Genes. *The Plant Cell* 10, 1307-1320. DOI: 10.1105/tpc.10.8.1307
- 132 Rygulla, W. *et al.* (2008) Identification of quantitative trait loci for resistance against *Verticillium longisporum* in oilseed rape (*Brassica napus*). *Phytopathology* 98, 215-221. DOI: 10.1094/PHYTO-98-2-0215
- 133 Shi, X. *et al.* (2010) Identification of the quantitative trait loci in japonica rice landrace Heikezijing responsible for broad-spectrum resistance to rice blast. *Phytopathology* 100, 822-829. DOI: 10.1094/PHYTO-100-8-0822
- 134 Hamon, C. *et al.* (2010) A complex genetic network involving a broad-spectrum locus and strain-specific loci controls resistance to different pathotypes of *Aphanomyces euteiches* in *Medicago truncatula*. *Theor. Appl. Genet.* 120, 955-970. DOI: 10.1007/s00122-009-1224-x
- 135 Lisec, J. *et al.* (2009) Identification of heterotic metabolite QTL in *Arabidopsis thaliana* RIL and IL populations. *The Plant Journal* 59, 777-788. DOI: 10.1111/j.1365-313X.2009.03910.x
- 136 Krasileva, K.V. *et al.* (2011) Global Analysis of *Arabidopsis*/Downy Mildew Interactions Reveals Prevalence of Incomplete Resistance and Rapid Evolution of Pathogen Recognition. *PLoS ONE* 6, e28765
- 137 Holub, E. (2008) Natural history of *Arabidopsis thaliana* and oomycete symbioses. *European Journal of Plant Pathology* 122, 91-109
- 138 Slusarenko, A.J. and Schlaich, N.L. (2003) Downy mildew of *Arabidopsis thaliana* caused by *Hyaloperonospora parasitica* (formerly *Peronospora parasitica*). *Mol. Plant. Pathol.* 4, 159-170. DOI: 10.1046/j.1364-3703.2003.00166.x
- 139 Holub, E.B. and Beynon, J. (1997) Symbiology of mouse-ear cress (*Arabidopsis thaliana*) and oomycetes. *Adv. Bot. Res.* 24, 228
- 140 Torjek, O. *et al.* (2008) Construction and analysis of two reciprocal *Arabidopsis* introgression line populations. *J. Hered.* 99, 396-406. DOI: 10.1093/jhered/esn014
- 141 Torjek, O. *et al.* (2006) Segregation distortion in *Arabidopsis* C24/Col-0 and Col-0/C24 recombinant inbred line populations is due to reduced fertility caused by epistatic interaction of two loci. *Theor. Appl. Genet.* 113, 1551-1561. DOI: 10.1007/s00122-006-0402-3
- 142 Lisec, J. *et al.* (2008) Identification of metabolic and biomass QTL in *Arabidopsis thaliana* in a parallel analysis of RIL and IL populations. *Plant J.* 53, 960-972. DOI: 10.1111/j.1365-313X.2007.03383.x
- 143 Sekine, K.T. *et al.* (2008) High level expression of a virus resistance gene, *RCY1*, confers extreme resistance to Cucumber mosaic virus in *Arabidopsis thaliana*. *Mol. Plant Microbe Interact.* 21, 1398-1407. DOI: 10.1094/MPMI-21-11-1398
- 144 Sekine, K.T. *et al.* (2006) Single amino acid alterations in *Arabidopsis thaliana* *RCY1* compromise resistance to Cucumber mosaic virus, but differentially suppress hypersensitive response-like cell death. *Plant Mol. Biol.* 62, 669-682. DOI: 10.1007/s11013-006-9048-4
- 145 Weigel, D. and Glazebrook, J. (2002) CTAB DNA miniprep. In *Arabidopsis: A Laboratory Manual*, pp. 165, Cold Spring Harbor Laboratory Press

- 146 Weigel, D. and Glazebrook, J. (2002) Trypan Blue Stain for Fungi, Oomycetes, and Dead Plant Cells. In *Arabidopsis: A Laboratory Manual*, pp. 86, Cold Spring Harbor Laboratory press
- 147 Broman, K.W. *et al.* (2003) R/qtl: QTL mapping in experimental crosses. *Bioinformatics* 19, 889-890
- 148 Yang, J. *et al.* (2008) QTLNetwork: mapping and visualizing genetic architecture of complex traits in experimental populations. *Bioinformatics* 24, 721-723. DOI: 10.1093/bioinformatics/btm494
- 149 Hruz, T. *et al.* (2011) RefGenes: identification of reliable and condition specific reference genes for RT-qPCR data normalization. *BMC Genomics* 12, 156. DOI: 10.1186/1471-2164-12-156
- 150 Reignault, P. *et al.* (1996) Four *Arabidopsis RPP* loci controlling resistance to the Noco2 isolate of *Peronospora parasitica* map to regions known to contain other *RPP* recognition specificities. *Mol. Plant Microbe Interact.* 9, 464-473
- 151 McDowell, J.M. *et al.* (1998) Intragenic recombination and diversifying selection contribute to the evolution of downy mildew resistance at the *RPP8* locus of *Arabidopsis*. *Plant Cell* 10, 1861-1874
- 152 Parker, J.E. *et al.* (1997) The *Arabidopsis* downy mildew resistance gene *RPP5* shares similarity to the toll and interleukin-1 receptors with *N* and *L6*. *Plant Cell* 9, 879-894
- 153 Salome, P.A. *et al.* (2011) Genetic architecture of flowering-time variation in *Arabidopsis thaliana*. *Genetics* 188, 421-433. DOI: 10.1534/genetics.111.126607
- 154 Takahashi, H. *et al.* (2002) *RCY1*, an *Arabidopsis thaliana RPP8/HRT* family resistance gene, conferring resistance to cucumber mosaic virus requires salicylic acid, ethylene and a novel signal transduction mechanism. *Plant J.* 32, 655-667
- 155 Bechtold, U. *et al.* (2010) Constitutive salicylic acid defences do not compromise seed yield, drought tolerance and water productivity in the *Arabidopsis* accession C24. *Plant. Cell. Environ.* 33, 1959-1973. DOI: 10.1111/j.1365-3040.2010.02198.x
- 156 Pieterse, C.M. *et al.* (2009) Networking by small-molecule hormones in plant immunity. *Nat. Chem. Biol.* 5, 308-316. DOI: 10.1038/nchembio.164
- 157 Spoel, S.H. and Dong, X. (2012) How do plants achieve immunity? Defence without specialized immune cells. *Nat Rev Immunol* 12, 89-100
- 158 Bomblies, K. and Weigel, D. (2007) Hybrid necrosis: autoimmunity as a potential gene-flow barrier in plant species. *Nat. Rev. Genet.* 8, 382-393. DOI: 10.1038/nrg2082
- 159 van Leeuwen, H. *et al.* (2007) Natural Variation among *Arabidopsis thaliana* Accessions for Transcriptome Response to Exogenous Salicylic Acid. *The Plant Cell* 19, 2099-2110. DOI: 10.1105/tpc.107.050641
- 160 Ahmad, S. *et al.* (2011) Genetic dissection of basal defence responsiveness in accessions of *Arabidopsis thaliana*. *Plant, Cell Environ.* 34, 1191-1206. DOI: 10.1111/j.1365-3040.2011.02317.x
- 161 Poland, J.A. *et al.* (2009) Shades of gray: the world of quantitative disease resistance. *Trends Plant Sci.* 14, 21-29. DOI: 10.1016/j.tplants.2008.10.006
- 162 Palloix, A. *et al.* (2009) Durability of plant major resistance genes to pathogens depends on the genetic background, experimental evidence and consequences for breeding strategies. *New Phytol.*

- 183, 190-199. DOI: 10.1111/j.1469-8137.2009.02827.x
- 163 Gollner, K. *et al.* (2008) Natural genetic resources of *Arabidopsis thaliana* reveal a high prevalence and unexpected phenotypic plasticity of *RPW8*-mediated powdery mildew resistance. *New Phytol.* 177, 725-742. DOI: 10.1111/j.1469-8137.2007.02339.x
- 164 Holub, E.B. (2001) The arms race is ancient history in *Arabidopsis*, the wildflower. *Nat. Rev. Genet.* 2, 516-527
- 165 Caranta, C. *et al.* (1997) Polygenic resistance of pepper to potyviruses consists of a combination of isolate-specific and broad-spectrum quantitative trait loci. *Mol. Plant-Microbe Interact.* 10, 872-878. DOI: 10.1094/MPMI.1997.10.7.872
- 166 Faris, J. and Friesen, T. (2005) Identification of quantitative trait loci for race-nonspecific resistance to tan spot in wheat. *Theor. Appl. Genet.* 111, 386-392. DOI: 10.1007/s00122-005-2033-5
- 167 Silvar, C. *et al.* (2011) Resistance to powdery mildew in Spanish barley landraces is controlled by different sets of quantitative trait loci. *Theor. Appl. Genet.* 123, 1019-1028. DOI: 10.1007/s00122-011-1644-2
- 168 Leonards-Schippers, C. *et al.* (1994) Quantitative Resistance to *Phytophthora infestans* in Potato - a Case-Study for QTL Mapping in an Allopolyploid Plant-Species. *Genetics* 137, 67-77
- 169 Wilfert, L. and Schmid-Hempel, P. (2008) The genetic architecture of susceptibility to parasites. *BMC Evol. Biol.* 8, 187. DOI: 10.1186/1471-2148-8-187
- 170 Kover, P. and Caicedo, A. (2001) The genetic architecture of disease resistance in plants and the maintenance of recombination by parasites. *Mol. Ecol.* 10, 1-16. DOI: 10.1046/j.1365-294X.2001.01124.x
- 171 Cook, D.E. *et al.* (2012) Copy Number Variation of Multiple Genes at *Rhg1* Mediates Nematode Resistance in Soybean. *Science* 1206. DOI: 10.1126/science.1228746
- 172 Kover, P.X. *et al.* (2009) A Multiparent Advanced Generation Inter-Cross to Fine-Map Quantitative Traits in *Arabidopsis thaliana*. *PLoS Genet* 5, e1000551
- 173 McMullen, M.D. *et al.* (2009) Genetic Properties of the Maize Nested Association Mapping Population. *Science* 325, 737-740. DOI: 10.1126/science.1174320
- 174 Kump, K.L. *et al.* (2011) Genome-wide association study of quantitative resistance to southern leaf blight in the maize nested association mapping population. *Nat. Genet.* 43, 163-168. DOI: 10.1038/ng.747; 10.1038/ng.747
- 175 Poland, J.A. *et al.* (2011) Genome-wide nested association mapping of quantitative resistance to northern leaf blight in maize. *Proc. Natl. Acad. Sci. U. S. A.* 108, 6893-6898. DOI: 10.1073/pnas.1010894108
- 176 Atwell, S. *et al.* (2010) Genome-wide association study of 107 phenotypes in *Arabidopsis thaliana* inbred lines. *Nature* 465, 627-631. DOI: 10.1038/nature08800; 10.1038/nature08800
- 177 Wissler, R.J. *et al.* (2011) Multivariate analysis of maize disease resistances suggests a pleiotropic genetic basis and implicates a *GST* gene. *Proc. Natl. Acad. Sci. U. S. A.* 108, 7339-7344. DOI: 10.1073/pnas.1011739108

- 178 Olukolu, B.A. *et al.* (2012) A Connected Set of Genes Associated with Programmed Cell Death Implicated in Controlling the Hypersensitive Response in Maize. *Genetics*. DOI: 10.1534/genetics.112.147595
- 179 Greene, E.A. *et al.* (2003) Spectrum of Chemically Induced Mutations From a Large-Scale Reverse-Genetic Screen in Arabidopsis. *Genetics* 164, 731-740
- 180 Krieg, D.R. (1963) Ethyl methanesulfonate-induced reversion of bacteriophage T4rII mutants. *Genetics* 48, 561-580
- 181 Schneeberger, K. *et al.* (2009) SHOREmap: simultaneous mapping and mutation identification by deep sequencing. *Nat. Methods* 6, 550-551. DOI: 10.1038/nmeth0809-550
- 182 Austin, R.S. *et al.* (2011) Next-generation mapping of Arabidopsis genes. *Plant J.* 67, 715-725. DOI: 10.1111/j.1365-313X.2011.04619.x
- 183 Abe, A. *et al.* (2012) Genome sequencing reveals agronomically important loci in rice using Mut-Map. *Nat. Biotechnol.* 30, 174-178. DOI: 10.1038/nbt.2095
- 184 Earley, E.J. and Jones, C.D. (2011) Next-generation mapping of complex traits with phenotype-based selection and introgression. *Genetics* 189, 1203-1209. DOI: 10.1534/genetics.111.129445
- 185 Takagi, H. *et al.* (2013) QTL-seq: rapid mapping of quantitative trait loci in rice by whole genome resequencing of DNA from two bulked populations. *Plant J.* 74, 174-183. DOI: 10.1111/tj.12105
- 186 Koornneef, M. and Meinke, D. (2010) The development of Arabidopsis as a model plant. *Plant J.* 61, 909-921. DOI: 10.1111/j.1365-313X.2009.04086.x
- 187 Sherrie, L.S. and Richard, M.A. (1996) Genetic and physiological analysis of flowering time in the C24 line of *Arabidopsis thaliana*. *WEEDS WORLD* 2, 2
- 188 Berendzen, K. *et al.* (2005) A rapid and versatile combined DNA/RNA extraction protocol and its application to the analysis of a novel DNA marker set polymorphic between *Arabidopsis thaliana* ecotypes Col-0 and Landsberg *erecta*. *Plant Methods* 1, 4. DOI: 10.1186/1746-4811-1-4
- 189 Stassen, J.H.M. *et al.* (2012) Effector identification in the lettuce downy mildew *Bremia lactucae* by massively parallel transcriptome sequencing. *Molecular Plant Pathology* 13, 719-731. DOI: 10.1111/j.1364-3703.2011.00780.x
- 190 Mokry, M. *et al.* (2011) Identification of factors required for meristem function in Arabidopsis using a novel next generation sequencing fast forward genetics approach. *BMC Genomics* 12, 256-2164-12-256. DOI: 10.1186/1471-2164-12-256; 10.1186/1471-2164-12-256
- 191 Benjamini, Y. and Hochberg, Y. (1995) Controlling the False Discovery Rate - a Practical and Powerful Approach to Multiple Testing. *J. R. Stat. Soc. Ser. B-Methodol.* 57, 289-300
- 192 R Development Core Team. (2012) *R: A Language and Environment for Statistical Computing*, R Foundation for Statistical Computing
- 193 Sarkar, D. (2008) *Lattice: Multivariate Data Visualization with R*, Springer
- 194 Warnes, G.R. (2013) gplots: Various R programming tools for plotting data: CRAN 2.11.0.1
- 195 Warthmann, N. *et al.* (2007) MSQT for choosing SNP assays from multiple DNA alignments.

Bioinformatics 23, 2784-2787. DOI: 10.1093/bioinformatics/btm428

196 Schneeberger, K. *et al.* (2011) Reference-guided assembly of four diverse *Arabidopsis thaliana* genomes. *Proc. Natl. Acad. Sci. U. S. A.* 108, 10249-10254. DOI: 10.1073/pnas.1107739108

197 Lamesch, P. *et al.* (2012) The Arabidopsis Information Resource (TAIR): improved gene annotation and new tools. *Nucleic Acids Res.* 40, D1202-D1210. DOI: 10.1093/nar/gkr1090

198 Copenhaver, G. *et al.* (1999) Genetic definition and sequence analysis of Arabidopsis centromeres. *Science* 286, 2468-2474. DOI: 10.1126/science.286.5449.2468

199 Huang, X. *et al.* (2011) Analysis of natural allelic variation in Arabidopsis using a multiparent recombinant inbred line population. *Proc. Natl. Acad. Sci. U. S. A.* DOI: 10.1073/pnas.1100465108

200 Lehner, B. (2011) Molecular mechanisms of epistasis within and between genes. *Trends Genet.* 27, 323-331. DOI: 10.1016/j.tig.2011.05.007

201 Rozen, S. and Skaletsky, H. (2000) Primer3 on the WWW for general users and for biologist programmers. *Methods Mol. Biol.* 132, 365-86

202 Vossen, R.H.A.M. *et al.* (2009) High-Resolution Melting Analysis (HRMA)-More Than Just Sequence Variant Screening. *Hum. Mutat.* 30, 860-866. DOI: 10.1002/humu.21019

203 Deslandes, L. and Rivas, S. (2012) Catch me if you can: bacterial effectors and plant targets. *Trends Plant Sci.* 17, 644-655. DOI: 10.1016/j.tplants.2012.06.011

204 Mentlak, T.A. *et al.* (2012) Effector-Mediated Suppression of Chitin-Triggered Immunity by *Magnaporthe oryzae* Is Necessary for Rice Blast Disease. *Plant Cell* 24, 322-335. DOI: 10.1105/tpc.111.092957

205 Shen, Q. *et al.* (2007) Nuclear activity of MLA immune receptors links isolate-specific and basal disease-resistance responses. *Science* 315, 1098-1103. DOI: 10.1126/science.1136372

206 Zhu, Z. *et al.* (2010) Arabidopsis resistance protein SNC1 activates immune responses through association with a transcriptional corepressor. *Proc. Natl. Acad. Sci. U. S. A.* 107, 13960-13965. DOI: 10.1073/pnas.1002828107

207 Padmanabhan, M.S. *et al.* (2013) Novel Positive Regulatory Role for the SPL6 Transcription Factor in the N TIR-NB-LRR Receptor-Mediated Plant Innate Immunity. *PLoS Pathog.* 9, e1003235. DOI: 10.1371/journal.ppat.1003235

208 Gao, X. *et al.* (2013) Bifurcation of Arabidopsis NLR Immune Signaling via Ca²⁺-Dependent Protein Kinases. *PLoS Pathog.* 9, e1003127. DOI: 10.1371/journal.ppat.1003127

209 Bellin, D. *et al.* (2013) Nitric Oxide as a Mediator for Defense Responses. *Mol. Plant-Microbe Interact.* 26, 271-277. DOI: 10.1094/MPMI-09-12-0214-CR

210 Yoshioka, H. *et al.* (2011) Regulatory mechanisms of nitric oxide and reactive oxygen species generation and their role in plant immunity. *Nitric Oxide-Biol. Chem.* 25, 216-221. DOI: 10.1016/j.niox.2010.12.008

211 Underwood, W. *et al.* (2007) The *Pseudomonas syringae* type III effector tyrosine phosphatase HopAO1 suppresses innate immunity in *Arabidopsis thaliana*. *Plant J.* 52, 658-672. DOI: 10.1111/j.1365-313X.2007.03262.x

- 212 Tsuda, K. *et al.* (2009) Network Properties of Robust Immunity in Plants. *Plos Genetics* 5, e1000772. DOI: 10.1371/journal.pgen.1000772
- 213 Tsuda, K. and Katagiri, F. (2010) Comparing signaling mechanisms engaged in pattern-triggered and effector-triggered immunity. *Curr. Opin. Plant Biol.* 13, 459-465. DOI: 10.1016/j.pbi.2010.04.006
- 214 Lacombe, S. *et al.* (2010) Interfamily transfer of a plant pattern-recognition receptor confers broad-spectrum bacterial resistance. *Nat. Biotechnol.* 28, 365-369. DOI: 10.1038/nbt.1613
- 215 Takai, R. *et al.* (2008) Analysis of Flagellin Perception Mediated by flg22 Receptor OsFLS2 in Rice. *Mol. Plant-Microbe Interact.* 21, 1635-1642. DOI: 10.1094/MPMI-21-12-1635
- 216 Maekawa, T. *et al.* (2012) Conservation of NLR-triggered immunity across plant lineages. *Proc. Natl. Acad. Sci. U. S. A.* 109, 20119-20123. DOI: 10.1073/pnas.1218059109
- 217 Lapin, D. and Van den Ackerveken, G. (2013) Susceptibility to plant disease: more than a failure of host immunity. *Trends Plant Sci.* . DOI: <http://dx.doi.org/10.1016/j.tplants.2013.05.005>
- 218 Zellerhoff, N. *et al.* (2006) Non-host resistance of barley is successfully manifested against *Magnaporthe grisea* and a closely related *Pennisetum*-infecting lineage but is overcome by *Magnaporthe oryzae*. *Mol. Plant-Microbe Interact.* 19, 1014-1022. DOI: 10.1094/MPMI-19-1014
- 219 Jarosch, B. *et al.* (1999) The ambivalence of the barley *Mlo* locus: Mutations conferring resistance against powdery mildew (*Blumeria graminis* f. sp. *hordei*) enhance susceptibility to the rice blast fungus *Magnaporthe grisea*. *Mol. Plant-Microbe Interact.* 12, 508-514. DOI: 10.1094/MPMI.1999.12.6.508
- 220 Mang, H.G. *et al.* (2009) The Arabidopsis *RESURRECTION1* gene regulates a novel antagonistic interaction in plant defense to biotrophs and necrotrophs. *Plant Physiol.* 151, 290-305. DOI: 10.1104/pp.109.142158
- 221 Pieterse, C.M.J. *et al.* (2012) Hormonal Modulation of Plant Immunity. *Annu. Rev. Cell Dev. Biol.* 28, 489-521. DOI: 10.1146/annurev-cellbio-092910-154055
- 222 Allen, R. *et al.* (2004) Host-parasite coevolutionary conflict between Arabidopsis and downy mildew. *Science* 306, 1957-1960. DOI: 10.1126/science.1104022
- 223 Bittner-Eddy, P. *et al.* (1999) Genetic and physical mapping of the *RPP13* locus, in Arabidopsis, responsible for specific recognition of several *Peronospora parasitica* (downy mildew) isolates. *Mol. Plant Microbe Interact.* 12, 792-802. DOI: 10.1094/MPMI.1999.12.9.792
- 224 Baxter, I. *et al.* (2010) A Coastal Cline in Sodium Accumulation in *Arabidopsis thaliana* Is Driven by Natural Variation of the Sodium Transporter AtHKT1;1. *PLoS Genet.* 6, e1001193. DOI: 10.1371/journal.pgen.1001193
- 225 Platt, A. *et al.* (2010) The Scale of Population Structure in *Arabidopsis thaliana*. *PLoS Genet.* 6, e1000843. DOI: 10.1371/journal.pgen.1000843
- 226 Chen, Z. *et al.* (2009) Two Seven-Transmembrane Domain MILDEW RESISTANCE LOCUS O Proteins Cofunction in Arabidopsis Root Thigmomorphogenesis. *Plant Cell* 21, 1972-1991. DOI: 10.1105/tpc.108.062653
- 227 Rashotte, A.M. *et al.* (2006) A subset of Arabidopsis AP2 transcription factors mediates cytokinin responses in concert with a two-component pathway. *Proc. Natl. Acad. Sci. U. S. A.* 103, 11081-11085. DOI: 10.1073/pnas.0602038103

- 228 Alonso, J. *et al.* (2003) Genome-wide Insertional mutagenesis of *Arabidopsis thaliana*. *Science* 301, 653-657. DOI: 10.1126/science.1086391
- 229 Sessions, A. *et al.* (2002) A high-throughput Arabidopsis reverse genetics system. *Plant Cell* 14, 2985-2994. DOI: 10.1105/tpc.004630
- 230 Karimi, M. *et al.* (2002) GATEWAY vectors for *Agrobacterium*-mediated plant transformation. *Trends Plant Sci.* 7, 193-195. DOI: 10.1016/S1360-1385(02)02251-3
- 231 Clough, S. and Bent, A. (1998) Floral dip: a simplified method for *Agrobacterium*-mediated transformation of *Arabidopsis thaliana*. *Plant Journal* 16, 735-743. DOI: 10.1046/j.1365-313x.1998.00343.x
- 232 Argueso, C.T. *et al.* (2012) Two-Component Elements Mediate Interactions between Cytokinin and Salicylic Acid in Plant Immunity. *PLoS Genet* 8, e1002448
- 233 Seren, U. *et al.* (2012) GWAPP: A Web Application for Genome-Wide Association Mapping in Arabidopsis. *Plant Cell* 24, 4793-4805. DOI: 10.1105/tpc.112.108068
- 234 Kang, H.M. *et al.* (March 2008) Efficient Control of Population Structure in Model Organism Association Mapping. *Genetics* 178, 1709-1723. DOI: 10.1534/genetics.107.080101
- 235 Waterhouse, A.M. *et al.* (2009) Jalview Version 2-a multiple sequence alignment editor and analysis workbench. *Bioinformatics* 25, 1189-1191. DOI: 10.1093/bioinformatics/btp033
- 236 Bradbury, P.J. *et al.* (2007) TASSEL: software for association mapping of complex traits in diverse samples. *Bioinformatics* 23, 2633-2635. DOI: 10.1093/bioinformatics/btm308
- 237 Carr, D. *et al.* (2009) Hexagonal Binning Routines. *CRAN* 1.26.2
- 238 Teng, S. *et al.* (2005) Sucrose-specific induction of anthocyanin biosynthesis in Arabidopsis requires the *MYB75/PAP1* gene. *Plant Physiol.* 139, 1840-1852. DOI: 10.1104/pp.105.066688
- 239 Kim, S. *et al.* (2007) Recombination and linkage disequilibrium in *Arabidopsis thaliana*. *Nat. Genet.* 39, 1151-1155. DOI: 10.1038/ng2115
- 240 Negi, J. *et al.* (2013) A Dof Transcription Factor, SCAP1, Is Essential for the Development of Functional Stomata in Arabidopsis. *Curr. Biol.* 23, 479-484. DOI: 10.1016/j.cub.2013.02.001
- 241 Park, J. *et al.* (2001) Overexpression of the tobacco *Tsi1* gene encoding an EREBP/AP2-Type transcription factor enhances resistance against pathogen attack and osmotic stress in tobacco. *Plant Cell* 13, 1035-1046. DOI: 10.1105/tpc.13.5.1035
- 242 Gu, Y. *et al.* (2002) Tomato transcription factors Pti4, Pti5, and Pti6 activate defense responses when expressed in Arabidopsis. *Plant Cell* 14, 817-831. DOI: 10.1105/tpc.000794
- 243 Hruz, T. *et al.* (2008) Genevestigator v3: a reference expression database for the meta-analysis of transcriptomes. *Advances in Bioinformatics* 2008, 420747. DOI: 10.1155/2008/420747
- 244 Carver, T.L.W. *et al.* (1999) Induction of cellular accessibility and inaccessibility and suppression and potentiation of cell death in oat attacked by *Blumeria graminis* f.sp. *avenae*. *Physiol. Mol. Plant Pathol.* 55, 183-196. DOI: 10.1006/pmpp.1999.0223
- 245 Lyngkjaer, M.F. *et al.* (2001) Virulent *Blumeria graminis* infection induces penetration susceptibility and suppresses race-specific hypersensitive resistance against avirulent attack in *Mla1*-barley. *Physiol.*

Mol. Plant Pathol. 59, 243-256. DOI: 10.1006/pmpp.2001.0360

246 Aghnoum, R. *et al.* (2010) Basal Host Resistance of Barley to Powdery Mildew: Connecting Quantitative Trait Loci and Candidate Genes. *Mol. Plant-Microbe Interact.* 23, 91-102. DOI: 10.1094/MPMI-23-1-0091

247 Boyle, B. *et al.* (2010) Molecular and histochemical characterisation of two distinct poplar *Melampsora* leaf rust pathosystems. *Plant Biol.* 12, 364-376. DOI: 10.1111/j.1438-8677.2009.00310.x

248 Azaiez, A. *et al.* (2009) Transcriptome Profiling in Hybrid Poplar Following Interactions with *Melampsora* Rust Fungi. *Mol. Plant-Microbe Interact.* 22, 190-200. DOI: 10.1094/MPMI-22-2-0190

249 Nakano, T. *et al.* (2006) Genome-wide analysis of the *ERF* gene family in Arabidopsis and rice. *Plant Physiol.* 140, 411-432. DOI: 10.1104/pp.105.073783

250 Zhou, J.M. *et al.* (1997) The Pto kinase conferring resistance to tomato bacterial speck disease interacts with proteins that bind a cis-element of pathogenesis-related genes. *EMBO J.* 16, 3207-3218. DOI: 10.1093/emboj/16.11.3207

251 Zarei, A. *et al.* (2011) Two GCC boxes and AP2/ERF-domain transcription factor ORA59 in jasmonate/ethylene-mediated activation of the *PDF1.2* promoter in Arabidopsis. *Plant Mol. Biol.* 75, 321-331. DOI: 10.1007/s11103-010-9728-y

252 Van der Does, D. *et al.* (2013) Salicylic Acid Suppresses Jasmonic Acid Signaling Downstream of SCFCO11-JAZ by Targeting GCC Promoter Motifs via Transcription Factor ORA59. *Plant Cell* 25, 744-761. DOI: 10.1105/tpc.112.108548

253 Roberts, A.M. and Walters, D.R. (1986) Stimulation of Photosynthesis in Uninfected Leaves of Rust-infected Leeks. *Annals of Botany* 57, 893-896. DOI: 10.1093/oxfordjournals.aob.a087174

254 Dempsey, D.A. and Klessig, D.F. (2012) SOS - too many signals for systemic acquired resistance? *Trends Plant Sci.* 17, 538-545. DOI: 10.1016/j.tplants.2012.05.011

255 Coll, N.S. *et al.* (2011) Programmed cell death in the plant immune system. *Cell Death Differ.* 18, 1247-1256. DOI: 10.1038/cdd.2011.37

256 Coll, N.S. *et al.* (2010) Arabidopsis Type I Metacaspases Control Cell Death. *Science* 330, 1393-1397. DOI: 10.1126/science.1194980

257 Liu, Y. *et al.* (2005) Autophagy Regulates Programmed Cell Death during the Plant Innate Immune Response. *Cell* 121, 567-577

258 Whisson, S.C. *et al.* (2007) A translocation signal for delivery of oomycete effector proteins into host plant cells. *Nature* 450, 115-118. DOI: 10.1038/nature06203

259 Wahl, R. *et al.* (2010) A Novel High-Affinity Sucrose Transporter Is Required for Virulence of the Plant Pathogen *Ustilago maydis*. *PLoS Biol* 8, e1000303

260 Wang, D. *et al.* (2012) Technologies for systems-level analysis of specific cell types in plants. *Plant Science* 197, 21-29. DOI: 10.1016/j.plantsci.2012.08.012

261 Balestrini, R. *et al.* (2009) Application of Laser Microdissection to plant pathogenic and symbiotic interactions. *Journal of Plant Interactions* 4, 81-92. DOI: 10.1080/17429140902770396

- 262 Libault, M. *et al.* (2010) Complete Transcriptome of the Soybean Root Hair Cell, a Single-Cell Model, and Its Alteration in Response to *Bradyrhizobium japonicum* Infection. *Plant Physiol.* 152, 541-552. DOI: 10.1104/pp.109.148379
- 263 Hoa, L.T. *et al.* (2004) Proteomic Analysis on Symbiotic Differentiation of Mitochondria in Soybean Nodules. *Plant and Cell Physiology* 45, 300-308. DOI: 10.1093/pcp/pch035
- 264 Dai, S. and Chen, S. (2012) Single-cell-type Proteomics: Toward a Holistic Understanding of Plant Function. *Molecular & Cellular Proteomics* 11, 1622-1630. DOI: 10.1074/mcp.R112.021550
- 265 Panter, S. *et al.* (2000) Identification with Proteomics of Novel Proteins Associated with the Peribacteroid Membrane of Soybean Root Nodules. *Mol. Plant-Microbe Interact.* 13, 325-333. DOI: 10.1094/MPMI.2000.13.3.325
- 266 Koroleva, O.A. and Cramer, R. (2011) Single-cell proteomic analysis of glucosinolate-rich S-cells in *Arabidopsis thaliana*. *Methods* 54, 413-423. DOI: 10.1016/j.ymeth.2011.06.005; 10.1016/j.ymeth.2011.06.005
- 267 Petricka, J.J. *et al.* (2012) The protein expression landscape of the Arabidopsis root. *Proc. Natl. Acad. Sci. U. S. A.* DOI: 10.1073/pnas.1202546109
- 268 America, A.H. and Cordewener, J.H. (2008) Comparative LC-MS: a landscape of peaks and valleys. *Proteomics* 8, 731-749. DOI: 10.1002/pmic.200700694; 10.1002/pmic.200700694
- 269 Ruiz-May, E. *et al.* (2012) The secreted plant N-glycoproteome and associated secretory pathways. *Front. Plant. Sci.* 3, 117. DOI: 10.3389/fpls.2012.00117; 10.3389/fpls.2012.00117
- 270 von Schaewen, A. *et al.* (1993) Isolation of a mutant Arabidopsis plant that lacks N-acetyl glucosaminyl transferase I and is unable to synthesize Golgi-modified complex N-linked glycans. *Plant Physiol.* 102, 1109-1118
- 271 Strasser, R. *et al.* (2005) Molecular basis of N-acetylglucosaminyltransferase I deficiency in Arabidopsis thaliana plants lacking complex N-glycans. *Biochem. J.* 387, 385-391. DOI: 10.1042/BJ20041686
- 272 Frank, J. *et al.* (2008) Comparative Analyses of Arabidopsis *complex glycan1* Mutants and Genetic Interaction with *staurosporin* and *temperature sensitive3a*. *Plant Physiol.* 148, 1354-1367. DOI: 10.1104/pp.108.127027
- 273 Strasser, R. *et al.* (2004) Generation of *Arabidopsis thaliana* plants with complex N-glycans lacking β 1,2-linked xylose and core α 1,3-linked fucose. *FEBS Lett.* 561, 132-136. DOI: [http://dx.doi.org/10.1016/S0014-5793\(04\)00150-4](http://dx.doi.org/10.1016/S0014-5793(04)00150-4)
- 274 Bardor, M. *et al.* (2003) Immunoreactivity in mammals of two typical plant glyco-epitopes, core a(1,3)-fucose and core xylose. *Glycobiology* 13, 427-434. DOI: 10.1093/glycob/cwg024
- 275 Wilson, I.B.H. *et al.* (1998) Core a1,3-fucose is a key part of the epitope recognized by antibodies reacting against plant N-linked oligosaccharides and is present in a wide variety of plant extracts. *Glycobiology* 8, 651-661
- 276 Galinha, C. *et al.* (2007) PLETHORA proteins as dose-dependent master regulators of Arabidopsis root development. *Nature* 449, 1053-1057. DOI: 10.1038/nature06206
- 277 Logemann, E. *et al.* (2006) An improved method for preparing *Agrobacterium* cells that simplifies the Arabidopsis transformation protocol. *Plant Methods* 2, 16. DOI: 10.1186/1746-4811-2-16

- 278 Weigel, D. and Glazebrook, J. (2002) Whole-mount GUS staining. In *Arabidopsis: A Laboratory Manual*, pp. 243, Cold Spring Harbor Laboratory Press
- 279 Liebrand, T.W.H. *et al.* (2012) Endoplasmic Reticulum-Quality Control Chaperones Facilitate the Biogenesis of Cf Receptor-Like Proteins Involved in Pathogen Resistance of Tomato. *Plant Physiol.* 159, 1819-1833. DOI: 10.1104/pp.112.196741
- 280 Gupta, R. *et al.* (2004) Prediction of N-glycosylation sites in human proteins. *Unpublished*
- 281 Petersen, T.N. *et al.* (2011) SignalP 4.0: discriminating signal peptides from transmembrane regions. *Nature Methods* 8, 785-786. DOI: 10.1038/nmeth.1701
- 282 Saeed, A.I. *et al.* (2003) TM4: A free, open-source system for microarray data management and analysis. *BioTechniques* 34, 374-+
- 283 Song, W. *et al.* (2011) N-glycoproteomics in plants: Perspectives and challenges. *Journal of Proteomics* 74, 1463-1474. DOI: 10.1016/j.jprot.2011.05.007
- 284 Iskratsch, T. *et al.* (2009) Specificity analysis of lectins and antibodies using remodeled glycoproteins. *Anal. Biochem.* 386, 133-146. DOI: 10.1016/j.ab.2008.12.005
- 285 Zhang, H. *et al.* (2003) Identification and quantification of N-linked glycoproteins using hydrazide chemistry, stable isotope labeling and mass spectrometry. *Nat. Biotechnol.* 21, 660-666. DOI: 10.1038/nbt827
- 286 Maley, F. *et al.* (1989) Characterization of Glycoproteins and their Associated Oligosaccharides through the use of Endoglycosidases. *Anal. Biochem.* 180, 195-204. DOI: 10.1016/0003-2697(89)90115-2
- 287 Rampitsch, C. and Bykova, N.V. (2012) Proteomics and plant disease: Advances in combating a major threat to the global food supply. *Proteomics* 12, 673-690. DOI: 10.1002/pmic.201100359
- 288 Asai, T. *et al.* (2002) MAP kinase signalling cascade in Arabidopsis innate immunity. *Nature* 415, 977-983. DOI: 10.1038/415977a
- 289 Qutob, D. *et al.* (2006) Phytotoxicity and innate immune responses induced by Nep1-like proteins. *Plant Cell* 18, 3721-3744. DOI: 10.1105/tpc.106.044180
- 290 Suarez-Rodriguez, M.C. *et al.* (2007) MEKK1 is required for flg22-induced MPK4 activation in Arabidopsis plants. *Plant Physiol.* 143, 661-669. DOI: 10.1104/pp.106.091389
- 291 Varet, A. *et al.* (2002) *NHL25* and *NHL3*, two *NDR1/HIN1*-like genes in *Arabidopsis thaliana* with potential role(s) in plant defense. *Mol. Plant-Microbe Interact.* 15, 608-616. DOI: 10.1094/MPMI.2002.15.6.608
- 292 Varet, A. *et al.* (2003) The Arabidopsis *NHL3* gene encodes a plasma membrane protein and its overexpression correlates with increased resistance to *Pseudomonas syringae* pv. *tomato* DC3000. *Plant Physiol.* 132, 2023-2033. DOI: 10.1104/pp.103.020438
- 293 Ham, B. *et al.* (2012) Overexpression of Arabidopsis Plasmodesmata Germin-Like Proteins Disrupts Root Growth and Development. *Plant Cell* 24, 3630-3648. DOI: 10.1105/tpc.112.101063
- 294 McDowell, J.M. *et al.* (2005) Genetic analysis of developmentally regulated resistance to downy mildew (*Hyaloperonospora parasitica*) in *Arabidopsis thaliana*. *Mol. Plant Microbe Interact.* 18, 1226-

1234. DOI: 10.1094/MPMI-18-1226

295 Niks, R.E. (1986) Failure of Haustorial Development as a Factor in Slow Growth and Development of *Puccinia hordei* in Partially Resistant Barley Seedlings. *Physiol. Mol. Plant Pathol.* 28, 309-322

296 Fu, D. *et al.* (2009) A Kinase-START Gene Confers Temperature-Dependent Resistance to Wheat Stripe Rust. *Science* 323, 1357-1360. DOI: 10.1126/science.1166289

297 Li, Y.H. *et al.* (2007) Microscopic and macroscopic studies of the development of *Puccinia hemerocallidis* in resistant and susceptible daylily cultivars. *Plant Dis.* 91, 664-668. DOI: 10.1094/PDIS-91-6-0664

298 Moldenhauer, J. *et al.* (2008) Histopathology and PR-protein markers provide insight into adult plant resistance to stripe rust of wheat (vol 9, pg 137, 2008). *Molecular Plant Pathology* 9, 561-561. DOI: 10.1111/J.1364-3703.2008.00490.X

299 Sillero, J. and Rubiales, D. (2002) Histological characterization of resistance to *Uromyces viciae-fabae* in faba bean. *Phytopathology* 92, 294-299. DOI: 10.1094/PHTO.2002.92.3.294

300 Krattinger, S.G. *et al.* (2009) A putative ABC transporter confers durable resistance to multiple fungal pathogens in wheat. *Science* 323, 1360-1363. DOI: 10.1126/science.1166453

301 Cook, D.E. *et al.* (2012) Copy Number Variation of Multiple Genes at *Rhg1* Mediates Nematode Resistance in Soybean. *Science* 338, 1206-1209. DOI: 10.1126/science.1228746

302 Cole, S.J. and Diener, A.C. (2013) Diversity in receptor-like kinase genes is a major determinant of quantitative resistance to *Fusarium oxysporum* f.sp. *matthioli*. *New Phytol.* . DOI: 10.1111/nph.12368

303 Hu, K.M. *et al.* (2008) Isolation and manipulation of quantitative trait loci for disease resistance in rice using a candidate gene approach. *Mol. Plant.* 1, 786-793. DOI: 10.1093/mp/ssn039; 10.1093/mp/ssn039

304 Periyannan, S. *et al.* (2013) The Gene *Sr33*, an Ortholog of Barley *Mla* Genes, Encodes Resistance to Wheat Stem Rust Race Ug99. *Science* . DOI: 10.1126/science.1239028

305 Hayashi, N. *et al.* (2010) Durable panicle blast-resistance gene *Pb1* encodes an atypical CC-NBS-LRR protein and was generated by acquiring a promoter through local genome duplication. *Plant Journal* 64, 498-510. DOI: 10.1111/j.1365-313X.2010.04348.x

306 Broglie, K.E. *et al.* (2011) Method for identifying maize plants with *RCG1* gene conferring resistance to *Colletotrichum* infection. US8062847 B2

307 Manosalva, P.M. *et al.* (2009) A Germin-Like Protein Gene Family Functions as a Complex Quantitative Trait Locus Conferring Broad-Spectrum Disease Resistance in Rice. *Plant Physiol.* 149, 286-296. DOI: 10.1104/pp.108.128348

308 Pajerowska-Mukhtar, K.M. *et al.* (2008) Natural variation of potato *ALLENE OXIDE SYNTHASE 2* causes differential levels of jasmonates and pathogen resistance in Arabidopsis. *Planta* 228, 293-306. DOI: 10.1007/s00425-008-0737-x

309 Fukuoka, S. *et al.* (2009) Loss of function of a proline-containing protein confers durable disease resistance in rice. *Science* 325, 998-1001. DOI: 10.1126/science.1175550

310 Vashisht, D. *et al.* (2011) Natural variation of submergence tolerance among *Arabidopsis thaliana*

accessions. *New Phytol.* 190, 299-310. DOI: 10.1111/j.1469-8137.2010.03552.x

311 Todesco, M. *et al.* (2010) Natural allelic variation underlying a major fitness trade-off in *Arabidopsis thaliana*. *Nature* 465, 632-636

312 Delaney, T.P. *et al.* (1994) A Central Role of Salicylic-Acid in Plant-Disease Resistance. *Science* 266, 1247-1250. DOI: 10.1126/science.266.5188.1247

313 Zimmerli, L. *et al.* (2004) Host and non-host pathogens elicit different jasmonate/ethylene responses in *Arabidopsis*. *Plant Journal* 40, 633-646. DOI: 10.1111/j.1365-313X.2004.02236.x

314 Caillaud, M.-. *et al.* (2012) Mechanisms of nuclear suppression of host immunity by *Arabidopsis* downy mildew effectors. *Abstract Book ICAR 2012*, 7

315 Makandar, R. *et al.* (2010) Involvement of Salicylate and Jasmonate Signaling Pathways in *Arabidopsis* Interaction with *Fusarium graminearum*. *Mol. Plant-Microbe Interact.* 23, 861-870. DOI: 10.1094/MPMI-23-7-0861

316 Thatcher, L.F. *et al.* (2009) *Fusarium oxysporum* hijacks COI1-mediated jasmonate signaling to promote disease development in *Arabidopsis*. *Plant Journal* 58, 927-939. DOI: 10.1111/j.1365-313X.2009.03831.x

317 He, Y. *et al.* (2012) Specific Missense Alleles of the *Arabidopsis* Jasmonic Acid Co-Receptor *COI1* Regulate Innate Immune Receptor Accumulation and Function. *Plos Genetics* 8, e1003018. DOI: 10.1371/journal.pgen.1003018

318 Neto, G.C. *et al.* (1991) Isolation and Identification of (-)-Jasmonic Acid from Wild-Rice, *Oryza officinalis*, as an Antifungal Substance. *Agric. Biol. Chem.* 55, 3097-3098

319 Schweizer, P. *et al.* (1993) Effect of Jasmonic Acid on the Interaction of Barley (*Hordeum vulgare* L.) with the Powdery Mildew *Erysiphe graminis* f. sp. *hordei*. *Plant Physiol.* 102, 503-511

320 Cohen, Y. *et al.* (1993) Local and Systemic Protection Against *Phytophthora infestans* Induced in Potato and Tomato Plants by Jasmonic Acid and Jasmonic Methyl-Ester. *Phytopathology* 83, 1054-1062. DOI: 10.1094/Phyto-83-1054

321 Antico, C. *et al.* (2012) Insights into the role of jasmonic acid-mediated defenses against necrotrophic and biotrophic fungal pathogens. *Frontiers in Biology* 7, 48-56. DOI: 10.1007/s11515-011-1171-1

322 Thaler, J.S. *et al.* (2004) The role of the jasmonate response in plant susceptibility to diverse pathogens with a range of lifestyles. *Plant Physiol.* 135, 530-538. DOI: 10.1104/pp.104.041566

323 Belhadj, A. *et al.* (2006) Methyl jasmonate induces defense responses in grapevine and triggers protection against *Erysiphe necator*. *J. Agric. Food Chem.* 54, 9119-9125. DOI: 10.1021/jf0618022

324 Walters, D. *et al.* (2002) Methyl jasmonate alters polyamine metabolism and induces systemic protection against powdery mildew infection in barley seedlings. *J. Exp. Bot.* 53, 747-756. DOI: 10.1093/jexbot/53.369.747

325 Dempsey, D.A. and Klessig, D.F. (2012) SOS - too many signals for systemic acquired resistance? *Trends Plant Sci.* 17, 538-545. DOI: 10.1016/j.tplants.2012.05.011

326 De Geyter, N. *et al.* (2012) Transcriptional machineries in jasmonate-elicited plant secondary metabolism. *Trends Plant Sci.* 17, 349-359. DOI: 10.1016/j.tplants.2012.03.001

- 327 Wahl, R. *et al.* (2010) A novel high-affinity sucrose transporter is required for virulence of the plant pathogen *Ustilago maydis*. *PLoS Biol.* 8, e1000303. DOI: 10.1371/journal.pbio.1000303
- 328 Giraldo, M.C. *et al.* (2013) Two distinct secretion systems facilitate tissue invasion by the rice blast fungus *Magnaporthe oryzae*. *Nature Communications* 4, 1996-1996. DOI: 10.1038/ncomms2996
- 329 Caillaud, M. *et al.* (2012) Subcellular localization of the *Hpa* RxLR effector repertoire identifies a tonoplast-associated protein HaRxL17 that confers enhanced plant susceptibility. *Plant Journal* 69, 252-265. DOI: 10.1111/j.1365-313X.2011.04787.x
- 330 Saito, C. *et al.* (2011) The occurrence of 'bulbs', a complex configuration of the vacuolar membrane, is affected by mutations of vacuolar SNARE and phospholipase in Arabidopsis. *Plant Journal* 68, 64-73. DOI: 10.1111/j.1365-313X.2011.04665.x
- 331 Saito, C. *et al.* (2002) A complex and mobile structure forms a distinct subregion within the continuous vacuolar membrane in young cotyledons of Arabidopsis. *Plant Journal* 29, 245-255. DOI: 10.1046/j.0960-7412.2001.01189.x
- 332 Elbein, A.D. *et al.* (2003) New insights on trehalose: a multifunctional molecule. *Glycobiology* 13, 17R-27R. DOI: 10.1093/glycob/cwg047
- 333 Zhang, C. *et al.* (2013) Crosstalk between the Circadian Clock and Innate Immunity in Arabidopsis. *Plos Pathogens* 9, e1003370. DOI: 10.1371/journal.ppat.1003370
- 334 Wang, W. *et al.* (2011) Timing of plant immune responses by a central circadian regulator. *Nature* 470, 110-114. DOI: 10.1038/nature09766
- 335 Deshmukh, S.S. *et al.* (1978) Reduction of Downy Mildew of Pearl Millet with Fertilizer Management. *Phytopathology* 68, 1350-1353
- 336 Hottes, A.K. *et al.* (2013) Bacterial Adaptation through Loss of Function. *PLoS Genetics* 9, e1003617-e1003617. DOI: 10.1371/journal.pgen.1003617
- 337 Windram, O. *et al.* (2012) Arabidopsis Defense against *Botrytis cinerea*: Chronology and Regulation Deciphered by High-Resolution Temporal Transcriptomic Analysis. *Plant Cell* 24, 3530-3557. DOI: 10.1105/tpc.112.102046

Summary

The plant immune system can detect pathogens and restrict their growth and development, although adapted pathogens can circumvent or suppress the activated immune responses. Also non-immunity related host factors and processes contribute to pathogenesis by attracting pathogens, stimulating their development and providing nutrition. The model plant species *Arabidopsis thaliana* and its biotrophic pathogen *Hyaloperonospora arabidopsidis* (*Hpa*), causing downy mildew, provide an excellent interaction to study the role of immunity and non-immunity related host processes in plant disease susceptibility. The work described in this thesis was aimed at identifying *Arabidopsis* genes that alter susceptibility to the downy mildew pathogen *Hpa*. In **Chapters 2, 3 and 4**, results of studies on susceptibility of natural *Arabidopsis* accessions to *Hpa* are presented. The genetic basis of broad-spectrum resistance (BSR) of *Arabidopsis* line C24 to downy mildew was analysed by segregation analysis and quantitative trait loci mapping. BSR was found to be multigenic and mediated by different combinations of isolate-specific resistance loci, some of which confer only partial resistance. In **Chapter 3**, the quantitative resistance of C24 to the *Hpa* isolate Waco9 was studied in more details. Backcross mapping facilitated by whole-genome sequencing revealed two major loci, which interact to confer strong quantitative resistance to *Hpa*. An alternative method to identify *Arabidopsis* genes contributing to susceptibility to downy mildew is by association mapping, and is described in chapter 4., The core *Arabidopsis* HapMap population was scored for susceptibility to a mixture of four *Hpa* isolates. Data analysis revealed that natural variation at three loci, *CYTOKININ RESPONSE FACTOR 1* (*CRF1*), *STOMATAL CARPENTER 1* (*SCAP1*), and the unknown gene At5g53750, was associated with susceptibility to *Hpa*. Analysis of mutants and silencing lines indicated that *SCAP1* and *CRF2*, a close homolog of *CRF1*, are candidate genes that affect susceptibility in the *Arabidopsis*-downy mildew interaction. However, role of these genes in *Arabidopsis* susceptibility remain unknown. Besides the genetic approaches, a complementary proteomics approach was taken to identify proteins present in haustoria-invaded host cells. These specialized infectious structures, called haustoria, are formed by the downy mildew pathogen via penetrating of the plant cell wall and invagination of the host plasma membrane. To gain insight the molecular events occurring specifically in the *Hpa*-infected cells of *Arabidopsis*, we used a N-glycotagging approach coupled to label-free quantitative proteomics (described in **Chapter 5**). Complex N-glycosylation was specifically restored in infected cells by making use of the downy mildew-induced *DMR6* (for *DOWNY MILDEW RESISTANT 6*) promoter. A total of 18 candidate complex N-glycoproteins of *Arabidopsis* were identified that were associated with downy mildew infection. Analysis of mutants in the corresponding genes suggested that *Arabidopsis* PLASMODESMATA GERMIN-LIKE PROTEIN 1 (PDGLP1) and the subtilase ATSBT3.5 affect host susceptibility to *Hpa*. Molecular mechanisms of how genes and proteins identified in this study affect the interaction between *Arabidopsis* and downy mildew are not known, and their further functional characterization might improve our knowledge of host processes that contribute to susceptibility of plants to (hemi-)biotrophic pathogens.

Samenvatting

Het immuunsysteem van planten detecteert ziekteverwekkers en activeert de afweer, zodat hun groei en ontwikkeling wordt inperkt. Echter, succesvolle ziekteverwekkers kunnen de geactiveerde immunoreacties omzeilen of onderdrukken, en dus toch ziekte veroorzaken. Ook niet-immuniteit-gerelateerde factoren en processen in de plant kunnen bijdragen aan vatbaarheid, door het aantrekken van ziekteverwekkers, het stimuleren van hun ontwikkeling, en het verstrekken van voedingsstoffen. De plant *Arabidopsis thaliana* en de biotrofe ziekteverwekker *Hyaloperonospora arabidopsidis* (*Hpa*), de veroorzaker van valse meeldauw, vormen een uitstekend modelsysteem om de rol van immuniteit- en niet-immuniteit-gerelateerde processen in planten te bestuderen. Het in dit proefschrift beschreven werk was gericht op het identificeren van genen van *Arabidopsis* die de gevoeligheid voor *Hpa* beïnvloeden. In de hoofdstukken 2, 3 en 4 zijn de resultaten beschreven van experimenten met betrekking tot de vatbaarheid voor *Hpa* van verschillende *Arabidopsis* accessies. De genetische basis van breed-spectrum resistentie (BSR) van de *Arabidopsis* lijn C24 voor valse meeldauw werd in kaart gebracht door segregatieanalyse en door het mappen van “quantitative trait loci”. BSR bleek bepaald door meerdere genen en veroorzaakt door verschillende combinaties van isolaat-specifieke resistentie loci, waarvan enkelen slechts gedeeltelijke resistentie opleverden. In hoofdstuk 3 is de kwantitatieve resistentie van C24 voor *Hpa* isolaat Waco9 in meer detail bestudeerd en beschreven. Via “backcross mapping” en door middel van “whole genome sequencing”, zijn twee belangrijke loci onthuld, die samen een sterke kwantitatieve resistentie tegen *Hpa* opleveren.

Een alternatieve methode om genen van *Arabidopsis* te identificeren die bijdragen aan de gevoeligheid voor valse meeldauw, is door middel van “association mapping”, welke is beschreven in hoofdstuk 4. Hiervoor werd de “core” *Arabidopsis* HapMap populatie getest op gevoeligheid voor een mix van vier *Hpa* isolaten. Data-analyse toonde aan dat natuurlijke variatie op drie loci, *CYTOKININE RESPONSE FACTOR 1* (*CRF1*), *STOMATAL CARPENTER 1* (*SCAP1*), en het onbekende gen *At5g53750*, was geassocieerd met vatbaarheid voor *Hpa*. Analyse van mutanten en gesilenteerde lijnen gaf aan dat *SCAP1* en *CRF2*, een homoloog van *CRF1*, kandidaat-genen zijn die invloed hebben op de vatbaarheid van *Arabidopsis* voor valse meeldauw. Naast de genetische benaderingen is middels een complementaire proteomics-aanpak een aantal eiwitten geïdentificeerd die aanwezig zijn in haustoria-bevattende gastheercellen. Haustoria zijn gespecialiseerde infectiestructuren gevormd door valse meeldauw ziekteverwekkers door penetratie van de plantencelwand en invaginatie van het plasmamembraan. Om inzicht te krijgen in de moleculaire processen die in *Hpa*-geïnfecteerde cellen van *Arabidopsis* plaatsvinden, is een gecombineerde aanpak van N-glycotagging gekoppeld aan label-vrije kwantitatieve proteomics gebruikt (beschreven in hoofdstuk 5). Complexe N-glycosylatie werd specifiek hersteld in geïnfecteerde cellen door gebruik te maken van de *DMR6* promotor die geïnduceerd wordt door valse meeldauw. In totaal werden 18 mogelijke complexe N-glycoproteïnen van *Arabidopsis* geïdentificeerd die geassocieerd waren met infectie door valse meeldauw. Analyse van mutanten in de overeenkomstige genen suggereerde dat *Arabidopsis* *PLASMODESMATA GERMIN-LIKE PROTEIN 1* (*PDGLP1*) en de subtilase *ATSBT3.5* de vatbaarheid voor *Hpa* beïnvloeden. De verdere functionele karakterisering van de geïdentificeerde genen en eiwitten kan nieuwe kennis opleveren over processen die bijdragen aan de vatbaarheid van planten voor biotrofe ziekteverwekkers.

Acknowledgements/Благодарности

First of all, I would like to thank Guido for the opportunity to have a PhD training in Utrecht University. Our frequent discussions are absolutely essential for my development into an independent researcher. No doubt, your constructive criticism and suggestions had main influence on my “scientific taste” and helped to set markers of good and bad scientific practice. Guido, I am thankful to you for the enormous chances you gave me to participate in different scientific conferences, meetings, symposia, meet with famous researchers. I hope I will be able to capitalize on this fundament. Corné, it was my honor to work and study in the PMI group, I am impressed with the extent of your scientific network and the ability to explain in simple words essence and significance of a scientific finding. Peter, our discussions on plagiarism, misconduct and fraud in science were also important for my training. Saskia, thank you for providing financial resources from the graduate school Life Sciences to attend different courses and meetings. Prof. dr. Weller, thank you for ensuring me that there is nothing wrong to be fascinated about the work-hobby I have.

Pim, I am thankful to you for the help during my first days in the lab. I still remember when you showed me the “best DNA isolation method ever”. Also your words of support and talking to you were essential to help me recover after different emotional deeps during my life in PMI. Miek, I do not exclude that your sweets and home-made cakes contributed to my energy levels and good mood during a day. You are one of the special people who remember birthdays and other important dates of PMI members, take care of cards and presents. I am glad you could take over several projects and responsibilities when my PhD research finished. I wish you success with it. Joyce, Arabidopsis seedlings and plants you grow look awesome. They get a prize from me. I was always impressed with the particular precision and clarity of your work. Nora, Ms. Phytophthora of our lab, thanks for showing me how to perform infection assays with the pathogen *P. capsici*. On top of that, I would like to thank you for valuable advice on music, it definitely enriched my playlists. Joost, your realistic and analytic view on the world always fascinated me. You are one of few people I know who are able to build up long, well-structured and yet making sense sentences. I hope one day I will also be able to talk like an actor in a play. Special thanks for restoration of the admin account on a PCR machine! Of course, you are the great party body: your vegetarian and soft drink-based life style leaves more opportunities for people, including me, whose party style is based on alcohol and meat. Tom, it is astonishing how many facts from different field of knowledge and every-day life are circulating inside your brain. Success with your exciting PhD projects! Stan, I really enjoy talking to you because you frequently have unusual reasoning or an opinion. Your Friday-afternoon experiments encouraged me for my own Friday-afternoon experiments that led to the chapter 4. All the best with the realization of your entrepreneurial spirit. Paul Mister X, I would like to thank you for the hard work in the C24 resistance and dedication to the project. Success with finishing your master studies!

My dear W305 roomies, Giannis, Paul, Silvia, Inez, Tieme, it was my pleasure to share the office with you. We had plenty of nice moments and interesting discussions. Especial thanks to Tieme for giving links to useful RTFM protocols, inviting to Muse concerts, introducing me to the hardstyle music etc. You impressed me with the exceptionally sharp and independent thinking. Silvia, thank you for the help in choosing proper “postdoc” clothing for my new work in Germany.

Roeland, thank you for “the guided tours” on racing bikes and invitations to your New Year parties. I was discovering the Netherlands mostly by following you or your advice. Your explanations on how to use the old machine to bind my thesis were instrumental when I was finishing the thesis for the reading committee. Also, I am greatly thankful to you for the help with my moving in Utrecht, Zeist and Cologne in all these years. Chiel, you are the guy

who made me to like sport/near-sport activities. Thank you so much for that! Probably, it will prolong my active life. Also, beers and dinners in the lab and outside of the lab with you and others were an essential part of my stay in the Netherlands. Glad I shared these moments with you! Dieuwertje, thank you for showing the western blot analysis, sharing dinners and beers in the lab and outside of the lab. It was good time. Richard and Marcel, I hope one day I will also be proficient in programming skills. Thank you for the interesting scientific discussions and sharing your opinions about papers. I enjoyed it a lot! Lotte and Irene, I take off my hat to your amazing organizational skills. I wish I were your student. Silvia, thank you so much for all the discussions we had about association mapping and the opportunity to use materials from your work. Christos, I thank you for help and advice in the lab, sharing your know-hows. I want to have a dinner with you when we talk only about science, let's arrange it one day. Yelling, I wish you all the best with your challenging projects. Anja, Hans, Inze, my projects were at least partially dependent on your consistent work in making sure that stocks and reagents are in good order and easily accessible. Ainhoa and Ivan, thank you for the nice coffee breaks and beers together. I wish you all the best with current postdoc studies and establishing an independent group. Dear PMI members, my PhD training in Utrecht was a pink page of life with a lot of positive emotions, I enjoyed my stay in the Netherlands over these four years, and it is mainly because of you. I wish to all of you interesting projects and a little bit of luck!

I would like to thank Rob Weide, my daily supervisor during the short internship in the group of prof. dr. Francine Govers in Wageningen. Essentially, this training opened for me the world of molecular phytopathology, molecular biology methods, the opportunity to have a PhD study in Utrecht University and, as a consequence, postdoc position in the group of prof. dr. Jane Parker.

Особую благодарность я бы хотел выразить своим родителям. Мама и папа, большое спасибо за вашу моральную и финансовую поддержку в течение моего обучения в Москве. Я бы, наверняка, не был сейчас постдоком в институте Макса Планка в Кельне, если бы я где-то подрабатывал. Я бы хотел поблагодарить весь коллектив бывшей кафедры генетики РГАУ-МСХА имени К.А. Тимирязева и в особенности проф. др. Соловьева Александра Александровича за возможности изучения генетики и доступ к уникальным учебникам и научно-познавательной литературе по генетике. Еще я бы хотел сказать «спасибо» Смолиной Татьяне Владимировне за интересные книги по биологии, факультатив и микроскоп, с которым я мог работать дома во время подготовки к олимпиаде. Конечно же, я не могу не поблагодарить своего классного руководителя Нестерову Галину Викторовну за беседы, которые, как мне кажется, играют важную роль в моем мироощущении, отношении к людям и до сих пор помогают быть уверенным в своих силах. Особая благодарность за Вашу помощь в улучшении моего стиля письма. Кроме того, это так здорово, что мы ездили в театры! Я не сомневаюсь, что это развило мою любовь ко всякого рода большим и маленьким театральным постановкам.

Curriculum vitae

EDUCATION

Utrecht University, Graduate School EPS, The Netherlands	Utrecht
PhD student in the Plant-Microbe Interactions group	2009 - 2013
Russian State Agrarian University, Russia	Moscow
MSc, Field Crop Breeding and Genetics	2004-2009

RESEARCH AND WORK EXPERIENCE

MPIPZ, Germany	Cologne
postdoc in the group of prof. dr. Jane Parker	started in Sept 2013
Utrecht University, The Netherlands	Utrecht
Graduate researcher in Plant-Microbe Interactions group;	2009 - 2013
supervisor a/prof. dr. ir. Guido van den Ackerveken	
promoter prof. dr. ir. Corné Pieterse	
Wageningen University, The Netherlands	Wageningen
Undergraduate in the Lab of Phytopathology;	3 months in 2009
supervisor prof. dr. ir. Francine Govers	
N.I. Vavilov Institute of Plant Industry (VIR), Russia	S.-Petersburg
Undergraduate in the lab of Biochemistry	3 months in 2008
supervisor dr. T.I. Peneva	
Centre of Molecular Biotechnology, Russia	Moscow
Undergraduate; supervisor dr. M.G. Divashuk	2006-2007
Department of Genetics, RSAU, Russia	Moscow
Undergraduate; supervisor prof. dr. A.A. Soloviev	2005-2006

List of publications

Lapin D and Van den Ackerveken G. Plant disease susceptibility: more than a failure of host immunity. *Trends Plant Sci.* (2013) 18(10): 546–54

Lapin D, Meyer RC, Takahashi H, Bechtold U, Van den Ackerveken G. Broad-spectrum resistance of Arabidopsis C24 to downy mildew is mediated by different combinations of isolate-specific loci. *New Phytologist* (2012) 196(4):1171-81.

ten Hove CA, de Jong M, **Lapin D**, Andel A, Sanchez-Perez GF, Tarutani Y, Suzuki Y, Heidstra R, van den Ackerveken G. Trans-repression of gene activity upstream of T-DNA tagged RLK902 links Arabidopsis root growth inhibition and downy mildew resistance. *PLoS One* (2011) 21;6(4):e1902.

